Finite Element Analysis for bulk–surface Partial Differential Equations in evolving Domains

Dissertation
der Mathematisch-Naturwissenschaftlichen Fakultät
der Eberhard Karls Universität Tübingen
zur Erlangung des Grades eines
Doktors der Naturwissenschaften
(Dr. rer. nat)

vorgelegt von
Dominik Edelmann
aus Stuttgart

Tübingen
2024

Gedruckt mit Genehmigung der Mathematisch-Naturwissenschaftlichen Fakultät der Eberhard Karls Universität Tübingen.

Tag der mündlichen Qualifikation:	10.07.2024
Dekan:	Prof. Dr. Thilo Stehle
1. Berichterstatter:	Prof. Dr. Christian Lubich
2. Berichterstatter:	Prof. Dr. Arnold Reusken

Abstract

This dissertation studies the numerical approximation of various partial bulk–surface differential equations in time-dependent domains. The main interest is an application to a model of tissue growth which is a slight modification of a model presented in Eyles et al. [2019]. The model couples a Poisson equation in the time-dependent domain with a forced mean curvature flow of the free boundary surface, with nontrivial bulk–surface coupling in both the velocity law of the evolving boundary surface and the boundary condition of the Poisson equation.

To prepare studying this elaborate system, we present two results on two closely related systems of partial differential equations without any coupling term.

In the first work [Edelmann, 2022], we derive convergence results for evolving finite elements applied to a diffusion-type equation on a time-dependent domain, whose velocity is given explicitly only for the boundary surface and then extended harmonically into the bulk, i.e. obtained by solving a Laplace equation with the given boundary velocity as boundary condition. The weak formulation is then discretized in space using isoparametric finite elements of polynomial degree at least two. We formulate and prove H^1-optimal error bounds for the spatial semi-discretization.

The second work [Edelmann, 2021] deals with an elliptic partial differential equation on a stationary domain, endowed with a generalized Robin boundary condition. This boundary condition includes the Laplace–Beltrami operator on the boundary surface of the domain. The weak formulation of this elliptic equation is discretized using isoparametric finite elements of arbitrary polynomial degree. We provide error bounds that are both L^2- and H^1-optimal.

The third work [Edelmann et al., 2024] studies the aforementioned model of tissue growth. The tissue pressure solves a Poisson equation with an inhomogeneous Robin boundary condition and the boundary surface follows a forced mean curvature flow with the boundary values of the tissue pressure being the forcing term. The presented analysis highly relies on results and techniques from the previous works and the literature cited within the paper. Paired with some additional auxiliary results, we state and prove error bounds for the spatial semi-discretization with evolving bulk–surface finite elements of polynomial degree at least two, which are H^1-optimal in the respective Sobolev spaces of the approximated quantities.

In the above mentioned three works, the convergence analysis is clearly separated into stability und consistency. Numerical experiments that illustrate and complement the proven theoretical results are given in the three works.

Zusammenfassung

Die vorliegende Arbeit untersucht die numerische Approximation verschiedener partieller *bulk–surface* Differentialgleichungen in zeitabhängigen Gebieten. Das Hauptziel ist eine Anwendung auf ein Modell für Tumorwachstum, welches eine leichte Abwandlung des in Eyles et al. [2019] präsentierten Modells ist. Das Modell koppelt eine Poisson Gleichung in einem zeitabhängigen Gebiet mit einem *forced mean curvature flow* des freien Randes, mit nichttrivialer Kopplung sowohl im Geschwindigkeitsgesetz des Randes als auch in der Randbedingung der Poisson Gleichung.

Bevor wir dieses umfangreiche System von partiellen Differentialgleichungen untersuchen, werden zunächst zwei Resultate über nahe verwandte Systeme ohne Kopplungsterme präsentiert. Zunächst werden in [Edelmann, 2022] Konvergenzergebnisse für finite Elemente angewandt auf eine Diffusionsgleichung in einem zeitabhängigen Gebiet hergeleitet. Die Bewegung des Gebiets ist nur für den Rand explizit gegeben und dann im inneren des Gebiets durch eine harmonische Erweiterung gegeben, d. h. durch die Lösung der Laplace Gleichung. Die schwache Formulierung des Systems wird mit isoparametrischen finiten Elementen mindestens zweiten Grades diskretisiert. Wir formulieren und beweisen H^1-optimale Fehlerschranken für die Semidiskretisierung.

Die zweite Arbeit [Edelmann, 2021] behandelt eine elliptische partielle Differentialgleichung auf einem stationären Gebiet mit verallgemeinerten Robin-Randbedingungen. Diese Randbedingung enthält den Laplace–Beltrami Operator auf der Randfläche des Gebiets. Die schwache Formulierung wird mit finiten Elementen beliebigen Grades diskretisiert und wir beweisen Fehlerschranken, die L^2- und H^1-optimal sind.

Die dritte Arbeit [Edelmann et al., 2024] untersucht das anfangs genannte Modell eines Tumorwachstums. Der Gewebedruck erfüllt eine Poisson Gleichung mit einer inhomogenen Robin-Randbedingung und der freie Rand bewegt sich gemäß einem *forced mean curvature flow*, wobei der *forcing term* durch die Randwerte des Gewebedrucks gegeben ist. Die Analyse dieses Modells benötigt die Resultate und Techniken der vorangegangenen Arbeiten sowie der dort zitierten Literatur. Zusammen mit weiteren Hilfsresultaten werden H^1-optimale Fehlerschranken für die Semidiskretisierung mit *evolving bulk–surface* finiten Elementen vom polynomiellen Grad mindestens zwei bewiesen - in den entsprechenden Sobolevräumen der approximierten Lösungen.

In den drei genannten Papers ist die Konvergenzanalyse klar getrennt in Stabilität und Konsistenz. Numerische Experimente, die die Ergebnisse illustrieren und abrunden, werden jeweils am Ende der Arbeiten präsentiert.

Danksagung

Zuerst möchte ich mich bei meinem Betreuer Prof. Dr. Christian Lubich bedanken. Du hast mir nicht nur die Möglichkeit zur Promotion gegeben, sondern hattest während der gesamten Zeit stets ein offenes Ohr, um bei mathematischen Herausforderungen zu helfen. Ein ganz besonderes Anliegen ist es mir, mich bei Dir für Deine uneingeschränkte Unterstützung und Deinen Rückhalt zu bedanken, auch und insbesondere in Zeiten, die von besonders großen persönlichen und mathematischen Herausforderungen geprägt waren.

Ein ganz besonderer Dank geht an Prof. Dr. Balázs Kovács, von dem ich insbesondere zu Beginn meiner Promotion unglaublich viel gelernt habe. Deine Betreuung und Hilfe zur Einarbeitung in die mathematischen Grundlagen, die zur Entstehung dieser Arbeit beigetragen haben, haben wesentlich zu meiner Wissensbildung und Motivation beigetragen. Außerdem bedanke ich mich für unsere unkomplizierte und produktive Zusammenarbeit bei der Entstehung unserer gemeinsamen Arbeit, welche Teil dieser Dissertation ist.

Wichtige Bestandteile für die Freude und Motivation über einen mehrjährigen Zeitraum sind auch eine gute Atmosphäre und freundliche Kollegen. Ich bedanke mich bei allen Doktoranden und Postdoktoranden, die ich im Laufe meiner Promotionszeit kennen und zu schätzen gelernt habe. Besonders hervorheben möchte ich an dieser Stelle Jörg Nick, Gianluca Ceruti, Dominik Sulz, Yanyan Shi, Bin Wang, Lukas Einkemmer, Hanna Walach, Buyang Li und Guilherme Fiusa. Die regelmäßigen Tee–Runden nach dem Mittagessen mit interessanten Gesprächen über das bestenfalls mittelmäßige Essen in der Mensa, unsere Kulturen, Reisen und in letzter Zeit insbesondere über linguistische Kuriositäten und Feinheiten unserer Muttersprachen waren eine stets geschätzte Abwechslung zur Arbeit mit Bleistift auf Papier und vor dem Bildschirm.

Abschließend möchte ich einen ganz besonderen Dank an meine Familie aussprechen, die mich seit Beginn meines Studiums stets und zuverlässig in allen Lebensbereichen unterstützt hat. Ich danke euch für euren bedingungslosen Rückhalt und eure Begleitung, insbesondere auch in Zeiten persönlicher und gesundheitlicher Krisen.

Contents

1. Introduction

1.1. Related work

Finite element analysis for coupled bulk–surface partial differential equations is a relatively new field in numerical analysis. While finite element methods for partial differential equations of many different types on stationary domains are widely studied, the literature for evolving bulk–surface partial differential equations is scarce. In this section we give a brief summary of the most important related works for this thesis.

In 1988, Dziuk [Dziuk, 1988] developed a linear finite element method for a simple elliptic equation on an arbitrary two-dimensional stationary surface and provided optimal-order error bounds in both H^1- and L^2-norm. This was extended to an algorithm for the mean curvature flow of arbitrary surfaces in [Dziuk, 1990], where the method developed in [Dziuk, 1988] is applied to a two-dimensional surface that moves with a normal velocity that is, at each point, proportional to the mean curvature of the surface at that point. However, a convergence proof was not given.

In [Dziuk and Elliott, 2007a], the authors construct a linear finite element method for parabolic equations on evolving surfaces. A diffusion equation is derived and its weak formulation is discretized in space using evolving surface finite elements. The authors state and prove error bounds that are optimal in H^1-norm, not in L^2-norm. Optimal-order L^2 error bounds were then proved in [Dziuk and Elliott, 2013a].

In [Demlow, 2009], the author defines higher-order surface finite elements for the Laplace–Beltrami problem of [Dziuk, 1988]. Based on a polyhedral approximation of the surface, isoparametric surface finite element spaces of arbitrary polynomial degree are constructed. The author proves optimal-order convergence rates in both H^1- and L^2-norm and thus generalizes the results of [Dziuk, 1988] to surface finite elements of arbitrary polynomial degree.

For an excellent review article on related surface partial differential equations and results up to 2012 we refer to [Dziuk and Elliott, 2013a].

In [Elliott and Ranner, 2013], the authors study a model elliptic problem on a bulk domain coupled to a surface partial differential equation posed on the boundary surface and prove H^1-norm and L^2-norm optimal-order error estimates for finite elements of arbitrary polynomial degree. This work contains crucial geometric estimates that are used frequently throughout this thesis.

In [Kovács, 2018], the results of [Dziuk, 1988], [Demlow, 2009] and [Dziuk and Elliott, 2007a] are generalized to high-order evolving surface finite elements. The setting is as in [Dziuk and Elliott, 2007a] (where linear finite elements are used for spatial discretization) and the results of [Demlow, 2009] are used to prove optimal-order error bounds for evolving surface finite elements of arbitrary polynomial degree.

The results up to this point have in common that either the surface is stationary or that the surface evolution is given explicitly. A crucial next step is done in [Kovács et al., 2017], where a diffusion equation on an evolving surface is considered together with a velocity law coupled to this diffusion equation. With the velocity no longer given explicitly, an additional approximation error arises, which together with the non-trivial couplings makes both the stability and the consistency analysis considerably more challenging. In [Kovács et al., 2020], a convergent evolving finite element algorithm for mean curvature flow of closed surfaces is presented. The techniques developed therein opened up the possibility to analyse geometric surface flows.

The results in this thesis borrow and adapt techniques and results mainly from the works mentioned so far to derive convergence analyses in the respective situations.

1.2. General setting

Throughout this work, we use the following setting: Let $T > 0$ and $t \in [0,T]$. We consider a time-dependent open and bounded domain $\Omega(t)$ with smooth boundary $\Gamma(t) = \partial\Omega(t)$. The initial domain is denoted by $\Omega_0 = \Omega(0)$, so is the boundary surface $\Gamma_0 = \Gamma(0)$. The closure is denoted by $\overline{\Omega(t)} = \Omega(t) \cup \Gamma(t)$. We assume that there exists a smooth map

$$X : \overline{\Omega_0} \to \overline{\Omega(t)} \,, \quad p \mapsto X(p,t)$$

that maps the initial domain $\overline{\Omega_0}$ to $\overline{\Omega(t)}$. It is convenient to think of $\overline{\Omega(t)}$ as a collection of particles, where a particle labeled with $p \in \overline{\Omega_0}$ is at the position $X(p,t) \in \overline{\Omega(t)}$ at time t. The VELOCITY $v(x,t)$ at a point $x = X(p,t)$ is given by

$$v(x,t) = \frac{\partial}{\partial t} X(p,t) \,.$$

We denote the space–time domain Ω_T and space–time surface Γ_T by

$$\Omega_T = \bigcup_{t\in[0,T]} \Omega(t) \cup \{t\} \,, \quad \Gamma_T = \bigcup_{t\in[0,T]} \Gamma(t) \cup \{t\} \,.$$

For a function u defined on Ω_T or Γ_T (or both), the MATERIAL DERIVATIVE at a point $x = X(p,t)$ is denoted by

$$\partial^\bullet u(x,t) = \frac{\mathrm{d}}{\mathrm{d}t} u(X(p,t),t) = \nabla u(x,t) \cdot v(x,t) + \frac{\partial}{\partial t} u(x,t) \,.$$

The notation used for the weak formulation as well as for the discretization is not given here since they slightly differ in each paper.

By $\mathrm{n} = \mathrm{n}(x,t)$ we denote the unit normal vector to $x \in \Gamma(t)$ pointing outside of $\Omega(t)$ and for a function u defined on Γ_T we denote by

$$\partial_\mathrm{n} u(\cdot,t) = \frac{\partial}{\partial \mathrm{n}} u(\cdot,t) = \mathrm{n}(\cdot,t) \cdot \nabla u(\cdot,t)$$

the NORMAL DERIVATIVE of u.

1.3. Summary: Contribution of the papers

In this section, we give a brief summary of the main results contributed by the three papers Edelmann [2022], Edelmann [2021] and Edelmann et al. [2024]. While also being of independent interest, the first two papers can be considered as crucial groundwork for the third paper, which relies on the previous results. In all works, spatial discretization is obtained with (evolving) bulk–surface finite elements, as described down below. For time discretization, we use linearly-implicit backward difference formulae, although the convergence results are only available for the spatial semi-discretization. The three papers are the main part of this thesis and are found below in sections A, B and C.

The first paper [Edelmann, 2022] studies the spatial semi-discretization of a parabolic partial differential equation on an evolving domain $\Omega(t)$. Here, the velocity $v(\cdot,t)$ of the domain is given explicitly only on the boundary surface $\Gamma(t)$ of $\Omega(t)$ and then determined as harmonic extension of the given boundary velocity. The main challenge is to bound the errors in the diffusion equation in terms of the position errors of the moving mesh. We provide H^1-optimal-order error estimates for finite elements of polynomial degree at least 2.

The second paper [Edelmann, 2021] studies the discretization of an elliptic partial differential equation on a (stationary) domain Ω endowed with a generalized Robin boundary condition. The challenge here, compared with previous related works, is to generalize the results from *conforming* finite elements (where the finite element space is a subspace of the space of the weak solution) to *non-conforming* finite elements (where the finite element space no longer is a subspace of the weak solution space) and to take the regularity of the weak solution into account. We provide optimal-order error estimates in both L^2- and H^1-norm for finite elements of arbitrary polynomial degree.

The third paper [Edelmann et al., 2024] studies the spatial discretization of a system of partial differential equations which are a model of tumour growth. This model was proposed in [Eyles et al., 2019] and is slightly modified in this thesis. The velocity of the domain and its boundary are no longer given explicitly. Instead, the boundary velocity satisfies a forced mean curvature flow with the trace of the tissue pressure being the forcing term. The tissue pressure is determined by a Robin boundary value problem in the evolving bulk. The main challenges here are the non-trivial couplings, which lead to a sophisticated stability analysis, as well as the consistency analysis, where different interpolation operators and Ritz maps are needed for all of the unknown quantities. We provide error estimates for finite elements of polynomial degree at least two, which are optimal in the H^1-norms of the respective Sobolev spaces.

1.3.1. Finite element analysis for a diffusion equation on a harmonically evolving domain

The first paper [Edelmann, 2022] studies the evolving finite element spatial semi-discretization of a diffusion equation on a time-dependent domain $\Omega(t)$. The diffusion equation for a scalar quantity $u(\cdot,t)$ on $\Omega(t)$ endowed with a Neumann boundary condition is given by

$$\begin{cases} \partial^\bullet u(x,t) + u(x,t)\nabla\cdot v(x,t) - \beta\Delta u(x,t) = f(x,t) & \text{in} \quad \Omega(t)\,, \\ \qquad\qquad \dfrac{\partial}{\partial \mathrm{n}} u(x,t) = g(x,t) & \text{on} \quad \Gamma(t)\,, \end{cases}$$

where f and g are given functions defined on Ω_T and Γ_T, respectively, and $\beta > 0$ is a given constant. The velocity v of $\Omega(t)$ and $\Gamma(t)$ is not given explicitly, instead, the velocity $v_\Gamma = v|_\Gamma$ of the boundary surface $\Gamma(t)$ is given, and the inner velocity $v(\cdot, t)$ in $\Omega(t)$ is determined as the harmonic extension of v_Γ, that is the solution to the Laplace equation:

$$\begin{cases} -\Delta v(\cdot, t) = 0 & \text{in} \quad \Omega(t)\,, \\ \quad v(\cdot, t) = v_\Gamma(\cdot, t) & \text{on} \quad \Gamma(t)\,. \end{cases}$$

Various applications and related works are listed in the introduction of the paper, see Section A.1. We state and prove optimal-order H^1-norm error bounds for the spatial semi-discretization with finite elements of polynomial degree at least two, which hold true in the two- and three-dimensional case. These restrictions are due to an $\mathcal{O}(h^{k-n/2})$-type inverse estimate in the stability analysis, where k is the polynomial degree of the finite elements and n is the spatial dimension. This can only be bound for $k - \frac{n}{2} > 0$ as $h \to 0$. In numerical experiments, we observe the expected optimal order in the case of linear finite elements as well, however with the presented techniques this can not be proved. The convergence result is stated in Theorem A.4.1. The proof is clearly separated into stability and consistency, with geometric arguments only entering the consistency part. The stability analysis is first done for the partial differential equation describing the motion of the domain and then extended to the parabolic equation, see Remark A.2.1. Numerical experiments are provided.

1.3.2. Isoparametric finite element analysis of a generalized Robin boundary value problem on curved domains

The second paper [Edelmann, 2021] studies the finite element discretization of an elliptic partial differential equation on a stationary domain with smooth boundary. We consider the following second-order partial differential equation endowed with a boundary condition that includes the Laplace–Beltrami operator:

$$\begin{cases} -\Delta u + \kappa u = f & \text{in} \quad \Omega\,, \\ \dfrac{\partial}{\partial \mathrm{n}} u + \alpha u - \beta \Delta_\Gamma u = g & \text{on} \quad \Gamma = \partial\Omega\,, \end{cases}$$

where $\alpha > 0, \beta > 0$ and $\kappa \geq 0$ are given constants and f and g are given functions on Ω and Γ, respectively. The results given in the paper can be considered as generalization of the results in [Kashiwabara et al., 2015], where existence and regularity results are provided for a similar boundary value problem, yet the convergence analysis therein only holds true for conforming finite elements, which is restrictive for domains with curved boundaries.

We give L^2- and H^1-optimal-order error estimates for isoparametric finite elements of arbitrary polynomial degree. As opposed to the previous paper, we do not need the restriction for the finite element spaces to be at least of second polynomial degree. This is due to the boundary value problem being stationary, so an inverse estimate in the stability analysis is not required. The proof is separated into stability and consistency. The regularity of the solution is taken into account in the consistency part. A two and a three-dimensional numerical example are provided.

1.3.3. Numerical Analysis of an evolving bulk–surface model of tumour growth

The third paper [Edelmann et al., 2024] studies an evolving bulk–surface finite element method for a model of tumour growth. Eyles, King and Styles [Eyles et al., 2019] recently proposed a model that couples a Poisson equation for the *tissue pressure* $u(\cdot,t)$ in the domain with a forced mean curvature flow of the boundary. The tissue pressure is the solution of the boundary value problem

$$\begin{cases} -\Delta u = -1 & \text{in} \quad \Omega(t)\,, \\ \dfrac{\partial}{\partial \mathrm{n}} u + \alpha u = \beta H + Q & \text{on} \quad \Gamma(t)\,, \end{cases} \tag{1.3.1}$$

where $\alpha > 0$ and $\beta > 0$ are given constants, $H(\cdot,t)$ is the mean curvature of $\Gamma(t)$ and $Q(\cdot,t)$ is a given surface source term. The velocity of the free boundary surface $\Gamma(t)$ is determined by a forced mean curvature flow, that is

$$v_\Gamma = V\mathrm{n}\,, \quad \text{with} \quad V = -\beta H + \alpha u \quad \text{on} \quad \Gamma(t)\,. \tag{1.3.2}$$

These equations are strongly coupled through the appearance of both $u(\cdot,t)$ as forcing term in the mean curvature flow and of $H(\cdot,t)$ as a source term in the boundary condition.

It is shown in [Kovács et al., 2020, Lemma 2.1] that for a surface evolving under forced mean curvature flow (1.3.2), the mean curvature and surface normal satisfy the following parabolic evolution equations:

$$\begin{cases} \partial^\bullet \mathrm{n} = \beta \Delta_\Gamma \mathrm{n} + \beta |A|^2 \mathrm{n} - \alpha \nabla_\Gamma u & \text{on} \quad \Gamma(t)\,, \\ \partial^\bullet H = \beta \Delta_\Gamma H + \beta |A|^2 H - \alpha \Delta_\Gamma u - \alpha\, |A|^2 u & \text{on} \quad \Gamma(t)\,. \end{cases} \tag{1.3.3}$$

For the finite element method, a moving mesh is required not only for the boundary surface $\Gamma(t)$ but also for $\Omega(t)$ in order to solve the above Robin boundary value problem for the tissue pressure u. To achieve this, we extend the velocity v_Γ harmonically into $\Omega(t)$:

$$\begin{cases} -\Delta v = 0 & \text{in} \quad \Omega(t)\,, \\ v = v_\Gamma & \text{on} \quad \Gamma(t)\,. \end{cases} \tag{1.3.4}$$

In view of the term $\Delta_\Gamma u$ in (1.3.3), we need the trace γu of u on $\Gamma(t)$ to be in $H^1(\Gamma(t))$ with controlled norm in the exact and numerical solution as well as in the approximation error. This cannot be ensured for the original Eyles–King–Styles model with the boundary condition (1.3.1). To overcome this, we add a regularization term to the boundary condition:

$$\frac{\partial}{\partial \mathrm{n}} u + \alpha u - \mu \Delta_\Gamma u = \beta H + Q \quad \text{on} \quad \Gamma(t)\,, \tag{1.3.5}$$

with a constant $\mu > 0$. It is shown in [Kashiwabara et al., 2015] that the solution u to (1.3.1) with boundary condition (1.3.5) has higher regularity on the boundary. We will show that with this added regularization term, we can control the $H^1(\Gamma(t))$ norm of the numerical error in γu. In Section C.4.5, we give a brief explanation why with the presented techniques, we see no way to achieve this bound without adding this regularization term.

The collected equations are listed in Section C.2.2.5. The weak formulation of these equations is discretized to obtain approximations to H and n which then are used to obtain an approximate surface velocity v and an approximation to u.

We state and prove optimal-order H^1-norm error bounds for all approximated quantities for bulk–surface finite elements of polynomial degree $k \geq 2$. The order restriction is again due to the use of inverse estimates in the stability analysis. The convergence proof is clearly separated into stability and consistency. We provide numerical experiments to illustrate the proven convergence rate and to study the dependence of the solution on the parameters α, β and μ.

A. Finite element analysis for a diffusion equation on a harmonically evolving domain

This chapter is identical to the paper [Edelmann, 2022] with the same title. An exception are citations, which are updated to the most recent versions of the cited papers. This work was first submitted in August 2019 and, after a major revision, got accepted in May 2021.

Abstract. We study convergence of the evolving finite element semi-discretization of a parabolic partial differential equation on an evolving bulk domain. The boundary of the domain evolves with a given velocity, which is then extended to the bulk by solving a Poisson equation. The numerical solution to the parabolic equation depends on the numerical evolution of the bulk, which yields the time-dependent mesh for the finite element method. The stability analysis works with the matrix–vector formulation of the semi-discretization only and does not require geometric arguments, which are then required in the proof of consistency estimates. We present various numerical experiments that illustrate the proven convergence rates.

A.1. Introduction

This paper studies the numerical discretization of a diffusion equation in a time-dependent domain that is specified by the velocity of its boundary. The interior velocity is determined as the solution of a Laplace equation with the given boundary velocity as Dirichlet data.

The strong formulation of this model is to find the time-dependent domain $\Omega(t) \subset \mathbb{R}^n$ ($n = 2, 3$), $t \in [0, T]$, which moves with a velocity v that is the harmonic extension of the a priori given velocity v^Γ of the boundary $\Gamma(t) = \partial\Omega(t)$. That is, v is not given explicitly but determined as the solution of the Laplace equation, for all $t \in [0, T]$,

$$-\Delta v(x,t) = 0\,, \qquad x \in \Omega(t)\,, \tag{A.1.1a}$$

$$v(x,t) = v^\Gamma(x,t)\,, \qquad x \in \Gamma(t)\,. \tag{A.1.1b}$$

In $\Omega(t)$ we seek a solution $u = u(x,t)$ with given initial data $u(\cdot, 0) = u_0$ to the partial differential equation

$$\partial^\bullet u(x,t) + u(x,t)\nabla \cdot v(x,t) - \beta\Delta u(x,t) = f(x,t)\,, \;\; x \in \Omega(t)\,, \;\; t \in [0,T]\,, \tag{A.1.2}$$

where $\partial^\bullet$ denotes the material derivative, $\nabla\cdot v$ is the divergence of the velocity and $\beta > 0$ is a given diffusion coefficient. On the boundary, we impose the Neumann condition $\frac{\partial u}{\partial \mathrm{n}}(x,t) = g(x,t)$, $x \in \Gamma(t)$, $t \in [0,T]$, where n denotes the unit outward pointing normal to $\Gamma(t)$.

Convection–diffusion equations in time-dependent domains have gained considerable interest in the past decades. A model similar to (A.1.2) (without (A.1.1)) with an additional convection

term, together with homogeneous Dirichlet boundary conditions is analyzed in Badia and Codina [2006] and Boffi and Gastaldi [2004] in an arbitrary Lagrangian–Eulerian (ALE) framework, where the velocity is determined by the ALE mapping. In Boffi and Gastaldi [2004], the velocity of the boundary is prescribed and the ALE mapping is constructed as the harmonic extension of the boundary positions. This approach is first proposed in Formaggia and Nobile [1999] in the context of a generic conservation law on a moving domain, see also Gastaldi [2001], Formaggia and Nobile [2004] and the references therein.

Diffusion equations on evolving surfaces are analyzed in Dziuk and Elliott [2007a,b, 2013a] for a given velocity, and there are recent works, where the velocity is not given explicitly but determined by various velocity laws that depend on the solution of the diffusion equation on the surface, see Kovács et al. [2017], Kovács and Lubich [2018], Kovács et al. [2020].

Of particular interest is Eyles et al. [2019], where a bulk–surface model for tissue growth is presented, together with a numerical algorithm. Instead of the coupled system (A.1.1)–(A.1.2), in [Eyles et al., 2019, (1.1)–(1.3) & Section 6.1.2] they consider the boundary velocity

$$v^\Gamma = \frac{u}{\alpha} + \beta H\,, \tag{A.1.3}$$

and instead of (A.1.2) they consider an elliptic boundary value problem in the moving bulk. Here H denotes the mean curvature of the boundary surface and α, β are given positive constants.

Through the numerical analysis of the problem with a given boundary velocity (A.1.1)–(A.1.2) we will develop techniques which are expected to be essential for the more involved tumor growth model of Eyles et al. [2019]. However the stability and error analysis of this free boundary value problem is beyond the scope of this paper, see the forced mean curvature flow problem in Kovács et al. [2020].

In this paper, we prove error bounds for the spatial semi-discretization of the coupled problem (A.1.1)–(A.1.2) with isoparametric finite elements of polynomial degree at least two. More precisely, we show H^1-norm error bounds in the positions and the velocity v that are uniform in time, and $L^\infty L^2$ norm and $L^2 H^1$ norm error bounds for the solution u of the diffusion equation. The proof clearly separates the stability and consistency analysis. To prove stability of the semi-discrete equations, we adapt techniques recently used in Kovács et al. [2017], Kovács [2018] to the present situation. The stability analysis of the semi-discrete problems use energy estimates. Transport formulae are used to relate mass and stiffness matrices corresponding to different discrete domains. In order to estimate errors between these matrices on different domains, a key issue is to control the $W^{1,\infty}$-norm of the position error uniformly in time. This is done with an inverse estimate, that yields an $\mathcal{O}(h^{k-n/2})$ bound uniformly in time, which is small only for $k \geq 2$. The stability analysis of the semi-discrete diffusion equation uses the same techniques and is based on the stability analysis of the semi-discrete velocity law. Moreover, it becomes clear how the position error affects the error in the numerical solution to (A.1.2).

The stability analysis relies on smallness assumptions on the defects. These are shown to be true in the following consistency analysis, that uses geometric approximation estimates and interpolation results. The final convergence result is then obtained by combining stability and consistency estimates together with interpolation error bounds.

The paper is organized as follows.

In Section A.2 we recall basic notation and formulate a diffusion equation on an evolving domain together with the above velocity law. We derive the weak formulation.

In Section A.3 we describe the high-order evolving finite element approximation of the problem. After introducing an *exact triangulation* of the curved domain, we define the computational domain and the finite element method. We describe the spatial semi-discretization and derive a matrix–vector formulation, which will be crucial for the stability analysis.

In Section A.4 we state the main result of the paper, which gives convergence estimates for the spatial semi-discretization with evolving isoparametric finite elements of polynomial degree at least 2. We outline the main ideas of the proof.

In Section A.5 we collect auxiliary results that will be needed for the following analysis. The first part deals with the evolving mass and stiffness matrices and their properties, which are crucial in the stability analysis. The second part collects geometric estimates which will be needed only for consistency analysis.

Section A.6 analyses the stability of the semi-discrete velocity law without a diffusion equation on the evolving domain. In Section A.7, we extend the stability analysis to the semi-discrete diffusion equation. Section A.8 contains the consistency analysis, that is, estimating the defects obtained on inserting the interpolated exact solutions into the numerical scheme.

In Section A.9 we prove the main convergence result by combining the stability and consistency estimates. Section A.10 provides several numerical experiments which illustrate the theoretical results.

A.2. Problem formulation

A.2.1. Basic notation

For $t \in [0,T]$, let $\Omega(t) \subseteq \mathbb{R}^n$ $(n = 2, 3)$ be an open bounded and connected set with smooth boundary $\Gamma(t) = \partial\Omega(t)$ and $\Omega_0 = \Omega(0)$, $\Gamma_0 = \Gamma(0)$. We denote $\overline{\Omega(t)} = \Omega(t) \cup \Gamma(t)$. We assume that there exists a sufficiently smooth map $X : \Omega_0 \cup \Gamma_0 \times [0,T] \to \mathbb{R}^n$ such that

$$\Omega(t) = \{X(p,t) : p \in \Omega_0\}\,, \quad \Gamma(t) = \{X(p,t) : p \in \Gamma_0\}\,.$$

The velocity $v(x,t)$ at a point $x = X(p,t) \in \overline{\Omega(t)}$ is defined by

$$v(X(p,t),t) = \frac{\partial}{\partial t} X(p,t)\,.$$

For a function $u = u(x,t)$, $x \in \overline{\Omega(t)}$, $t \in [0,T]$, the material derivative at $x = X(p,t)$ is defined by

$$\partial^\bullet u(x,t) = \frac{\mathrm{d}}{\mathrm{d}t} u(X(p,t),t) = \frac{\partial}{\partial t} u(x,t) + \nabla u(x,t) \cdot v(x,t)\,. \tag{A.2.1}$$

For $x \in \Gamma(t)$, we denote by $\mathrm{n} = \mathrm{n}(x,t)$ the unit outward pointing normal to $\Gamma(t)$. We define the space–time domain Ω_T and the space–time surface Γ_T by

$$\Omega_T = \bigcup_{t\in[0,T]} \Omega(t) \times \{t\}\,, \quad \Gamma_T = \bigcup_{t\in[0,T]} \Gamma(t) \times \{t\}\,. \tag{A.2.2}$$

For functions φ, ψ defined on $\Omega(t)$, we have bilinear forms

$$\begin{aligned} m(\varphi, \psi) &= \int_{\Omega(t)} \varphi\psi \mathrm{d}x\,, \\ a(\varphi, \psi) &= \int_{\Omega(t)} \nabla\varphi \cdot \nabla\psi \mathrm{d}x\,. \end{aligned} \tag{A.2.3}$$

Note that these bilinear forms explicitly depend on t, but we will omit the argument t, for brevity. It will always be clear from context for which $t \in [0, T]$ the bilinear forms are evaluated.

A.2.2. Diffusion equation

We assume that $u = u(\cdot, t)$ is the density of a scalar quantity on $\Omega(t)$ (for example, mass per unit volume). We follow a construction of [Dziuk and Elliott, 2007a, Section 3] to obtain a diffusion equation with Neumann boundary conditions:

$$\begin{cases} \partial^\bullet u + u\nabla \cdot v - \beta\Delta u = f & \text{in} \quad \Omega(t)\,, \\ \dfrac{\partial u}{\partial \mathrm{n}} = \nabla u \cdot \mathrm{n} = g & \text{on} \quad \Gamma(t)\,, \end{cases} \tag{A.2.4}$$

where $\nabla \cdot v$ denotes the divergence of the velocity, $\beta > 0$ is a given diffusion coefficient and n the unit outward pointing normal to $\Gamma(t)$.

A.2.3. Harmonic velocity law

Contrary to existing works (cf. Elliott and Ranner [2021]), the velocity $v(\cdot, t)$ of $\Omega(t)$ is not given explicitly. Instead, only the velocity of the boundary $\Gamma(t) = \partial\Omega(t)$ is given; the velocity of the bulk is then determined as the harmonic extension, i.e. as the solution to the Laplace equation. More precisely, we have the following differential equation for $v(x, t)$: for each $t \in [0, T]$

$$\begin{cases} -\Delta v(\cdot, t) = 0 & \text{in} \quad \Omega(t)\,, \\ v(\cdot, t) = v^\Gamma(\cdot, t) & \text{on} \quad \Gamma(t)\,. \end{cases} \tag{A.2.5}$$

We assume that v^Γ is defined on a neighborhood of Γ_T, as defined in (A.2.2). This system is considered together with the position ODEs: for each $p \in \overline{\Omega(0)}$

$$\begin{cases} \dfrac{\mathrm{d}}{\mathrm{d}t} X(p, t) = v(X(p, t), t)\,, \\ X(p, 0) = p\,. \end{cases}$$

We consider an equivalent problem with homogeneous Dirichlet boundary conditions: assume that $v^\Gamma(\cdot, t)$ is the trace of a given function $w(\cdot, t) \in H^1(\Omega(t))^n$ and consider the equivalent problem: find $\widetilde{v}(\cdot, t) \in H^1_0(\Omega(t))^n$ such that

$$\begin{cases} -\Delta\widetilde{v}(\cdot, t) = \Delta w(\cdot, t) & \text{in} \quad \Omega(t)\,, \\ \widetilde{v}(\cdot, t) = 0 & \text{on} \quad \Gamma(t)\,. \end{cases} \tag{A.2.6}$$

It is easily seen that the solution $v = \widetilde{v} + w$ to (A.2.5) does not depend on the choice of w.

A.2.4. Coupled problem: strong and weak formulation

We consider the following system of partial differential equations: for given $\beta > 0$, $f : \mathbb{R}^n \times [0,T] \to \mathbb{R}$, $g : \mathbb{R}^n \times [0,T] \to \mathbb{R}$ and $v^\Gamma : \mathbb{R}^n \times [0,T] \to \mathbb{R}^n$, find the unknown function $u : \Omega_T \to \mathbb{R}$, the unknown velocity field $v : \Omega_T \to \mathbb{R}^n$ and the unknown position function $X : \Omega_0 \cup \Gamma_0 \times [0,T] \to \mathbb{R}^n$ such that for all $t \in [0,T]$

$$\begin{cases} \partial^\bullet u(\cdot,t) + u(\cdot,t)\nabla \cdot v(\cdot,t) - \beta \Delta u(\cdot,t) = f(\cdot,t) & \text{in} \quad \Omega(t)\,, \\ \dfrac{\partial u}{\partial \mathrm{n}}(\cdot,t) = g(\cdot,t) & \text{on} \quad \Gamma(t)\,, \\ \dfrac{\mathrm{d}X}{\mathrm{d}t}(\cdot,t) = v(X(\cdot,t),t) & \text{in} \quad \Omega_0 \cup \Gamma_0\,, \\ -\Delta v(\cdot,t) = 0 & \text{in} \quad \Omega(t)\,, \\ v(\cdot,t) = v^\Gamma(\cdot,t) & \text{on} \quad \Gamma(t)\,. \end{cases} \tag{A.2.7}$$

Without loss of generality, we assume $\beta = 1$ and $g \equiv 0$ in the following.

Remark A.2.1. *The last three equations of* (A.2.7) *purely describe the motion of the domain* $\Omega(t)$ *and are independent of the parabolic equation for* u*. The latter includes the velocity* v *in the material derivative as well as the divergence of the velocity in the equation. This is reflected in the stability analysis, which is first done for the discretization of the domain motion, and then extended to the parabolic equation. On the other hand, if the velocity field* v *was given for the whole domain, the finite element analysis for the parabolic equation alone would be remarkably easier. Convergence results for these types of problems with given velocity are found in [Elliott and Ranner, 2021, Section 8].*

We now derive a weak formulation. By multiplying the first equation with an arbitrary test function $\varphi \in H^1(\Omega(t))$ such that $\partial^\bullet \varphi$ exists in $L^2(\Omega(t))$, integrating over $\Omega(t)$, using the Leibniz formula, Green's formula and the Neumann boundary condition, we arrive at

$$\frac{\mathrm{d}}{\mathrm{d}t}\int_{\Omega(t)} u\varphi + \int_{\Omega(t)} \nabla u \cdot \nabla \varphi = \int_{\Omega(t)} f\varphi + \int_{\Omega(t)} u\partial^\bullet \varphi\,.$$

Multiplying (A.2.6) with arbitrary test function $\psi \in H_0^1(\Omega(t))^n$, integrating over $\Omega(t)$ and using Green's formula, we obtain

$$\int_{\Omega(t)} \nabla \widetilde{v} \cdot \nabla \psi = -\int_{\Omega(t)} \nabla w \cdot \nabla \varphi\,,$$

where we have used that the boundary integrals vanish thanks to $\psi \in H_0^1(\Omega(t))^n$. Here, the dot denotes the Euclidean inner product of the vectorizations of the matrices, i.e. the Frobenius norm inner product of the matrices. Again, it can be shown that the weak solution $v = \widetilde{v} + w$ does not depend on w.

The weak formulation of the diffusion equation and the domain evolution thus reads: find $u(\cdot,t) \in H^1(\Omega(t))$, $\widetilde{v}(\cdot,t) \in H_0^1(\Omega(t))^n$ such that for all $\varphi \in H^1(\Omega(t))$ with $\partial^\bullet \varphi \in L^2(\Omega(t))$,

$\psi \in H_0^1(\Omega(t))^n$ and all $t \in [0,T]$

$$\begin{aligned} \frac{\mathrm{d}}{\mathrm{d}t}\int_{\Omega(t)} u\varphi + \int_{\Omega(t)} \nabla u \cdot \nabla \varphi &= \int_{\Omega(t)} f\varphi + \int_{\Omega(t)} u\partial^\bullet \varphi \,, \\ \int_{\Omega(t)} \nabla \widetilde{v} \cdot \nabla \psi &= -\int_{\Omega(t)} \nabla w \cdot \nabla \psi \,, \\ v &= \widetilde{v} + w \,, \\ \frac{\mathrm{d}X}{\mathrm{d}t} &= v \,. \end{aligned} \tag{A.2.8}$$

This is considered together with given initial data $u(\cdot,t) = u_0(\cdot)$, $X(\cdot,0) = Id$.

We assume throughout the paper that there exists a unique weak solution with sufficiently high Sobolev regularity on $[0,T]$. Precise regularity assumptions will be given in Theorem A.4.1.

From now on, we will be working in the more technically challenging three-dimensional case. All of the upcoming results are valid in the two-dimensional case as well.

A.3. Evolving bulk finite elements

In this section we briefly recall the evolving isoparametric finite element method which is used for semi-discretization in space. We refer to Elliott and Ranner [2013, 2021] for a more detailed introduction into the construction of isoparametric finite elements.

In the following, we denote $\Omega_0 = \Omega(0)$ for brevity. The initial domain Ω_0 is triangulated and the nodes are then evolved in time by solving the position ODE $\dot{x}_i = v(x_i,t)$ in each node, together with (A.2.5).

A.3.1. High-order domain approximation

We construct a triangulation $\mathcal{T}_h^{(1)}$ of Ω_0 consisting of closed simplices with maximal diameter h. The union of all simplices of $\mathcal{T}_h^{(1)}$ defines a polyhedral approximation Ω_h of Ω_0, whose boundary $\Gamma_h = \partial\Omega_h$ is an interpolation of Γ_0.

Each simplex $T \in \mathcal{T}_h^{(1)}$ corresponds to a curved simplex $T^{\mathrm{c}} \subset \Omega$, which is parametrized over the unit simplex $\widehat{T}$ with a map $\Phi_T^{\mathrm{c}} = \Phi_T + \rho_T$. Here, Φ_T denotes the usual affine function that maps $\widehat{T}$ onto T. For the construction of an appropriate ρ_T, we refer to Elliott and Ranner [2013]. The union of those curved simplices can be considered as an *exact triangulation* of Ω_0. Using the map Φ_T^{c}, we can define an isoparametric mapping $\Phi_T^{(k)}$, that maps the unit simplex $\widehat{T}$ to a polynomial simplex $T^{(k)}$. $\Omega_h^{(k)}$ is then defined as the union of elements in $\mathcal{T}_h^{(k)}$, where

$$\mathcal{T}_h^{(k)} := \{T^{(k)} : T \in \mathcal{T}_h^{(1)}\}\,, \quad T^{(k)} := \{\Phi_T^{(k)}(\widehat{x}) : \widehat{x} \in \widehat{T}\}\,.$$

A.3.2. Evolving finite element method

Here and in the following, we use the notational convention that vectors and matrices are denoted with bold-face letters. As mentioned, we set $n = 3$ and assume that the order $k \geq 2$ is fixed.

Based on the previous subsection, we obtain a triangulation of Ω_0, whose nodes $x_1^0, \dots, x_N^0$ are collected in a vector $\mathbf{x}^0 = (x_1^0, \dots, x_N^0) \in \mathbb{R}^{3N}$. We assume that the enumeration is such that exactly the first N_Γ nodes lie on the boundary $\Gamma_0 = \partial\Omega_0$. The nodes are evolved in time and collected in a vector $\mathbf{x}(t) = (x_1(t), \dots, x_N(t))$ with $\mathbf{x}(0) = \mathbf{x}^0$. We use the notation

$$\mathbf{x}(t) = \begin{pmatrix} \mathbf{x}^\Gamma(t) \\ \mathbf{x}^\Omega(t) \end{pmatrix}$$

to indicate which nodes live on the boundary. The nodal vector $\mathbf{x} = \mathbf{x}(t)$ defines a computational domain $\Omega_h(\mathbf{x}) = \Omega_h(\mathbf{x}(t))$ with boundary $\Gamma_h(\mathbf{x})$. The finite element basis functions $\varphi_j(\cdot, t) : \Omega_h(\mathbf{x}(t)) \to \mathbb{R}$ satisfy

$$\varphi_j(x_k(t), t) = \delta_{jk}\,, \quad 1 \le j, k \le N\,,$$

and their pullback to the reference triangle is polynomial of degree k. Note that, since the velocity is not given explicitly, we are in general not able to find the exact positions $x_j^*(t) = X(x_j^0, t)$, so that $\Omega_h(\mathbf{x}(t))$ is *not* the triangulation of $\Omega(t)$ corresponding to the exact positions $X(x_j^0, t)$. It is therefore more convenient to denote the dependence on $\mathbf{x}$ instead of t, i.e. to write $\Omega_h(\mathbf{x})$ and not $\Omega_h(t)$, etc.

The finite element space is now given as

$$S_h(\mathbf{x}) = \operatorname{span}\{\varphi_1[\mathbf{x}], \dots, \varphi_N[\mathbf{x}]\}\,,$$

where $\varphi_j[\mathbf{x}](\cdot) = \varphi_j(\cdot, t)$ for $\mathbf{x} = \mathbf{x}(t)$.

We use the notation

$$S_{0,h}(\mathbf{x}) = \{\varphi_h[\mathbf{x}] \in S_h(\mathbf{x}) : \gamma_h\varphi_h[\mathbf{x}] = 0\} = \operatorname{span}\{\varphi_{N_\Gamma+1}(\mathbf{x}), \dots, \varphi_N[\mathbf{x}]\}\,,$$

where $\gamma_h\varphi_h$ denotes the trace of a function φ_h defined on $\Omega_h(\mathbf{x})$ on $\Gamma_h(\mathbf{x})$. We set

$$X_h(p_h, t) = \sum_{j=1}^N x_j(t)\varphi_j[\mathbf{x}(0)](p_h)\,, \quad p_h \in \Omega_h^0 \cup \Gamma_h^0\,,$$

which has the properties that $X_h(x_k^0, t) = x_k(t)$ and $X_h(x_j^0, 0) = x_j^0$, implying that $X_h(x, 0) = x$ for all $x \in \Omega_h^0 \cup \Gamma_h^0$. The discrete velocity $v_h(x, t)$ at a particle $x = X_h(p_h, t)$ is given by

$$v_h(X_h(p_h, t), t) = \frac{\mathrm{d}}{\mathrm{d}t} X_h(p_h, t)\,.$$

The basis functions satisfy the transport property

$$\frac{\mathrm{d}}{\mathrm{d}t}\left(\varphi_j[\mathbf{x}(t)](X_h(p_h, t))\right) = 0\,, \tag{A.3.1}$$

which implies $\varphi_j[\mathbf{x}(t)](X_h(p_h, t)) = \varphi_j[\mathbf{x}(0)](p_h)$. For the discrete velocity, this means

$$\begin{aligned} v_h(x, t) = v_h(X_h(p_h, t), t) &= \frac{\mathrm{d}}{\mathrm{d}t} \sum_{j=1}^N x_j(t)\varphi_j[\mathbf{x}(0)](p_h) \\ &= \sum_{j=1}^N v_j(t)\varphi_j[\mathbf{x}(t)](x) \text{ with } v_j = \dot{x}_j\,. \end{aligned}$$

In particular, $v_h(\cdot,t) \in S_h(\mathbf{x}(t))$. For a finite element function

$$u_h(x,t) = \sum_{j=1}^{N} u_j(t)\varphi_j[\mathbf{x}(t)](x) \;,$$

the discrete material derivative at $x = X_h(p_h,t)$ is defined by

$$\partial_h^\bullet u_h(x,t) = \frac{\mathrm{d}}{\mathrm{d}t} u_h(X_h(p_h,t),t) = \sum_{j=1}^{N} \dot{u}_j(t)\varphi_j[\mathbf{x}(t)](x)\,,$$

where we have used the transport property again. In particular: $\partial_h^\bullet u_h(\cdot,t) \in S_h(\mathbf{x}(t))$.

A.3.3. Spatial semi-discretization and matrix–vector formulation

The evolving finite element discretization of (A.2.8) reads: find the unknown position vector $\mathbf{x}(t) \in \mathbb{R}^{3N}$ and the unknown finite element functions $u_h(\cdot,t) \in S_h(\mathbf{x}(t))$, $\widetilde{v}_h(\cdot,t) \in S_{0,h}(\mathbf{x}(t))^3$ such that for all $\varphi_h(\cdot,t) \in S_h(\mathbf{x}(t))$ with $\partial_h^\bullet \varphi_h \in S_h(\mathbf{x}(t))$ and all $\psi_h(\cdot,t) \in S_{0,h}(\mathbf{x}(t))^3$

$$\begin{aligned} \frac{\mathrm{d}}{\mathrm{d}t}\int_{\Omega_h(\mathbf{x}(t))} u_h\varphi_h + \int_{\Omega_h(\mathbf{x}(t))} \nabla u_h\cdot\nabla\varphi_h &= \int_{\Omega_h(\mathbf{x}(t))} f\varphi_h + \int_{\Omega_h(\mathbf{x}(t))} u_h\partial_h^\bullet\varphi_h\,, \\ \int_{\Omega_h(\mathbf{x}(t))} \nabla\widetilde{v}_h\cdot\nabla\psi_h &= -\int_{\Omega_h(\mathbf{x}(t))} \nabla w_h\cdot\nabla\psi_h\,, \end{aligned} \tag{A.3.2}$$

together with

$$\frac{\partial}{\partial t} X_h(p_h,t) = v_h(X_h(p_h,t),t)\,, \quad X_h(p_h,0) = p_h\,,$$

for $p_h \in \Omega_h^0 \cup \Gamma_h^0$, where $v_h = \widetilde{v}_h + w_h$. The initial values for the nodal vector $\mathbf{u}$ corresponding to $u_h(\cdot,0)$ and the nodal vector $\mathbf{x}(0)$ are taken as the exact initial values of the nodes x_j^0 of the initial triangulation of Ω_0:

$$u_j(0) = u(x_j^0,0)\,, \quad x_j(0) = x_j^0 \quad (j=1,\dots,N)\,. \tag{A.3.3}$$

We now show that the nodal vectors $\mathbf{u} \in \mathbb{R}^N$ and $\mathbf{v} \in \mathbb{R}^{3N}$ corresponding to the finite element functions u_h and v_h, respectively, together with the position vector $\mathbf{x} \in \mathbb{R}^{3N}$ satisfy a system of differential equations. We set (omitting the omnipresent argument t)

$$u_h = \sum_{j=1}^{N} u_j\varphi_j[\mathbf{x}]\,, \quad v_h = \sum_{j=1}^{N} v_j\varphi_j[\mathbf{x}]$$

with $u_j \in \mathbb{R}$, $v_j \in \mathbb{R}^3$ and collect the nodal values in vectors $\mathbf{u} \in \mathbb{R}^N$, $\mathbf{v} \in \mathbb{R}^{3N}$. The domain-dependent mass and stiffness matrices $\mathbf{M}(\mathbf{x})$ and $\mathbf{A}(\mathbf{x})$ are defined by

$$\begin{aligned} \mathbf{M}(\mathbf{x})_{jk} &= \int_{\Omega_h(\mathbf{x})} \varphi_j[\mathbf{x}]\varphi_k[\mathbf{x}]\mathrm{d}x\,, \\ \mathbf{A}(\mathbf{x})_{jk} &= \int_{\Omega_h(\mathbf{x})} \nabla\varphi_j[\mathbf{x}]\cdot\nabla\varphi_k[\mathbf{x}]\mathrm{d}x\,. \end{aligned}$$

In view of the following discretization of the velocity law, we use the notation

$$\mathbf{A}(\mathbf{x}) = \begin{pmatrix} \mathbf{A}_{11}(\mathbf{x}) & \mathbf{A}_{12}(\mathbf{x}) \\ \mathbf{A}_{21}(\mathbf{x}) & \mathbf{A}_{22}(\mathbf{x}) \end{pmatrix},$$

where $\mathbf{A}_{11}(x) \in \mathbb{R}^{N_\Gamma \times N_\Gamma}$ and $\mathbf{A}_{22}(\mathbf{x}) \in \mathbb{R}^{N_\Omega \times N_\Omega}$. $\mathbf{A}_{22}(\mathbf{x})$ thus corresponds to the finite element functions which vanish on the boundary. We will use the same notation for $\mathbf{M}(\mathbf{x})$ when it is necessary. It is important to note that the sub-matrix $\mathbf{A}_{22}(\mathbf{x})$ is invertible.

For the right-hand side of the diffusion equation, we define the vector

$$\mathbf{f}(\mathbf{x}(t))_k = \int_{\Omega_h(\mathbf{x})} f \varphi_k[\mathbf{x}] \mathrm{d}x \,.$$

By linearity, the transport property implies $\partial_h^\bullet \varphi_h = 0$, so the first equation of (A.3.2) is equivalent to

$$\frac{\mathrm{d}}{\mathrm{d}t} \left(\mathbf{M}(\mathbf{x}(t))\mathbf{u}(t) \right) + \mathbf{A}(\mathbf{x}(t))\mathbf{u}(t) = \mathbf{f}(\mathbf{x}(t)) \,.$$

For the velocity law, we remind that the nodes $x_j(t)$, $j = 1, \dots, N_\Gamma$, on the boundary are known explicitly since $v^\Gamma(\cdot, t)$ is prescribed. Writing $v_j(t) = v^\Gamma(x_j(t), t)$, we have the finite element interpolation of v^Γ:

$$v_h^\Gamma(\cdot, t) = \sum_{j=1}^{N_\Gamma} v_j(t) \varphi_j[\mathbf{x}(t)](\cdot) \,.$$

We write

$$w_h(\cdot, t) = \sum_{j=1}^{N} w_j(t) \varphi_j[\mathbf{x}(t)](\cdot) \,, \quad w_j(t) = v_j(t) \text{ for } j = 1, \dots, N_\Gamma \,,$$

for an arbitrary extension of v_h^Γ. Noting that $\mathbf{v}$ has three components, a short calculation shows that the second equation of (A.3.2) is equivalent to

$$\left(I_3 \otimes \mathbf{A}_{22}(\mathbf{x}) \right) \mathbf{v}^\Omega = - \left(I_3 \otimes \begin{pmatrix} \mathbf{A}_{21}(\mathbf{x}) & \mathbf{A}_{22}(\mathbf{x}) \end{pmatrix} \right) \begin{pmatrix} \mathbf{v}^\Gamma \\ \mathbf{w}^\Omega \end{pmatrix},$$

where $\mathbf{w}^\Omega$ is the vector containing the nodal values of w_h in the inner nodes. Here, I_3 denotes the identity matrix of size 3×3 and $\otimes$ denotes the Kronecker product. The solution v_h we are seeking is then obtained by $v_h = v_h^\Gamma + \widetilde{v}_h$ and corresponds to the nodal vector

$$\mathbf{v} = \begin{pmatrix} \mathbf{v}^\Gamma \\ \mathbf{v}^\Omega + \mathbf{w}^\Omega \end{pmatrix}, \quad \text{i.e. } v_h = \sum_{j=1}^{N} v_j \varphi_j[\mathbf{x}] \,.$$

Using the fact that $\mathbf{A}_{22}(\mathbf{x})$ is invertible, it is easily seen that the solution $\mathbf{v}$ does not depend on the particular choice of $\mathbf{w}^\Omega$, which is why we use $\mathbf{w}^\Omega = 0$.

The matrix–vector formulation reads (omitting the Kronecker product notation)

$$\begin{aligned}\frac{\mathrm{d}}{\mathrm{d}t}(\mathbf{M}(\mathbf{x})\mathbf{u}) + \mathbf{A}(\mathbf{x})\mathbf{u} &= \mathbf{f}(\mathbf{x})\,,\\ -\mathbf{A}_{22}(\mathbf{x})\mathbf{v}^{\Omega}(\mathbf{x}) &= \mathbf{A}_{21}(\mathbf{x})\mathbf{v}^{\Gamma}(\mathbf{x})\,,\\ \frac{\mathrm{d}}{\mathrm{d}t}\begin{pmatrix}\mathbf{x}^{\Gamma}\\ \mathbf{x}^{\Omega}\end{pmatrix} = \dot{\mathbf{x}} = \mathbf{v} &= \begin{pmatrix}\mathbf{v}^{\Gamma}\\ \mathbf{v}^{\Omega}\end{pmatrix}.\end{aligned}$$

The initial nodal vectors $\mathbf{u}(0)$ and $\mathbf{x}(0)$ are chosen as in (A.3.3).

We will see in the following sections that the matrix–vector formulation is the only tool used in the stability analysis, where geometric estimates are only needed for the consistency analysis.

A.3.4. Lifted finite element space

In the error analysis, we compare functions on three different domains: the exact domain $\Omega(t)$, the discrete domain $\Omega_h(t) = \Omega_h(\mathbf{x}(t))$ obtained by the finite element method and the *interpolated exact domain* $\Omega_h^*(t) = \Omega_h(\mathbf{x}^*(t))$, which is the computational domain corresponding to the nodal vector $\mathbf{x}^*(t)$ with the exact positions $x_j^*(t) = X(x_j^0, t)$ of the nodes at time t.

Any finite element function $u_h \in S_h(\mathbf{x})$ on the discrete computational domain, with nodal values u_j, $j = 1, \dots, N$, is related to a finite element function $\widehat{u}_h \in S_h(\mathbf{x}^*)$ with the same nodal values:

$$\widehat{u}_h = \sum_{j=1}^{N} u_j \varphi_j[\mathbf{x}^*]\,.$$

Based on Section A.3.1, we obtain a map $\Lambda_h(\cdot, t) : \Omega_h(\mathbf{x}^*(t)) \to \Omega(t)$ (cf. Elliott and Ranner [2013, 2021]), that is defined element-wise and maps the curved elements of the triangulation of $\Omega_h(\mathbf{x}^*(t))$ onto the corresponding parts of $\Omega(t)$. Restricted to interior simplices with at most one node on the boundary, this map is the identity. On boundary simplices, Λ_h is of class C^k if the boundary is of class C^k (see [Elliott and Ranner, 2013, Lemma 4.6]).

Definition A.3.1. *For a function $\widehat{u}_h \in S_h(\mathbf{x}^*(t))$, we define its lift $\widehat{u}_h^{\ell} : \Omega(t) \to \mathbb{R}$ by*

$$\widehat{u}_h^{\ell}(\Lambda_h(x,t),t) := \widehat{u}_h(x,t)\,.$$

The composed lift from finite element functions u_h on $\Omega_h(\mathbf{x}(t))$ to functions on $\Omega(t)$ is denoted by

$$u_h^L = \widehat{u}_h^{\ell}\,.$$

For any $u \in H^{k+1}(\Omega)$, there exists a unique finite element interpolation in the nodes x_j^*, denoted by $\widetilde{I}_h u \in S_h(\mathbf{x}^*)$. We set $I_h u = (\widetilde{I}_h u)^{\ell} : \Omega \to \mathbb{R}$. An interpolation estimate is obtained from [Elliott and Ranner, 2013, Proposition 5.4], based on Bernardi [1989].

Proposition A.3.2 (Interpolation error)**.** *There exists a constant $c > 0$ independent of $h \le h_0$ (h_0 sufficiently small) and t such that for all $1 \le m \le k$, $u(\cdot, t) \in H^{m+1}(\Omega(t))$ and $t \in [0, T]$*

$$\|u - I_h u\|_{L^2(\Omega(t))} + h\|\nabla(u - I_h u)\|_{L^2(\Omega(t))} \le c h^m \|u\|_{H^{m+1}(\Omega(t))}\,.$$

A.4. Statement of the main result

We are now able to formulate the main result of this paper, which yields error bounds for the spatial semi-discretization of (A.2.8) with evolving isoparametric finite elements of polynomial degree $k \geq 2$. We introduce the notation

$$x_h^L(x,t) = X_h^L(p,t) \in \Omega_h(t) \quad \text{for} \quad x = X(p,t) \in \Omega(t)\,.$$

Theorem A.4.1. *Consider the spatial semi-discretization* (A.3.2) *of* (A.2.8) *with evolving isoparametric finite elements of order $k \geq 2$. We assume a quasi-uniform admissible triangulation of the initial domain and initial values chosen by finite element interpolations of the exact initial data. Assume that the problem admits an exact solution (u, v, X) that is sufficiently smooth ($u \in H^{k+1}(\Omega(t))$, $v, X \in H^{k+1}(\Omega(t))^n$, $n = 2, 3$) for $t \in [0,T]$ and that the solution v is such that the triangulation of the interpolated exact domain $\Omega_h^*(t)$ remains quasi-uniform for $t \in [0,T]$. Then there exists an $h_0 > 0$ such that for all mesh widths $h \leq h_0$ the following error bounds hold on $\Omega(t)$, for $t \in [0,T]$:*

$$\begin{aligned}
\left(\|u_h^L(\cdot,t) - u(\cdot,t)\|^2_{L^2(\Omega(t))} + \int_0^t \|u_h^L(\cdot,s) - u(\cdot,s)\|^2_{H^1(\Omega(s))} \mathrm{d}s \right)^{\frac{1}{2}} &\leq c h^k\,, \\
\|v_h^L(\cdot,t) - v(\cdot,t)\|_{H^1(\Omega(t))^n} &\leq c h^k\,, \\
\|X_h^L(\cdot,t) - X(\cdot,t)\|_{H^1(\Omega_0)^n} &\leq c h^k\,.
\end{aligned}$$

The constant c depends on the regularity of the exact solution (u, v, X), on T and on the regularity of f.

In the following proof of error bounds, we clearly separate the stability and consistency analysis. The stability analysis, which is the significantly more difficult task in this work, borrows techniques used in Kovács et al. [2017] and extends them to the present evolving bulk problem. The crucial differences are that in the stability analysis for the domain evolution the boundary has to be taken into account and the error only lives in the interior of the domain, whereas for the diffusion equation there is also an error on the boundary. The stability analysis relies on auxiliary results from Section A.5, which require a bound on the $W^{1,\infty}$-norm of the position errors. With the H^1-norm error bound together with an inverse estimate, we obtain an $\mathcal{O}(h^{k-n/2})$ error bound for the position error, which is only small for $k \geq 2$. This is why we impose the condition $k \geq 2$ in the above result.

The consistency analysis requires geometric estimates for the evolving isoparametric finite element method. Such estimates are mainly taken from Elliott and Ranner [2013], which are generalized to the time-dependent case in Elliott and Ranner [2021].

The stability proof will yield h-independent bounds of the errors in terms of the defects. The stability analysis is done in the matrix–vector formulation, which allows a compact and manageable representation of the computations. We use energy estimates and transport formulae to relate mass and stiffness matrices for different nodal vectors. This allows us to work with the interpolated exact domain $\Omega_h(\mathbf{x}^*(t))$, which is a finite element triangulation of $\Omega(t)$ and only available in theoretical consideration.

In Section A.5 we prove auxiliary results that are used in the stability analysis, and then collect geometric estimates which are needed for the consistency analysis. In Section A.6 we analyze stability of the semi-discrete velocity law without a diffusion equation on the evolving domain. The stability analysis of the semi-discrete diffusion equation, which requires results from Section A.6, is then done in Section A.7. The defects are then bounded in Section A.8 and the proof of Theorem A.4.1 is completed in Section A.9.

A.5. Auxiliary results

A.5.1. Properties of the evolving mass and stiffness matrix

The following construction and results are similar to [Kovács et al., 2017, Section 4], where similar identities are shown for surfaces only. We extend these results to the present case of domains. In the stability analysis, we have to relate finite element matrices corresponding to different nodal vectors. Let $\mathbf{x}, \mathbf{y} \in \mathbb{R}^{3N}$ be two nodal vectors defining discrete domains $\Omega_h(\mathbf{x})$, $\Omega_h(\mathbf{y})$, respectively. We set $\mathbf{e} = \mathbf{x} - \mathbf{y}$. For any $\theta \in [0,1]$, we have the intermediate domain $\Omega_h^\theta = \Omega_h(\mathbf{y} + \theta\mathbf{e})$ which is the discrete domain corresponding to the intermediate nodal vector $\mathbf{y} + \theta\mathbf{e}$.

For any vector $\mathbf{w} \in \mathbb{R}^N$, we set

$$w_h^\theta = \sum_{j=1}^N w_j \varphi_j[\mathbf{y} + \theta\mathbf{e}] \in S_h(\mathbf{y} + \theta\mathbf{e})\,.$$

In particular, we have the finite element function e_h^θ corresponding to $\mathbf{e}$:

$$e_h^\theta = \sum_{j=1}^N e_j \varphi_j[\mathbf{y} + \theta\mathbf{e}]\,.$$

Lemma A.5.1. *In the above setting, the following identities hold for any $\mathbf{w}, \mathbf{z} \in \mathbb{R}^N$:*

$$\mathbf{w}^{\mathrm{T}}(\mathbf{M}(\mathbf{x}) - \mathbf{M}(\mathbf{y}))\mathbf{z} = \int_0^1 \int_{\Omega_h^\theta} w_h^\theta (\nabla \cdot e_h^\theta) z_h^\theta \mathrm{d}x \mathrm{d}\theta\,,$$

$$\mathbf{w}^{\mathrm{T}}(\mathbf{A}(\mathbf{x}) - \mathbf{A}(\mathbf{y}))\mathbf{z} = \int_0^1 \int_{\Omega_h^\theta} \nabla w_h^\theta \cdot (D_{\Omega_h^\theta} e_h^\theta) \nabla z_h^\theta \mathrm{d}x \mathrm{d}\theta\,,$$

where $D_{\Omega_h^\theta} = \mathrm{trace}(\nabla e_h^\theta) I_3 - (\nabla e_h^\theta + (\nabla e_h^\theta)^{\mathrm{T}})$.

Proof. We use transport formulae from Elliott and Ranner [2021]:

$$\begin{aligned}\mathbf{w}^{\mathrm{T}}(\mathbf{A}(\mathbf{x})-\mathbf{A}(\mathbf{y}))\mathbf{z} &= \int_{\Omega_h(\mathbf{x})} \nabla w_h^1 \cdot \nabla z_h^1 \mathrm{d}x - \int_{\Omega_h(\mathbf{y})} \nabla w_h^0 \cdot \nabla z_h^0 \mathrm{d}x \\ &= \int_0^1 \frac{\mathrm{d}}{\mathrm{d}\theta} \int_{\Omega_h^\theta} \nabla w_h^\theta \cdot \nabla z_h^\theta \mathrm{d}x\mathrm{d}\theta \\ &= \int_0^1 \int_{\Omega_h^\theta} \nabla \partial_\theta^\bullet w_h^\theta \cdot \nabla z_h^\theta + \nabla w_h^\theta \cdot \nabla \partial_\theta^\bullet z_h^\theta \\ &\quad + \left((\nabla \cdot e_h^\theta) I_3 - \left(\nabla e_h^\theta + (\nabla e_h^\theta)^{\mathrm{T}} \right) \right) \nabla w_h^\theta \cdot \nabla z_h^\theta \mathrm{d}x\mathrm{d}\theta \,.\end{aligned}$$

The first two terms vanish thanks to the transport property. This shows the second identity, since $\nabla \cdot e_h^\theta = \mathrm{trace}(\nabla e_h^\theta)$. The first identity is proven similarly. □

A direct consequence is the following lemma, where for any symmetric and positive (semi-)definite matrix $\mathbf{K}$, we denote the induced (semi-)norm on $\mathbb{R}^N$ by $\|\mathbf{w}\|_{\mathbf{K}} := (\mathbf{w}^{\mathrm{T}}\mathbf{K}\mathbf{w})^{1/2}$.

Lemma A.5.2. *If $\|\nabla \cdot e_h^\theta\|_{L^\infty(\Omega_h^\theta)} \leq \mu$ for $\theta \in [0,1]$, then*

$$\|\mathbf{w}\|_{\mathbf{M}(\mathbf{y}+\theta\mathbf{e})} \leq e^{\frac{\mu}{2}} \|\mathbf{w}\|_{\mathbf{M}(\mathbf{y})} \quad \text{for } \theta \in [0,1] \,.$$

If $\|D_{\Omega_h^\theta} e_h^\theta\|_{L^\infty(\Omega_h^\theta)} \leq \eta$ for $\theta \in [0,1]$, then

$$\|\mathbf{w}\|_{\mathbf{A}(\mathbf{y}+\theta\mathbf{e})} \leq e^{\frac{\eta}{2}} \|\mathbf{w}\|_{\mathbf{A}(\mathbf{y})} \quad \text{for } \theta \in [0,1] \,.$$

Proof. We use the previous lemma and an L^2-L^∞-L^2-estimate and compute for $0 \leq \tau \leq 1$:

$$\begin{aligned}\|\mathbf{w}\|^2_{\mathbf{M}(\mathbf{y}+\tau\mathbf{e})} - \|\mathbf{w}\|^2_{\mathbf{M}(\mathbf{y})} &= \mathbf{w}^{\mathrm{T}} \left(\mathbf{M}(\mathbf{y}+\tau\mathbf{e}) - \mathbf{M}(\mathbf{y}) \right) \mathbf{w} \\ &= \int_0^\tau \int_{\Omega_h^\theta} w_h^\theta \nabla \cdot e_h^\theta w_h^\theta \mathrm{d}x\mathrm{d}\theta \\ &= \int_0^\tau \|\mathbf{w}\|^2_{\mathbf{M}(\mathbf{y}+\theta\mathbf{e})} \|\nabla \cdot e_h^\theta\|_{L^\infty(\Omega_h^\theta)} \mathrm{d}\theta \\ &\leq \mu \int_0^\tau \|\mathbf{w}\|^2_{\mathbf{M}(\mathbf{y}+\theta\mathbf{e})} \mathrm{d}\theta \,.\end{aligned}$$

A Gronwall argument shows the first result. The second estimate is shown analogously. □

Lemma A.5.3. *Assume that*

$$\|\nabla e_h^0\|_{L^\infty(\Omega_h(\mathbf{y}))} \leq \frac{1}{2} \,. \tag{A.5.1}$$

Then, for $0 \leq \theta \leq 1$ the function $w_h^\theta = \sum_{j=1}^N w_j \varphi_j[\mathbf{y}+\theta\mathbf{e}]$ on Ω_h^θ is bounded by

$$\|\nabla w_h^\theta\|_{L^p(\Omega_h^\theta)} \leq c_p \|\nabla w_h^0\|_{L^p(\Omega_h^0)} \,,$$

$$\|w_h^\theta\|_{L^p(\Omega_h^\theta)} \leq \widetilde{c}_p \|w_h^0\|_{L^p(\Omega_h^0)} \,,$$

for $1 \leq p \leq \infty$, where c_p and $\widetilde{c}_p$ depend only on p.

Proof. We parametrize Ω_h^θ over Ω_h^0:

$$\begin{aligned} Y_h^\theta(p_h) = Y_h(p_h,\theta) &= \sum_{j=1}^N (y_j + \theta e_j)\varphi_j[\mathbf{y}](p_h) \qquad \big(p_h \in \Omega_h^0 = \Omega_h(\mathbf{y})\big) \\ &= \sum_{j=1}^N y_j \varphi_j[\mathbf{y}](p_h) + \theta \sum_{j=1}^N e_j \varphi_j[\mathbf{y}](p_h) = p_h + \theta e_h^0(p_h)\,, \end{aligned}$$

where we have used that $Y_h^0(p_h) = p_h$. Differentiating with respect to p_h yields

$$DY_h^\theta(p_h) = I + \theta De_h^0(p_h)\,. \tag{A.5.2}$$

By the transport property, we have $w_h^\theta(Y_h^\theta(p_h)) = w_h^0(Y_h^0(p_h)) = w_h^0(p_h)$. Differentiation with respect to p_h yields

$$Dw_h^\theta(Y_h^\theta(p_h))DY_h^\theta(p_h) = Dw_h^0(p_h)\,. \tag{A.5.3}$$

From (A.5.2) we have under the assumption $\|\nabla e_h^0\|_{L^\infty(\Omega_h(\mathbf{y}))} \le \frac{1}{2}$:

$$|DY_h^\theta(p_h)z| = |z + \theta(\nabla e_h^0)^{\mathrm{T}} z| \ge |z| - \theta|(\nabla e_h^0)^{\mathrm{T}} z| \ge \frac{1}{2}|z|\,.$$

Thus, the matrix $DY_h^\theta(p_h)$ is invertible and we have with (A.5.3)

$$Dw_h^\theta(Y_h^\theta(p_h)) = Dw_h^0(p_h)\left(DY_h^\theta(p_h)\right)^{-1},$$

implying $|Dw_h^\theta(Y_h^\theta(p_h))| \le 2|Dw_h^0(p_h)|$ and thus

$$\|\nabla w_h^\theta\|_{L^\infty(\Omega_h^\theta)} \le 2\|\nabla w_h^0\|_{L^\infty(\Omega_h^0)}\,.$$

For $1 \le p < \infty$, we use the transformation formula and the fact that $\|De_h^0(p_h)\|_{L^\infty(\Omega_h^0)} \le \frac{1}{2}$ to obtain

$$\begin{aligned} \|\nabla w_h^\theta\|^p_{L^p(\Omega_h^\theta)} &= \int_{\Omega_h^\theta} |Dw_h^\theta(y_h^\theta)|^p \mathrm{d}y_h^\theta = \int_{\Omega_h^0} \left|Dw_h^\theta(Y_h^\theta(p_h))\right|^p \left|\det DY_h^\theta(p_h)\right| \mathrm{d}p_h \\ &= \int_{\Omega_h^0} |Dw_h^0(p_h)(DY_h^\theta(p_h))^{-1}|^p |\det DY_h(p_h)| \mathrm{d}p_h \\ &\le c\int_{\Omega_h^0} |Dw_h^0(p_h)|^p \mathrm{d}p_h = c\|\nabla w_h^0\|^p_{L^p(\Omega_h^0)}\,. \end{aligned}$$

For the second estimate, we note that the transport property immediately implies

$$\|w_h^\theta\|_{L^\infty(\Omega_h^\theta)} = \left\|w_h^0\right\|_{L^\infty(\Omega_h^0)}\,.$$

For $1 \le p < \infty$, we use the transformation formula and the same arguments as above. □

Another consequence of Lemma A.5.2 is the following.

Lemma A.5.4. *Let $\mathbf{x}^*(t)$ be the vector of the exact positions $x_j^*(t) = X(x_j^0, t)$. Then, we have for all $\mathbf{w}, \mathbf{z} \in \mathbb{R}^N$:*

$$\mathbf{w}^{\mathrm{T}} \left(\frac{\mathrm{d}}{\mathrm{d}t} \mathbf{M}(\mathbf{x}^*(t)) \right) \mathbf{z} \leq c \|\mathbf{w}\|_{\mathbf{M}(\mathbf{x}^*(t))} \|\mathbf{z}\|_{\mathbf{M}(\mathbf{x}^*(t))} ,$$

$$\mathbf{w}^{\mathrm{T}} \left(\frac{\mathrm{d}}{\mathrm{d}t} \mathbf{A}(\mathbf{x}^*(t)) \right) \mathbf{z} \leq c \|\mathbf{w}\|_{\mathbf{A}(\mathbf{x}^*(t))} \|\mathbf{z}\|_{\mathbf{A}(\mathbf{x}^*(t))} .$$

The constant c depends on the $W^{1,\infty}(\Omega_T)$-norm of v, the dimension n and the length T of the time interval, but is independent of h and t.

Proof. The proof can be found in [Dziuk et al., 2012, Lemma 4.1] for surfaces and can directly be transferred to the present situation, using arguments from the proof of Lemma A.5.2. □

A.5.2. Geometric estimates

We collect geometric estimates that are used later in the consistency analysis. For a finite element function $\eta_h : \Omega_h^*(t) \to \mathbb{R}$, its lift is denoted by $\eta_h^\ell : \Omega(t) \to \mathbb{R}$ (see Definition A.3.1). The following lemma shows that the norms of finite element functions and their lifts are equivalent. A proof can be found in [Elliott and Ranner, 2013, Proposition 4.9], based on Ciarlet and Raviart [1972].

Lemma A.5.5. *Let $\eta_h : \Omega_h^*(t) \to \mathbb{R}$ with lift $\eta_h^\ell : \Omega(t) \to \mathbb{R}$. Then there exist constants $c_1, c_2 > 0$ such that*

$$\begin{aligned} c_1 \|\eta_h\|_{L^2(\Omega_h^*(t))} \leq \|\eta_h^\ell\|_{L^2(\Omega(t))} &\leq c_2 \|\eta_h\|_{L^2(\Omega_h^*(t))} , \\ c_1 \|\nabla \eta_h\|_{L^2(\Omega_h^*(t))} \leq \|\nabla \eta_h^\ell\|_{L^2(\Omega(t))} &\leq c_2 \|\nabla \eta_h\|_{L^2(\Omega_h^*(t))} . \end{aligned}$$

The constants depend on the dimension n, the length T of the time interval and the geometry of Ω_T but are independent of h and t.

We define discrete analogues of the bilinear forms m and a, defined in (A.2.3): For η_h, χ_h: $\Omega_h^*(t) \to \mathbb{R}$, we define

$$\begin{aligned} m_h^*(\eta_h, \chi_h) &= \int_{\Omega_h^*(t)} \eta_h \chi_h , \\ a_h^*(\eta_h, \chi_h) &= \int_{\Omega_h^*(t)} \nabla \eta_h \cdot \nabla \chi_h . \end{aligned}$$

The following lemma estimates the difference between the discrete bilinear form on the interpolated exact domain and the exact bilinear form of the lifted functions on the exact domain. A proof can be found in Elliott and Ranner [2021].

Lemma A.5.6 (Geometric approximation errors)**.** *For $\eta_h, \chi_h \in S_h(\mathbf{x}^*(t))$ with corresponding lifts η_h^ℓ, χ_h^ℓ, the following estimates hold: there exists a constant c such that*

$$\begin{aligned}\left|m_h^*(\eta_h,\chi_h) - m(\eta_h^\ell,\chi_h^\ell)\right| &\leq ch^k \|\eta_h^\ell\|_{L^2(\Omega(t))}\|\chi_h^\ell\|_{L^2(\Omega(t))}\,,\\ \left|a_h^*(\eta_h,\chi_h) - a(\eta_h^\ell,\chi_h^\ell)\right| &\leq ch^k \|\nabla\eta_h^\ell\|_{L^2(\Omega(t))}\|\nabla\chi_h^\ell\|_{L^2(\Omega(t))}\,.\end{aligned}$$

The constant c depends on the dimension n, the length T of the interval and the geometry of Ω_T but is independent of h and t.

A.6. Stability of the semi-discrete harmonic velocity law

We will start with analyzing stability of the semi-discrete velocity law without the diffusion equation, since the domain evolution is independent of the parabolic equation, see Remark A.2.1. The stability analysis of the semi-discrete diffusion equation, which is based on the following results, is presented in the next section.

We consider the nodal vectors $\mathbf{v}, \mathbf{x} \in \mathbb{R}^{3N}$ which satisfy

$$\begin{aligned}(I_3 \otimes \mathbf{A}_{22}(\mathbf{x}))\mathbf{v}^\Omega &= -(I_3 \otimes \mathbf{A}_{21}(\mathbf{x}))\mathbf{v}^\Gamma\,,\\ \dot{\mathbf{x}} &= \mathbf{v}.\end{aligned} \tag{A.6.1}$$

with given $\mathbf{v}^\Gamma$. We denote by

$$\mathbf{x}^*(t) = \begin{pmatrix}\mathbf{x}^{\Gamma,*}(t)\\ \mathbf{x}^{\Omega,*}(t)\end{pmatrix}$$

the vector of the exact positions at time $t \in [0,T]$. Note that $x_j^*(t) = x_j(t)$ for all $j = 1,\dots,N_\Gamma$ since $\mathbf{v}^\Gamma$ is given explicitly. i.e. $\mathbf{x}^\Gamma(t) = \mathbf{x}^{\Gamma,*}(t)$.

We consider the interpolated exact velocity $v_h^*(\cdot,t) = \sum_{j=1}^N v_j^*(t)\varphi_j[\mathbf{x}^*(t)]$ with the corresponding nodal vector

$$\mathbf{v}^*(t) = \begin{pmatrix}\mathbf{v}^{\Gamma,*}(t)\\ \mathbf{v}^{\Omega,*}(t)\end{pmatrix}\,.$$

Note again that $\mathbf{v}^{\Gamma,*}(t) = \mathbf{v}^\Gamma(t)$.

A.6.1. Error equations

The vectors $\mathbf{x}^*$ and $\mathbf{v}^*$ satisfy (A.6.1) up to a defect $\mathbf{d}_{\mathbf{v}^\Omega}$:

$$\begin{aligned}(I_3 \otimes \mathbf{A}_{22}(\mathbf{x}^*))\mathbf{v}^{\Omega,*} &= -(I_3 \otimes \mathbf{A}_{21}(\mathbf{x}^*))\mathbf{v}^{\Gamma,*} + \mathbf{M}_{22}(\mathbf{x}^*)\mathbf{d}_{\mathbf{v}^\Omega}\,,\\ \dot{\mathbf{x}}^* &= \mathbf{v}^*\,.\end{aligned} \tag{A.6.2}$$

We set $\mathbf{d}_\mathbf{v} = (\mathbf{d}_{\mathbf{v}^\Gamma}, \mathbf{d}_{\mathbf{v}^\Omega}) \in \mathbb{R}^{3N}$ with $\mathbf{d}_{\mathbf{v}^\Gamma} = 0 \in \mathbb{R}^{3N_\Gamma}$. This notation will be useful in the stability analysis. The defect $\mathbf{d}_\mathbf{v}$ corresponds to a finite element function $d_h^v(\cdot,t) = \sum_{j=1}^N d_j^v(t)\varphi_j[\mathbf{x}^*(t)] \in$

$S_{0,h}(\mathbf{x}(t))^3$. We denote the errors in the nodes and in the velocity by $\mathbf{e}_{\mathbf{x}^\Omega} = \mathbf{x}^\Omega - \mathbf{x}^{\Omega,*}$, $\mathbf{e}_{\mathbf{v}^\Omega} = \mathbf{v}^\Omega - \mathbf{v}^{\Omega,*}$ and use the notation

$$\mathbf{e}_\mathbf{x} = \begin{pmatrix} 0 \\ \mathbf{e}_{\mathbf{x}^\Omega} \end{pmatrix} = \begin{pmatrix} \mathbf{e}_{\mathbf{x}^\Gamma} \\ \mathbf{e}_{\mathbf{x}^\Omega} \end{pmatrix}, \quad \mathbf{e}_\mathbf{v} = \begin{pmatrix} 0 \\ \mathbf{e}_{\mathbf{v}^\Omega} \end{pmatrix} = \begin{pmatrix} \mathbf{e}_{\mathbf{v}^\Gamma} \\ \mathbf{e}_{\mathbf{v}^\Omega} \end{pmatrix}.$$

In the following, we write $\mathbf{A}(\mathbf{x})$ instead of $I_3 \otimes \mathbf{A}(\mathbf{x})$, for brevity. We rewrite (A.6.1) as

$$\begin{aligned} \mathbf{A}_{22}(\mathbf{x}^*)\mathbf{v}^\Omega = &- (\mathbf{A}_{22}(\mathbf{x}) - \mathbf{A}_{22}(\mathbf{x}^*))\mathbf{v}^{\Omega,*} \\ &- (\mathbf{A}_{22}(\mathbf{x}) - \mathbf{A}_{22}(\mathbf{x}^*))\mathbf{e}_{\mathbf{v}^\Omega} - \mathbf{A}_{21}(\mathbf{x})\mathbf{v}^\Gamma . \end{aligned} \tag{A.6.3}$$

Subtracting (A.6.2) from (A.6.3) and using $\mathbf{v}^\Gamma = \mathbf{v}^{\Gamma,*}$ yields the error equations

$$\begin{aligned} \mathbf{A}_{22}(\mathbf{x}^*)\mathbf{e}_{\mathbf{v}^\Omega} = \quad &- (\mathbf{A}_{22}(\mathbf{x}) - \mathbf{A}_{22}(\mathbf{x}^*))\mathbf{v}^{\Omega,*} - (\mathbf{A}_{22}(\mathbf{x}) - \mathbf{A}_{22}(\mathbf{x}^*))\mathbf{e}_{\mathbf{v}^\Omega} \\ &- (\mathbf{A}_{21}(\mathbf{x}) - \mathbf{A}_{21}(\mathbf{x}^*))\mathbf{v}^{\Gamma,*} - \mathbf{M}_{22}(\mathbf{x}^*)\mathbf{d}_{\mathbf{v}^\Omega} , \\ \dot{\mathbf{e}}_{\mathbf{x}^\Omega} = \quad &\mathbf{e}_{\mathbf{v}^\Omega} . \end{aligned} \tag{A.6.4}$$

A.6.2. Dual norm

We recall that the mass and stiffness matrices $\mathbf{M}_{22}(\mathbf{x})$ and $\mathbf{A}_{22}(\mathbf{x})$, respectively, induce norms on $S_{0,h}(\mathbf{x})$. Note that $\mathbf{A}_{22}(\mathbf{x})$ defines a norm on $S_{0,h}(\mathbf{x})$, whereas $\mathbf{A}(\mathbf{x})$ defines only a semi-norm on $S_h(\mathbf{x})$. We define the dual norm

$$\begin{aligned} \|d_h^v\|_{H^{-1}_{0,h}(\Omega_h(\mathbf{x}^*))} &= \sup_{0\neq\psi_h\in S_{0,h}(\mathbf{x}^*)^3} \frac{\int_{\Omega_h(\mathbf{x}^*)} d_h^v \cdot \psi_h \mathrm{d}x}{\|\psi_h\|_{H^1_0(\Omega_h(\mathbf{x}^*))}} = \sup_{0\neq\mathbf{z}\in\mathbb{R}^{3N_\Omega}} \frac{\mathbf{d}_{\mathbf{v}^\Omega}^{\mathrm{T}}\mathbf{M}_{22}(\mathbf{x}^*)\mathbf{z}}{(\mathbf{z}^{\mathrm{T}}\mathbf{A}_{22}(\mathbf{x}^*)\mathbf{z})^{1/2}} \\ &= \sup_{0\neq\mathbf{w}\in\mathbb{R}^{3N_\Omega}} \frac{\mathbf{d}_{\mathbf{v}^\Omega}^{\mathrm{T}}\mathbf{M}_{22}(\mathbf{x}^*)\mathbf{A}_{22}(\mathbf{x}^*)^{-1/2}\mathbf{w}}{(\mathbf{w}^{\mathrm{T}}\mathbf{w})^{1/2}} = \|\mathbf{A}_{22}(\mathbf{x}^*)^{-1/2}\mathbf{M}_{22}(\mathbf{x}^*)\mathbf{d}_{\mathbf{v}^\Omega}\|_2 \\ &= \left(\mathbf{d}_{\mathbf{v}^\Omega}^{\mathrm{T}}\mathbf{M}_{22}(\mathbf{x}^*)\mathbf{A}_{22}(\mathbf{x}^*)^{-1}\mathbf{M}_{22}(\mathbf{x}^*)\mathbf{d}_{\mathbf{v}^\Omega}\right)^{\frac{1}{2}} =: \|\mathbf{d}_{\mathbf{v}^\Omega}\|_{\star,\mathbf{x}^*} . \end{aligned} \tag{A.6.5}$$

A.6.3. Stability estimate

We are now ready to state and prove the first main stability result. The following stability result holds under a smallness assumption on the defect. It will be proven in Section A.8 that this assumption is satisfied for $\kappa = k \geq 2$, where k is the order of the finite element method.

Lemma A.6.1. *Assume that, for some $\kappa > \frac{3}{2}$, the defect is bounded as follows:*

$$\|\mathbf{d}_{\mathbf{v}^\Omega}(t)\|_{\star,\mathbf{x}^*(t)} \leq ch^\kappa , \quad t \in [0,T] . \tag{A.6.6}$$

Then there exists an $h_0 > 0$ such that for $h \leq h_0$ and $t \in [0,T]$, the following error bounds hold.

$$\|\mathbf{e}_{\mathbf{x}^\Omega}(t)\|^2_{\mathbf{A}_{22}(\mathbf{x}^*(t))} \leq c\int_0^t \|\mathbf{d}_{\mathbf{v}^\Omega}(s)\|^2_{\star,\mathbf{x}^*(s)}\mathrm{d}s , \tag{A.6.7}$$

$$\|\mathbf{e}_{\mathbf{v}^\Omega}(t)\|^2_{\mathbf{A}_{22}(\mathbf{x}^*(t))} \leq c\|\mathbf{d}_{\mathbf{v}^\Omega}(t)\|^2_{\star,\mathbf{x}^*(t)} + c\int_0^t \|\mathbf{d}_{\mathbf{v}^\Omega}(s)\|^2_{\star,\mathbf{x}^*(s)}\mathrm{d}s . \tag{A.6.8}$$

Proof. The proof uses energy estimates that are similar to techniques used in Kovács et al. [2017] and Kovács et al. [2019]. We extend their results for coupled surface problems to the present evolving bulk problem. Since the structure of the proof is similar to the cited works, we might skip some non-trivial steps. However there are some crucial differences that need to be pointed out: The evolving bulk $\Omega(t)$ has a boundary $\Gamma(t)$ that has to be taken into account, whereas in Kovács et al. [2017], Kovács et al. [2019] the considered evolving surfaces have no boundaries or interiors. Moreover, we exploit the fact there is no position or velocity error in the boundary because the boundary velocity is given. This implies that the lift of the finite element function corresponding to the error is a H_0^1-function and turns out to be crucial to estimate the error equations, see (A.6.11) and (A.6.12) below. In addition, the space dimension $n \in \{2,3\}$ requires the assumption $\kappa > n/2$, which is due to an inverse estimate at the end of this proof, see Remark A.6.2.

In view of the auxiliary results from Section A.5 and in particular condition (A.5.1), we need to control the $W^{1,\infty}$-norm of the position error $e_x(\cdot,t)$. Let $0 < t^* \leq T$ as the maximal time such that

$$\|\nabla e_x(\cdot,t)\|_{L^\infty(\Omega_h(\mathbf{x}^*(t)))} \leq h^{(\kappa-3/2)/2}\,. \tag{A.6.9}$$

Note that $e_x(\cdot,0) = 0$ implies $t^* > 0$. We prove the stated error bounds for $t \in [0,t^*]$ and then show that $t^* = T$.

We test the first equation of (A.6.4) with $\mathbf{e}_{\mathbf{v}^\Omega}$ and obtain

$$\begin{aligned}\|\mathbf{e}_{\mathbf{v}^\Omega}\|^2_{\mathbf{A}_{22}(\mathbf{x}^*)} =& -\mathbf{e}_{\mathbf{v}^\Omega}^{\mathrm{T}}(\mathbf{A}_{22}(\mathbf{x})-\mathbf{A}_{22}(\mathbf{x}^*))\mathbf{v}^{\Omega,*}\\ &-\mathbf{e}_{\mathbf{v}^\Omega}^{\mathrm{T}}(\mathbf{A}_{22}(\mathbf{x})-\mathbf{A}_{22}(\mathbf{x}^*))\mathbf{e}_{\mathbf{v}^\Omega}\\ &-\mathbf{e}_{\mathbf{v}^\Omega}^{\mathrm{T}}(\mathbf{A}_{21}(\mathbf{x})-\mathbf{A}_{21}(\mathbf{x}^*))\mathbf{v}^{\Gamma,*}-\mathbf{e}_{\mathbf{v}^\Omega}^{\mathrm{T}}\mathbf{M}_{22}(\mathbf{x}^*)\mathbf{d}_{\mathbf{v}^\Omega}\,.\end{aligned} \tag{A.6.10}$$

It is crucial to combine the first and third term of (A.6.10). Note that

$$\begin{aligned}(0,\mathbf{e}_{\mathbf{v}^\Omega}^{\mathrm{T}})\mathbf{A}(\mathbf{x})\begin{pmatrix}\mathbf{v}^\Gamma\\ \mathbf{v}^\Omega\end{pmatrix} &= (0,\mathbf{e}_{\mathbf{v}^\Omega}^{\mathrm{T}})\begin{pmatrix}\mathbf{A}_{11}(\mathbf{x}) & \mathbf{A}_{12}(\mathbf{x})\\ \mathbf{A}_{21}(\mathbf{x}) & \mathbf{A}_{22}(\mathbf{x})\end{pmatrix}\begin{pmatrix}\mathbf{v}^\Gamma\\ \mathbf{v}^\Omega\end{pmatrix}\\ &= \mathbf{e}_{\mathbf{v}^\Omega}^{\mathrm{T}}\mathbf{A}_{21}(\mathbf{x})\mathbf{v}^\Gamma + \mathbf{e}_{\mathbf{v}^\Omega}^{\mathrm{T}}\mathbf{A}_{22}(\mathbf{x})\mathbf{v}^\Omega\,.\end{aligned} \tag{A.6.11}$$

We set $\mathbf{e}_{\mathbf{v}^\Gamma} = 0$ and $\mathbf{e}_{\mathbf{v}}^{\mathrm{T}} = (\mathbf{e}_{\mathbf{v}^\Gamma}^{\mathrm{T}}, \mathbf{e}_{\mathbf{v}^\Omega}^{\mathrm{T}})$. Applying (A.6.11) to (A.6.10), we obtain

$$\begin{aligned}\|\mathbf{e}_{\mathbf{v}}\|^2_{\mathbf{A}(\mathbf{x}^*)} =& -\mathbf{e}_{\mathbf{v}}^{\mathrm{T}}(\mathbf{A}(\mathbf{x})-\mathbf{A}(\mathbf{x}^*))\mathbf{v}^* - \mathbf{e}_{\mathbf{v}^\Omega}^{\mathrm{T}}(\mathbf{A}_{22}(\mathbf{x})-\mathbf{A}_{22}(\mathbf{x}^*))\mathbf{e}_{\mathbf{v}^\Omega}\\ &-\mathbf{e}_{\mathbf{v}^\Omega}^{\mathrm{T}}\mathbf{M}_{22}(\mathbf{x}^*)\mathbf{d}_{\mathbf{v}^\Omega}\\ =& -\mathbf{e}_{\mathbf{v}}^{\mathrm{T}}(\mathbf{A}(\mathbf{x})-\mathbf{A}(\mathbf{x}^*))\mathbf{v}^* - \mathbf{e}_{\mathbf{v}}^{\mathrm{T}}(\mathbf{A}(\mathbf{x})-\mathbf{A}(\mathbf{x}^*))\mathbf{e}_{\mathbf{v}} - \mathbf{e}_{\mathbf{v}}^{\mathrm{T}}\mathbf{M}(\mathbf{x}^*)\mathbf{d}_{\mathbf{v}}\,.\end{aligned} \tag{A.6.12}$$

We estimate these three terms separately.

(i) We use that

$$D_{\Omega_h^\theta} e_x^\theta = \operatorname{trace}(\nabla e_x^\theta) I_3 - \left(\nabla e_x^\theta + (\nabla e_x^\theta)^{\mathrm{T}}\right)$$

and thus $\|D_{\Omega_h^\theta} e_x^\theta\| \le c\|\nabla e_x^\theta\|$. With Lemma A.5.1, an L^2-L^2-L^∞-estimate and Lemma A.5.2, we arrive at

$$\begin{aligned}
\mathbf{e}_\mathbf{v}^{\mathrm{T}} \left(\mathbf{A}(\mathbf{x}) - \mathbf{A}(\mathbf{x}^*)\right) \mathbf{v}^* &= \int_0^1 \int_{\Omega_h^\theta} \nabla e_v^\theta \cdot (D_{\Omega_h^\theta} e_x^\theta) \nabla v_h^{*,\theta} \mathrm{d}x \mathrm{d}\theta \\
&\le \int_0^1 \|\nabla e_v^\theta\|_{L^2(\Omega_h^\theta)} \|D_{\Omega_h^\theta} e_x^\theta\|_{L^2(\Omega_h^\theta)} \|\nabla v_h^{*,\theta}\|_{L^\infty(\Omega_h^\theta)} \mathrm{d}\theta \\
&\le c\|\nabla e_v^0\|_{L^2(\Omega_h^0)} \|\nabla e_x^0\|_{L^2(\Omega_h^0)} \|\nabla v_h^{*,0}\|_{L^\infty(\Omega_h^0)} \\
&= c\|\mathbf{e}_\mathbf{v}\|_{\mathbf{A}(\mathbf{x}^*)} \|\mathbf{e}_\mathbf{x}\|_{\mathbf{A}(\mathbf{x}^*)} \|\nabla v_h^*\|_{L^\infty(\Omega_h(\mathbf{x}^*))} .
\end{aligned}$$

The last factor is bounded by a constant independent of h, since v_h^* is the finite element interpolation of the exact velocity (see [Bernardi, 1989, Theorem 4.1]). Using Young's inequality together with the fact that $\|\mathbf{e}_\mathbf{v}\|_{\mathbf{A}(\mathbf{x}^*)} = \|\mathbf{e}_{\mathbf{v}^\Omega}\|_{\mathbf{A}_{22}(\mathbf{x}^*)}$, we obtain

$$\mathbf{e}_\mathbf{v}^{\mathrm{T}} (\mathbf{A}(\mathbf{x}) - \mathbf{A}(\mathbf{x}^*)) \mathbf{v}^* \le \frac{1}{4} \|\mathbf{e}_{\mathbf{v}^\Omega}\|_{\mathbf{A}_{22}(\mathbf{x}^*)}^2 + C \|\mathbf{e}_{\mathbf{x}^\Omega}\|_{\mathbf{A}_{22}(\mathbf{x}^*)}^2 .$$

(ii) Similarly, using the smallness assumption (A.6.9), we obtain

$$\begin{aligned}
\mathbf{e}_\mathbf{v}^{\mathrm{T}} (\mathbf{A}(\mathbf{x}) - \mathbf{A}(\mathbf{x}^*)) \mathbf{e}_\mathbf{v} &\le c\|\nabla e_v^0\|_{L^2(\Omega_h(\mathbf{x}^*))}^2 \|\nabla e_x^0\|_{L^\infty(\Omega_h(\mathbf{x}^*))} \\
&\le c h^{(\kappa-3/2)/2} \|\mathbf{e}_\mathbf{v}\|_{\mathbf{A}(\mathbf{x}^*)}^2 = c h^{(\kappa-3/2)/2} \|\mathbf{e}_{\mathbf{v}^\Omega}\|_{\mathbf{A}_{22}(\mathbf{x}^*)}^2 .
\end{aligned}$$

(iii) Using the Cauchy–Schwarz inequality together with Young's inequality, we estimate

$$\begin{aligned}
\mathbf{e}_{\mathbf{v}^\Omega}^{\mathrm{T}} \mathbf{M}_{22}(\mathbf{x}^*) \mathbf{d}_{\mathbf{v}^\Omega} &= \mathbf{e}_{\mathbf{v}^\Omega}^{\mathrm{T}} \mathbf{A}_{22}(\mathbf{x}^*)^{\frac{1}{2}} \mathbf{A}_{22}(\mathbf{x}^*)^{-\frac{1}{2}} \mathbf{M}_{22}(\mathbf{x}^*) \mathbf{d}_{\mathbf{v}^\Omega} \\
&\le \frac{1}{4} \|\mathbf{A}_{22}(\mathbf{x}^*)^{\frac{1}{2}} \mathbf{e}_{\mathbf{v}^\Omega}\|^2 + c\|\mathbf{A}_{22}(\mathbf{x}^*)^{-\frac{1}{2}} \mathbf{M}_{22}(\mathbf{x}^*) \mathbf{d}_{\mathbf{v}^\Omega}\|^2 \\
&= \frac{1}{4} \|\mathbf{e}_{\mathbf{v}^\Omega}\|_{\mathbf{A}_{22}(\mathbf{x}^*)}^2 + c\|\mathbf{d}_{\mathbf{v}^\Omega}\|_{\star,\mathbf{x}^*}^2 .
\end{aligned}$$

The combination of the three estimates with absorptions (for $h \le h_0$ sufficiently small) yields

$$\|\dot{\mathbf{e}}_{\mathbf{x}^\Omega}\|_{\mathbf{A}_{22}(\mathbf{x}^*)}^2 = \|\mathbf{e}_{\mathbf{v}^\Omega}\|_{\mathbf{A}_{22}(\mathbf{x}^*)}^2 \le c\|\mathbf{e}_{\mathbf{x}^\Omega}\|_{\mathbf{A}_{22}(\mathbf{x}^*)}^2 + c\|\mathbf{d}_{\mathbf{v}^\Omega}\|_{\star,\mathbf{x}^*}^2 . \tag{A.6.13}$$

We connect $\frac{\mathrm{d}}{\mathrm{d}t}\|\mathbf{e}_{\mathbf{x}^\Omega}\|_{\mathbf{A}_{22}(\mathbf{x}^*)}^2$ and $\|\dot{\mathbf{e}}_{\mathbf{x}^\Omega}\|_{\mathbf{A}_{22}(\mathbf{x}^*)}^2$. We have

$$\frac{1}{2} \frac{\mathrm{d}}{\mathrm{d}t} \|\mathbf{e}_{\mathbf{x}^\Omega}\|_{\mathbf{A}_{22}(\mathbf{x}^*)}^2 = \mathbf{e}_{\mathbf{x}^\Omega}^{\mathrm{T}} \mathbf{A}_{22}(\mathbf{x}^*) \dot{\mathbf{e}}_{\mathbf{x}^\Omega} + \frac{1}{2} \mathbf{e}_{\mathbf{x}^\Omega}^{\mathrm{T}} \left(\frac{\mathrm{d}}{\mathrm{d}t} \mathbf{A}_{22}(\mathbf{x}^*(t)) \right) \mathbf{e}_{\mathbf{x}^\Omega} .$$

With the Cauchy–Schwarz and Young inequalities, we obtain

$$\mathbf{e}_{\mathbf{x}^\Omega}^{\mathrm{T}} \mathbf{A}_{22}(\mathbf{x}^*) \dot{\mathbf{e}}_{\mathbf{x}^\Omega} \le \|\mathbf{e}_{\mathbf{x}^\Omega}\|_{\mathbf{A}_{22}(\mathbf{x}^*)} \|\dot{\mathbf{e}}_{\mathbf{x}^\Omega}\|_{\mathbf{A}_{22}(\mathbf{x}^*)} \le \|\dot{\mathbf{e}}_{\mathbf{x}^\Omega}\|_{\mathbf{A}_{22}(\mathbf{x}^*)}^2 + \frac{1}{4} \|\mathbf{e}_{\mathbf{x}^\Omega}\|_{\mathbf{A}_{22}(\mathbf{x}^*)}^2 .$$

For the second term Lemma A.5.4 yields

$$\frac{1}{2} \mathbf{e}_{\mathbf{x}^\Omega}^{\mathrm{T}} \left(\frac{\mathrm{d}}{\mathrm{d}t} \mathbf{A}_{22}(\mathbf{x}^*(t)) \right) \mathbf{e}_{\mathbf{x}^\Omega} \le C \|\mathbf{e}_{\mathbf{x}^\Omega}(t)\|_{\mathbf{A}_{22}(\mathbf{x}^*(t))}^2 .$$

We thus obtain, using (A.6.13)

$$\frac{1}{2}\frac{\mathrm{d}}{\mathrm{d}t}\|\mathbf{e}_{\mathbf{x}^\Omega}\|^2_{\mathbf{A}_{22}(\mathbf{x}^*)} \leq c\|\mathbf{e}_{\mathbf{x}^\Omega}\|^2_{\mathbf{A}_{22}(\mathbf{x}^*)} + c\|\mathbf{d}_{\mathbf{v}^\Omega}\|^2_{\star,\mathbf{x}^*}\,.$$

Integrating from 0 to t and using $\mathbf{e}_{\mathbf{x}^\Omega}(0) = 0$, we obtain

$$\|\mathbf{e}_{\mathbf{x}^\Omega}(t)\|^2_{\mathbf{A}_{22}(\mathbf{x}^*(t))} \leq c\int_0^t \|\mathbf{d}_{\mathbf{v}^\Omega}(s)\|^2_{\star,\mathbf{x}^*(s)}\mathrm{d}s + \int_0^t c\|\mathbf{e}_{\mathbf{x}^\Omega}(s)\|^2_{\mathbf{A}_{22}(\mathbf{x}^*(s))}\mathrm{d}s\,.$$

The Gronwall inequality thus yields (A.6.7), which then inserted into (A.6.13) yields (A.6.8).

Now it remains to show that for $h \leq h_0$ sufficiently small we in fact have $t^* = T$. For $0 \leq t \leq t^*$ we have with an inverse inequality (see Brenner and Scott [2008]) and for $h \leq h_0$ sufficiently small:

$$\begin{aligned}\|\nabla e_x(\cdot,t)\|_{L^\infty(\Omega_h(\mathbf{x}^*(t)))} &\leq ch^{-3/2}\|\nabla e_x(\cdot,t)\|_{L^2(\Omega_h(\mathbf{x}^*(t)))}\\ &= ch^{-3/2}\|\mathbf{e}_{\mathbf{x}^\Omega}(t)\|^2_{\mathbf{A}_{22}(\mathbf{x}^*(t))} \leq ch^{\kappa-3/2}\\ &\leq \frac{1}{2}h^{\frac{\kappa-3/2}{2}}\,.\end{aligned}$$

This shows that the bound (A.6.9) can be extended beyond t^*, which contradicts the maximality of t^* unless $t^* = T$. □

Remark A.6.2. *The previous lemma remains valid in the two-dimensional case, where the assumption* (A.6.6) *is only required for $\kappa > 1$. Either way it requires the finite element method to be of order two, at least.*

A.7. Stability of the semi-discrete diffusion equation

In this section, we extend the stability result to the nodal vector $\mathbf{u}(t)$ of the numerical solution to the semi-discrete diffusion equation.

A.7.1. Error equations

The numerical solution $u_h(x,t) = \sum_{j=1}^N u_j(t)\varphi_j[\mathbf{x}(t)](x)$ with corresponding nodal vector $\mathbf{u} = \mathbf{u}(t) = (u_j(t))_{j=1}^N$, satisfies

$$\frac{\mathrm{d}}{\mathrm{d}t}\left(\mathbf{M}(\mathbf{x})\mathbf{u}\right) + \mathbf{A}(\mathbf{x})\mathbf{u} = \mathbf{f}(\mathbf{x})\,. \tag{A.7.1}$$

The finite element interpolation $u_h^*(\cdot,t)$ of the exact solution $u(\cdot,t)$ with corresponding nodal vector $\mathbf{u}^*(t)$, when inserted into the matrix–vector formulation, yields defects $\mathbf{d}_\mathbf{u}$, corresponding to a finite element function d_h^u, such that

$$\frac{\mathrm{d}}{\mathrm{d}t}\left(\mathbf{M}(\mathbf{x}^*)\mathbf{u}^*\right) + \mathbf{A}(\mathbf{x}^*)\mathbf{u}^* = \mathbf{f}(\mathbf{x}^*) + \mathbf{M}(\mathbf{x}^*)\mathbf{d}_\mathbf{u}\,. \tag{A.7.2}$$

Rewriting (A.7.1) in a similar way as (A.6.3) and subtracting from (A.7.2) yields the error equation

$$\begin{aligned}\frac{\mathrm{d}}{\mathrm{d}t}\big(\mathbf{M}(\mathbf{x}^*)\mathbf{e_u}\big) + \mathbf{A}(\mathbf{x}^*)\mathbf{e_u} = &-\frac{\mathrm{d}}{\mathrm{d}t}\big((\mathbf{M}(\mathbf{x})-\mathbf{M}(\mathbf{x}^*))\mathbf{u}^*\big) - \frac{\mathrm{d}}{\mathrm{d}t}\big((\mathbf{M}(\mathbf{x})-\mathbf{M}(\mathbf{x}^*))\mathbf{e_u}\big)\\ &-\big(\mathbf{A}(\mathbf{x})-\mathbf{A}(\mathbf{x}^*)\big)\mathbf{u}^*\\ &-\big(\mathbf{A}(\mathbf{x})-\mathbf{A}(\mathbf{x}^*)\big)\mathbf{e_u} + (\mathbf{f}(\mathbf{x})-\mathbf{f}(\mathbf{x}^*)) - \mathbf{M}(\mathbf{x}^*)\mathbf{d_u}\,.\end{aligned} \tag{A.7.3}$$

A.7.2. Dual norm

In order to bound the defect in u we need to introduce a different dual norm than in the previous section, which is due to the fact that the defect d_h^u lives on the whole domain $\Omega(t)$ and does not vanish on the boundary. We use the notation $\mathbf{K}(\mathbf{x}^*) = \mathbf{M}(\mathbf{x}^*) + \mathbf{A}(\mathbf{x}^*)$ and consider the dual norm (cf. (A.6.5))

$$\begin{aligned}\|d_h^u\|_{H_h^{-1}(\Omega_h(\mathbf{x}^*))} &= \sup_{0\neq\psi_h\in S_h(\mathbf{x}^*)} \frac{\int_{\Omega_h(\mathbf{x}^*)} d_h^u\psi_h \mathrm{d}x}{\|\psi_h\|_{H^1(\Omega_h(\mathbf{x}^*))}}\\ &= \big(\mathbf{d_u}^{\mathrm{T}}\mathbf{M}(\mathbf{x}^*)\mathbf{K}(\mathbf{x}^*)^{-1}\mathbf{M}(\mathbf{x}^*)\mathbf{d_u}\big)^{1/2} =: \|\mathbf{d_u}\|_{\star,\mathbf{x}^*}\,.\end{aligned} \tag{A.7.4}$$

For simplicity we do not use another notation for the dual norm of $\mathbf{d_u}$, as it will always be clear from context which dual norm is meant. In the following stability proof we need the following technical lemma.

Lemma A.7.1. *For a function $w = w(x,t) : \Omega(t) \to \mathbb{R}^3$, we have*

$$\partial^\bullet(\nabla\cdot w) = \nabla\cdot\partial^\bullet w - \nabla v\cdot\nabla w\,,$$

where $v = v(x,t)$ is the velocity and $\nabla v\cdot\nabla w$ denotes the Frobenius norm inner product, i.e. the Euclidean product of the vectorizations of the matrices.

Proof. Based on Dziuk et al. [2013] a similar identity for the surface divergence is shown in Kovács et al. [2019]. The proof is adapted by embedding everything into a surface $\Gamma(t) = \Omega(t)\times\{0\}\in\mathbb{R}^4$. □

A.7.3. Stability estimate

We are now able to state and prove the stability result for the error $\mathbf{e_u}$. Note that the previous stability estimates for $\mathbf{e_x}$ and $\mathbf{e_v}$ remain valid since the solution to the domain evolution does not depend on the numerical solution u_h, but the solution u_h to the diffusion equation depends on the solution $\mathbf{x}$ of the position vectors, which is reflected in the following proof.

Lemma A.7.2. *Assume that, for some $\kappa > \frac{3}{2}$, the defects are bounded as follows:*

$$\|\mathbf{d_u}(t)\|_{\star,\mathbf{x}^*(t)} \le ch^\kappa\,,\quad \|\mathbf{d}_{\mathbf{v}^\Omega}(t)\|_{\star,\mathbf{x}^*(t)} \le ch^\kappa\,,\quad t\in[0,T]\,. \tag{A.7.5}$$

Then there exists an $h_0 > 0$ such that the following estimate holds for $h \le h_0$ and $t\in[0,T]$, where the constant C is independent of h:

$$\|\mathbf{e_u}(t)\|^2_{\mathbf{M}(\mathbf{x}^*)} + \int_0^t \|\mathbf{e_u}(s)\|^2_{\mathbf{A}(\mathbf{x}^*(s))}\mathrm{d}s \le C\int_0^t \|\mathbf{d_u}(s)\|^2_{\star,\mathbf{x}^*(s)} + \|\mathbf{d_v}(s)\|^2_{\star,\mathbf{x}^*(s)}\mathrm{d}s\,.$$

Proof. The proof is similar to the proof of Lemma A.6.1. Let $0 < t^* \leq T$ be the maximal time such that

$$\begin{aligned} \|\nabla e_x(\cdot,t)\|_{L^\infty(\Omega_h(\mathbf{x}^*(t)))} &\leq h^{(\kappa-3/2)/2}\,, \\ \|e_u(\cdot,t)\|_{L^\infty(\Omega_h(\mathbf{x}^*(t)))} &\leq 1\,. \end{aligned}$$

for all $t \in [0,t^*]$. Note that $e_x(\cdot,0) = 0 = e_u(\cdot,0)$ implies $t^* > 0$. Again, we will prove the error bound for $t \in [0,t^*]$ and then show that t^* coincides with T.

Testing (A.7.3) with $\mathbf{e}_\mathbf{u}^\mathrm{T}$, we obtain (omitting the argument t)

$$\begin{aligned} \mathbf{e}_\mathbf{u}^\mathrm{T}\frac{\mathrm{d}}{\mathrm{d}t}\left(\mathbf{M}(\mathbf{x}^*)\mathbf{e}_\mathbf{u}\right) + \mathbf{e}_\mathbf{u}^\mathrm{T}\mathbf{A}(\mathbf{x}^*)\mathbf{e}_\mathbf{u} = &- \mathbf{e}_\mathbf{u}^\mathrm{T}\frac{\mathrm{d}}{\mathrm{d}t}\left((\mathbf{M}(\mathbf{x})-\mathbf{M}(\mathbf{x}^*))\mathbf{u}^*\right) \\ &- \mathbf{e}_\mathbf{u}^\mathrm{T}\frac{\mathrm{d}}{\mathrm{d}t}\left((\mathbf{M}(\mathbf{x})-\mathbf{M}(\mathbf{x}^*))\mathbf{e}_\mathbf{u}\right) \\ &- \mathbf{e}_\mathbf{u}^\mathrm{T}\left(\mathbf{A}(\mathbf{x})-\mathbf{A}(\mathbf{x}^*)\right)\mathbf{u}^* - \mathbf{e}_\mathbf{u}^\mathrm{T}\left(\mathbf{A}(\mathbf{x})-\mathbf{A}(\mathbf{x}^*)\right)\mathbf{e}_\mathbf{u} \\ &- \mathbf{e}_\mathbf{u}^\mathrm{T}(\mathbf{f}(\mathbf{x})-\mathbf{f}(\mathbf{x}^*)) - \mathbf{e}_\mathbf{u}^\mathrm{T}\mathbf{M}(\mathbf{x}^*)\mathbf{d}_\mathbf{u}\,. \end{aligned} \tag{A.7.6}$$

We estimate the six terms on the right-hand side separately.

(i) We apply the product rule to obtain

$$\mathbf{e}_\mathbf{u}^\mathrm{T}\frac{\mathrm{d}}{\mathrm{d}t}\left((\mathbf{M}(\mathbf{x})-\mathbf{M}(\mathbf{x}^*))\mathbf{u}^*\right) = \mathbf{e}_\mathbf{u}^\mathrm{T}\left(\mathbf{M}(\mathbf{x})-\mathbf{M}(\mathbf{x}*)\right)\dot{\mathbf{u}}^* + \mathbf{e}_\mathbf{u}^\mathrm{T}\left(\frac{\mathrm{d}}{\mathrm{d}t}\left(\mathbf{M}(\mathbf{x})-\mathbf{M}(\mathbf{x}^*)\right)\right)\mathbf{u}^* \tag{A.7.7}$$

For the first term of (A.7.7) we use Lemma A.5.1, an L^2-L^2-L^∞-estimate and Lemma A.5.3 to obtain

$$\begin{aligned} \left|\mathbf{e}_\mathbf{u}^\mathrm{T}\left(\mathbf{M}(\mathbf{x})-\mathbf{M}(\mathbf{x}^*)\right)\dot{\mathbf{u}}^*\right| &= \left|\int_0^1\int_{\Omega_h^\theta} e_u^\theta(\nabla\cdot e_x^\theta)\partial_h^\bullet u_h^{*,\theta}\mathrm{d}x\mathrm{d}\theta\right| \\ &\leq \int_0^1 \left\|e_u^\theta\right\|_{L^2(\Omega_h^\theta)}\left\|\nabla\cdot e_x^\theta\right\|_{L^2(\Omega_h^\theta)}\left\|\partial_h^\bullet u_h^{*,\theta}\right\|_{L^\infty(\Omega_h^\theta)}\mathrm{d}\theta \\ &\leq c\,\|\mathbf{e}_\mathbf{u}\|_{\mathbf{M}(\mathbf{x}^*)}\,\|\mathbf{e}_\mathbf{x}\|_{\mathbf{A}(\mathbf{x}^*)}\left\|\partial_h^\bullet u_h^{*,0}\right\|_{L^\infty(\Omega_h(\mathbf{x}^*))}\,. \end{aligned}$$

With an elementary computation the last term can be bounded by

$$\|\partial_h^\bullet u_h^{*,0}\|_{L^\infty(\Omega_h(\mathbf{x}^*))} \leq c\|\dot{\mathbf{u}}^*(t)\|_\infty\,,$$

and the nodal values of $\dot{\mathbf{u}}^*(t)$ are exactly the nodal values of $\partial^\bullet u(\cdot,t)$. The smoothness assumption on u and $\partial^\bullet u$ thus implies $\|\dot{\mathbf{u}}^*\|_\infty \leq c$, and we arrive at

$$\left|\mathbf{e}_\mathbf{u}^\mathrm{T}\left(\mathbf{M}(\mathbf{x})-\mathbf{M}(\mathbf{x}^*)\right)\dot{\mathbf{u}}^*\right| \leq c\|\mathbf{e}_\mathbf{u}\|_{\mathbf{M}(\mathbf{x}^*)}\|\mathbf{e}_\mathbf{x}\|_{\mathbf{A}(\mathbf{x}^*)}\,.$$

Using the basis functions, Lemma A.5.1 and the Leibniz formula, a tedious but elementary computation yields

$$\begin{aligned} \mathbf{e}_\mathbf{u}^\mathrm{T}\frac{\mathrm{d}}{\mathrm{d}t}\left(\mathbf{M}(\mathbf{x})-\mathbf{M}(\mathbf{x}^*)\right)\mathbf{u}^* = &\int_0^1\int_{\Omega_h^\theta} e_u^\theta\partial_h^\bullet\nabla\cdot e_x^\theta u_h^{*,\theta}\mathrm{d}x\mathrm{d}\theta \\ &+ \int_0^1\int_{\Omega_h^\theta} e_u^\theta\left(\nabla\cdot e_x^\theta\right)u_h^{*,\theta}\nabla\cdot v_h^\theta\mathrm{d}x\mathrm{d}\theta\,, \end{aligned}$$

where v_h^θ is the velocity of Ω_h^θ as a function of t, i. e. the finite element function in $S_h(\mathbf{x}^*(t) + \theta\mathbf{e}_\mathbf{x}(t))$ with nodal vector $\dot{\mathbf{x}}^* + \theta\dot{\mathbf{e}}_\mathbf{x} = \mathbf{v}^* + \theta\mathbf{e}_\mathbf{v}$, implying $v_h^\theta = v_h^{*,\theta} + \theta e_v^\theta$. We will estimate both integrals separately, where we use the identity from Lemma A.7.1. With $\partial_h^\bullet e_x^\theta = e_v^\theta$ and writing $v_h^\theta = v_h^{*,\theta} + \theta e_v^\theta$ we obtain the following estimate for the first integral: (we write L^p instead of $L^p(\Omega_h^\theta)$ and $\mathbf{M}$ and $\mathbf{A}$ instead of $\mathbf{M}(\mathbf{x}^*)$ and $\mathbf{A}(\mathbf{x}^*)$ in the occurring norms)

$$
\begin{aligned}
&\left| \int_0^1 \int_{\Omega_h^\theta} e_u^\theta \partial_h^\bullet \nabla \cdot e_x^\theta u_h^{*,\theta} \mathrm{d}x\mathrm{d}\theta \right| \\
&\leq \int_0^1 \left\| e_u^\theta \right\|_{L^2} \left(\left\| \nabla \cdot e_v^\theta \right\|_{L^2} + \left\| \nabla v_h^{*,\theta} \right\|_{L^\infty} \left\| \nabla e_x^\theta \right\|_{L^2} + \theta \left\| \nabla e_v^\theta \right\|_{L^2} \left\| \nabla e_x^\theta \right\|_{L^\infty} \right) \left\| u_h^{*,\theta} \right\|_{L^\infty} \\
&\leq c \left\| \mathbf{e_u} \right\|_{L^2} \left(\|\nabla e_v\|_{L^2} + \|\nabla v_h^*\|_{L^\infty} \|\nabla e_x\|_{L^2} + \|\nabla e_v\|_{L^2} \|\nabla e_x\|_{L^\infty} \right) \|u_h^*\|_{L^\infty} \\
&\leq c \|\mathbf{e_u}\|_{\mathbf{M}} \left(\|\mathbf{e_v}\|_{\mathbf{A}} + \|\nabla v_h^*\|_{L^\infty} \|\mathbf{e_x}\|_{\mathbf{A}} + \|\mathbf{e_v}\|_{\mathbf{A}} \|\nabla e_x\|_{L^\infty} \right) \|\mathbf{u}^*\|_\infty \\
&\leq c \|\mathbf{e_u}\|_{\mathbf{M}(\mathbf{x}^*)} \left(\|\mathbf{e_v}\|_{\mathbf{A}(\mathbf{x}^*)} + \|\mathbf{e_x}\|_{\mathbf{A}(\mathbf{x}^*)} \right) .
\end{aligned}
$$

We analogously estimate the second integral and obtain

$$
\left| \int_0^1 \int_{\Omega_h^\theta} e_u^\theta \left(\nabla \cdot e_x^\theta \right) u_h^{*,\theta} \nabla \cdot v_h^\theta \mathrm{d}x\mathrm{d}\theta \right| \leq c \|\mathbf{e_u}\|_{\mathbf{M}(\mathbf{x}^*)} \left(\|\mathbf{e_v}\|_{\mathbf{A}(\mathbf{x}^*)} + \|\mathbf{e_x}\|_{\mathbf{A}(\mathbf{x}^*)} \right) .
$$

Finally, we obtain for the first term of (A.7.6):

$$
-\mathbf{e_u}^\mathrm{T} \frac{\mathrm{d}}{\mathrm{d}t} \left((\mathbf{M}(\mathbf{x}) - \mathbf{M}(\mathbf{x}^*)) \mathbf{u}^* \right) \leq c \left\| \mathbf{e_u} \right\|_{\mathbf{M}(\mathbf{x}^*)} \left(\left\| \mathbf{e_v} \right\|_{\mathbf{A}(\mathbf{x}^*)} + \left\| \mathbf{e_x} \right\|_{\mathbf{A}(\mathbf{x}^*)} \right) .
$$

(ii) For the second term of (A.7.6), we obtain similarly

$$
\begin{aligned}
&- \mathbf{e_u}^\mathrm{T} \frac{\mathrm{d}}{\mathrm{d}t} \left((\mathbf{M}(\mathbf{x}) - \mathbf{M}(\mathbf{x}^*)) \mathbf{e_u} \right) \\
&= -\frac{1}{2} \mathbf{e_u}^\mathrm{T} \left(\frac{\mathrm{d}}{\mathrm{d}t} (\mathbf{M}(\mathbf{x}) - \mathbf{M}(\mathbf{x}^*)) \right) \mathbf{e_u} - \frac{1}{2} \frac{\mathrm{d}}{\mathrm{d}t} \left(\mathbf{e_u}^\mathrm{T} (\mathbf{M}(\mathbf{x}) - \mathbf{M}(\mathbf{x}^*) \mathbf{e_u} \right) \\
&\leq c \|\mathbf{e_u}\|_{\mathbf{M}(\mathbf{x}^*)} \left(\|\mathbf{e_v}\|_{\mathbf{A}(\mathbf{x}^*)} + \|\mathbf{e_x}\|_{\mathbf{A}(\mathbf{x}^*)} \right) \|e_u\|_{L^\infty(\Omega_h(\mathbf{x}^*))} - \frac{1}{2} \frac{\mathrm{d}}{\mathrm{d}t} \left(\mathbf{e_u}^\mathrm{T} (\mathbf{M}(\mathbf{x}) - \mathbf{M}(\mathbf{x}^*)) \mathbf{e_u} \right) \\
&\leq C \|\mathbf{e_u}\|_{\mathbf{M}(\mathbf{x}^*)} \left(\|\mathbf{e_v}\|_{\mathbf{A}(\mathbf{x}^*)} + \|\mathbf{e_x}\|_{\mathbf{A}(\mathbf{x}^*)} \right) - \frac{1}{2} \frac{\mathrm{d}}{\mathrm{d}t} \left(\mathbf{e_u}^\mathrm{T} (\mathbf{M}(\mathbf{x}) - \mathbf{M}(\mathbf{x}^*)) \mathbf{e_u} \right) .
\end{aligned}
$$

(iii) For the third term we use Lemma A.5.1 and Lemma A.5.3 and estimate

$$
\begin{aligned}
\left| \mathbf{e_u}^\mathrm{T} (\mathbf{A}(\mathbf{x}) - \mathbf{A}(\mathbf{x}^*)) \mathbf{u}^* \right| &\leq c \int_0^1 \|\nabla e_u^\theta\|_{L^2(\Omega_h^\theta)} \|\nabla e_x^\theta\|_{L^2(\Omega_h^\theta)} \|\nabla u_h^{*,\theta}\|_{L^\infty(\Omega_h^\theta)} \mathrm{d}x\mathrm{d}\theta \\
&\leq c \|\nabla e_u\|_{L^2(\Omega_h(\mathbf{x}^*))} \|\nabla e_x\|_{L^2(\Omega_h(\mathbf{x}^*))} \|\nabla u_h^*\|_{L^\infty(\Omega_h(\mathbf{x}^*))} \\
&\leq C \|\mathbf{e_u}\|_{\mathbf{A}(\mathbf{x}^*)} \|\mathbf{e_x}\|_{\mathbf{A}(\mathbf{x}^*)} ,
\end{aligned}
$$

where we have used the smoothness assumption on u.

(iv) Similarly, we estimate

$$\begin{aligned}\left|\mathbf{e}_\mathbf{u}^\mathrm{T}(\mathbf{A}(\mathbf{x})-\mathbf{A}(\mathbf{x}^*))\mathbf{e}_\mathbf{u}\right| &= \left|\int_0^1\int_{\Omega_h^\theta}\nabla e_u^\theta\left(D_{\Omega_h^\theta}e_x^\theta\right)\nabla e_u^\theta \mathrm{d}x\mathrm{d}\theta\right| \\ &\le c\|\nabla e_u\|^2_{L^2(\Omega_h(\mathbf{x}^*))}\|\nabla e_x\|_{L^\infty(\Omega_h(\mathbf{x}^*))} \\ &\le ch^{(\kappa-3/2)/2}\|\mathbf{e}_\mathbf{u}\|^2_{\mathbf{A}(\mathbf{x}^*)}\,.\end{aligned}$$

(v) For the fifth term we use the Leibniz formula, an L^∞-L^2-L^2-estimate and Lemma A.5.3, to obtain

$$\begin{aligned}&\mathbf{e}_\mathbf{u}^\mathrm{T}(\mathbf{f}(\mathbf{x})-\mathbf{f}(\mathbf{x}^*)) \\ &= \int_{\Omega_h^1} fe_u^1\mathrm{d}x - \int_{\Omega_h^0} fe_u^0\mathrm{d}x = \int_0^1\frac{\mathrm{d}}{\mathrm{d}\theta}\int_{\Omega_h^\theta} fe_u^\theta\mathrm{d}x\mathrm{d}\theta \\ &= \int_0^1\int_{\Omega_h^\theta}\partial_\theta^\bullet fe_u^\theta + f\underbrace{\partial_\theta^\bullet e_u^\theta}_{=0} + fe_u^\theta\nabla\cdot e_x^\theta\mathrm{d}x\mathrm{d}\theta \\ &= \int_0^1\int_{\Omega_h^\theta} f'e_x^\theta e_u^\theta + fe_u^\theta\nabla\cdot e_x^\theta\mathrm{d}x\mathrm{d}\theta \\ &\le \int_0^1 \|f'\|_{L^\infty(\Omega_h^\theta)}\|e_x^\theta\|_{L^2(\Omega_h^\theta)}\|e_u^\theta\|_{L^2(\Omega_h^\theta)} + \|f\|_{L^\infty(\Omega_h^\theta)}\|e_u^\theta\|_{L^2(\Omega_h^\theta)}\|\nabla\cdot e_x^\theta\|_{L^2(\Omega_h^\theta)}\mathrm{d}\theta \\ &\le c\|\mathbf{e}_\mathbf{x}\|_{\mathbf{M}(\mathbf{x}^*)}\|\mathbf{e}_\mathbf{u}\|_{\mathbf{M}(\mathbf{x}^*)} + c\|\mathbf{e}_\mathbf{x}\|_{\mathbf{A}(\mathbf{x}^*)}\|\mathbf{e}_\mathbf{u}\|_{\mathbf{M}(\mathbf{x}^*)} \\ &\le c\|\mathbf{e}_\mathbf{x}\|_{\mathbf{A}(\mathbf{x}^*)}\|\mathbf{e}_\mathbf{u}\|_{\mathbf{M}(\mathbf{x}^*)}\,,\end{aligned}$$

where we have used the Poincaré inequality in the last step, which yields for $e_x^\ell \in H_0^1(\Omega(t))$

$$\|\mathbf{e}_\mathbf{x}\|_{\mathbf{M}(\mathbf{x}^*)} = \|e_x\|_{L^2(\Omega_h(\mathbf{x}^*(t)))} \le c\|e_x^\ell\|_{L^2(\Omega(t))} \le c\|\nabla e_x^\ell\|_{L^2(\Omega(t))} \le c\|\mathbf{e}_\mathbf{x}\|_{\mathbf{A}(\mathbf{x}^*)}\,.$$

(vi) For the last term of (A.7.6), we use

$$\begin{aligned}\mathbf{e}_\mathbf{u}^\mathrm{T}\mathbf{M}(\mathbf{x}^*)\mathbf{d}_\mathbf{u} &= \mathbf{e}_\mathbf{u}^\mathrm{T}\mathbf{K}(\mathbf{x}^*)^{\frac12}\mathbf{K}(\mathbf{x}^*)^{-\frac12}\mathbf{M}(\mathbf{x}^*)\mathbf{d}_\mathbf{u} \\ &\le \frac16\|\mathbf{K}(\mathbf{x}^*)^{\frac12}\mathbf{e}_\mathbf{u}\|_2^2 + C\|\mathbf{K}(\mathbf{x}^*)^{-\frac12}\mathbf{M}(\mathbf{x}^*)\mathbf{d}_\mathbf{u}\|_2^2 \\ &= \frac16\|\mathbf{e}_\mathbf{u}\|^2_{\mathbf{M}(\mathbf{x}^*)} + \frac16\|\mathbf{e}_\mathbf{u}\|^2_{\mathbf{A}(\mathbf{x}^*)} + C\|\mathbf{d}_\mathbf{u}\|^2_{\star,\mathbf{x}^*}\,.\end{aligned}$$

Combining estimates (i)-(vi), using Young's inequality on each product, for $h \le h_0$ sufficiently small such that $ch^{(\kappa-3/2)/2} \le 1/6$, we obtain after absorbing $\|\mathbf{e}_\mathbf{u}\|^2_{\mathbf{A}(\mathbf{x}^*)}$:

$$\begin{aligned}\frac12\frac{\mathrm{d}}{\mathrm{d}t}\|\mathbf{e}_\mathbf{u}\|^2_{\mathbf{M}(\mathbf{x}^*)} + \frac12\|\mathbf{e}_\mathbf{u}\|^2_{\mathbf{A}(\mathbf{x}^*)} &\le c\|\mathbf{e}_\mathbf{u}\|^2_{\mathbf{M}(\mathbf{x}^*)} + c\|\mathbf{e}_\mathbf{x}\|^2_{\mathbf{A}(\mathbf{x}^*)} + c\|\mathbf{e}_\mathbf{v}\|^2_{\mathbf{A}(\mathbf{x}^*)} \\ &\quad - \frac12\frac{\mathrm{d}}{\mathrm{d}t}\left(\mathbf{e}_\mathbf{u}^\mathrm{T}(\mathbf{M}(\mathbf{x})-\mathbf{M}(\mathbf{x}^*))\mathbf{e}_\mathbf{u}\right) + c\|\mathbf{d}_\mathbf{u}\|^2_{\star,\mathbf{x}^*}\,.\end{aligned}$$

Inserting the estimates from Lemma A.6.1, we have

$$\frac{\mathrm{d}}{\mathrm{d}t}\|\mathbf{e_u}\|^2_{\mathbf{M}(\mathbf{x}^*)} + \|\mathbf{e_u}\|^2_{\mathbf{A}(\mathbf{x}^*)} \leq c\|\mathbf{e_u}\|^2_{\mathbf{M}(\mathbf{x}^*)} + c\|\mathbf{d_v}\|^2_{\star,\mathbf{x}^*} + c\int_0^t \|\mathbf{d_v}(s)\|^2_{\star,\mathbf{x}^*}\mathrm{d}s \\ - \frac{\mathrm{d}}{\mathrm{d}t}\left(\mathbf{e}_\mathbf{u}^{\mathrm{T}}(\mathbf{M}(\mathbf{x}) - \mathbf{M}(\mathbf{x}^*))\mathbf{e_u}\right) + c\|\mathbf{d_u}\|^2_{\star,\mathbf{x}^*}\,.$$

Integrating from 0 to t for $t \in [0, t^*]$ and using a Gronwall argument as in part (C) of [Kovács et al., 2019, Proposition 6.1], we finally obtain the desired result for $t \in [0, t^*]$. The proof is then finished by showing that t^* coincides with T, which is due to the same argument as in the previous section. □

Remark A.7.3. *The previous lemma remains valid in the two-dimensional case, where the assumption* (A.7.5) *is only required for* $\kappa > 1$.

A.8. Defect bounds

In this section we show that the smallness assumptions in Lemma A.6.1 and Lemma A.7.2 are satisfied for $\kappa = k \geq 2$, which in combination with the stability results will lead to the desired error bounds. We remind that we have different dual norm definitions (A.6.5) and (A.7.4) since the defect functions live in different finite element spaces. We avoid using different notations, because the dual norms only appear on $\mathbf{d_v}$ and $\mathbf{d_u}$, so it is always clear from context which definition is meant.

A.8.1. The interpolating domain

In order to estimate the defect $\mathbf{d_u}$ we need to introduce a discrete velocity on the smooth domain, which is denoted by $\widehat{v}_h$.

Recall that $\Omega(t)$ can be described as image $X(\cdot, t)(\Omega_0)$ with a sufficiently smooth map $X : \Omega_0 \times [0, T] \to \mathbb{R}^3$. The nodes $x_j^*(t) = X(x_j^0, t)$ define an interpolating domain which is parametrized over Ω_h^0 via

$$X_h^*(p_h, t) = \sum_{j=1}^N x_j^*(t)\varphi_j[\mathbf{x}(0)](p_h)\,, \quad p_h \in \Omega_h^0\,.$$

The velocity of the interpolating domain is given, using the transport property of the basis functions (A.3.1), by

$$v_h^*(\cdot, t) = \sum_{j=1}^N v_j^*(t)\varphi_j[\mathbf{x}^*(t)](\cdot) \quad \text{with } v_j^*(t) = \frac{\mathrm{d}}{\mathrm{d}t}x_j^*(t)\,.$$

For a material point $p_h(t) = X_h^*(p_h, t) \in \Omega_h(\mathbf{x}^*(t))$, $p_h \in \Omega_h^0$, on the interpolated exact domain, this velocity satisfies

$$v_h^*(p_h(t), t) = \frac{\mathrm{d}}{\mathrm{d}t}X_h^*(p_h, t)\,.$$

Associated with $p_h(t)$ is its lifted material point $y(t) = \Lambda_h(p_h(t), t) \in \Omega(t)$. This lifted point moves with velocity

$$\widehat{v}_h(y(t), t) = \frac{\mathrm{d}}{\mathrm{d}t} y(t) = \frac{\mathrm{d}}{\mathrm{d}t} \Lambda_h(p_h(t), t) = (\partial_t \Lambda_h)(p_h(t), t) + v_h^*(p_h(t), t) \nabla \Lambda_h(p_h(t), t)\,.$$

We can use these velocities to define discrete material derivatives for functions φ_h and φ defined on $\Omega_h(\mathbf{x}^*(t))$ and $\Omega(t)$, respectively, via

$$\begin{aligned} \partial^\bullet_{v_h^*} \varphi_h &= \partial_t \varphi_h + v_h^* \cdot \nabla \varphi_h\,, \\ \partial^\bullet_{\widehat{v}_h} \varphi &= \partial_t \varphi + \widehat{v}_h \cdot \nabla \varphi\,. \end{aligned}$$

The basis functions $\varphi_j[\mathbf{x}^*]$ enjoy the transport property $\partial^\bullet_{v_h^*} \varphi_j = 0$. It is not true in general that the lifted basis functions satisfy $\partial^\bullet_v \varphi_j^\ell = 0$, with $\partial^\bullet_v = \partial^\bullet$ as defined in (A.2.1). In particular, we have $(\partial^\bullet_{v_h^*} \varphi_j)^\ell \neq \partial^\bullet \varphi_j^\ell$ in general. The following lemma shows that the transport property is satisfied with the discrete velocity defined above, which will be crucial in the following.

Lemma A.8.1. *For $j = 1, \dots, N$, we have*

$$\partial^\bullet_{\widehat{v}_h} \varphi_j^\ell = 0\,.$$

In particular, we have for any finite element function $\eta_h \in S_h(\mathbf{x}^*(t))$ and for any $u \in H^{k+1}(\Omega(t))$

$$\left(\partial^\bullet_{v_h^*} \eta_h\right)^\ell = \partial^\bullet_{\widehat{v}_h} \eta_h^\ell \quad \text{and} \quad \left(\partial^\bullet_{v_h^*} \widetilde{I}_h u\right)^\ell = \partial^\bullet_{\widehat{v}_h} I_h u = I_h \partial^\bullet_{\widehat{v}_h} u\,.$$

Proof. Follows from Definition A.3.1, the chain rule and the transport property of the basis functions, cf. [Dziuk and Elliott, 2013a, Lemma 4.1]. □

For the following defect estimate, we introduce the notation

$$\begin{aligned} q_h^*(\eta_h, \chi_h) &= \int_{\Omega_h^*(t)} \eta_h \chi_h \nabla \cdot v_h^* \mathrm{d}x\,, \\ \widehat{q}_h(\eta, \chi) &= \int_{\Omega(t)} \eta \chi \nabla \cdot \widehat{v}_h \mathrm{d}x\,. \end{aligned}$$

Lemma A.8.2. *For any $\eta(\cdot, t)$, $\chi(\cdot, t) \in H^1(\Omega(t))$, we have*

$$\begin{aligned} \frac{\mathrm{d}}{\mathrm{d}t} m(\eta, \chi) &= m(\partial^\bullet \eta, \chi) + m(\eta, \partial^\bullet \chi) + q(\eta, \chi)\,, \\ \frac{\mathrm{d}}{\mathrm{d}t} m(\eta, \chi) &= m\left(\partial^\bullet_{\widehat{v}_h} \eta, \chi\right) + m\left(\eta, \partial^\bullet_{\widehat{v}_h} \chi\right) + \widehat{q}_h(\eta, \chi)\,. \end{aligned}$$

On the discrete domain, for $\eta_h(\cdot, t)$, $\chi_h(\cdot, t) \in S_h(\Omega_h(\mathbf{x}^*(t)))$, we have

$$\frac{\mathrm{d}}{\mathrm{d}t} m_h^*(\eta_h, \chi_h) = m_h^*\left(\partial^\bullet_{v_h^*} \eta_h, \chi_h\right) + m_h^*\left(\eta_h, \partial^\bullet_{v_h^*} \chi_h\right) + q_h^*(\eta_h, \chi_h)\,.$$

Proof. Follows directly from the Leibniz formula (see [Elliott and Ranner, 2021, Section 8.3]). □

We are now in position to formulate and prove the required defect estimates.

Lemma A.8.3. *Let the domain $\Omega(t)$ and the exact solution (u, v, X) be sufficiently smooth. Then there is a constant $c > 0$ and an $h_0 > 0$, such that for all $h \leq h_0$ and all $t \in [0, T]$, the defects $\mathbf{d}_{\mathbf{v}^\Omega}$ and $\mathbf{d}_{\mathbf{u}}$ are bounded by*

$$\begin{aligned} \|\mathbf{d}_{\mathbf{v}^\Omega}\|_{\star,\mathbf{x}^*} &\leq ch^k\,, \\ \|\mathbf{d}_{\mathbf{u}}\|_{\star,\mathbf{x}^*} &\leq ch^k\,. \end{aligned}$$

Proof. We start with estimating $\mathbf{d}_{\mathbf{u}}$. The defect equation (A.7.2) is equivalent to

$$\begin{aligned} m_h^*(d_u, \varphi_h) &= \frac{\mathrm{d}}{\mathrm{d}t} m_h^*(\widetilde{I}_h u, \varphi_h) + a_h^*(\widetilde{I}_h u, \varphi_h) - m_h^*(f, \varphi_h) \\ &= m_h^*\left(\partial^\bullet_{v_h^*} \widetilde{I}_h u, \varphi_h\right) + q_h^*(\widetilde{I}_h u, \varphi_h) + a_h^*(\widetilde{I}_h u, \varphi_h) - m_h^*(f, \varphi_h) \end{aligned}$$

for all $\varphi_h \in S_h(\mathbf{x}^*)$. The exact solution u satisfies, using Lemma A.8.2 and Lemma A.8.1,

$$\begin{aligned} 0 &= \frac{\mathrm{d}}{\mathrm{d}t} m(u, \varphi_h^\ell) + a(u, \varphi_h^\ell) - m(f, \varphi_h^\ell) \\ &= m\left(\partial^\bullet_{\widehat{v}_h} u, \varphi_h^\ell\right) + \widehat{q}_h(u, \varphi_h^\ell) + a(u, \varphi_h^\ell) - m(f, \varphi_h^\ell)\,. \end{aligned}$$

Subtracting both terms yields

$$\begin{aligned} m_h^*(d_u, \varphi_h) = &\left(m_h^*\left(\partial^\bullet_{v_h^*} \widetilde{I}_h u, \varphi_h\right) - m\left(\partial^\bullet_{\widehat{v}_h} u, \varphi_h^\ell\right)\right) \\ &+ \left(q_h^*(\widetilde{I}_h u, \varphi_h) - \widehat{q}_h(u, \varphi_h^\ell)\right) \\ &+ \left(a_h^*(\widetilde{I}_h u, \varphi_h) - a(u, \varphi_h^\ell)\right) - \left((m_h^*(f, \varphi_h) - m(f, \varphi_h^\ell))\right)\,. \end{aligned} \tag{A.8.1}$$

We will estimate the four differences separately.

(i) For the first difference we use $\partial^\bullet_{\widehat{v}_h} I_h u = I_h \partial^\bullet_{\widehat{v}_h} u$:

$$\begin{aligned} \left|m_h^*\left(\partial^\bullet_{v_h^*} \widetilde{I}_h u, \varphi_h\right) - m\left(\partial^\bullet_{\widehat{v}_h} u, \varphi_h^\ell\right)\right| \leq &\left|m_h^*\left(\partial^\bullet_{v_h^*} \widetilde{I}_h u, \varphi_h\right) - m\left(\partial^\bullet_{\widehat{v}_h} I_h u, \varphi_h^\ell\right)\right| \\ &+ \left|m\left(I_h \partial^\bullet_{\widehat{v}_h} u - \partial^\bullet_{\widehat{v}_h} u, \varphi_h^\ell\right)\right|\,. \end{aligned}$$

For the first term note that $(\partial^\bullet_{v_h^*} \widetilde{I}_h u)^\ell = \partial^\bullet_{\widehat{v}_h} I_h u$, so Lemma A.5.6 yields

$$\left|m_h^*\left(\partial^\bullet_{v_h^*} \widetilde{I}_h u, \varphi_h\right) - m\left(\partial^\bullet_{\widehat{v}_h} I_h u, \varphi_h^\ell\right)\right| \leq ch^k \left\|\partial^\bullet_{\widehat{v}_h} I_h u\right\|_{L^2(\Omega)} \|\varphi_h^\ell\|_{L^2(\Omega)}\,.$$

Now we bound

$$\begin{aligned} \left\|\partial^\bullet_{\widehat{v}_h} I_h u\right\|_{L^2(\Omega)} &= \left\|I_h \partial^\bullet_{\widehat{v}_h} u - \partial^\bullet_{\widehat{v}_h} u + \partial^\bullet_{\widehat{v}_h} u\right\|_{L^2(\Omega)} \\ &\leq (ch^k + 1)\left\|\partial^\bullet_{\widehat{v}_h} u - \partial^\bullet u + \partial^\bullet u\right\|_{L^2(\Omega)} \leq c\,, \end{aligned}$$

where we have used that $\|\partial^\bullet_{\widehat{v}_h} u - \partial^\bullet u\|_{L^2(\Omega)} \leq ch^{k+1}$ (see [Elliott and Ranner, 2021, Lemma 8.23]) and the regularity assumption on u. Similarly

$$\begin{aligned}\left|m\left(I_h\partial^\bullet_{\widehat{v}_h} u - \partial^\bullet_{\widehat{v}_h} u, \varphi_h^\ell\right)\right| &\leq \left\|I_h\partial^\bullet_{\widehat{v}_h} u - \partial^\bullet_{\widehat{v}_h} u\right\|_{L^2(\Omega)} \left\|\varphi_h^\ell\right\|_{L^2(\Omega)} \\ &\leq ch^k \left\|\partial^\bullet_{\widehat{v}_h} u\right\| \left\|\varphi_h^\ell\right\|_{L^2(\Omega)} \leq ch^k \left\|\varphi_h^\ell\right\|_{L^2(\Omega)} .\end{aligned}$$

Altogether, we have for the first difference of (A.8.1)

$$\left|m_h^*\left(\partial^\bullet_{v_h^*}\widetilde{I}_h u, \varphi_h\right) - m\left(\partial^\bullet_{\widehat{v}_h} u, \varphi_h^\ell\right)\right| \leq ch^k \left\|\varphi_h^\ell\right\|_{L^2(\Omega)} .$$

(ii) In a similar way:

$$\left|q_h^*(\widetilde{I}_h u, \varphi_h) - \widehat{q}_h(u, \varphi_h^\ell)\right| \leq \left|q_h^*(\widetilde{I}_h u, \varphi_h) - \widehat{q}_h(I_h u, \varphi_h^\ell)\right| + \left|\widehat{q}_h(I_h u - u, \varphi_h^\ell)\right| .$$

For the first term, we use [Elliott and Ranner, 2021, Lemma 8.24]:

$$\left|q_h^*(\widetilde{I}_h u, \varphi_h) - \widehat{q}_h(I_h u, \varphi_h^\ell)\right| \leq ch^{k+1} \|I_h u\|_{L^2(\Omega)} \left\|\varphi_h^\ell\right\| \leq ch^{k+1} \left\|\varphi_h^\ell\right\|_{L^2(\Omega)} .$$

For the second term, we use an L^2-L^2-L^∞ estimate and [Elliott and Ranner, 2021, Lemma 8.24] to bound $\|\nabla \widehat{v}_h\|_{L^\infty(\Omega)}$:

$$\begin{aligned}\left|\widehat{q}_h(I_h u - u, \varphi_h^\ell)\right| &\leq \|I_h u - u\|_{L^2(\Omega)} \|\varphi_h^\ell\|_{L^2(\Omega)} \|\nabla \cdot \widehat{v}_h\|_{L^\infty(\Omega)} \\ &\leq ch^{k+1} \|\varphi_h^\ell\|_{L^2(\Omega)} \|\nabla \widehat{v}_h\|_{L^\infty(\Omega)} \leq ch^{k+1} \|\varphi_h^\ell\|_{L^2(\Omega)} .\end{aligned}$$

(iii) The third term of (A.8.1) is estimated similarly:

$$\begin{aligned}\left|a_h^*(\widetilde{I}_h u, \varphi_h) - a(u, \varphi_h^\ell)\right| &\leq \left|a_h^*(\widetilde{I}_h u, \varphi_h) - a(I_h u, \varphi_h^\ell)\right| + \left|a(I_h u - u, \varphi_h^\ell)\right| \\ &\leq ch^k \|\nabla I_h u\|_{L^2(\Omega)} \|\nabla \varphi_h^\ell\|_{L^2(\Omega)} + \|\nabla (I_h u - u)\|_{L^2(\Omega)} \|\nabla \varphi_h^\ell\|_{L^2(\Omega)} \\ &\leq ch^k \|\varphi_h^\ell\|_{H^1(\Omega)} .\end{aligned}$$

(iv) For the last term of (A.8.1) we immediately have

$$\left|m_h^*(f, \varphi_h) - m(f, \varphi_h^\ell)\right| \leq ch^k \|f\|_{L^2(\Omega)} \|\varphi_h^\ell\|_{L^2(\Omega)} .$$

Putting those four estimates together, using norm equivalence, we obtain

$$\|\mathbf{d_u}\|_{\star,\mathbf{x}^*} = \|d_u\|_{H_h^{-1}(\Omega(\mathbf{x}^*))} = \sup_{0 \neq \varphi_h \in S_h(\mathbf{x}^*)} \frac{m_h^*(d_u, \varphi_h)}{\|\varphi_h\|_{H^1(\Omega(\mathbf{x}^*))}} \leq ch^k .$$

Now we estimate $\mathbf{d}_{\mathbf{v}^\Omega}$, which is defined by the defect equation (A.6.2). We set $\mathbf{d}_{\mathbf{v}}^{\mathrm{T}} = (0, \mathbf{d}_{\mathbf{v}^\Omega}^{\mathrm{T}})$ and $\mathbf{w}^{\mathrm{T}} = (0, \mathbf{w}^{\Omega,\mathrm{T}})$ for $\mathbf{w}^\Omega \in \mathbb{R}^{3N_\Omega}$ and test with $\mathbf{w}^\Omega$ to obtain with a computation similar to (A.6.11) (omitting the tensor notation) $\mathbf{w}^{\mathrm{T}}\mathbf{M}(\mathbf{x}^*)\mathbf{d}_{\mathbf{v}} = \mathbf{w}^{\mathrm{T}}\mathbf{A}(\mathbf{x}^*)\mathbf{v}^*$ which is equivalent to

$$\begin{aligned}\int_{\Omega_h(\mathbf{x}^*)} \varphi_h \cdot d_h \mathrm{d}x &= \int_{\Omega_h(\mathbf{x}^*)} \nabla \varphi_h \cdot \nabla v_h^* \mathrm{d}x \\ &= a_h(\varphi_h, \widetilde{I}_h v) - a(\varphi_h^\ell, I_h v) + a(\varphi_h^\ell, I_h v)\end{aligned} \tag{A.8.2}$$

for all $\varphi_h \in S_{0,h}(\mathbf{x}^*)$. We will estimate the first difference and the second term of (A.8.2) separately, starting with the second term. Since $\varphi_h \in S_{0,h}(\mathbf{x}^*)$ we have $\varphi_h^\ell \in H_0^1(\Omega(t))$ and thus $a(\varphi_h^\ell, v) = 0$. With Proposition A.3.2, we obtain

$$\begin{aligned} a(\varphi_h^\ell, I_h v) = a(\varphi_h^\ell, I_h v - v) &\leq \|\nabla \varphi_h^\ell\|_{L^2(\Omega)} \|\nabla(I_h v - v)\|_{L^2(\Omega)} \\ &\leq c h^k \|\nabla \varphi_h^\ell\|_{L^2(\Omega)} \|v\|_{H^{k+1}(\Omega)} \,. \end{aligned}$$

The first difference in (A.8.2) is estimated analogously to (iii) in the first part of this proof and yields

$$|a_h(\varphi_h, \widetilde{I}_h v) - a(\varphi_h^\ell, I_h v)| \leq c h^k \|\nabla \varphi_h^\ell\|_{L^2(\Omega)}$$

for $h \leq h_0$ sufficiently small using the regularity assumption.

Putting these estimates together yields with Lemma A.5.5:

$$\|\mathbf{d}_{\mathbf{v}^\Omega}\|_{\star,\mathbf{x}^*} = \sup_{0 \neq \mathbf{w}^\Omega \in \mathbb{R}^{3N_\Omega}} \frac{\mathbf{d}_{\mathbf{v}^\Omega}^{\mathrm{T}} \mathbf{M}_{22}(\mathbf{x}*) \mathbf{w}^\Omega}{\|\mathbf{w}^\Omega\|_{\mathbf{A}_{22}(\mathbf{x}^*)}} \leq c h^k \,.$$

□

A.9. Proof of Theorem A.4.1

We prove the first error bound. The remaining ones are shown analogously. The error is decomposed using interpolation and lift:

$$u_h^L - u = \left(\widehat{u}_h - \widetilde{I}_h u\right)^\ell + (I_h u - u) \,.$$

The right term can be bounded by ch^k in the H^1-norm using an interpolation estimate. For the first term we obtain, using norm equivalence, Lemma A.6.1 and Lemma A.8.3

$$\begin{aligned} \left\| (\widehat{u}_h - \widetilde{I}_h u)^\ell \right\|_{L^2(\Omega(t))} &\leq c \|\widehat{u}_h - \widetilde{I}_h u\|_{L^2(\Omega_h(\mathbf{x}^*(t)))} = c \|\mathbf{e}_\mathbf{u}\|_{\mathbf{M}(\mathbf{x}^*)} \\ &\leq c \int_0^t \|\mathbf{d}_\mathbf{u}(s)\|_{\star,\mathbf{x}^*}^2 + \|\mathbf{d}_\mathbf{v}(s)\|_{\star,\mathbf{x}^*}^2 \mathrm{d}s \leq c h^k \,. \end{aligned}$$

Analogously

$$\|\nabla(\widehat{u}_h - \widetilde{I}_h u)^\ell\|_{L^2(\Omega(t))} \leq c \|\nabla(\widehat{u}_h - \widetilde{I}_h u)\|_{L^2(\Omega_h(\mathbf{x}^*(t)))} = c \|\mathbf{e}_\mathbf{u}\|_{\mathbf{A}(\mathbf{x}^*)} \,.$$

Lemma A.7.2 and Lemma A.8.3 yield the result. The remaining estimates are shown analogously.

Remark A.9.1. (L^2-estimate)
The convergence rate in u, v and X in the L^2-norm is expected to be of order $k+1$, which is also reflected in the numerical experiments down below. In order to prove $\mathcal{O}(h^{k+1})$-error bounds for the diffusion equation one could work with the Ritz projection $R_h u$ instead of the interpolation $I_h u$. In fact, defining a Ritz projection as described in [Elliott and Ranner, 2021, Section 3.3],

cf. Dziuk and Elliott [2013a], we are able to prove $\sup_{t\in[0,T]}\|\mathbf{d}_\mathbf{u}(t)\|^2_{\star,\mathbf{x}^*(t)} \leq ch^{k+1}$. *This yields the error bound*

$$\|\mathbf{e}_\mathbf{u}(t)\|^2_{\mathbf{M}(\mathbf{x}^*)} + \int_0^t \|\mathbf{e}_\mathbf{u}(s)\|^2_{\mathbf{A}(\mathbf{x}^*(s))}\mathrm{d}s \leq Ch^{2k+} + c\int_0^t \|\mathbf{d}_\mathbf{v}(s)\|^2_{\star,\mathbf{x}^*(s)}\mathrm{d}s\,.$$

It is further possible to define a Ritz map for the Laplace equation for the velocity, taking the inhomogeneous boundary conditions into account. However, taking the Ritz projection instead of the finite element interpolation implies that the corresponding error $\mathbf{e}_\mathbf{v}$ *does not vanish on the boundary anymore. This induces a different defect* $\mathbf{d}_\mathbf{v}$ *in* v *and an additional defect* $\mathbf{d}_\mathbf{x}$ *in the equation* $\dot{\mathbf{e}}_\mathbf{x} = \mathbf{e}_\mathbf{v} + \mathbf{d}_\mathbf{x}$, *where* $\mathbf{d}_\mathbf{x}$ *can be considered as the error between the finite element interpolation* $I_h v$ *and the Ritz projection* $R_h v$ *of* v. *While it is indeed possible to obtain an* $\mathcal{O}(h^{k+1})$ *bound for* $\mathbf{d}_\mathbf{v}$ *this is no longer true for the new defect* $\mathbf{d}_\mathbf{x}$, *which still has to be estimated in the* $\mathbf{A}$*-norm, see* (A.6.13), *yielding only an* h^k *error bound.*

A.10. Numerical experiments

In this section we illustrate the theoretical results with various numerical experiments. Fitting the layout of the stability proof we start with an evolving domain problem in two dimensions without solving a diffusion equation on that domain. The second example is similar to the first one, but three-dimensional. In the third example we show convergence plots for a diffusion equation with nonhomogeneous Neumann boundary conditions on a rotating and growing sphere.

All experiments were implemented in MATLAB® R2018a and performed in reasonable time on an MSI GE63VR notebook with Intel Core i7-7700HQ processor and 16 GB DDR4-RAM.

A.10.1. An evolving open domain

We consider problem (A.2.5) for $t \in [0,1]$, with $\Omega(0)$ being the unit circle in $\mathbb{R}^2$. As exact solution, we choose

$$v(x,t) = \begin{pmatrix} \exp(-2t)\left(\exp(x_1)\sin(x_2) - \exp(x_2)\sin(x_1)\right) \\ 2\exp(-5t)\left(x_1^2 - x_2^2\right) \end{pmatrix},$$

which satisfies $-\Delta v = 0$. Exemplary triangulations of $\Omega(t_j)$ for $t_j = j/5$, $j = 0,\dots,5$ are shown in Figures A.1 and A.2.

We apply a second-order isoparametric finite element method. The degrees of freedom range from 143 to 28315. For time discretization we use a linearly implicit 4-step BDF method with a time step size $\tau = 8\cdot 10^{-3}$, such that the time discretization error is negligible. To compute a reference solution, we use the fact that the above v satisfies $-\Delta v(\cdot,t) = 0$, and solve the position ODEs

$$\frac{\mathrm{d}}{\mathrm{d}t}x_j(t) = v(x_j(t),t)\,, \quad x_j(0) = x_j^0\,,$$

in *all* nodes x_j^0, $j = 1,\dots,N$, of the initial triangulation with a RK4 method and time step size $\tau = 2 * 10^{-4}$. Since stiffness is no issue in the position ODEs, an explicit high-order time discretization scheme is sufficient to compute a reference solution.

We record the position error

$$\|\mathrm{err}_{\mathbf{x}}\|_{L^\infty(L^2)} := \sup_{n:n\tau\le 1} \|(x_h^n)^L - \mathrm{id}_{\Omega(t_n)}\|_{L^2(\Omega(t_n))^2}\,,$$
$$\|\mathrm{err}_{\mathbf{x}}\|_{L^\infty(H^1)} := \sup_{n:n\tau\le 1} \|\nabla\left((x_h^n)^L - \mathrm{id}_{\Omega(t_n)}\right)\|_{L^2(\Omega(t_n))^2}\,.$$

and the velocity error $\mathrm{err}_{\mathbf{v}}$ in the same norms for different choices of h. Figure A.3 shows the results. The error in H^1-norm converges with the expected order, whereas the convergence rate of the L^2-norm error is one order higher. This is not covered by the theory of this paper and left to possible future works.

Remark A.10.1 (Linear finite elements)**.** *We solved the same problem with linear finite elements. Although not covered by the theory of this paper, we observe the expected $\mathcal{O}(h^2)$-convergence in L^2-norm and $\mathcal{O}(h)$-convergence in H^1-norm.*

A.10.2. An evolving 3d domain

This example is similar to the previous one, but in three dimensions. We consider (A.2.5) for $t \in [0, 0.1]$, with $\Omega(0)$ being the unit ball in $\mathbb{R}^3$. As exact solution, we choose

$$v(x,t) = \begin{pmatrix} \sin(-t/10)(x_1^2 - 2x_2^2 + x_3^2) \\ \sin(-t/10)(\exp(x_2)\sin(x_3) - \exp(x_3)\sin(x_2)) \\ \exp(-5t)(x_1^2 - x_3^2) \end{pmatrix}$$

which satisfies $-\Delta v = 0$. We use isoparametric finite elements of second order. The degrees of freedom range from 177 to 843. For the time discretization and reference solution, we proceed as in the previous example, with $\tau = 10^{-3}$ for the BDF method and $\tau = 10^{-6}$ for the reference solution. We record the $L^\infty(L^2)$- and $L^\infty(H^1)$-norm of the position and velocity error. The results are shown in Figure A.4.

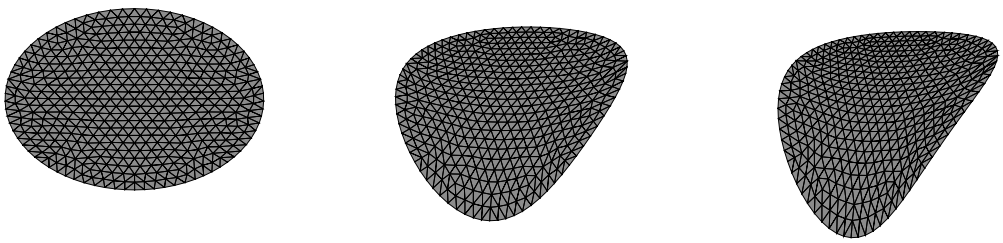

Figure A.1.: Triangulation of $\Omega(t)$ at $t_0 = 0$ (left), $t_1 = 0.2$ (center) and $t_2 = 0.4$ (right).

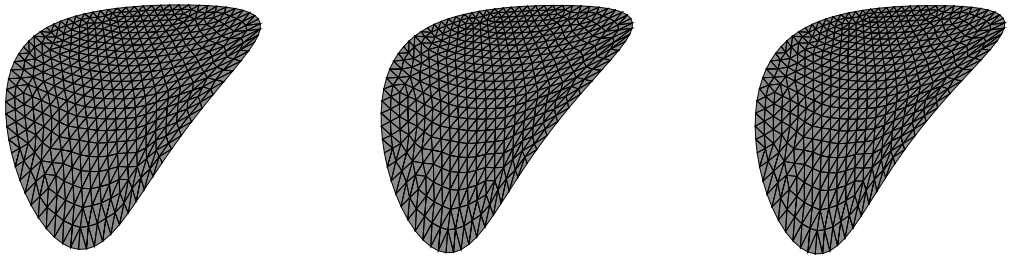

Figure A.2.: Triangulation of $\Omega(t)$ at $t_3 = 0.6$ (left), $t_4 = 0.8$ (center) and $t_5 = 1.0$ (right).

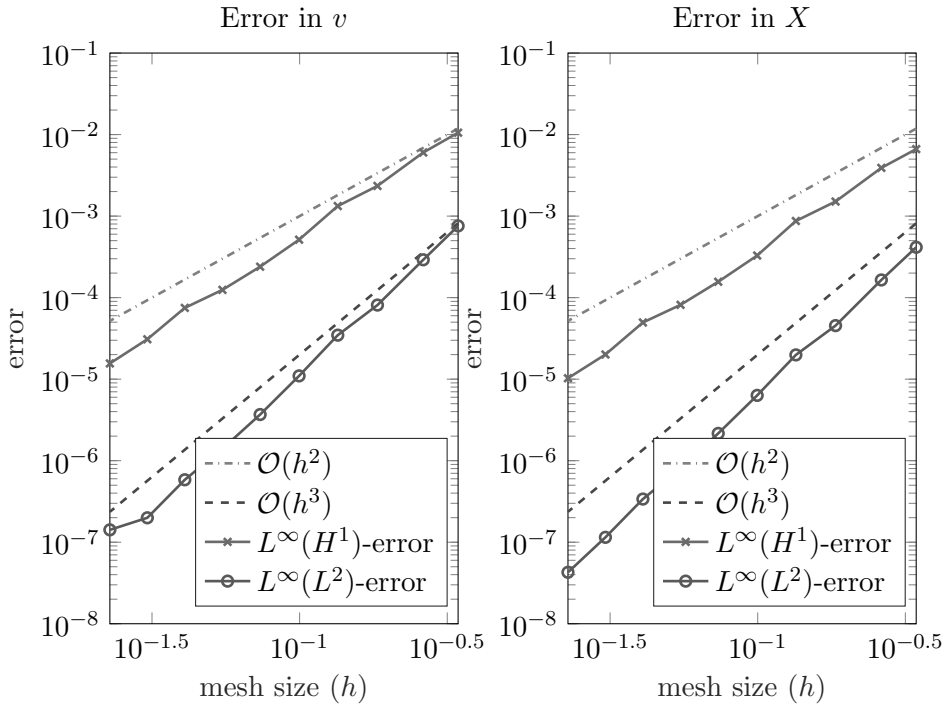

Figure A.3.: Convergence rate of the evolving quadratic finite element discretization of Example A.10.1.

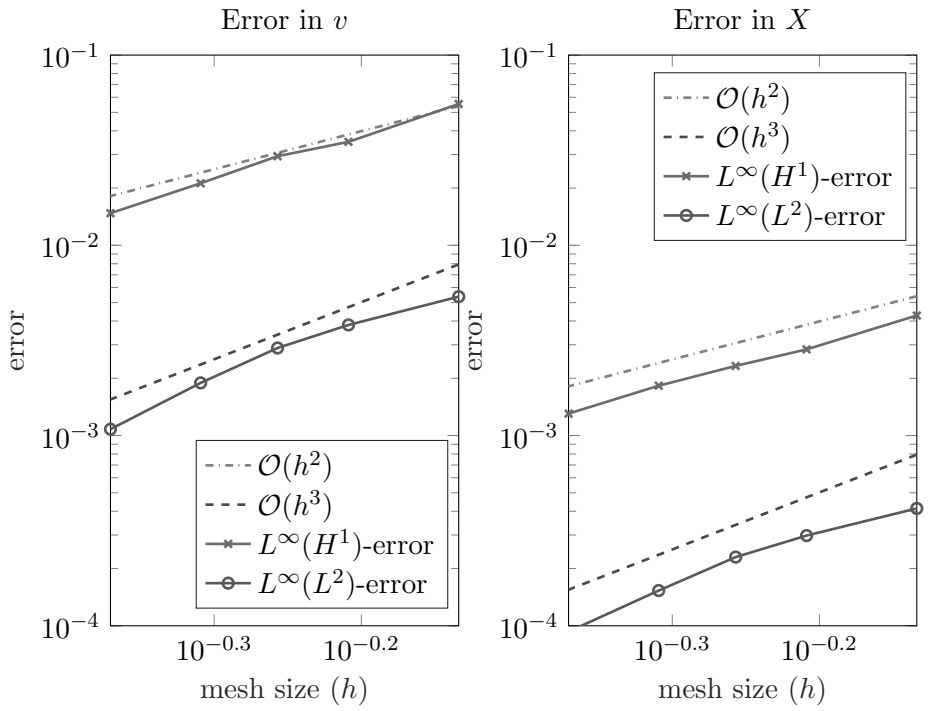

Figure A.4.: Convergence rate of the evolving quadratic finite element discretization of Example A.10.2.

A.10.3. Diffusion equation

In this example, we consider the diffusion equation (A.2.4), where the velocity again satisfies (A.2.5). As exact solution, we choose $\beta = 1$ and

$$u(x,y,t) = e^{-t}(x^2+y^2)(x^2-y^2)\,,$$
$$v(x,y,t) = \left(1 - \frac{1}{r(t)}\right)\begin{pmatrix} x \\ y \end{pmatrix} + \begin{pmatrix} -y \\ x \end{pmatrix}\,, \quad \text{where} \quad r(t) = \frac{2}{1+e^{-t}}\,.$$

The velocity v describes a growing ball which in addition is rotating anti-clockwise (cf. [Kovács et al., 2017, Example 11.1]), $r(t)$ is the radius of the ball at $t \in [0,T]$. We compute the right-hand side functions f and g of (A.2.4) and apply second order isoparametric finite elements in space and a linearly implicit 4 step BDF method with time step-size $\tau = 10^{-3}$ in time.

Note that v is linear in x and y, so the solution to $-\Delta v = 0$ is computed exactly by the finite element method. This is reflected in the convergence plot in v, which shows a purely temporal

convergence and is thus not shown here. We record the error

$$\|\mathrm{err}_{\mathbf{u}}\|_{L^\infty(L^2)} := \sup_{n:t_n\leq 1} \|(u_h^n)^L - u(\cdot,t_n)\|_{L^2(\Omega(t_n))}\,,$$

$$\|\mathrm{err}_{\mathbf{u}}\|_{L^2(H^1)} := \left(\tau \sum_{n:t_n\leq 1} \|(u_h^n)^L - u(\cdot,t_n)\|^2_{H^1(\Omega(t_n))}\right)^{\frac{1}{2}},$$

where τ denotes the time step size and $t_n = n\tau$ the n-th time step. Figure A.5 shows the results. As expected the error in the $L^2(H^1)$-norm converges with the expected order, whereas the L^2-norm convergence rate is one order higher.

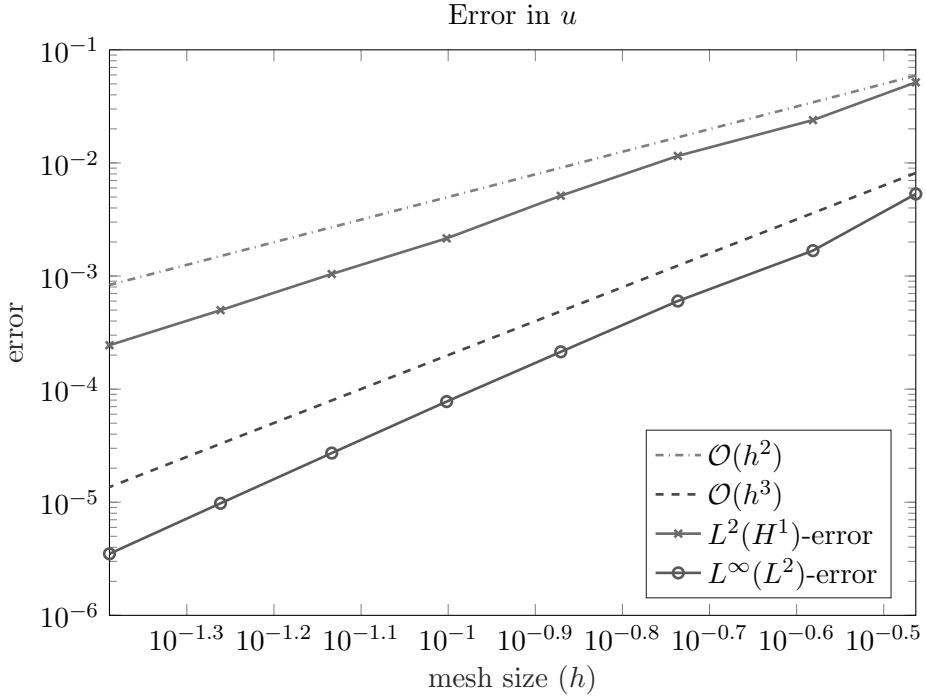

Figure A.5.: Convergence rate in u of the evolving quadratic finite element discretization of Example A.10.3.

B. Isoparametric finite element analysis of a generalized Robin boundary value problem on curved domains

This chapter is identical to the paper [Edelmann, 2021] with the same title. It was first submitted in September 2020 and got accepted in 2021.

Abstract. We study the discretization of an elliptic partial differential equation, posed on a two- or three-dimensional domain with smooth boundary, endowed with a generalized Robin boundary condition which involves the Laplace–Beltrami operator on the boundary surface. The boundary is approximated with piecewise polynomial faces and we use isoparametric finite elements of arbitrary order for the discretization. We derive optimal-order error bounds for this non-conforming finite element method in both L^2- and H^1-norm. Numerical examples illustrate the theoretical results.

B.1. Introduction

B.1.1. The generalized Robin boundary value problem

In this paper, we study the following second-order partial differential equation endowed with a boundary condition including the Laplace–Beltrami operator

$$\begin{cases} -\Delta u + \kappa u = f & \text{in } \Omega\,, \\ \dfrac{\partial u}{\partial \mathrm{n}} + \alpha u - \beta \Delta_\Gamma u = g & \text{on } \Gamma = \partial\Omega\,, \end{cases} \tag{B.1.1}$$

where $\Omega \subset \mathbb{R}^n$ $(n = 2, 3)$ is a domain with curved boundary $\Gamma = \partial\Omega$, $\alpha > 0, \beta > 0$ and $\kappa \geq 0$ are given constants and f, g are given functions on Ω and $\partial\Omega$, respectively.

The generalized Robin problem (B.1.1) is studied in Kashiwabara et al. [2015] (with $\kappa = 0$). The authors prove existence and uniqueness of the weak solution and analyze the regularity of the solution given the regularity of f and g. It turns out that the solution to the generalized problem possesses better regularity properties than the solution to the standard Robin problem, that is (B.1.1) with $\beta = 0$. Moreover, they analyze the *conforming* finite element discretization of (B.1.1) and prove optimal-order error bounds in both L^2- and H^1-norm. However, in Kashiwabara et al. [2015] the authors have to assume that Ω can be represented exactly by the finite element mesh such that the numerical domain coincides with the exact domain or, equivalently, that the finite element space V_h is contained in the solution space V. Two different cases are considered: either Γ is polyhedral, or of class $C^{1,1}$. In the first case, they have to introduce mixed boundary conditions, because the generalized boundary condition cannot be imposed

on the entire boundary (see [Kashiwabara et al., 2015, Remark 3.1]). In the second case, it is restrictive to assume that the computational mesh is capable of representing the boundary exactly.

The purpose of this paper is to generalize the results of Kashiwabara et al. [2015] to *non-conforming* finite elements, where the additional error that stems from the approximation of the geometry is taken into account. Based on a polyhedral approximation of Ω, on which linear finite elements can be used, we construct a piecewise polynomial approximation domain and isoparametric finite elements of arbitrary order. Since the finite element space is no longer contained in the solution space, we cannot compare the finite element solution and the exact solution directly. To overcome this, we lift the finite element solution to the solution space to be able to analyze the error of the method.

The above setting allows us to treat different types of boundary conditions in a unified setting. Here we focus on the generalized Robin problem, and the convergence results for the isoparametric finite element discretization of (B.1.1) with the standard Robin boundary condition ($\beta = 0$) or Neumann boundary condition ($\alpha = \beta = 0$) are obtained as a consequence. We derive error bounds between the exact solution and the lifted finite element solution that are optimal with respect to the regularity of the right-hand side functions f and g. Under suitable regularity assumptions, the error satisfies optimal-order error bounds.

B.1.2. Applications

The problem (B.1.1) has applications for example in heat conduction processes, see Goldstein [2006], or in the context of Schrödinger operators [Gesztesy and Mitrea, 2008]. Generalized Robin boundary conditions appear also in the context of domain decomposition methods [Gerardo-Giorda et al., 2010, Quarteroni and Valli, 1999] and in the Schwarz waveform relaxation algorithm [Gander and Halpern, 2007, Halpern, 2009]. A more comprehensive list of applications can be found in Kashiwabara et al. [2015].

B.1.3. Outline of the paper

In Section 2, we introduce basic notations and derive a variational form of the generalized Robin problem. In Section 3, the approximation of the geometry is described, followed by the isoparametric finite element method in Section 4. In Section 5, we derive error estimates in both L^2- and H^1-norm. We begin by stating the main results in Section 5.1, followed by a convergence proof for the H^1-estimate that is clearly separated into stability and consistency, and finally the proof of the L^2-estimate. We finish with some numerical experiments in two and three space dimensions in Section 6.

B.2. Continuous problem

B.2.1. Preliminaries

Let $\Omega \subset \mathbb{R}^n$, $(n = 2, 3)$ be an open, bounded and connected domain with sufficiently smooth boundary $\Gamma = \partial\Omega$. In the following, we require Γ at least of class C^2. For a more thorough

introduction to the following concepts and definitions, we refer to [Dziuk and Elliott, 2013b, Section 2], where more details about the following concepts can be found, cf. Dziuk and Elliott [2007a], Elliott and Ranner [2013].

The outer unit normal on Γ is denoted by n. The tangential gradient of a function w defined on some open neighborhood of Γ is given by

$$\nabla_\Gamma w = \nabla w - (\nabla w \cdot \mathrm{n})\,\mathrm{n}$$

and depends on values of w on Γ only. The Laplace–Beltrami operator is given by

$$\Delta_\Gamma w = \nabla_\Gamma \cdot \nabla_\Gamma w = \sum_{j=1}^{n} (\nabla_\Gamma)_j \, (\nabla_\Gamma)_j \, w \,.$$

We denote by $d : \mathbb{R}^n \to \mathbb{R}$ the signed distance function

$$d(x) = \begin{cases} -\mathrm{dist}(x,\Gamma) & \text{if } x \in \Omega \,, \\ 0 & \text{if } x \in \Gamma \,, \\ \mathrm{dist}(x,\Gamma) & \text{otherwise,} \end{cases}$$

where $\mathrm{dist}(x,\Gamma) = \inf\{|x-y| : y \in \Gamma\}$ denotes the distance of x to Γ. Since Γ is a C^2-manifold, there exists a $\delta > 0$ and a strip

$$\mathcal{U}_\delta = \{x \in \mathbb{R}^n : |d(x)| < \delta\} \tag{B.2.1}$$

such that for each $x \in \mathcal{U}_\delta$ there exists a unique $p(x) \in \Gamma$ such that

$$x = p(x) + d(x)\mathrm{n}(p(x)) \,, \tag{B.2.2}$$

see [Dziuk and Elliott, 2013b, Section 2]. $p(x)$ is the closest point to x on Γ.

We let $c > 0$ denote a generic constant that assumes different values on different occurrences. We use the standard notation for Sobolev spaces, i.e. $H^0(\Omega) := L^2(\Omega) = \{u : \Omega \to \mathbb{R} : \int_\Omega u^2 \mathrm{d}x < \infty\}$, $H^{k+1}(\Omega) := \{u \in L^2(\Omega) : \nabla u \in H^k(\Omega)^n\}$. It is well known that the trace γu of a function $u \in H^k(\Omega)$ is in $H^{k-1/2}(\Gamma)$ if $\Gamma \in C^{k-1,1}$. Due to the Laplace–Beltrami operator in the boundary condition of (B.1.1), it turns out that we need $\gamma u \in H^1(\Gamma)$ to derive a weak formulation. Therefore $H^1(\Omega)$ is not the suitable weak solution space. Instead, we work with the space

$$H^k(\Omega;\Gamma) := \left\{ u \in H^k(\Omega) : \, \gamma u \in H^k(\Gamma) \right\}$$

endowed with the norm

$$\|u\|_{H^k(\Omega;\Gamma)} = \left(\|u\|^2_{H^k(\Omega)} + \|\gamma u\|^2_{H^k(\Gamma)} \right)^{1/2} . \tag{B.2.3}$$

Recall that for a function $w \in H^k(\Gamma)$, the $H^k(\Gamma)$-norm is defined using tangential derivatives, i.e.

$$\|w\|_{H^k(\Gamma)} = \left(\|w\|^2_{L^2(\Gamma)} + \|\nabla_\Gamma w\|^2_{H^{k-1}(\Gamma)^n} \right)^{1/2} .$$

It is shown in [Kashiwabara et al., 2015, Lemma 2.5] that the space $H^k(\Omega;\Gamma)$ with the inner product that induces (B.2.3) is a Hilbert space.

B.2.2. Variational form

To derive the weak formulation, we make use of the integration by parts formula on Γ: for $w \in H^1(\Gamma)$, we have (see Dziuk and Elliott [2013b])

$$\int_\Gamma -\Delta_\Gamma u w \mathrm{d}\sigma = \int_\Gamma \nabla_\Gamma u \cdot \nabla_\Gamma w \mathrm{d}\sigma \,. \tag{B.2.4}$$

We multiply (B.1.1) with a test function φ, integrate over Ω and obtain

$$\int_\Omega \nabla u \cdot \nabla \varphi + \kappa u \varphi \mathrm{d}x - \int_\Gamma \frac{\partial u}{\partial \mathrm{n}} \gamma\varphi \mathrm{d}\sigma = \int_\Omega f\varphi \mathrm{d}x \,.$$

Substituting the boundary condition and using (B.2.4) with $w = \gamma\varphi$, we arrive at

$$\begin{aligned} &\int_\Omega \nabla u \cdot \nabla \varphi + \kappa u \varphi \mathrm{d}x + \alpha \int_\Gamma (\gamma u)(\gamma\varphi)\mathrm{d}\sigma + \beta \int_\Gamma \nabla_\Gamma(\gamma u) \cdot \nabla_\Gamma(\gamma\varphi)\mathrm{d}\sigma \\ &= \int_\Omega f\varphi \mathrm{d}x + \int_\Gamma g(\gamma\varphi)\mathrm{d}\sigma \,. \end{aligned}$$

We use the following notation for bilinear forms defined on $H^1(\Omega;\Gamma) \times H^1(\Omega;\Gamma)$:

$$\begin{aligned} m^\Omega(u,v) &= \int_\Omega uv \mathrm{d}x \,, \\ a^\Omega(u,v) &= \int_\Omega \nabla u \cdot \nabla v \mathrm{d}x \,, \\ m^\Gamma(u,v) &= \int_\Gamma (\gamma u)(\gamma v)\mathrm{d}\sigma \,, \\ a^\Gamma(u,v) &= \int_\Gamma \nabla_\Gamma(\gamma u) \cdot \nabla_\Gamma(\gamma v)\mathrm{d}\sigma \,, \\ a(u,v) &= a^\Omega(u,v) + \kappa m^\Omega(u,v) + \alpha m^\Gamma(u,v) + \beta a^\Gamma(u,v) \,. \end{aligned} \tag{B.2.5}$$

The right hand side is denoted by

$$\ell(\varphi) = \int_\Omega f\varphi \mathrm{d}x + \int_\Gamma g(\gamma\varphi)\mathrm{d}\sigma \,.$$

The variational form thus reads: find $u \in V = H^1(\Omega;\Gamma)$ such that

$$a(u,\varphi) = \ell(\varphi) \tag{B.2.6}$$

for all $\varphi \in H^1(\Omega;\Gamma)$. The following regularity result is proved in Kashiwabara et al. [2015].

Proposition B.2.1. *Let $\alpha, \beta > 0$, $\kappa \geq 0$ and $j \geq 1$. If $\Gamma \in C^{j,1}$, $f \in H^{j-1}(\Omega)$, $g \in H^{j-1}(\Gamma)$, then there exists a unique solution $u \in H^{j+1}(\Omega;\Gamma)$ that satisfies the a priori bound*

$$\|u\|_{H^{j+1}(\Omega;\Gamma)} \leq c \left(\|f\|_{H^{j-1}(\Omega)} + \|g\|_{H^{j-1}(\Gamma)} \right) .$$

Let us remark that for the standard Robin boundary value problem, i.e. (B.1.1) with $\beta = 0$, we need $g \in H^{j-1/2}(\Gamma)$ to have $u \in H^{j+1}(\Omega)$, and the trace theorem then yields $\gamma u \in H^{j+1/2}(\Gamma)$, so the generalized problem requires less regularity in the data to produce a more regular solution, cf. [Kashiwabara et al., 2015, Remark 3.5].

B.3. Domain approximation

Before we describe the finite element method, we need to construct an approximation of Ω and Γ. We follow the construction of Elliott and Ranner [2013], which is based on Lenoir [1986], Bernardi [1989] and Demlow [2009].

B.3.1. Linear approximation

Let $\Omega_h^{(1)}$ be a polyhedral approximation of Ω with boundary $\Gamma_h^{(1)} = \partial\Omega_h^{(1)}$. We construct $\Omega_h^{(1)}$ such that the faces of $\Gamma_h^{(1)}$ are simplices whose vertices lie on Γ (triangles in $\mathbb{R}^3$ and straight lines in $\mathbb{R}^2$). We construct a quasi-uniform triangulation $\mathcal{T}_h^{(1)}$ of $\Omega_h^{(1)}$ consisting of simplices (tetrahedrons on $\mathbb{R}^3$ and triangles in $\mathbb{R}^2$). We set

$$h = \max\{\operatorname{diam}(T) : T \in \mathcal{T}_h^{(1)}\}$$

and assume that $h \leq h_0$, where h_0 is sufficiently small such that $\Gamma_h^{(1)} \subset \mathcal{U}_\delta$, where $\mathcal{U}_\delta$ is defined in (B.2.1).

B.3.2. Exact triangulation

Before we define the computational domain, we define an *exact triangulation* of Ω. We denote by $\widehat{T}$ the unit n-simplex. For each $T \in \mathcal{T}_h^{(1)}$, there exists an affine transformation $\Phi_T : \mathbb{R}^n \to \mathbb{R}^n$ that maps $\widehat{T}$ onto T, which we write as

$$\Phi_T(\widehat{x}) = B_T\widehat{x} + b_T\,,$$

where $B_T \in \mathbb{R}^{n\times n}$, $b_T \in \mathbb{R}^n$. Φ_T is exactly the map used for linear finite elements. We now call T^c a curved simplex if there exists a C^1-mapping Φ_T^c that maps $\widehat{T}$ onto T^c which is of the form

$$\Phi_T^c = \Phi_T + \varrho_T\,,$$

where Φ_T is an affine map as defined above and $\varrho_T : \widehat{T} \to \mathbb{R}^N$ is a C^1-mapping satisfying

$$C_T := \sup_{\widehat{x}\in\widehat{T}} |D\varrho_T(\widehat{x})B_T^{-1}| \leq C < 1\,. \tag{B.3.1}$$

There are several ways to define ϱ_T. We follow the construction of Elliott and Ranner [2013], based on Dubois [1990]. Note that each $T \in \mathcal{T}_h^{(1)}$ is either an internal simplex with at most one node on the boundary, or T has more than one node on the boundary. In the first case, we set $\varrho_T = 0$. For the latter case, we denote by l the number of nodes of T that lie on the boundary $\Gamma_h^{(1)}$. The vertices $x_1^T, \dots, x_{n+1}^T$ of T are ordered such that $x_1^T, \dots, x_l^T$ lie on $\Gamma_h^{(1)}$. For each $x^T \in T$, there is a unique representation

$$x^T = \sum_{j=1}^{n+1} \lambda_j x_j^T$$

in barycentric coordinates. Note that

$$\lambda_{n+1} = 1 - \sum_{j=1}^{n} \lambda_j \,.$$

We write $\widehat{x}^T = (\lambda_1, \dots, \lambda_N)$ for the coordinates of x in $\widehat{T}$. We introduce

$$\lambda^*(\widehat{x}) = \sum_{j=1}^{l} \lambda_j \,, \quad \widehat{\sigma} = \{\widehat{x} \in \widehat{T} : \lambda^*(\widehat{x}) = 0\} \,.$$

We have $\lambda^*(\widehat{x}) = 0$ if $\widehat{x}$ is a node which is not belonging to the boundary (or if $\widehat{x}$ is on the edge between such nodes in the three-dimensional case, when $l = 2$), and $\lambda^*(\widehat{x}) = 1$ if $\widehat{x} \in T \cap \Gamma_h^{(1)}$.

We denote by τ_T the face of $\Gamma_h^{(1)}$ that corresponds to the boundary face of T, i. e. $\tau_T = T \cap \Gamma_h^{(1)}$. For $\widehat{x} \notin \widehat{\sigma}$, we denote the projection of $x = \Phi_T(\widehat{x})$ onto τ_T by

$$y(\widehat{x}) = \sum_{j=1}^{l} \frac{\lambda_j}{\lambda^*} x_j^T \,.$$

Then, using the normal projection p defined in (B.2.2), we define ϱ_T by

$$\varrho_T(\widehat{x}) = \begin{cases} (\lambda^*(\widehat{x}))^{k+2}(p(y(\widehat{x})) - y(\widehat{x}))\,, & \text{if } \widehat{x} \notin \widehat{\sigma}\,, \\ 0\,, & \text{if } \widehat{x} \in \widehat{\sigma}\,. \end{cases}$$

Basic regularity properties of the above maps are stated and proved in Elliott and Ranner [2013]. In particular, it is shown that ρ_T satisfies (B.3.1) for $h \le h_0$ sufficiently small.

B.3.3. Computational domain and lifts

We can now define the higher-order computational domain $\Omega_h^{(k)}$ for $k \ge 1$. Let $T \in \mathcal{T}_h^{(1)}$ and $\varphi_1^k, \dots, \varphi_{n_k}^k$ be the Lagrangian basis functions of degree k on $\widehat{T}$ corresponding to the nodal points $\widehat{x}^1, \dots, \widehat{x}^{n_k}$ on $\widehat{T}$. Here, n_k denotes the number of nodal points on each element, for example $n_k = 4$ or $n_k = 10$ for linear or quadratic finite elements in three dimensions. Then, we define a parametrization of a polynomial simplex $T^{(k)}$ by

$$\Phi_T^{(k)}(\widehat{x}) = \sum_{j=1}^{n_k} \Phi_T^c(\widehat{x}^j)\varphi_j^k(\widehat{x}) \,.$$

Note that, by the Lagrangian property, we have

$$\Phi_T^{(k)}(\widehat{x}^l) = \Phi_T^c(\widehat{x}^l) \,.$$

We can apply this to each $T \in \mathcal{T}_h^{(1)}$ and then define $\Omega_h^{(k)}$ as the union of elements in $\mathcal{T}_h^{(k)}$, defined by

$$\mathcal{T}_h^{(k)} := \{T^{(k)} : T \in \mathcal{T}_h^{(1)}\} \,, \quad T^{(k)} := \{\Phi_T^{(k)}(\widehat{x}) : \widehat{x} \in \widehat{T}\} \,.$$

For $k = 1$, this notation is consistent with the notation of $\Omega_h^{(1)}$ in the previous subsection.

Definition B.3.1. *For a function $w_h : \Omega_h^{(k)} \to \mathbb{R}$, its lift $w_h^l : \Omega \to \mathbb{R}$ is defined by $w_h^l = w_h \circ (\Phi_T^{(k)})^{-1}$, i.e.*

$$w_h^l \left(\Phi_T^{(k)}(x) \right) = w_h(x) , \quad x \in \Omega_h^{(k)} .$$

For a continuous function $w : \Omega \to \mathbb{R}$, its inverse lift is defined by $w^{-l} = w \circ \Phi_T^{(k)}$.

The following lemma states that both the L^2-norm and the H^1-seminorm of functions on $\Omega_h^{(k)}$ and their lifts are equivalent.

Proposition B.3.2. *There exists a constant $c > 0$ independent of h (but depending on k, n and the geometry of Ω), such that for all $w_h : \Omega_h^{(k)} \to \mathbb{R}$*

$$\begin{aligned}
\frac{1}{c} \|w_h\|_{L^2(\Omega_h^{(k)};\Gamma_h^{(k)})} &\leq \|w_h^l\|_{L^2(\Omega;\Gamma)} \leq c \|w_h\|_{L^2(\Omega_h^{(k)};\Gamma_h^{(k)})} , \\
\frac{1}{c} \|\nabla w_h\|_{L^2(\Omega_h^{(k)})} &\leq \|\nabla w_h^l\|_{L^2(\Omega)} \leq c \|\nabla w_h\|_{L^2(\Omega_h^{(k)})} , \\
\frac{1}{c} \|\nabla_{\Gamma_h} (\gamma_h w_h)\|_{L^2(\Gamma_h^{(k)})} &\leq \|\nabla_\Gamma (\gamma w_h^l)\|_{L^2(\Gamma)} \leq c \|\nabla_{\Gamma_h} (\gamma_h w_h)\|_{L^2(\Gamma_h^{(k)})} .
\end{aligned}$$

Proof. See [Elliott and Ranner, 2013, Proposition 4.9] for the bulk estimate and Demlow [2009] for the estimate on the boundary. □

B.4. The isoparametric finite element method

In this section we introduce the finite element method. We use piecewise polynomial finite element functions of degree k, which lead to isoparametric finite elements. Isoparametric finite elements are also used in Elliott and Ranner [2013] in the context of bulk–surface equations; the traces of isoparametric bulk finite element functions on the boundary can be considered as surface finite elements, see e.g. Dziuk and Elliott [2007a, 2013b].

From now on, we write Ω_h and Γ_h instead of $\Omega_h^{(k)}$ and $\Gamma_h^{(k)}$. We collect the nodes $x_1, \dots, x_N \in \mathbb{R}^n$ of the triangulation in a vector $\mathbf{x} = (x_1, \dots, x_N) \in \mathbb{R}^{nN}$ such that exactly the first N_Γ nodes $x_1, \dots, x_{N_\Gamma}$ lie on Γ. We use Lagrangian basis functions $\varphi_1, \dots, \varphi_N$, which are defined elementwise such that their pullback to the reference element is polynomial of degree k. The basis functions satisfy the property $\varphi_j(x_k) = \delta_{jk}$ for $1 \leq j, k \leq N$. The finite element space is then defined as

$$V_h = \operatorname{span} \{ \varphi_1, \dots, \varphi_N \} .$$

Recall that, as opposed to Kashiwabara et al. [2015], the finite element space V_h is *not* contained in $V = H^1(\Omega; \Gamma)$. The right-hand side functions are approximated with appropriate functions $f_h : \Omega_h \to \mathbb{R}$ and $g_h : \Gamma_h \to \mathbb{R}$. If f and g are continuous, one could use the inverse lifts or the finite element interpolations, for example.

We use the following discrete analogues of the bilinear forms defined in (B.2.5):

$$\begin{aligned}
m_h^\Omega(u_h, v_h) &= \int_{\Omega_h} u_h v_h \mathrm{d}x \,, \\
a_h^\Omega(u_h, v_h) &= \int_{\Omega_h} \nabla u_h \cdot \nabla v_h \mathrm{d}x \,, \\
m_h^\Gamma(u_h, v_h) &= \int_{\Gamma_h} (\gamma_h u_h)(\gamma_h v_h) \mathrm{d}\sigma_h \,, \\
a_h^\Gamma(u_h, v_h) &= \int_{\Gamma_h} \nabla_{\Gamma_h}(\gamma_h u_h) \cdot \nabla_{\Gamma_h}(\gamma_h v_h) \mathrm{d}\sigma_h \,, \\
a_h(u_h, v_h) &= a_h^\Omega(u_h, v_h) + \kappa m_h^\Omega(u_h, v_h) + \alpha m_h^\Gamma(u_h, v_h) + \beta a_h^\Gamma(u_h, v_h) \,.
\end{aligned}$$

Here, γ_h denotes the discrete trace operator on Γ_h, $\mathrm{d}\sigma_h$ denotes the discrete surface measure on Γ_h (see Elliott and Ranner [2013], Demlow [2009], Dziuk and Elliott [2013b] for further details). Moreover, we denote

$$\ell_h(\varphi_h) = \int_{\Omega_h} f_h \varphi_h \mathrm{d}x + \int_{\Gamma_h} g_h(\gamma_h \varphi_h) \mathrm{d}\sigma_h \,.$$

The bilinear forms are defined on $V_h \times V_h$ and ℓ_h is defined on V_h.

The discretized formulation of (B.2.6) now reads: given $f_h, g_h \in V_h$, find $u_h \in V_h$ such that

$$a_h(u_h, \varphi_h) = \ell_h(\varphi_h) \tag{B.4.1}$$

for all $\varphi_h \in V_h$. Since a_h is coercive and bounded and V_h is a (finite-dimensional) Hilbert space, we get existence and uniqueness of the discrete solution by the Lax-Milgram lemma.

B.4.1. Matrix–vector formulation

We derive a matrix–vector formulation of the discretized problem. First, we note that (B.4.1) is equivalent to: find $u_h \in V_h$ such that

$$a_h(u_h, \varphi_j) = \ell_h(\varphi_j)$$

for all basis functions φ_j, $j = 1, \dots, N$. The functions f_h and g_h, which are assumed to be finite element functions, can be written as $f_h(\cdot) = \sum_{j=1}^N f_h(x_j)\varphi_j(\cdot)$, $g_h(\cdot) = \sum_{j=1}^{N_\Gamma} g_h(x_j)\varphi_j(\cdot)$. We collect the nodal values in vectors

$$\mathbf{f} = (f_h(x_j))_{j=1}^N \,, \quad \mathbf{g} = (g_h(x_j))_{j=1}^{N_\Gamma} \,.$$

We define the bulk and surface mass and stiffness matrices:

$$
\begin{aligned}
(\mathbf{M}_\Omega)_{jk} &= \int_{\Omega_h} \varphi_j \varphi_k \mathrm{d}x\,, \\
(\mathbf{A}_\Omega)_{jk} &= \int_{\Omega_h} \nabla\varphi_j \cdot \nabla\varphi_k \mathrm{d}x\,, \quad 1 \le j,k \le N\,, \\
(\mathbf{M}_\Gamma)_{jk} &= \int_{\Gamma_h} (\gamma_h\varphi_j)(\gamma_h\varphi_k) \mathrm{d}\sigma_h\,, \\
(\mathbf{A}_\Gamma)_{jk} &= \int_{\Gamma_h} \nabla_{\Gamma_h}(\gamma_h\varphi_j) \cdot \nabla_{\Gamma_h}(\gamma_h\varphi_k) \mathrm{d}\sigma_h\,, \quad 1 \le j,k \le N_\Gamma\,.
\end{aligned}
$$

We introduce the matrix $\boldsymbol{\gamma} = (I_{N_\Gamma}, 0) \in \mathbb{R}^{N_\Gamma \times N}$, where I_{N_Γ} denotes the identity matrix of size $N_\Gamma \times N_\Gamma$. For a finite element function w_h with nodal values collected in a vector $\mathbf{w}$, $\boldsymbol{\gamma}\mathbf{w} \in \mathbb{R}^{N_\Gamma}$ is the vector of the nodal values on the boundary nodes.

Proposition B.4.1. *Let $u_h(\cdot) = \sum_{j=1}^N u_j\varphi_j(\cdot) \in V_h$ denote the finite element solution to* (B.4.1) *and $\mathbf{u} = (u_j)_{j=1}^N$ the vector of nodal values. Then the spatially discretized problem* (B.4.1) *is equivalent to the linear system*

$$
\mathbf{K}\mathbf{u} = \mathbf{b}\,, \tag{B.4.2}
$$

where $\mathbf{K} = \boldsymbol{\gamma}^{\mathrm{T}}(\alpha\mathbf{M}_\Gamma + \beta\mathbf{A}_\Gamma)\boldsymbol{\gamma} + \kappa\mathbf{M}_\Omega + \mathbf{A}_\Omega$ and $\mathbf{b} = \mathbf{M}_\Omega\mathbf{f} + \boldsymbol{\gamma}^{\mathrm{T}}\mathbf{M}_\Gamma\mathbf{g}$.

Proof. Follows from linearity and a direct computation. □

The following properties of $\mathbf{K}$ are needed in the error analysis.

Lemma B.4.2. *For a finite element function $w_h = \sum_{j=1}^N w_j\varphi_j$ with corresponding nodal vector $\mathbf{w} \in \mathbb{R}^n$, the a_h-norm of w_h, defined by $\|w_h\|_{a_h} = (a_h(w_h,w_h))^{1/2} = (\mathbf{w}^{\mathrm{T}}\mathbf{K}\mathbf{w})^{1/2}$ and the $H^1(\Omega_h,\Gamma_h)$-norm are equivalent.*

Proof. For $\alpha = \beta = \kappa = 1$, we have $\|w_h\|_{a_h} = \|w_h\|_{H^1(\Omega_h;\Gamma_h)}$. In the general case, denote $c_1 = \min(\alpha,\beta,\kappa,1)$ and $c_2 = \max(\alpha,\beta,\kappa,1)$ and we have

$$
c_1\|w_h\|_{a_h} \le \|w_h\|_{H^1(\Omega_h;\Gamma_h)} \le c_2\|w_h\|_{a_h}\,.
$$

□

Remark B.4.3. *If the right-hand side functions f and g are not approximated with finite element functions, the vector $\mathbf{b}$ in* (B.4.2) *is defined by integrals over Ω and Γ, which then have to be approximated with quadrature rules. In this paper, we do not intend analyzing these numerical integration errors and therefore assume that f and g are approximated with finite element functions f_h and g_h. This is not fully practical for $f \in L^2(\Omega)$, $g \in L^2(\Gamma)$, cf. Dziuk [1988], Elliott and Ranner [2013]. We will carefully carry out the error analysis such that this approximation error is taken into account. If f and g are continuous, f_h and g_h can be chosen as finite element interpolations of f and g, and provided that f and g are sufficiently regular this interpolation error is of the same order as the order of the finite element method.*

Definition B.4.4. *For a function $w \in H^2(\Omega)$, its finite element interpolation $\widetilde{I}_h w \in V_h$ is given by*

$$\widetilde{I}_h w(\cdot) = \sum_{j=1}^{N} w(x_j)\varphi_j(\cdot)\,.$$

The lifted finite element interpolation $I_h w : \Omega \to \mathbb{R}$ is then defined as

$$I_h w = \left(\widetilde{I}_h w\right)^l .$$

Note that since $n \in \{2,3\}$, we have $H^2(\Omega) \subset C^0(\Omega)$, so the pointwise evaluation is well-defined. The following two approximation properties are crucial in order to prove optimal-order error bounds with respect to the regularity of the exact solution.

Proposition B.4.5. *Let $k \geq 1$. There exists a constant c independent of h and j, such that for all $2 \leq j \leq k+1$*

$$\begin{aligned}\|w - I_h w\|_{L^2(\Omega;\Gamma)} &\leq c h^j \|w\|_{H^j(\Omega;\Gamma)}\,,\\ \|w - I_h w\|_{H^1(\Omega;\Gamma)} &\leq c h^{j-1} \|w\|_{H^j(\Omega;\Gamma)}\end{aligned}$$

for all $w \in H^j(\Omega;\Gamma)$.

Proof. See [Bernardi, 1989, Corollary 4.1] and Demlow [2009]. □

Proposition B.4.6. *For any $u_h, w_h \in V_h$ with lifts $u_h^l, w_h^l \in V_h^l \subset H^1(\Omega)$, we have the following estimates:*

$$\begin{aligned}\left|m_h^\Omega(u_h,w_h) - m^\Omega(u_h^l,w_h^l)\right| &\leq c h^k \|u_h^l\|_{L^2(\Omega)} \|w_h^l\|_{L^2(\Omega)}\,,\\ \left|m_h^\Omega(u_h,w_h) - m^\Omega(u_h^l,w_h^l)\right| &\leq c h^{k+1} \|u_h^l\|_{H^1(\Omega)} \|w_h^l\|_{H^1(\Omega)}\,,\\ \left|a_h^\Omega(u_h,w_h) - a^\Omega(u_h^l,w_h^l)\right| &\leq c h^k \|u_h^l\|_{H^1(\Omega)} \|w_h^l\|_{H^1(\Omega)}\,.\end{aligned}$$

The traces of u_h, w_h on Γ_h and their lifts on Γ satisfy

$$\begin{aligned}\left|m_h^\Gamma(u_h,w_h) - m^\Gamma(u_h^l,w_h^l)\right| &\leq c h^{k+1} \|u_h^l\|_{L^2(\Gamma)} \|w_h^l\|_{L^2(\Gamma)}\,,\\ \left|a_h^\Gamma(u_h,w_h) - a^\Gamma(u_h^l,w_h^l)\right| &\leq c h^{k+1} \|\nabla_\Gamma u_h^l\|_{L^2(\Gamma)} \|\nabla_\Gamma w_h^l\|_{L^2(\Gamma)}\,.\end{aligned}$$

For $u, w \in H^2(\Omega)$ with inverse lifts u^{-l}, w^{-l}, we have

$$\left|a_h^\Omega(u^{-l},w^{-l}) - a^\Omega(u,w)\right| \leq c h^{k+1} \|u\|_{H^2(\Omega)} \|w\|_{H^2(\Omega)}\,.$$

Proof. See in the proof of [Elliott and Ranner, 2013, Lemma 6.2]. □

B.5. Error analysis

In this section, we analyze the error of the isoparametric finite element method. Since the exact solution and the numerical solution are defined on different domains, we cannot compare them directly. Instead, we compare the exact solution to the lift of the numerical solution. We derive optimal-order error estimates for finite elements of arbitrary order $k \geq 1$, with respect to both the regularity of the solution and the approximation of the data.

We begin by stating the main results of this paper. The proof of the following theorems follows down below and is clearly separated into stability and consistency.

B.5.1. Statement of the main result

Theorem B.5.1. *Let $j \geq 1$ be a natural number, $f \in H^{j-1}(\Omega)$, $g \in H^{j-1}(\Gamma)$, let $u \in H^{j+1}(\Omega;\Gamma)$ be the solution of* (B.2.6)*. Denote by $u_h : \Omega_h^{(k)} \to \mathbb{R}$ the numerical solution to* (B.4.1) *computed with isoparametric finite elements of order $k \geq 1$, f_h and g_h approximations to f and g. Then, the error between the exact solution and the lifted finite element solution is bounded by*

$$\|u - u_h^l\|_{H^1(\Omega;\Gamma)} \leq Ch^{\min(k,j)} + c\|f - f_h^l\|_{L^2(\Omega)} + c\|g - g_h^l\|_{L^2(\Gamma)}\,,$$

where C and c are independent of h, C depends on $\|f\|_{L^2(\Omega)}$, $\|g\|_{L^2(\Gamma)}$ and $\|u\|_{H^{\min(k,j)+1}(\Omega;\Gamma)}$ and c is independent of these quantities.

In particular: If $j \geq k$ and f_h and g_h are chosen such that $\|f - f_h^l\|_{L^2(\Omega)} \leq ch^k$ and $\|g - g_h^l\|_{L^2(\Gamma)} \leq ch^k$, then the error is bounded by

$$\|u - u_h^l\|_{H^1(\Omega;\Gamma)} \leq Ch^k\,, \tag{B.5.1}$$

where C depends on the regularity of f and g and on $\|u\|_{H^{k+1}(\Omega;\Gamma)}$.

Remark B.5.2. *The assumptions in the second part of Theorem B.5.1 are satisfied if $f \in H^k(\Omega)$, $g \in H^k(\Gamma)$ for $k \geq 2$. In this case f_h and g_h can be chosen as finite element interpolations of f and g. The interpolation errors are then bounded using Proposition B.4.5, and we arrive at* (B.5.1)*.*

For the L^2-estimate, we need slightly more assumptions, see Remark B.5.6.

Theorem B.5.3. *Let $j \geq 1$ be a natural number, $f \in H^{j-1}(\Omega) \cap H^1(\Omega)$, $g \in H^{j-1}(\Gamma)$, let $u \in H^{j+1}(\Omega;\Gamma)$ be the solution of* (B.2.6)*. Denote by $u_h : \Omega_h^{(k)} \to \mathbb{R}$ the numerical solution of* (B.4.1) *computed with isoparametric finite elements of order $k \geq 1$. Then, the error between the exact solution and the lifted finite element solution is bounded by*

$$\begin{aligned}\|u - u_h^l\|_{L^2(\Omega;\Gamma)} \leq\ & Ch^{\min(k,j)+1} + c\|f - f_h^l\|_{L^2(\Omega)} \\ & + c\|g - g_h^l\|_{L^2(\Gamma)} + ch^{k+1}\|f - f_h^l\|_{H^1(\Omega)}\,,\end{aligned}$$

where C and c are independent of h, C depends on $\|f\|_{H^1(\Omega)}$, $\|g\|_{L^2(\Gamma)}$ and $\|u\|_{H^{\min(k,j)+1}(\Omega;\Gamma)}$ and c is independent of these quantities.

In particular: If $j \geq k$ and f_h and g_h are chosen such that $\|f - f_h^l\|_{L^2(\Omega)} \leq ch^{k+1}$, $\|f - f_h^l\|_{H^1(\Omega)} \leq c$ and $\|g - g_h^l\|_{L^2(\Gamma)} \leq ch^{k+1}$, then the error is bounded by

$$\|u - u_h^l\|_{L^2(\Omega;\Gamma)} \leq Ch^{k+1}\,.$$

Remark B.5.4. *The assumptions in the second part of Theorem B.5.3 are satisfied if $f \in H^{k+1}(\Omega)$, $g \in H^{k+1}(\Gamma)$ for $k \geq 1$ with $f_h = \widetilde{I}_h f$, $g_h = \widetilde{I}_h g$, see Proposition B.4.5.*

The proof of Theorems B.5.1 and B.5.3 follows down below and is clearly separated into stability and consistency.

B.5.2. Stability

The finite element interpolation $u_h^* : \Omega_h^{(k)} \to \mathbb{R}$ of the exact solution, which corresponds to the nodal vector $\mathbf{u}^* = (u(x_j))_{j=1}^N$, satisfies the numerical scheme up to a defect $\mathbf{d}$, which corresponds to a finite element function $d_h \in V_h$:

$$\mathbf{K}\mathbf{u}^* = \mathbf{b} + (\mathbf{M}_\Omega + \boldsymbol{\gamma}^{\mathrm{T}}\mathbf{M}_\Gamma\boldsymbol{\gamma})\mathbf{d}\,. \tag{B.5.2}$$

Note that $\mathbf{K}$ is symmetric and positive definite and thus both $\mathbf{K}^{-1}$ and $\mathbf{K}^{-1/2}$ exist. Subtracting (B.5.2) from (B.4.2), we find that the error $\mathbf{e} = \mathbf{u} - \mathbf{u}^*$ satisfies

$$\mathbf{K}\mathbf{e} = -(\mathbf{M}_\Omega + \boldsymbol{\gamma}^{\mathrm{T}}\mathbf{M}_\Gamma\boldsymbol{\gamma})\mathbf{d}\,.$$

We test this equation with $\mathbf{e}$ and obtain

$$\|\mathbf{e}\|_{\mathbf{K}}^2 := \mathbf{e}^{\mathrm{T}}\mathbf{K}\mathbf{e} = -\mathbf{e}^{\mathrm{T}}(\mathbf{M}_\Omega + \boldsymbol{\gamma}^{\mathrm{T}}\mathbf{M}_\Gamma\boldsymbol{\gamma})\mathbf{d}\,.$$

The defect will be estimated in the dual norm induced by the bilinear form a_h:

$$\begin{aligned}\|\mathbf{d}\|_\star := \|\mathbf{K}^{-1/2}(\mathbf{M}_\Omega + \boldsymbol{\gamma}^{\mathrm{T}}\mathbf{M}_\Gamma\boldsymbol{\gamma})\mathbf{d}\|_2 &= \sup_{0\neq\mathbf{w}\in\mathbb{R}^N} \frac{\mathbf{d}^{\mathrm{T}}(\mathbf{M}_\Omega + \boldsymbol{\gamma}^{\mathrm{T}}\mathbf{M}_\Gamma\boldsymbol{\gamma})\mathbf{K}^{-1/2}\mathbf{w}}{(\mathbf{w}^{\mathrm{T}}\mathbf{w})^{1/2}} \\ = \sup_{0\neq\mathbf{z}\in\mathbb{R}^N} \frac{\mathbf{d}^{\mathrm{T}}(\mathbf{M}_\Omega + \boldsymbol{\gamma}^{\mathrm{T}}\mathbf{M}_\Gamma\boldsymbol{\gamma})\mathbf{z}}{(\mathbf{z}^{\mathrm{T}}\mathbf{K}\mathbf{z})^{1/2}} &= \sup_{0\neq\varphi_h\in V_h} \frac{\int_{\Omega_h} d_h\varphi_h \mathrm{d}x + \int_{\Gamma_h}(\gamma_h d_h)(\gamma_h\varphi_h)\mathrm{d}\sigma_h}{\|\varphi_h\|_{a_h}}\,.\end{aligned}$$

With the Cauchy–Schwarz and Young inequality, we obtain

$$\begin{aligned}\|\mathbf{e}\|_{\mathbf{K}}^2 &= -\mathbf{e}^{\mathrm{T}}(\mathbf{M}_\Omega + \boldsymbol{\gamma}^{\mathrm{T}}\mathbf{M}_\Gamma\boldsymbol{\gamma})\mathbf{d} = -\mathbf{e}^{\mathrm{T}}\mathbf{K}^{1/2}\mathbf{K}^{-1/2}(\mathbf{M}_\Omega + \boldsymbol{\gamma}^{\mathrm{T}}\mathbf{M}_\Gamma\boldsymbol{\gamma})\mathbf{d} \\ &\leq \|\mathbf{K}^{1/2}\mathbf{e}\|_2\|\mathbf{K}^{-1/2}(\mathbf{M}_\Omega + \boldsymbol{\gamma}^{\mathrm{T}}\mathbf{M}_\Gamma\boldsymbol{\gamma})\mathbf{d}\|_2 \\ &= \|\mathbf{e}\|_{\mathbf{K}}\|\mathbf{d}\|_\star\,.\end{aligned} \tag{B.5.3}$$

We thus have shown that

$$\|\mathbf{e}\|_{\mathbf{K}} \leq \|\mathbf{d}\|_\star\,.$$

B.5.3. Consistency

In this section, we bound the dual norm of the defect in order to obtain an optimal order H^1-estimate. In order to prove error bounds of order j, we assume that the solution $u \in H^{j+1}(\Omega;\Gamma)$, which is provided if Γ is a C^{j+1}-manifold, $g \in H^{j-1}(\Gamma)$, $f \in H^{j-1}(\Omega)$ (see Proposition B.2.1). Note that since $j \geq 1$ and the dimension $n \in \{2,3\}$, we have $H^{j+1}(\Omega) \subseteq C^0(\Omega)$ and the finite element interpolation $\widetilde{I}_h u$ of u is well-defined.

Proposition B.5.5. *Under the assumptions of Theorem B.5.1, the defect is bounded by*

$$\|\mathbf{d}\|_\star \leq Ch^{\min(k,j)} + c\|f_h^l - f\|_{L^2(\Omega)} + c\|g_h^l - g\|_{L^2(\Gamma)}\,, \tag{B.5.4}$$

where $C = C(\|f\|_{L^2(\Omega)}, \|g\|_{L^2(\Gamma)}, \|u\|_{H^{j+1}(\Omega;\Gamma)})$.

Proof. The defect equation (B.5.2) is equivalent to

$$\begin{aligned} m_h^\Omega(d_h,\varphi_h) + m_h^\Gamma(d_h,\varphi_h) = {}& \alpha m_h^\Gamma(\widetilde{I}_h u,\varphi_h) + \beta a_h^\Gamma(\widetilde{I}_h u,\varphi_h) \\ & + \kappa m_h^\Omega(\widetilde{I}_h u,\varphi_h) + a_h^\Omega(\widetilde{I}_h u,\varphi_h) - \ell_h(\varphi_h) \end{aligned}$$

for all finite element functions $\varphi_h \in V_h$. Since $\varphi_h^l \in H^1(\Omega;\Gamma)$, the exact solution u satisfies

$$0 = \alpha m^\Gamma(u,\varphi_h^l) + \beta a^\Gamma(u,\varphi_h^l) + \kappa m^\Omega(u,\varphi_h^l) + a^\Omega(u,\varphi_h^l) - \ell(\varphi_h^l)\,.$$

Subtracting both equations yields

$$\begin{aligned} m_h^\Omega(d_h,\varphi_h) + m_h^\Gamma(d_h,\varphi_h) = {}& \alpha\left(m_h^\Gamma(\widetilde{I}_h u,\varphi_h) - m^\Gamma(u,\varphi_h^l)\right) \\ & + \beta\left(a_h^\Gamma(\widetilde{I}_h u,\varphi_h) - a^\Gamma(u,\varphi_h^l)\right) \\ & + \kappa\left(m_h^\Omega(\widetilde{I}_h u,\varphi_h) - m^\Omega(u,\varphi_h^l)\right) \\ & + \left(a_h^\Omega(\widetilde{I}_h u,\varphi_h) - a^\Omega(u,\varphi_h^l)\right) \\ & + \left(\ell_h(\varphi_h) - \ell(\varphi_h^l)\right)\,. \end{aligned}$$

We estimate the five terms separately.

(i) We write

$$\begin{aligned} & m_h^\Gamma(\widetilde{I}_h u,\varphi_h) - m^\Gamma(u,\varphi_h^l) \\ =& m_h^\Gamma(\widetilde{I}_h u,\varphi_h) - m^\Gamma(I_h u,\varphi_h^l) + m^\Gamma(I_h u - u,\varphi_h^l)\,. \end{aligned}$$

With the Cauchy–Schwarz inequality and Proposition B.4.5 we obtain for the second term:

$$\begin{aligned} m^\Gamma(I_h u - u,\varphi_h^l) &\leq \|\gamma(I_h u - u)\|_{L^2(\Gamma)}\|\gamma\varphi_h^l\|_{L^2(\Gamma)} \\ &\leq \|I_h u - u\|_{L^2(\Omega;\Gamma)}\|\varphi_h^l\|_{H^1(\Omega;\Gamma)} \\ &\leq ch^{j+1}\|u\|_{H^{j+1}(\Omega;\Gamma)}\|\varphi_h^l\|_{H^1(\Omega;\Gamma)}\,. \end{aligned}$$

For the first term, we use Proposition B.4.6 and then Proposition B.4.5:

$$\begin{aligned}
&\left|m_h^\Gamma(\widetilde{I}_h u, \varphi_h) - m^\Gamma(I_h u, \varphi_h^l)\right| \\
&\leq ch^{k+1}\|\gamma I_h u\|_{L^2(\Gamma)}\|\gamma\varphi_h^l\|_{L^2(\Gamma)} \\
&\leq ch^{k+1}\|I_h u\|_{L^2(\Omega;\Gamma)}\|\varphi_h^l\|_{H^1(\Omega;\Gamma)} \\
&\leq ch^{k+1}\left(\|I_h u - u\|_{L^2(\Omega;\Gamma)} + \|u\|_{L^2(\Omega;\Gamma)}\right)\|\varphi_h^l\|_{H^1(\Omega;\Gamma)} \\
&\leq ch^{k+1}\left(ch^{j+1}\|u\|_{H^{j+1}(\Omega;\Gamma)} + \|u\|_{H^1(\Omega;\Gamma)}\right)\|\varphi_h^l\|_{H^1(\Omega;\Gamma)} \\
&\leq ch^{k+1}\|u\|_{H^{j+1}(\Omega;\Gamma)}\|\varphi_h^l\|_{H^1(\Omega;\Gamma)}\,.
\end{aligned}$$

(ii) Similarly, we write

$$\begin{aligned}
&a_h^\Gamma(\widetilde{I}_h u, \varphi_h) - a^\Gamma(u, \varphi_h^l) \\
=&a_h^\Gamma(\widetilde{I}_h u, \varphi_h) - a^\Gamma(I_h u, \varphi_h^l) + a^\Gamma(I_h u - u, \varphi_h^l)\,.
\end{aligned}$$

We then proceed as in the first step and obtain

$$\left|a_h^\Gamma(\widetilde{I}_h u, \varphi_h) - a^\Gamma(u, \varphi_h^l)\right| \leq ch^{\min(k+1,j)}\|u\|_{H^{j+1}(\Omega;\Gamma)}\|\varphi_h^l\|_{H^1(\Omega;\Gamma)}\,.$$

(iii,iv) Using Propositions B.4.5 and B.4.6, we obtain analogously

$$\left|m_h^\Omega(\widetilde{I}_h u, \varphi_h) - m^\Omega(u, \varphi_h^l)\right| \leq ch^{\min(k,j)+1}\|u\|_{H^{j+1}(\Omega;\Gamma)}\|\varphi_h^l\|_{H^1(\Omega;\Gamma)}$$

and

$$\left|a_h^\Omega(\widetilde{I}_h u, \varphi_h) - a^\Omega(u, \varphi_h^l)\right| \leq ch^{\min(k,j)}\|u\|_{H^{j+1}(\Omega;\Gamma)}\|\varphi_h^l\|_{H^1(\Omega;\Gamma)}\,.$$

(v) For the last term we note that

$$\begin{aligned}
\ell_h(\varphi_h) - \ell(\varphi_h^l) = m_h^\Omega(f_h, \varphi) - m^\Omega(f, \varphi_h^l) \\
+ m_h^\Gamma(g_h, \gamma_h\varphi_h) - m^\Gamma(g, \gamma\varphi_h^l)\,.
\end{aligned}$$

We write

$$m_h^\Omega(f_h, \varphi_h) - m^\Omega(f, \varphi_h^l) = m_h^\Omega(f_h, \varphi_h) - m^\Omega(f_h^l, \varphi_h^l) + m^\Omega(f_h^l - f, \varphi_h^l)\,.$$

By the Cauchy–Schwarz inequality the last term is bounded by

$$m^\Omega(f_h^l - f, \varphi_h^l) \leq \|f_h^l - f\|_{L^2(\Omega)}\|\varphi_h^l\|_{H^1(\Omega;\Gamma)}\,.$$

For the first term we use Proposition B.4.6:

$$\begin{aligned}
\left|m_h^\Omega(f_h, \varphi_h) - m^\Omega(f_h^l, \varphi_h^l)\right| &\leq ch^k\|f_h^l\|_{L^2(\Omega)}\|\varphi_h^l\|_{L^2(\Omega)} \\
&\leq ch^k\left(\|f_h^l - f\|_{L^2(\Omega)} + \|f\|_{L^2(\Omega)}\right)\|\varphi_h^l\|_{H^1(\Omega;\Gamma)}\,,
\end{aligned}$$

so that we obtain the bound

$$\left|m_h^\Omega(f_h,\varphi_h)-m^\Omega(f,\varphi_h^l)\right| \le ch^k\|f\|_{L^2(\Omega)}\|\varphi_h^l\|_{H^1(\Omega;\Gamma)} + c\|f_h^l-f\|_{L^2(\Omega)}\|\varphi_h^l\|_{H^1(\Omega;\Gamma)}\,.$$

In a similar fashion we estimate

$$\left|m_h^\Gamma(g_h,\varphi_h)-m^\Gamma(g,\varphi_h^l)\right| \le \left(ch^{k+1}\|g\|_{L^2(\Gamma)} + \|g_h^l-g\|_{L^2(\Gamma)}\right)\|\varphi_h^l\|_{H^1(\Omega;\Gamma)}\,.$$

Adding the five estimates, using definition (B.5.3) of the dual norm together with the coercivity of a_h, we obtain (B.5.4). □

Now we can prove Theorem B.5.1.

Proof of Theorem B.5.1. The error is decomposed in the following way:

$$u-u_h^l = (u-I_hu) + \left(I_hu-u_h^l\right)\,.$$

With Proposition B.4.5, we obtain $\|u-I_hu\|_{H^1(\Omega;\Gamma)} \le ch^j\|u\|_{H^{j+1}(\Omega;\Gamma)}$. For the second term, we note that $\widetilde{I}_hu-u_h$ is the finite element function corresponding to the nodal vector $\mathbf{u}^*-\mathbf{u}=-\mathbf{e}$, so using Proposition B.3.2 and Lemma B.4.2, we obtain

$$\|I_hu-u_h^l\|_{H^1(\Omega;\Gamma)} \le c\|\widetilde{I}_hu-u_h\|_{H^1(\Omega_h;\Gamma_h)} \le c\|\mathbf{e}\|_{\mathbf{K}} \le c\|\mathbf{d}\|_\star\,,$$

so the result follows from Proposition B.5.5. □

B.5.4. L^2-estimate

In order to derive an optimal-order L^2-estimate, we apply the Aubin–Nitsche trick.

Proof of Theorem B.5.3. Consider the dual problem

$$\begin{aligned}&\text{for } \eta\in L^2(\Omega;\Gamma),\ \text{find } z_\eta\in H^1(\Omega;\Gamma) \text{ such that}\\ &\quad a(z_\eta,\psi)=m^\Omega(\eta,\psi)+m^\Gamma(\gamma\eta,\gamma\psi) \text{ for all } \psi\in H^1(\Omega;\Gamma)\,.\end{aligned}$$

This is the weak formulation of (B.1.1) with $f=\eta$, $g=\gamma\eta$. Since $\eta\in L^2(\Omega;\Gamma)$, we have $z_\eta\in H^2(\Omega;\Gamma)$ and z_η satisfies the a priori estimate (see Proposition B.2.1)

$$\|z_\eta\|_{H^2(\Omega;\Gamma)} \le c\|\eta\|_{L^2(\Omega;\Gamma)}\,. \tag{B.5.5}$$

With $\eta = e = u - u_h^l$ and writing $z = z_e$ for brevity, we have

$$\begin{aligned}
\|e\|^2_{L^2(\Omega;\Gamma)} &= m^\Omega(e,e) + m^\Gamma(\gamma e, \gamma e) = a(e,z) \\
&= a(u - u_h^l, z - I_h z) + a(u, I_h z) - a(u_h^l, I_h z) \\
&= a(u - u_h^l, z - I_h z) + \ell(I_h z) - a(u_h^l, I_h z - z) - a(u_h^l, z) \\
&= a(u - u_h^l, z - I_h z) + \ell(I_h z) - \ell_h(\widetilde{I}_h z) + a_h(u_h, \widetilde{I}_h z) \\
&\quad - a(u_h^l, I_h z - z) - a(u_h^l - u, z) - a(u, z) \\
&= a(u - u_h^l, z - I_h z) \\
&\quad + \Big(\ell(I_h z) - \ell_h(\widetilde{I}_h z)\Big) \\
&\quad + \Big(a_h(u_h, \widetilde{I}_h z - z^{-l}) - a(u_h^l, I_h z - z)\Big) \\
&\quad + \Big(a_h(u_h - u^{-l}, z^{-l}) - a(u_h^l - u, z)\Big) \\
&\quad + \Big(a_h(u^{-l}, z^{-l}) - a(u, z)\Big)\,.
\end{aligned} \tag{B.5.6}$$

We estimate the five terms separately.

(i) Using the boundedness of a, Theorem B.5.1, Proposition B.4.5 and the a priori bound (B.5.5), we obtain

$$\begin{aligned}
a(u - u_h^l, z - I_h z) &\le c\|u - u_h^l\|_{H^1(\Omega;\Gamma)} \|z - I_h z\|_{H^1(\Omega;\Gamma)} \\
&\le ch\|z\|_{H^2(\Omega;\Gamma)} \|u - u_h^l\|_{H^1(\Omega;\Gamma)} \\
&\le ch\|e\|_{L^2(\Omega;\Gamma)} \left(Ch^{\min(k,j)} + c\|f - f_h^l\|_{L^2(\Omega)} + c\|g - g_h^l\|_{L^2(\Gamma)}\right) \\
&\le \left(Ch^{\min(k,j)+1} + ch\|f - f_h^l\|_{L^2(\Omega)} + ch\|g - g_h^l\|_{L^2(\Gamma)}\right) \|e\|_{L^2(\Omega;\Gamma)}\,.
\end{aligned}$$

(ii) We write

$$\begin{aligned}
\ell(I_h z) - \ell_h(\widetilde{I}_h z) &= m^\Omega(f, I_h z) - m_h^\Omega(f_h, \widetilde{I}_h z) \\
&\quad + m^\Gamma(g, I_h z) - m_h^\Gamma(g_h, \widetilde{I}_h z) \\
&= m^\Omega(f - f_h^l, I_h z) + \Big(m^\Omega(f_h^l, I_h z) - m_h^\Omega(f_h, \widetilde{I}_h z)\Big) \\
&\quad + m^\Gamma(g - g_h^l, I_h z) + \Big(m^\Gamma(g_h^l, I_h z) - m_h^\Gamma(g_h, \widetilde{I}_h z)\Big)\,.
\end{aligned}$$

Using Cauchy–Schwarz, Proposition B.4.5 and (B.5.5), we see that the first term is bounded by

$$\begin{aligned}
m^\Omega(f - f_h^l, I_h z) &\le \|f - f_h^l\|_{L^2(\Omega)} \left(\|I_h z - z\|_{L^2(\Omega;\Gamma)} + \|z\|_{L^2(\Omega;\Gamma)}\right) \\
&\le \|f - f_h^l\|_{L^2(\Omega;\Gamma)} \left(ch^2 + 1\right) \|z\|_{H^2(\Omega;\Gamma)} \\
&\le c\|f - f_h^l\|_{L^2(\Omega)} \|e\|_{L^2(\Omega;\Gamma)}\,.
\end{aligned}$$

For the third term we proceed similarly and obtain

$$\begin{aligned} m^\Gamma(g - g_h^l, I_h z) &\leq \|g - g_h^l\|_{L^2(\Gamma)} \|I_h z\|_{L^2(\Gamma)} \\ &\leq \|g - g_h^l\|_{L^2(\Gamma)} \left(\|I_h z - z\|_{L^2(\Omega;\Gamma)} + \|z\|_{L^2(\Omega;\Gamma)} \right) \\ &\leq c \|g - g_h^l\|_{L^2(\Gamma)} \|e\|_{L^2(\Omega;\Gamma)} \,. \end{aligned}$$

For the second term we use Propositions B.4.6 and B.4.5 to obtain

$$\begin{aligned} m^\Omega(f_h^l, I_h z) - m_h^\Omega(f_h, \widetilde{I}_h z) &\leq c h^{k+1} \left(\|f_h^l - f\|_{H^1(\Omega)} + \|f\|_{H^1(\Omega)} \right) \|I_h z\|_{H^1(\Omega)} \\ &\leq c h^{k+1} \left(\|f_h^l - f\|_{H^1(\Omega)} + \|f\|_{H^1(\Omega)} \right) \|e\|_{L^2(\Omega;\Gamma)} \,. \end{aligned} \tag{B.5.7}$$

With Proposition B.4.6, we similarly obtain

$$m^\Gamma(g_h^l, I_h z) - m_h^\Gamma(g_h, \widetilde{I}_h z) \leq c h^{k+1} \left(\|g\|_{L^2(\Gamma)} + \|g_h^l - g\|_{L^2(\Gamma)} \right) \|e\|_{L^2(\Omega;\Gamma)} \,.$$

(iii) With Proposition B.4.6 and Theorem B.5.1, we obtain

$$\begin{aligned} &a_h(u_h, \widetilde{I}_h z - z^{-l}) - a(u_h^l, I_h z - z) \\ &\leq c h^k \|u_h^l\|_{H^1(\Omega;\Gamma)} \|I_h z - z\|_{H^1(\Omega;\Gamma)} \\ &\leq c h^k \|u_h^l - u + u\|_{H^1(\Omega;\Gamma)} c h \|z\|_{H^2(\Omega;\Gamma)} \\ &\leq c h^{k+1} \left(\|u_h^l - u\|_{H^1(\Omega;\Gamma)} + \|u\|_{H^1(\Omega;\Gamma)} \right) \|z\|_{H^2(\Omega;\Gamma)} \\ &\leq c h^{k+1} \left(C h^{\min(k,j)} + c \|f - f_h^l\|_{L^2(\Omega)} + c \|g - g_h^l\|_{L^2(\Gamma)} \right) \|e\|_{L^2(\Omega;\Gamma)} \,. \end{aligned}$$

(iv) Using the same arguments, we obtain for the fourth term

$$\begin{aligned} &a(u_h - u^{-l}, z^{-l}) - a(u_h^l - u, z) \\ &\leq c h^k \|u_h^l - u\|_{H^1(\Omega;\Gamma)} \|z\|_{H^1(\Omega;\Gamma)} \\ &\leq c h^k \left(C h^{\min(k,j)} + c \|f - f_h^l\|_{L^2(\Omega)} + c \|g - g_h^l\|_{L^2(\Gamma)} \right) \|e\|_{L^2(\Omega;\Gamma)} \,. \end{aligned}$$

(v) For the fifth term, using $u, z \in H^2(\Omega)$, we have with Proposition B.4.6 and Theorem B.5.1

$$\begin{aligned} a_h(u^{-l}, z^{-l}) - a(u, z) &\leq c h^{k+1} \|u\|_{H^2(\Omega;\Gamma)} \|z\|_{H^2(\Omega;\Gamma)} \\ &\leq c h^{k+1} \|u\|_{H^{k+1}(\Omega;\Gamma)} \|e\|_{L^2(\Omega;\Gamma)} \,. \end{aligned}$$

Inserting all the bounds into (B.5.6) gives the bound:

$$\|e\|_{L^2(\Omega;\Gamma)} \leq C h^{\min(k,j)+1} + c \|f - f_h^l\|_{L^2(\Omega)} + c \|g - g_h^l\|_{L^2(\Gamma)} + c h^{k+1} \|f - f_h^l\|_{H^1(\Omega)} \,,$$

where C depends on $\|u\|_{H^{j+1}(\Omega;\Gamma)}$, $\|f\|_{H^1(\Omega)}$ and $\|g\|_{L^2(\Gamma)}$. This completes the proof of Theorem B.5.3. □

Remark B.5.6. *Compared with Theorem B.5.1, we need for $j = 1$ the additional assumption that $f \in H^1(\Omega)$. This is due to the first two estimates of Proposition B.4.6, which only give a h^k-error bound for $f \in L^2(\Omega)$ in* (B.5.7)*. Alternatively, since $f_h^l \in H^1(\Omega)$, we could simply estimate*

$$m^\Omega(f_h^l, I_h z) - m_h^\Omega(f_h, \widetilde{I}_h z) \leq c h^{k+1} \|f_h^l\|_{H^1(\Omega)} \|e\|_{L^2(\Omega;\Gamma)}$$

in (B.5.7) *without using the triangle inequality and then make the reasonable assumption that f_h can be chosen such that $\|f_h^l\|_{H^1(\Omega)} \leq c\|f\|_{L^2(\Omega)}$ with a constant independent of h. Keeping in mind that we need $f \in H^{k+1}(\Omega)$ anyway to obtain the full order, the assumption $f \in H^1(\Omega)$ becomes redundant in this case.*

Corollary B.5.7. *Consider the standard Robin problem*

$$\begin{cases} -\Delta u + \kappa u = f & \text{in } \Omega\,, \\ \dfrac{\partial u}{\partial \mathrm{n}} + \alpha u = g & \text{on } \Gamma = \partial\Omega\,, \end{cases}$$

Here, the weak solution u is in $H^1(\Omega)$, and with minor modifications to the above convergence proof, we obtain under suitable assumptions the error estimate

$$\|u - u_h^l\|_{L^2(\Omega)} + h\|u - u_h^l\|_{H^1(\Omega)} \leq C h^{k+1}$$

for the isoparametric finite element method. The same result holds for the Neumann boundary condition, i.e. $\alpha = 0$ and $\kappa > 0$.

B.6. Numerical examples

We illustrate the theoretical results with some numerical examples. We use isoparametric finite elements of degree one and two to solve a generalized Robin problem in two and three space dimensions. Polyhedral approximations are obtained with *distmesh* [Persson and Strang, 2004]. For quadratic finite elements, we add new nodes and project the boundary nodes on the boundary. All functions are implemented in MATLAB, the isoparametric elements are implemented based on the ideas of Bartels et al. [2006].

Example B.6.1. (Two-dimensional)
We solve the generalized Robin boundary value problem

$$\begin{cases} -\Delta u + u = f & \text{in } \Omega\,, \\ \dfrac{\partial u}{\partial \mathrm{n}} + u - \Delta_\Gamma u = g & \text{on } \Gamma = \partial\Omega\,, \end{cases} \tag{B.6.1}$$

where $\Omega = \{x \in \mathbb{R}^2 : |x| < 1\}$ is the unit circle, with isoparametric finite elements of degree one and two. As exact solution, we chose

$$u(x, y) = xy(x^2 + y^2)^2$$

from which we compute the right-hand side functions f and g. We compute numerical solutions for different mesh sizes. The finest mesh we used for linear finite elements has around 18000 nodes and the refined version used for quadratic finite elements has around 73500 nodes. The error between the lifted numerical solution and the exact solution corresponding to each mesh size h is reported in Figure B.1 with a double logarithmic scale for finite elements of polynomial degree 1 and 2. The error $\mathrm{err}(h)$ *is expected to converge with order k and $k+1$ ($k = 1, 2$) as stated in Theorem B.5.1 for the $H^1(\Omega;\Gamma)$-norm and in Theorem B.5.3 for the $L^2(\Omega;\Gamma)$-norm, respectively. The numerical results therefore illustrate the expected rates of convergence.*

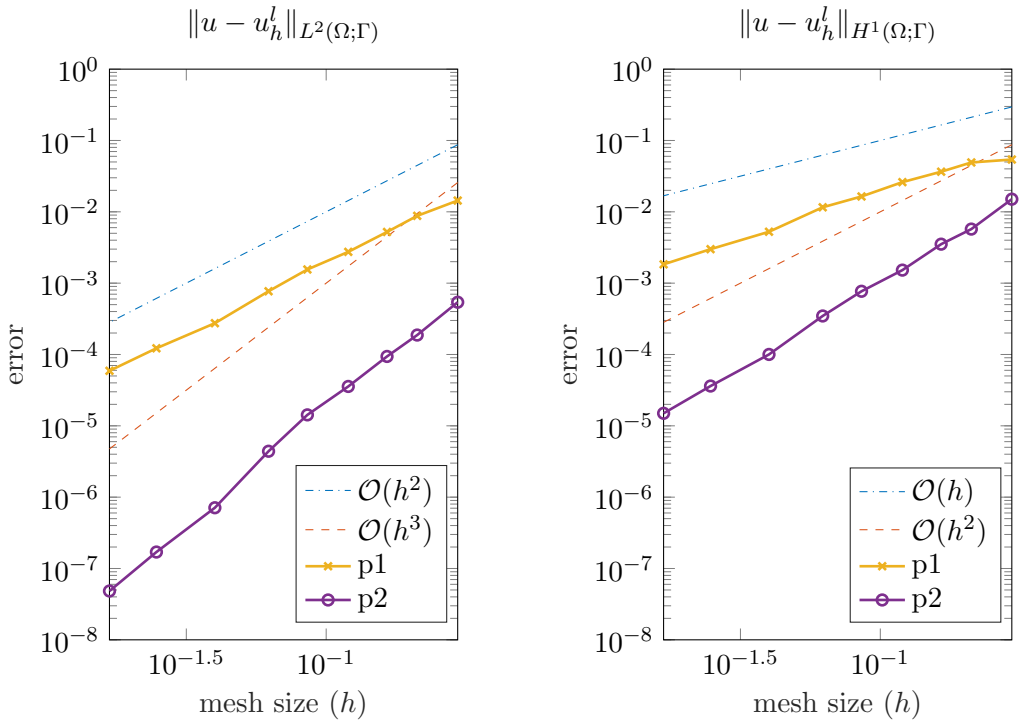

Figure B.1.: Convergence rate of the GRP discretization of Example B.6.1 with isoparametric finite elements of degree 1 and 2 in two dimensions.

Example B.6.2. (Three-dimensional)
We solve the generalized Robin boundary value problem (B.6.1) *where*

$$\Omega = \{x \in \mathbb{R}^3 : |x| < 1\}$$

is the unit ball, with isoparametric finite elements of degree one and two. As exact solution, we

chose

$$u(x, y) = x^2 + y^2 - x^2 z^2$$

from which we compute the right-hand side functions f and g. The finest mesh we used for linear finite elements has around 7000 nodes, and the refined version used for quadratic finite elements has around 55000 nodes. The error between the lifted numerical solution and the exact solution is reported in Figure B.2 for elements of polynomial degree 1 and 2. The numerical results illustrate the expected rates of convergence as stated in Theorem B.5.1 and Theorem B.5.3.

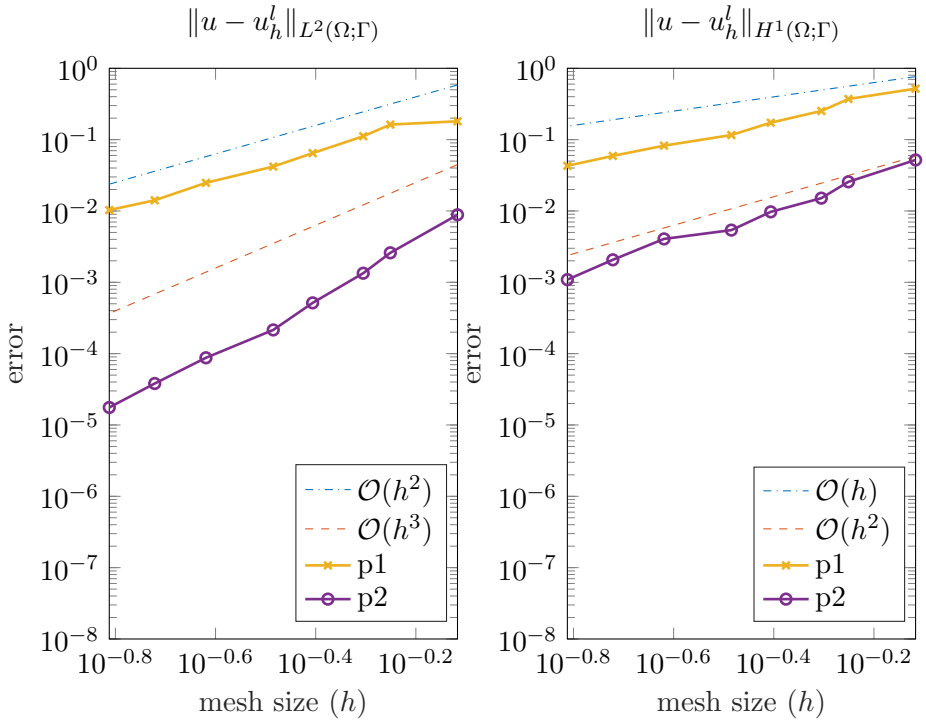

Figure B.2.: Convergence rate of the GRP discretization of Example B.6.2 with isoparametric finite elements of degree 1 and 2 in three dimensions.

C. Numerical analysis of an evolving bulk–surface model of tumour growth

This chapter is an updated version of [Edelmann et al., 2024], which is currently undergoing a minor review process and is about to be accepted in IMA J. Numer. Anal.

Abstract. This paper studies an evolving bulk–surface finite element method for a model of tissue growth, which is a modification of the model of Eyles, King and Styles (2019). The model couples a Poisson equation on the domain with a forced mean curvature flow of the free boundary, with nontrivial bulk–surface coupling in both the velocity law of the evolving surface and the boundary condition of the Poisson equation. The numerical method discretizes evolution equations for the mean curvature and the outer normal and it uses a harmonic extension of the surface velocity into the bulk. The discretization admits a convergence analysis in the case of continuous finite elements of polynomial degree at least two. The stability of the discretized bulk–surface coupling is a major concern. The error analysis combines stability estimates and consistency estimates to yield optimal-order H^1-norm error bounds for the computed tissue pressure and for the surface position, velocity, normal vector and mean curvature. Numerical experiments illustrate and complement the theoretical results.

C.1. Introduction

Eyles, King and Styles [Eyles et al., 2019] proposed and studied a 'tractable' model for tumour growth that determines the evolving tumour domain $\Omega(t)$ at time t with the free boundary surface $\Gamma(t)$ together with the tissue pressure $u(x,t)$ on $\Omega(t)$:

- The tissue pressure u solves a Poisson equation on the bulk $\Omega(t)$ with an inhomogeneous Robin boundary condition, where the inhomogeneity is a sum of the mean curvature on $\Gamma(t)$ and a given source term.
- The surface $\Gamma(t)$ follows a forced mean curvature flow with the tissue pressure on the boundary as the forcing term.

This model has non-trivial bulk–surface coupling in both the velocity law of the evolving surface and the boundary condition for the tissue pressure. A related model based on the Stokes flow, instead of Darcy's law which yields the Poisson equation, was proposed in [King and Venkataraman, 2021].

While the original model of [Eyles et al., 2019] turned out intractable to us, we show that a modified tumour model is indeed tractable by numerical analysis (alas, not the tumour itself). The modification replaces the Robin boundary condition by a generalized Robin boundary condition that adds the surface Laplacian of u as a regularizing term. This allows us to control the

$H^1(\Gamma(t))$ norm of the error in u in the numerical discretization, which is essential in the stability analysis.

We propose and analyse an evolving finite element method for the modified bulk–surface problem, which differs from the method proposed in [Eyles et al., 2019] in how the forced mean curvature flow is handled numerically. We use the numerical approach of [Kovács et al., 2019, 2020], which discretizes evolution equations for the outer normal and the mean curvature, and which allows for an error analysis that yields convergence with optimal-order error bounds.

In Section C.2 we formulate the model equations and further equations that are to be solved numerically. In Section C.3 we describe the evolving finite element semi-discretization and formulate the main result on optimal-order error bounds in the H^1 norm (Theorem C.3.1). This theorem is proved in the course of Section C.4 on stability (bounding errors in terms of defects) and Section C.5 on consistency (bounding defects), using also auxiliary results from the appendix (Section C.8). In Subsection C.4.5 we explain which term in the error equations prevents us from a stability analysis for the original Eyles–King–Styles model. Numerical experiments in Section C.7 illustrate the behaviour of the numerical method and the (tiny) effect of the regularization on the solution.

C.2. The Eyles–King–Styles model of tumour growth

C.2.1. Basic notions and notation

For times t in an interval $[0,T]$, we consider a time-dependent closed surface $\Gamma(t)$ in $\mathbb{R}^3$ that is the boundary of a bounded domain $\Omega(t) \subset \mathbb{R}^3$. With $\Omega^0 = \Omega(0)$ and $\Gamma^0 = \Gamma(0)$, we assume that the closure $\overline{\Omega(t)} = \Omega(t) \cup \Gamma(t) \subset \mathbb{R}^3$ is the image of a smooth map $X\colon \Omega^0 \cup \Gamma^0 \times [0,T] \to \mathbb{R}^3$ with the properties that $X(\cdot,0)$ is the identity map and, for each t, $X(\cdot,t)$ is an embedding and in particular

$$\Omega(t) = \{X(q,t) \ : \ q \in \Omega^0\}\,, \qquad \Gamma(t) = \{X(q,t) \ : \ q \in \Gamma^0\}\,.$$

In view of the subsequent numerical discretization, it is convenient to think of $X(q,t) \in \overline{\Omega(t)}$ as the position at time t of a particle labelled by its initial position $q \in \Omega^0 \cup \Gamma^0$, and of $\overline{\Omega(t)}$ as a collection of such particles. Particles that are initially in the interior Ω^0 remain in the interior $\Omega(t)$ and those on the boundary surface Γ^0 remain on the boundary surface $\Gamma(t)$. In the following, we will refer to $\Omega(t)$ as the bulk and to $\Gamma(t)$ as the boundary.

To indicate the dependence of the domain and its boundary on X, we will write

$$\Omega(t) = \Omega[X(\cdot,t)] \quad \text{and} \quad \Gamma(t) = \Gamma[X(\cdot,t)],$$

or briefly $\Omega[X]$ and $\Gamma[X]$ when the time t is clear from the context. The velocity $v(x,t) \in \mathbb{R}^3$ at a point $x = X(q,t) \in \Omega(t) \cup \Gamma(t)$ equals

$$\partial_t X(q,t) = v(X(q,t),t). \tag{C.2.1}$$

For a known velocity field v, the position $X(q,t)$ at time t of the particle with label q is obtained by solving the ordinary differential equation (C.2.1) from 0 to t for a fixed q. We denote the surface velocity and surface position

$$v_\Gamma(\cdot,t) = v(\cdot,t)|_{\Gamma(t)} \quad \text{and} \quad X_\Gamma(\cdot,t) = X(\cdot,t)|_{\Gamma^0}.$$

For a function $u(x,t)$ ($x \in \Omega(t) \cup \Gamma(t)$, $0 \le t \le T$) we denote the material derivative (with respect to the parametrization X) as

$$\partial^\bullet u(x,t) = \frac{\mathrm{d}}{\mathrm{d}t}\, u(X(q,t),t) = \nabla u(x,t) \cdot v(x,t) + \partial_t u(x,t) \qquad \text{for } \; x = X(q,t).$$

On any regular surface $\Gamma \subset \mathbb{R}^3$, we denote by $\nabla_\Gamma u \colon \Gamma \to \mathbb{R}^3$ the tangential gradient of a function $u \colon \Gamma \to \mathbb{R}$, and in the case of a vector-valued function $u = (u_1, u_2, u_3)^T \colon \Gamma \to \mathbb{R}^3$, we let $\nabla_\Gamma u = (\nabla_\Gamma u_1, \nabla_\Gamma u_2, \nabla_\Gamma u_3)$. We thus use the convention that the gradient of u has the gradient of the components as column vectors. We denote by $\nabla_\Gamma \cdot f = \mathrm{tr}(\nabla_\Gamma f)$ the surface divergence of a vector field f on Γ, cf. [Dziuk and Elliott, 2013b, equation (2.7)], and by $\Delta_\Gamma u = \nabla_\Gamma \cdot \nabla_\Gamma u$ the Laplace–Beltrami operator applied to u; see the review [Deckelnick et al., 2005] or [Ecker, 2012, Appendix A] or any textbook on differential geometry for these notions.

We denote the unit outer normal vector field to Γ by $\mathrm{n} \colon \Gamma \to \mathbb{R}^3$. Its surface gradient contains the (extrinsic) curvature data of the surface Γ. At every $x \in \Gamma$, the matrix of the extended Weingarten map,

$$A(x) = \nabla_\Gamma \mathrm{n}(x),$$

is a symmetric 3×3 matrix (see, e.g., [Walker, 2015, Proposition 20]). Apart from the eigenvalue 0 with eigenvector $\mathrm{n}(x)$, its other two eigenvalues are the principal curvatures κ_1 and κ_2 at the point x on the surface. They determine the fundamental quantities

$$H := \mathrm{tr}(A) = \kappa_1 + \kappa_2, \qquad |A|^2 = \kappa_1^2 + \kappa_2^2, \tag{C.2.2}$$

where H is the mean curvature (as in most of the literature, defined here without a factor $1/2$) and $|A|$ is the Frobenius norm of the matrix A.

C.2.2. Model equations and more equations

C.2.2.1. A 'tractable' model for tumour growth

In [Eyles et al., 2019], Eyles, King and Styles studied the following model for tumour growth, which determines the tissue pressure $u(x,t)$ on the evolving tumour domain $\Omega(t)$ with the free boundary $\Gamma(t)$ by the following Robin boundary value problem (α here corresponds to $1/\alpha$ in [Eyles et al., 2019]):

$$-\Delta u = -1 \qquad \text{in } \Omega(t)\,, \tag{C.2.3a}$$

$$\partial_{\mathrm{n}} u + \alpha u = \beta H + Q \qquad \text{on } \Gamma(t)\,, \tag{C.2.3b}$$

where ∂_{n} is the outer normal derivative, $\alpha > 0$ and $\beta > 0$ are given constants, $H(x,t)$ is the mean curvature of the surface $\Gamma(t)$, and $Q(x,t)$ is a given surface source term. (In Eyles et al. [2019] the authors state that "α and β are regularising parameters, the unregularised case being associated with the limit $\alpha \to 0$ with β fixed".) We assume throughout that $Q \colon \mathbb{R}^3 \times \mathbb{R} \to \mathbb{R}$ is a smooth function. The surface velocity is determined by the velocity law of a forced mean curvature flow:

$$v_\Gamma = V\mathrm{n}, \quad \text{with the normal velocity} \quad V = -\beta H + \alpha u \quad \text{on } \Gamma(t)\,. \tag{C.2.4}$$

Note that the above equations are strongly coupled through the appearance of H as a source term in (C.2.3b) and of u as the forcing term in (C.2.4).

C.2.2.2. Forced mean curvature flow

The velocity law (C.2.4) describes a forced mean curvature flow. In [Kovács et al., 2020, Lemma 2.1] it was shown that the mean curvature and surface normal from (C.2.4) satisfy parabolic evolution equations along the flow, which read (note that here αu corresponds to u of [Kovács et al., 2020]):

$$\partial^\bullet \mathrm{n} = \beta \Delta_\Gamma \mathrm{n} + \beta |A|^2 \mathrm{n} - \alpha \nabla_\Gamma u \qquad \text{on } \Gamma(t)\,, \tag{C.2.5a}$$

$$\partial^\bullet H = \beta \Delta_\Gamma H + \beta |A|^2 H - \alpha \Delta_\Gamma u - \alpha\, |A|^2 u \qquad \text{on } \Gamma(t)\,. \tag{C.2.5b}$$

In our numerical method, we will discretize the weak form of these equations by evolving finite elements and use the so obtained approximations to H and n in (C.2.4) to compute an approximate surface velocity. The second-order term $\Delta_\Gamma u$ in (C.2.5b) requires special attention in the stability analysis.

C.2.2.3. Harmonic extension of the surface velocity into the bulk

For the finite element method, a moving mesh is required not only on the boundary $\Gamma(t)$ but also on $\Omega(t)$; cf. [Eyles et al., 2019, Section 6.1.2]. This is achieved by extending the velocity v_Γ, which is given by the forced mean curvature flow, harmonically into $\Omega(t)$, i.e., we have the equation

$$\begin{aligned} -\Delta v &= 0 \qquad && \text{in } \Omega(t)\,, \\ v &= v_\Gamma \qquad && \text{on } \Gamma(t)\,. \end{aligned} \tag{C.2.6}$$

With this velocity, the positions $X(q,t)$ are obtained by solving the ordinary differential equation (C.2.1). The equations given so far fully describe the coupled bulk–surface model of [Eyles et al., 2019].

C.2.2.4. Regularization

In view of the term $\Delta_\Gamma u$ in the evolution equation (C.2.5b) for the forced mean curvature flow, it is crucial that the trace of u on Γ, denoted γu, be in $H^1(\Gamma)$ with controlled norm in the exact and the numerical solution, and in the error. We cannot ensure this for the original Eyles–King–Styles model. We therefore add a regularization term in the boundary condition (C.2.3b),

$$\partial_\mathrm{n} u - \mu \Delta_\Gamma u + \alpha u = Q + \beta H \qquad \text{on } \Gamma(t),$$

with a positive constant $\mu > 0$. Such a boundary condition is sometimes referred to as a *generalized Robin boundary condition*. It is shown in [Kashiwabara et al., 2015, Section 3.2] that the solution u has improved regularity on the boundary. We will show that here we can control the $H^1(\Gamma)$ norm of the numerical error in u whenever the bulk inhomogeneity in the error equation is suitably bounded in the dual space of $H^1(\Omega)$ but not necessarily in $L^2(\Omega)$.

C.2.2.5. Collected equations used for the discretization

Altogether, we consider the following strong formulation of the modified model problem, which consists of four coupled groups of equations:

$$\left.\begin{aligned} -\Delta u &= -1 && \text{in } \Omega(t),\\ \partial_{\mathrm{n}} u - \mu\Delta_\Gamma u + \alpha u &= \beta H + Q && \text{on } \Gamma(t); \end{aligned}\right\} \tag{C.2.7}$$

$$\left.\begin{aligned} \partial^\bullet \mathrm{n} &= \beta\Delta_\Gamma \mathrm{n} + \beta|A|^2\mathrm{n} - \alpha\nabla_\Gamma u && \text{on } \Gamma(t),\\ \partial^\bullet H &= \beta\Delta_\Gamma H + \beta|A|^2 H - \alpha\Delta_\Gamma u - \alpha|A|^2 u && \text{on } \Gamma(t),\\ v_\Gamma &= V\mathrm{n} \quad \text{with } V = -\beta H + \alpha u && \text{on } \Gamma(t); \end{aligned}\right\} \tag{C.2.8}$$

$$\left.\begin{aligned} -\Delta v &= 0 && \text{in } \Omega(t),\\ v &= v_\Gamma && \text{on } \Gamma(t); \end{aligned}\right\} \tag{C.2.9}$$

$$\partial_t X = v \circ X \qquad \text{on } \Omega^0 \cup \Gamma^0. \tag{C.2.10}$$

In the following weak formulation and matrix–vector formulation of the discretization and in the error analysis, the corresponding equations are clearly separated into these four parts. We refer to (C.2.7) as the generalized Robin boundary value problem, to (C.2.8) as the forced mean curvature flow, to (C.2.9) as the harmonic velocity extension, and to (C.2.10) as the ODE for the positions.

C.2.3. Weak formulation

C.2.3.1. Generalized Robin boundary value problem

In this subsection, we briefly write Ω and Γ and omit the argument X or t. The weak formulation of the Robin boundary value problem (C.2.3) is to find $u \in H^1(\Omega)$ such that (with γ denoting the trace operator):

$$\begin{aligned} &\int_\Omega \nabla u \cdot \nabla \varphi^u + \mu \int_\Gamma \nabla_\Gamma(\gamma u)\cdot\nabla_\Gamma(\gamma\varphi^u) + \alpha\int_\Gamma (\gamma u)(\gamma\varphi^u)\\ =& -\int_\Omega \varphi^u + \int_\Gamma (\beta H + Q)(\gamma\varphi^u) \end{aligned} \tag{C.2.11}$$

for all $\varphi^u \in H^1(\Omega)$.

C.2.3.2. Forced mean curvature flow

The weak formulation of the parabolic equations for n and H in (C.2.8) reads:

$$\begin{aligned} \int_\Gamma \partial^\bullet \mathrm{n}\,\varphi^{\mathrm{n}} + \beta\int_\Gamma \nabla_\Gamma \mathrm{n}\cdot\nabla_\Gamma\varphi^{\mathrm{n}} &= \beta\int_\Gamma |A|^2\mathrm{n}\cdot\varphi^{\mathrm{n}} - \alpha\int_\Gamma \nabla_\Gamma(\gamma u)\cdot\varphi^{\mathrm{n}},\\ \int_\Gamma \partial^\bullet H\varphi^H + \beta\int_\Gamma \nabla_\Gamma H\cdot\nabla_\Gamma\varphi^H &= -\int_\Gamma |A|^2 V\varphi^H + \alpha\int_\Gamma \nabla_\Gamma(\gamma u)\cdot\nabla_\Gamma\varphi^H, \end{aligned} \tag{C.2.12}$$

for all test functions $\varphi^{\mathrm{n}} \in H^1(\Gamma[X])^3$ and $\varphi^H \in H^1(\Gamma[X])$. Recall that the system is coupled to the velocity law (C.2.4) and the ordinary differential equation (C.2.1) that determines the boundary surface $\Gamma[X(\cdot,t)] = \partial\Omega[X(\cdot,t)]$.

C.2.3.3. Harmonic velocity extension

After extending $v_\Gamma \in H^{1/2}(\Gamma)$ to an (arbitrary) function $w \in H^1(\Omega)$ with $\gamma w = v_\Gamma$, the weak formulation of the harmonic extension (C.2.9) (which is an inhomogeneous Dirichlet problem) reads: Find $v \in H^1(\Omega)^3$ with $v - w \in H^1_0(\Omega)^3$ that satisfies

$$\int_{\Omega(t)} \nabla v \cdot \nabla \varphi^v = 0, \tag{C.2.13}$$

for all $\varphi^v \in H^1_0(\Omega)^3$. Recall that the equation for v is coupled to the ordinary differential equation (C.2.1) that determines the domain $\Omega[X(\cdot,t)]$.

C.3. Spatial semi-discretization with bulk–surface finite elements

We formulate the isoparametric evolving bulk–surface finite element discretization for the coupled tumour growth system, following the descriptions in [Elliott and Ranner, 2013] and [Kovács et al., 2019], as well as details from [Dziuk, 1988] and [Demlow, 2009]. We use tetrahedral and triangular finite elements in the bulk and on the surface, respectively, and continuous piecewise polynomial basis functions of degree k, which are compatible on the boundary. For details on higher-order finite elements we refer to [Elliott and Ranner, 2013, Section 5], [Demlow, 2009, Section 2.5], [Edelmann, 2022, 2021], [Kovács, 2018], and [Elliott and Ranner, 2021].

C.3.1. Evolving bulk–surface finite elements

The initial bulk–surface domain $\Omega^0 \cup \Gamma^0$ is discretized by an isoparametric tetrahedral mesh of degree k, denoted by Ω^0_h. The meshes are assumed to form an admissible family of triangulations $\mathcal{T}_h$ of decreasing maximal element diameter h; see [Dziuk and Elliott, 2007a, Elliott and Ranner, 2013] for the notion of an admissible bulk–surface approximation, which includes quasi-uniformity and shape regularity. By piecewise polynomial interpolation of degree k, the nodal vector defines an approximate bulk–surface domain Ω^0_h that interpolates Ω^0 in the nodes q_j. By construction, the boundary of the tetrahedral mesh Ω^0_h forms an equally admissible triangular approximation $\Gamma^0_h = \partial\Omega^0_h$ of the initial boundary Γ^0.

The nodes q_j of the triangulation are collected in the vector

$$\mathbf{x}^0 = \begin{pmatrix} \mathbf{x}^0_\Gamma \\ \mathbf{x}^0_\Omega \end{pmatrix} \in \left(\mathbb{R}^3\right)^N,$$

where we assume that the boundary nodes $\mathbf{x}^0_\Gamma = (q_j)_{j=1}^{N_\Gamma}$ lie on the boundary Γ^0, while the remaining ($N_\Omega = N - N_\Gamma$) nodes $\mathbf{x}^0_\Omega$ are in the interior of Ω^0.

The nodes $\mathbf{x}^0$ will evolve in time and at time t they are collected in the vector

$$\mathbf{x}(t) = \begin{pmatrix} \mathbf{x}_\Gamma(t) \\ \mathbf{x}_\Omega(t) \end{pmatrix} \in \big(\mathbb{R}^3\big)^N,$$

which employs the same partitioning as before. We will often suppress the omnipresent argument t.

By piecewise polynomial interpolation on the plane reference tetrahedron that corresponds to every curved tetrahedron of the triangulation, the nodal vector $\mathbf{x}$ defines a domain $\Omega_h[\mathbf{x}]$ and its boundary surface $\Gamma_h[\mathbf{x}]$, which actually depends only on $\mathbf{x}_\Gamma$.

We then define globally continuous finite element *basis functions*

$$\begin{aligned} \varphi_i[\mathbf{x}] &\colon \Omega_h[\mathbf{x}] \to \mathbb{R}, \qquad i = 1, \dots, N, \\ \psi_i[\mathbf{x}] &\colon \Gamma_h[\mathbf{x}] \to \mathbb{R}, \qquad i = 1, \dots, N_\Gamma, \end{aligned}$$

which have the property that on every tetrahedron and triangle, respectively, their pullbacks to the reference element are polynomials of degree k, and which satisfy at the node x_j

$$\begin{aligned} \varphi_i[\mathbf{x}](x_j) &= \delta_{ij} \quad \text{for all } i, j = 1, \dots, N, \\ \psi_i[\mathbf{x}](x_j) &= \delta_{ij} \quad \text{for all } i = 1, \dots, N_\Gamma,\ j = 1, \dots, N. \end{aligned}$$

Since we have $\Gamma_h(t) = \partial\Omega_h(t)$, by construction the basis functions satisfy the crucial property that $\psi_j[\mathbf{x}]$ is the discrete trace of $\varphi_j[\mathbf{x}]$, i.e.

$$\psi_j[\mathbf{x}] = \gamma_h \varphi_j[\mathbf{x}]. \tag{C.3.1}$$

These functions span the bulk and surface finite element spaces in $\Omega_h[\mathbf{x}]$ and on $\Gamma_h[\mathbf{x}]$, respectively:

$$\mathcal{V}_h[\mathbf{x}] = \operatorname{span}\{\varphi_1[\mathbf{x}], \dots, \varphi_N[\mathbf{x}]\}, \tag{C.3.2}$$

$$\mathcal{S}_h[\mathbf{x}] = \operatorname{span}\{\psi_1[\mathbf{x}], \dots, \psi_{N_\Gamma}[\mathbf{x}]\}. \tag{C.3.3}$$

For a finite element function $u_h \in \mathcal{S}_h[\mathbf{x}]$, the tangential gradient $\nabla_{\Gamma_h[\mathbf{x}]} u_h$ is defined piecewise on each element. Note that $\mathcal{V}_h[\mathbf{x}] \subset H^1(\Omega_h[\mathbf{x}]; \Gamma_h[\mathbf{x}])$ and $\mathcal{S}_h[\mathbf{x}] \subset H^1(\Gamma_h[\mathbf{x}])$. We denote the space of discrete functions with vanishing trace by

$$\mathcal{V}_h^0[\mathbf{x}] = \{v \in \mathcal{V}_h[\mathbf{x}] \,:\, \gamma_h v = 0\} = \operatorname{span}\{\varphi_{N_\Gamma+1}[\mathbf{x}], \dots, \varphi_N[\mathbf{x}]\}. \tag{C.3.4}$$

The discrete domain at time t is parametrized by the initial discrete domain via the map $X_h(\cdot, t) \colon \overline{\Omega}_h^0 \to \overline{\Omega}_h[\mathbf{x}(t)]$ defined by

$$X_h(q_h, t) = \sum_{j=1}^{N} x_j(t)\, \varphi_j[\mathbf{x}(0)](q_h), \qquad q_h \in \Omega_h^0, \tag{C.3.5}$$

which has the properties that $X_h(q_j, t) = x_j(t)$ for $j = 1, \dots, N$ and $X_h(q_h, 0) = q_h$ for all $q_h \in \Omega_h^0$. We then have

$$\Omega_h[\mathbf{x}(t)] = \Omega[X_h(\cdot, t)] \quad \text{and} \quad \Gamma_h[\mathbf{x}(t)] = \Gamma[X_h(\cdot, t)],$$

where the right-hand sides equal the domain $\{X_h(q_h,t) : q_h \in \Omega_h^0\}$ and surface $\{X_h(q_h,t) : q_h \in \Gamma_h^0\}$, respectively, as in Section C.2.1.

The discrete velocity $v_h(x,t) \in \mathbb{R}^3$ at a point $x = X_h(q_h,t) \in \Omega[X_h(\cdot,t)]$ is given by

$$\partial_t X_h(q_h,t) = v_h(X_h(q_h,t),t).$$

In view of the transport property of the basis functions [Dziuk and Elliott, 2007a],

$$\begin{aligned} \frac{\mathrm{d}}{\mathrm{d}t}\Big(\varphi_j[\mathbf{x}(t)](X_h(q_h,t))\Big) &= 0 \quad \text{for} \quad q_h \in \Omega_h^0, \\ \frac{\mathrm{d}}{\mathrm{d}t}\Big(\psi_j[\mathbf{x}(t)](X_h(q_h,t))\Big) &= 0 \quad \text{for} \quad q_h \in \Gamma_h^0, \end{aligned} \tag{C.3.6}$$

the discrete velocity equals, for $x \in \Omega_h[\mathbf{x}(t)]$,

$$v_h(x,t) = \sum_{j=1}^N v_j(t)\,\varphi_j[\mathbf{x}(t)](x) \qquad \text{with} \quad v_j(t) = \dot{x}_j(t),$$

where the dot denotes the time derivative $\mathrm{d}/\mathrm{d}t$. Hence, the discrete velocity $v_h(\cdot,t)$ is in the bulk finite element space $\mathcal{V}_h[\mathbf{x}(t)]$, with nodal vector $\mathbf{v}(t) = \dot{\mathbf{x}}(t)$, while its discrete trace $v_{\Gamma_h}(\cdot,t) = \gamma_h v_h(\cdot,t)$ is in the surface finite element space $\mathcal{S}_h[\mathbf{x}(t)]$, with nodal values $\mathbf{v}_\Gamma = (v_j(t))_{j=1}^{N_\Gamma} = (\dot{x}_j(t))_{j=1}^{N_\Gamma} = \dot{\mathbf{x}}_\Gamma(t)$.

The discrete material derivative of a finite element function $u_h(\cdot,t) \in \mathcal{V}_h[\mathbf{x}(t)]$, with nodal values $(u_j(t))_{j=1}^N$, at $x = X_h(q_h,t) \in \Omega_h[\mathbf{x}(t)]$ is

$$\partial_h^\bullet u_h(x,t) = \frac{\mathrm{d}}{\mathrm{d}t} u_h(X_h(q_h,t)) = \sum_{j=1}^N \dot{u}_j(t)\varphi_j[\mathbf{x}(t)](x), \tag{C.3.7}$$

and similarly, for $w_h(\cdot,t) \in \mathcal{S}_h[\mathbf{x}(t)]$, at $x = X_h(q_h,t) \in \Gamma_h[\mathbf{x}(t)]$ is

$$\partial_h^\bullet w_h(x,t) = \frac{\mathrm{d}}{\mathrm{d}t} w_h(X_h(q_h,t)) = \sum_{j=1}^{N_\Gamma} \dot{w}_j(t)\psi_j[\mathbf{x}(t)](x). \tag{C.3.8}$$

Since $\psi_j = \gamma_h\varphi_j$, for $j = 1,\dots,N_\Gamma$, this directly implies that we have $\partial_h^\bullet(\gamma_h u_h) = \gamma_h\big(\partial_h^\bullet u_h\big)$.

C.3.1.1. Lifts

We now introduce a lift operator for bulk–surface functions, following [Dziuk, 1988, Elliott and Ranner, 2013, 2021]. Let us denote the interpolated surface by $\Gamma_h^* = \Gamma_h[\mathbf{x}^*]$ and the corresponding interpolated domain by $\Omega_h^* = \Omega_h[\mathbf{x}^*]$, with $\mathbf{x}^*(t) = X(\mathbf{x}^0,t)$.

Following [Dziuk, 1988], we define the *lift* of functions $w_h \colon \Gamma_h^* \to \mathbb{R}$ as

$$w_h^\ell \colon \Gamma \to \mathbb{R} \qquad \text{with} \qquad w_h^\ell(p) = w_h(x), \quad \forall p \in \Gamma, \tag{C.3.9}$$

where $x \in \Gamma_h^*$ is the *unique* point on Γ_h^* with $x - p$ orthogonal to the tangent space $T_p\Gamma$. We further consider the *lift* of functions $w_h \colon \Omega_h^* \to \mathbb{R}$ to $w_h^\ell \colon \Omega \to \mathbb{R}$ by setting $w_h^\ell(p) = w_h(x)$ if

$x \in \Omega_h^*$ and $p \in \Omega$ are related as described in detail in [Elliott and Ranner, 2013, Section 4]. The mapping $G_h \colon \Omega_h^* \to \Omega$ is defined piecewise, for an element $E \in \mathcal{T}_h$, by

$$G_h|_E(x) = F_e\big((F_E)^{-1}(x)\big), \qquad \text{for any } x \in E, \tag{C.3.10}$$

where F_e is a C^1 map (see [Elliott and Ranner, 2013, equation (4.2) & (4.4)]) from the reference element onto the smooth element $e \subset \Omega$, and F_E is the standard affine linear map between the reference element and E, see, e.g. [Elliott and Ranner, 2013, equation (4.1)]. The *inverse lift* $w^{-\ell} \colon \Gamma_h^* \to \mathbb{R}$ denotes a function whose lift is $w \colon \Gamma \to \mathbb{R}$, and similarly for the bulk as well. Note that both definitions of the lift coincide on Γ. Finally, the lifted finite element space is denoted by $\mathcal{S}_h^\ell$, and is given as $\mathcal{S}_h^\ell = \{w_h^\ell \mid w_h \in \mathcal{S}_h\}$.

Then the *composed lift operator* ^{L}, as used in [Kovács et al., 2019], lifts finite element functions $w_h = \sum_{j=1}^N w_j \phi_j[\mathbf{x}]$ on the discrete surface $\Gamma_h[\mathbf{x}]$ to functions on the exact surface $\Gamma[X]$ via the finite element function $\widehat{w}_h = \sum_{j=1}^N w_j \phi_j[\mathbf{x}^*]$ on the interpolated surface $\Gamma_h[\mathbf{x}^*]$, by setting

$$w_h^L = (\widehat{w}_h)^\ell. \tag{C.3.11}$$

We will compare the positions of the exact surface $\Gamma[X(\cdot,t)]$ and the discrete surface $\Gamma_h[\mathbf{x}(t)]$ by comparing any point $x \in \Gamma[X(\cdot,t)]$ with its associated point $x_h^L(x,t) \in \Gamma_h[\mathbf{x}(t)]$, which is defined as

$$x_h^L(x,t) = X_h^L(q,t) \in \Gamma_h[\mathbf{x}(t)] \qquad \text{for } q \in \Gamma^0 \text{ such that} \quad X(q,t) = x \in \Gamma[X(\cdot,t)]. \tag{C.3.12}$$

Here, the discrete flow map $X_h(\cdot,t) \colon \Gamma_h[\mathbf{x}^*(0)] \to \mathbb{R}^3$ is defined in (C.3.5) and we denote its composed lift by $X_h^L(\cdot,t) = \big(X_h(\cdot,t)\big)^L \colon \Gamma^0 \to \mathbb{R}^3$.

C.3.2. Semi-discretization of the coupled bulk–surface system

C.3.2.1. Semi-discretization of the generalized Robin boundary value problem

The semi-discretization of the Robin boundary value problem (C.2.3) computes $u_h \in \mathcal{V}_h[\mathbf{x}]$ such that (with γ_h denoting the discrete trace operator)

$$\begin{aligned} &\int_{\Omega_h[\mathbf{x}]} \nabla u_h \cdot \nabla \varphi_h^u + \mu \int_{\Gamma_h(\mathbf{x})} \nabla_{\Gamma_h}(\gamma_h u_h) \cdot \nabla_{\Gamma_h}(\gamma_h \varphi_h^u) + \alpha \int_{\Gamma_h(\mathbf{x})} (\gamma_h u_h)(\gamma_h \varphi_h^u) \\ &= -\int_{\Omega_h(\mathbf{x})} \varphi_h^u + \int_{\Gamma_h(\mathbf{x})} (\beta H_h + Q_h)(\gamma_h \varphi_h^u) \end{aligned} \tag{C.3.13}$$

for all $\varphi_h^u \in \mathcal{V}_h[\mathbf{x}]$. Here Q_h is the finite element interpolation of Q on $\Gamma_h(\mathbf{x})$.

C.3.2.2. Semi-discretization of the forced mean curvature flow

A finite element semi-discretization of the parabolic equations (C.2.12) for n and H reads as follows: Find $\mathrm{n}_h(\cdot,t) \in \mathcal{S}_h[\mathbf{x}(t)]^3$ and $H_h(\cdot,t) \in \mathcal{S}_h[\mathbf{x}(t)]$ that satisfy, with u_h from (C.3.13) and

with $A_h = (\nabla_{\Gamma_h} \mathrm{n}_h + (\nabla_{\Gamma_h} \mathrm{n}_h)^T)/2$ and $V_h = -\beta H_h + \alpha\gamma_h u_h$,

$$\begin{aligned}
\int_{\Gamma_h[\mathbf{x}]} \partial_h^\bullet \mathrm{n}_h \varphi_h^{\mathrm{n}} + \beta \int_{\Gamma_h[\mathbf{x}]} \nabla_{\Gamma_h} \mathrm{n}_h \cdot \nabla_{\Gamma_h} \varphi_h^{\mathrm{n}} &= \beta \int_{\Gamma_h[\mathbf{x}]} |A_h|^2 \mathrm{n}_h \cdot \varphi_h^{\mathrm{n}} - \alpha \int_{\Gamma_h[\mathbf{x}]} \nabla_{\Gamma_h} u_h \cdot \varphi_h^{\mathrm{n}}, \\
\int_{\Gamma_h[\mathbf{x}]} \partial_h^\bullet H_h \varphi_h^H + \beta \int_{\Gamma_h[\mathbf{x}]} \nabla_{\Gamma_h} H_h \cdot \nabla_{\Gamma_h} \varphi_h^H &= -\int_{\Gamma_h[\mathbf{x}]} |A_h|^2 V_h \varphi_h^H + \alpha \int_{\Gamma_h[\mathbf{x}]} \nabla_{\Gamma_h} u_h \cdot \nabla_{\Gamma_h} \varphi_h^H,
\end{aligned} \tag{C.3.14}$$

for all test functions $\varphi_h^{\mathrm{n}} \in \mathcal{S}_h[\mathbf{x}]^3$ and $\varphi_h^H \in \mathcal{S}_h[\mathbf{x}]$.

The discrete surface velocity $v_{\Gamma_h}(\cdot,t) \in \mathcal{S}_h[\mathbf{x}(t)]^3$ with nodal vector $\mathbf{v}_\Gamma$ is determined by

$$v_{\Gamma_h} = \widetilde{I}_h\big(V_h \mathrm{n}_h\big), \qquad \text{where} \quad V_h = -\beta H_h + \alpha\gamma_h u_h \in \mathcal{S}_h[\mathbf{x}] \tag{C.3.15}$$

and $\widetilde{I}_h \colon C(\Gamma_h[\mathbf{x}]) \to \mathcal{S}_h[\mathbf{x}]$ denotes the Lagrangian finite element interpolation operator on $\Gamma_h[\mathbf{x}]$. The nodal vector $\mathbf{x}_\Gamma(t)$ that determines the discrete surface $\Gamma_h[\mathbf{x}(t)]$ is obtained by integrating

$$\dot{\mathbf{x}}_\Gamma = \mathbf{v}_\Gamma, \qquad \mathbf{x}_\Gamma(0) = \mathbf{x}_\Gamma^0. \tag{C.3.16}$$

C.3.2.3. Discrete harmonic velocity extension and ODE for positions

We compute $v_h \in \mathcal{V}_h[\mathbf{x}]^3$ with $\gamma_h v_h = v_{\Gamma_h}$ such that

$$\int_{\Omega_h(\mathbf{x})} \nabla v_h \cdot \nabla \varphi_h^v = 0 \tag{C.3.17}$$

for all $\varphi_h^v \in \mathcal{V}_h^0[\mathbf{x}]^3$. From the nodal vector $\mathbf{v} = (\mathbf{v}_\Gamma; \mathbf{v}_\Omega)$ of the finite element function v_h, the nodal vector $\mathbf{x}(t)$ that determines the discrete domain $\Omega_h[\mathbf{x}(t)]$ is obtained by integrating

$$\dot{\mathbf{x}}_\Omega = \mathbf{v}_\Omega, \qquad \mathbf{x}_\Omega(0) = \mathbf{x}_\Omega^0. \tag{C.3.18}$$

C.3.3. Matrix–vector formulation

C.3.3.1. Mass and stiffness matrices

We collect the nodal values of the semi-discrete approximations to tissue pressure $u_h(\cdot,t)$, velocity $v_h(\cdot,t)$, normal vector $\mathrm{n}_h(\cdot,t)$, mean curvature $H_h(\cdot,t)$ in the column vectors

$$\mathbf{u} = (u_j) \in \mathbb{R}^N, \qquad \mathbf{v} = (v_j) \in \mathbb{R}^{3N}, \qquad \mathbf{n} = (\mathrm{n}_j) \in \mathbb{R}^{3N_\Gamma}, \qquad \mathbf{H} = (H_j) \in \mathbb{R}^{N_\Gamma},$$

respectively. As we did with the position vector $\mathbf{x}$, we partition

$$\mathbf{u} = \begin{pmatrix} \mathbf{u}_\Gamma \\ \mathbf{u}_\Omega \end{pmatrix}, \quad \mathbf{v} = \begin{pmatrix} \mathbf{v}_\Gamma \\ \mathbf{v}_\Omega \end{pmatrix},$$

corresponding to the nodes on the surface and in the bulk. Furthermore, the nodal values of the semi-discrete normal velocity $V_h = -\beta H_h + \alpha\gamma_h u_h \in \mathcal{S}_h[\mathbf{x}]$ are collected in the vector $\mathbf{V} = (V_j) \in \mathbb{R}^{N_\Gamma}$:

$$\mathbf{V} = -\beta\mathbf{H} + \alpha\mathbf{u}_\Gamma.$$

We denote the domain-dependent bulk stiffness and mass matrices by $\mathbf{A}_{\bar\Omega}(\mathbf{x}) \in \mathbb{R}^{N\times N}$ and $\mathbf{M}_{\bar\Omega}(\mathbf{x}) \in \mathbb{R}^{N\times N}$, respectively, and define them as

$$\begin{aligned} \mathbf{M}_{\bar\Omega}(\mathbf{x})|_{ij} &= \int_{\Omega_h(\mathbf{x})} \varphi_i[\mathbf{x}]\varphi_j[\mathbf{x}], \\ \mathbf{A}_{\bar\Omega}(\mathbf{x})|_{ij} &= \int_{\Omega_h(\mathbf{x})} \nabla\varphi_i[\mathbf{x}]\cdot\nabla\varphi_j[\mathbf{x}], \end{aligned} \qquad i,j=1,\dots,N. \tag{C.3.19}$$

We partition these matrices as

$$\mathbf{A}_{\bar\Omega}(\mathbf{x}) = \begin{pmatrix} \mathbf{A}_{\Gamma\Gamma}(\mathbf{x}) & \mathbf{A}_{\Gamma\Omega}(\mathbf{x}) \\ \mathbf{A}_{\Omega\Gamma}(\mathbf{x}) & \mathbf{A}_{\Omega\Omega}(\mathbf{x}) \end{pmatrix} \tag{C.3.20}$$

and similarly for $\mathbf{M}_{\bar\Omega}(\mathbf{x})$.

We denote the surface mass and stiffness matrices, (recall $\psi_j = \gamma_h\varphi_j$, $j=1,\dots,N_\Gamma$), by

$$\begin{aligned} \mathbf{M}_\Gamma(\mathbf{x})|_{ij} &= \int_{\Gamma_h(\mathbf{x})} \psi_i[\mathbf{x}]\,\psi_j[\mathbf{x}], \\ \mathbf{A}_\Gamma(\mathbf{x})|_{ij} &= \int_{\Gamma_h(\mathbf{x})} \nabla_{\Gamma_h[\mathbf{x}]}\psi_i[\mathbf{x}]\cdot\nabla_{\Gamma_h[\mathbf{x}]}\psi_j[\mathbf{x}], \end{aligned} \qquad i,j=1,\dots,N_\Gamma. \tag{C.3.21}$$

The discrete trace matrix, corresponding to the discrete trace operator γ_h, is given by

$$\boldsymbol{\gamma} = \begin{pmatrix} I_{N_\Gamma} & 0 \end{pmatrix} \in \mathbb{R}^{N_\Gamma\times N},$$

where I_{N_Γ} denotes the $N_\Gamma\times N_\Gamma$ identity matrix. For any nodal vector $\mathbf{u}\in\mathbb{R}^N$ corresponding to a finite element function $u_h\in\mathcal{V}_h[\mathbf{x}]$, the vector $\boldsymbol{\gamma}\mathbf{u} = \mathbf{u}_\Gamma \in \mathbb{R}^{N_\Gamma}$ is the nodal vector of the finite element function $\gamma_h u_h \in \mathcal{S}_h[\mathbf{x}]$, cf. (C.3.1).

Moreover, for a matrix and for an arbitrary dimension d, we use the notation

$$\mathbf{M}_\Gamma^{[d]}(\mathbf{x}) = I_d \otimes \mathbf{M}_\Gamma(\mathbf{x}), \qquad \mathbf{A}_\Gamma^{[d]}(\mathbf{x}) = I_d \otimes \mathbf{A}_\Gamma(\mathbf{x}), \tag{C.3.22}$$

where $I_d \in \mathbb{R}^{d\times d}$ denotes the identity matrix, and $\otimes$ denotes the Kronecker product of matrices. If the dimension d is clear from the context, we will drop the superscript $^{[d]}$.

Finally, we define the tangential gradient matrix $\mathbf{D}(\mathbf{x}) \in \mathbb{R}^{3N_\Gamma\times N_\Gamma}$

$$\mathbf{D}(\mathbf{x})|_{i+(\ell-1)N_\Gamma,j} = \int_{\Gamma_h(\mathbf{x})} \psi_i[\mathbf{x}](\nabla_{\Gamma_h[\mathbf{x}]}\psi_j[x])_\ell$$

for $i,j=1,\dots,N_\Gamma$, $\ell=1,2,3$. Alternatively, this could be written as

$$\mathbf{D}(\mathbf{x}) = \begin{pmatrix} \mathbf{D}_1(\mathbf{x}) \\ \mathbf{D}_2(\mathbf{x}) \\ \mathbf{D}_3(\mathbf{x}) \end{pmatrix} \quad \text{with} \quad \mathbf{D}_\ell(\mathbf{x})|_{ij} = \int_{\Gamma_h} \psi_i \underline{D}_{h,\ell}\psi_j,$$

where $\underline{D}_{h,\ell}\psi_j$ denotes the ℓ-th component of the discrete tangential gradient of ψ_j.

C.3.3.2. Matrix–vector formulation of the generalized Robin boundary value problem

We define the vector $\mathbf{f}_u(\mathbf{x},\mathbf{H}) \in \mathbb{R}^N$ by

$$\mathbf{f}_u(\mathbf{x},\mathbf{H})|_j = -\int_{\Omega_h(\mathbf{x})} \varphi_j[\mathbf{x}] + \int_{\Gamma_h(\mathbf{x})} (\beta H_h + Q_h)\,\gamma_h \varphi_j[\mathbf{x}]\ , \quad j=1,\dots,N\ , \tag{C.3.23}$$

so that

$$\mathbf{f}_u(\mathbf{x},\mathbf{H}) = -\mathbf{M}_{\bar\Omega}(\mathbf{x})\mathbf{1} + \boldsymbol{\gamma}^{\mathrm{T}}\mathbf{M}_\Gamma(\mathbf{x})(\beta\mathbf{H}+\mathbf{Q}(\mathbf{x})),$$

where $\mathbf{1} \in \mathbb{R}^N$ is the vector with all entries equal to 1 and $\mathbf{Q}(\mathbf{x})$ is the nodal vector of Q on $\Gamma_h(\mathbf{x})$, i.e. $\mathbf{Q}(\mathbf{x}) = \big(Q(x_i)\big)$.

The discretized Robin boundary value problem (C.3.13) determines the nodal vector $\mathbf{u} \in \mathbb{R}^N$ as the solution of the linear system of equations

$$\Big(\mathbf{A}_{\bar\Omega}(\mathbf{x}) + \mu\boldsymbol{\gamma}^{\mathrm{T}}\mathbf{A}_\Gamma(\mathbf{x})\boldsymbol{\gamma} + \alpha\boldsymbol{\gamma}^{\mathrm{T}}\mathbf{M}_\Gamma(\mathbf{x})\boldsymbol{\gamma}\Big)\mathbf{u} = \mathbf{f}_u(\mathbf{x},\mathbf{H}). \tag{C.3.24}$$

C.3.3.3. Matrix–vector formulation of forced mean curvature flow

The discrete velocity law (C.3.15) written in terms of the nodal vectors becomes simply

$$\mathbf{v}_\Gamma = \mathbf{V} \bullet \mathbf{n} \qquad \text{with} \qquad \mathbf{V} = -\beta\mathbf{H} + \alpha\boldsymbol{\gamma}\mathbf{u}, \tag{C.3.25}$$

where $\bullet$ denotes the componentwise product of vectors, i.e. $(\mathbf{V}\bullet\mathbf{n})_j = V_j \mathrm{n}_j$ for $\mathbf{V} = (V_j) \in \mathbb{R}^{N_\Gamma}$ and $\mathbf{n} = (\mathrm{n}_j) \in (\mathbb{R}^3)^{N_\Gamma}$. We define the functions $\mathbf{f}_{\mathrm{n}}(\mathbf{x},\mathbf{n}) \in \mathbb{R}^{3N_\Gamma}$ and $\mathbf{f}_H(\mathbf{x},\mathbf{n},\mathbf{V}) \in \mathbb{R}^{N_\Gamma}$ by

$$\mathbf{f}_{\mathrm{n}}(\mathbf{x},\mathbf{n})|_{j+(\ell-1)N_\Gamma} = \beta \int_{\Gamma_h(\mathbf{x})} |A_h|^2\,(\mathrm{n}_h)_\ell\,\psi_j[\mathbf{x}],$$

$$\mathbf{f}_H(\mathbf{x},\mathbf{n},\mathbf{V})|_j = -\int_{\Gamma_h(\mathbf{x})} |A_h|^2\,V_h\,\psi_j[\mathbf{x}],$$

for $j=1,\dots,N_\Gamma$ and $\ell = 1,2,3$.

The formulation of the semi-discretized forced mean curvature flow equations (C.3.14) then leads to the matrix–vector formulation

$$\mathbf{M}_\Gamma^{[3]}(\mathbf{x})\dot{\mathbf{n}} + \beta\mathbf{A}_\Gamma^{[3]}(\mathbf{x})\mathbf{n} = \mathbf{f}_{\mathrm{n}}(\mathbf{x},\mathbf{n}) - \alpha\mathbf{D}_\Gamma(\mathbf{x})\boldsymbol{\gamma}\mathbf{u}, \tag{C.3.26a}$$

$$\mathbf{M}_\Gamma(\mathbf{x})\dot{\mathbf{H}} + \beta\mathbf{A}_\Gamma(\mathbf{x})\mathbf{H} = \mathbf{f}_H(\mathbf{x},\mathbf{n},-\beta\mathbf{H}+\alpha\gamma\mathbf{u}) + \alpha\mathbf{A}_\Gamma(\mathbf{x})\boldsymbol{\gamma}\mathbf{u}. \tag{C.3.26b}$$

Without the coupling terms containing $\mathbf{u}$ or $\dot{\mathbf{u}}$, these are the discrete equations studied in [Kovács et al., 2019] for the discretization of pure mean curvature flow.

C.3.3.4. Matrix–vector formulation of the harmonic velocity extension

In view of the partitioning (C.3.20), the matrix–vector formulation for the discrete harmonic velocity extension (C.3.17) reads

$$\mathbf{A}_{\Omega\Omega}^{[3]}(\mathbf{x})\mathbf{v}_\Omega = -\mathbf{A}_{\Omega\Gamma}^{[3]}(\mathbf{x})\mathbf{v}_\Gamma\,. \tag{C.3.27}$$

In summary, the matrix–vector formulation of the bulk–surface finite element semi-discretization of the coupled problem (C.2.7)–(C.2.9) is given by equations (C.3.24)–(C.3.27).

C.3.3.5. Matrix–vector formulation of the coupled bulk–surface problem

In summary, with $\mathbf{x} = (\mathbf{x}_\Gamma; \mathbf{x}_\Omega)$, $\mathbf{v} = (\mathbf{v}_\Gamma; \mathbf{v}_\Omega)$, and

$$\mathbf{L}(\mathbf{x}) := \mathbf{A}_{\bar\Omega}(\mathbf{x}) + \mu\boldsymbol{\gamma}^{\mathrm{T}}\mathbf{A}_\Gamma(\mathbf{x})\boldsymbol{\gamma} + \alpha\boldsymbol{\gamma}^{\mathrm{T}}\mathbf{M}_\Gamma(\mathbf{x})\boldsymbol{\gamma}, \tag{C.3.28}$$

the full matrix–vector formulation of the bulk–surface finite element semi-discretization of the coupled problem (C.2.7)–(C.2.9) thus reads as follows:

$$\mathbf{L}(\mathbf{x})\mathbf{u} = \ \mathbf{f}_u(\mathbf{x}, \mathbf{H}) \tag{C.3.29a}$$

$$\mathbf{M}_\Gamma(\mathbf{x})\dot{\mathbf{n}} + \beta\mathbf{A}_\Gamma(\mathbf{x})\mathbf{n} = \mathbf{f}_{\mathrm{n}}(\mathbf{x}, \mathbf{n}) - \alpha\mathbf{D}_\Gamma(\mathbf{x})\mathbf{u}_\Gamma \tag{C.3.29b}$$

$$\mathbf{M}_\Gamma(\mathbf{x})\dot{\mathbf{H}} + \beta\mathbf{A}_\Gamma(\mathbf{x})\mathbf{H} = \mathbf{f}_H(\mathbf{x}, \mathbf{n}, \mathbf{V}) + \alpha\mathbf{A}_\Gamma(\mathbf{x})\mathbf{u}_\Gamma \tag{C.3.29c}$$

$$\mathbf{V} = -\beta\mathbf{H} + \alpha\mathbf{u}_\Gamma \tag{C.3.29d}$$

$$\mathbf{v}_\Gamma = \mathbf{V} \bullet \mathbf{n} \tag{C.3.29e}$$

$$\mathbf{A}_{\Omega\Omega}(\mathbf{x})\mathbf{v}_\Omega = -\mathbf{A}_{\Omega\Gamma}(\mathbf{x})\mathbf{v}_\Gamma \tag{C.3.29f}$$

$$\dot{\mathbf{x}} = \mathbf{v}. \tag{C.3.29g}$$

C.3.4. Error bounds

Our main result yields optimal-order error bounds for the finite element semi-discretization using finite elements of polynomial degree $k \geq 2$ under the assumption that the exact solution is sufficiently regular. The following result will be proved in the course of this paper.

Theorem C.3.1. *Consider the space discretization of Section C.3.2 of the coupled bulk–surface problem* (C.2.7)–(C.2.10)*, using evolving bulk–surface finite elements of polynomial degree $k \geq 2$. Suppose that the problem admits an exact solution (X, v, n, H, u) that is sufficiently differentiable on the time interval $t \in [0, T]$, and that for each t, the flow map $X(\cdot, t)$ is an embedding.*

Then, there exists a constant $h_0 > 0$ such that for all mesh sizes $h \leq h_0$ the following error bounds for the lifts (C.3.11) *of the approximate tissue pressure and the discrete boundary position hold over the exact domain $\Omega(t) = \Omega[X(\cdot, t)]$ and exact surface $\Gamma(t) = \Gamma[X(\cdot, t)]$ for $0 \leq t \leq T$:*

$$\begin{aligned}\|u_h^L(\cdot, t) - u(\cdot, t)\|_{H^1(\Omega(t),\Gamma(t))} &\leq Ch^k,\\ \|x_h^L(\cdot, t) - \mathrm{id}_{\Gamma(t)}\|_{H^1(\Omega(t),\Gamma(t))^3} &\leq Ch^k,\end{aligned}$$

where x_h^L is defined in (C.3.12)*.*

Furthermore, $\|X_h^\ell(\cdot, t) - X(\cdot, t)\|_{H^1(\Omega^0,\Gamma^0)^3} \leq Ch^k$, and there are analogous error bounds for velocity, normal vector and mean curvature:

$$\begin{aligned}\|v_h^L(\cdot, t) - v(\cdot, t)\|_{H^1(\Omega(t),\Gamma(t))^3} &\leq Ch^k,\\ \|\mathrm{n}_h^L(\cdot, t) - \mathrm{n}(\cdot, t)\|_{H^1(\Gamma(t))^3} &\leq Ch^k,\\ \|H_h^L(\cdot, t) - H(\cdot, t)\|_{H^1(\Gamma(t))} &\leq Ch^k.\end{aligned}$$

The constant C is independent of h and t, but depends on bounds of higher derivatives of the solution (u, X, v, n, H) and on the length T of the time interval.

Theorem C.3.1 will be proved in the course of Sections C.4 and C.5, using also results from the appendix (Section C.8). We note that Eyles et al. [2019] does not study well-posedness of the original system, and we are also not aware of any well-posedness results for the coupled problem either.

The observations after [Kovács et al., 2019, Theorem 4.1] are valid for the present result. These include, that in particular the error bound for the positions implies that the bulk–surface mesh satisfies our admissibility assumptions on the meshes, which includes quasi-uniformity and shape regularity. For more details we refer to the detailed discussion after Theorem 4.1 in Kovács et al. [2019].

C.4. Stability of the spatially discretized bulk–surface problem

In this section we prove stability of the semi-discretization of the coupled bulk–surface problem in the sense that errors are bounded by defects in the semi-discrete equations in appropriate norms. The precise result is stated in Proposition C.4.3 below. Its proof requires error bounds for each of the three sub-problems (generalized Robin boundary value problem, forced mean curvature flow, harmonic velocity extension) and their non-trivial coupling.

For ease of presentation we choose in the following the parameters

$$\alpha = \beta = \mu = 1.$$

The general case just leads to different constants, as we will not study asymptotic limits as α or β or μ goes to zero or infinity.

C.4.1. Preparation: Estimates relating different mass and stiffness matrices

In the following stability proof, we use technical results relating different finite element domains, which were proved in [Kovács et al., 2017] for the surface mass and stiffness matrices and in [Edelmann, 2022] for the bulk mass and stiffness matrices. We use the following setting.

Let $\mathbf{x} \in \mathbb{R}^{3N}$ be a nodal vector defining the discrete domain $\Omega_h(\mathbf{x})$ with boundary $\Gamma_h(\mathbf{x})$. We denote by $\mathbf{x}_\Gamma \in \mathbb{R}^{3N_\Gamma}$ the nodes of $\mathbf{x}$ that lie on the boundary $\Gamma_h(\mathbf{x})$. For any nodal vector $\mathbf{u} = (u_j) \in \mathbb{R}^N$ and $\mathbf{w} = (w_j) \in \mathbb{R}^{N_\Gamma}$ with corresponding finite element functions $u_h = \sum_{j=1}^N u_j \varphi_j[\mathbf{x}] \in \mathcal{V}_h[\mathbf{x}]$ and $w_h = \sum_{j=1}^{N_\Gamma} w_j \varphi_j[\mathbf{x}] \in \mathcal{S}_h[\mathbf{x}]$, respectively, the mass and stiffness matrices define norms on $\Omega_h(\mathbf{x})$:

$$\begin{aligned} \|\mathbf{u}\|^2_{\mathbf{M}_{\bar\Omega}(\mathbf{x})} &= \mathbf{u}^{\mathrm{T}} \mathbf{M}_{\bar\Omega}(\mathbf{x}) \mathbf{u} = \|u_h\|^2_{L^2(\Omega_h(\mathbf{x}))}\,, \\ \|\mathbf{u}\|^2_{\mathbf{A}_{\bar\Omega}(\mathbf{x})} &= \mathbf{u}^{\mathrm{T}} \mathbf{A}_{\bar\Omega}(\mathbf{x}) \mathbf{u} = \|\nabla u_h\|^2_{L^2(\Omega_h(\mathbf{x}))}\,, \end{aligned} \tag{C.4.1}$$

and in the same way for the surface mass and stiffness matrices.

Let $\mathbf{x}, \mathbf{x}^* \in \mathbb{R}^{3N}$ be two nodal vectors that define discrete domains $\Omega_h[\mathbf{x}]$ and $\Omega_h[\mathbf{x}^*]$ with boundaries $\Gamma_h(\mathbf{x})$ and $\Gamma_h[\mathbf{x}^*]$. We denote the difference by $\mathbf{e} = \mathbf{x} - \mathbf{x}^*$. For $\theta \in [0,1]$, we consider the intermediate domain $\Omega_h^\theta = \Omega_h[\mathbf{x}^* + \theta\mathbf{e}]$ and the corresponding finite element function given by

$$e_h^\theta = \sum_{j=1}^N e_j \phi_j[\mathbf{x}^* + \theta\mathbf{e}]\,.$$

In the same way, any vectors $\mathbf{u} \in \mathbb{R}^N$ or $\mathbf{w} \in \mathbb{R}^{N_\Gamma}$ define finite element functions $u_h^\theta \in \mathcal{V}_h[\mathbf{x}^* + \theta\mathbf{e}]$ and $w_h^\theta \in \mathcal{S}_h[\mathbf{x}^* + \theta\mathbf{e}]$, respectively.

Lemma C.4.1. *In the above setting, the following identities hold for any bulk nodal vectors* $\mathbf{w}, \mathbf{z} \in \mathbb{R}^N$ *or surface nodal vectors* $\mathbf{w}, \mathbf{z} \in \mathbb{R}^{N_\Gamma}$*:*

$$\begin{aligned}
\mathbf{w}^{\mathrm{T}}\Big(\mathbf{M}_{\bar\Omega}(\mathbf{x}) - \mathbf{M}_{\bar\Omega}(\mathbf{x}^*)\Big)\mathbf{z} &= \int_0^1 \int_{\Omega_h^\theta} w_h^\theta (\nabla \cdot e_h^\theta) z_h^\theta \ \mathrm{d}\theta \\
\mathbf{w}^{\mathrm{T}}\Big(\mathbf{A}_{\bar\Omega}(\mathbf{x}) - \mathbf{A}_{\bar\Omega}(\mathbf{x}^*)\Big)\mathbf{z} &= \int_0^1 \int_{\Omega_h^\theta} \nabla w_h^\theta \cdot \Big(D_{\Omega_h^\theta} e_h^\theta\Big) \nabla z_h^\theta \ \mathrm{d}\theta \\
\mathbf{w}^{\mathrm{T}}\Big(\mathbf{M}_{\Gamma}(\mathbf{x}) - \mathbf{M}_{\Gamma}(\mathbf{x}^*)\Big)\mathbf{z} &= \int_0^1 \int_{\Gamma_h^\theta} w_h^\theta (\nabla_{\Gamma_h^\theta} \cdot e_h^\theta) z_h^\theta \ \mathrm{d}\theta \\
\mathbf{w}^{\mathrm{T}}\Big(\mathbf{A}_{\Gamma}(\mathbf{x}) - \mathbf{A}_{\Gamma}(\mathbf{x}^*)\Big)\mathbf{z} &= \int_0^1 \int_{\Gamma_h^\theta} \nabla_{\Gamma_h^\theta} w_h^\theta \cdot \Big(D_{\Gamma_h^\theta} e_h^\theta\Big) \nabla_{\Gamma_h^\theta} z_h^\theta \ \mathrm{d}\theta,
\end{aligned} \tag{C.4.2}$$

where we have $D_{\Omega_h^\theta} e_h^\theta = \mathrm{tr}(E^\theta) I_3 - (E^\theta + (E^\theta)^T)$ *with* $E^\theta = \nabla e_h^\theta \in \mathbb{R}^{3\times 3}$ *and* $D_{\Gamma_h^\theta} e_h^\theta = \mathrm{tr}(G^\theta) I_3 - (G^\theta + (G^\theta)^T)$ *with* $G^\theta = \nabla_{\Gamma_h^\theta} e_h^\theta \in \mathbb{R}^{3\times 3}$.

Furthermore, for any $\mathbf{w} \in \mathbb{R}^{3N_\Gamma}$*,* $z \in \mathbb{R}^{N_\Gamma}$*, the following identity holds:*

$$\mathbf{w}^{\mathrm{T}}\Big(\mathbf{D}(\mathbf{x}) - \mathbf{D}(\mathbf{x}^*)\Big)\mathbf{z} = \int_0^1 \int_{\Gamma_h^\theta} \Big(w_h^\theta \cdot \nabla_{\Gamma_h^\theta} z_h^\theta\Big) \nabla_{\Gamma_h^\theta} \cdot e_h^\theta \, \mathrm{d}\theta \,. \tag{C.4.3}$$

Proof. The formulae result from the Leibniz rule (transport formula). A proof of the first pair of identities is found in [Edelmann, 2022, Lemma 5.1], for the second pair in [Kovács et al., 2017, Lemma 4.1]. The last identity follows from the third one. □

The following lemma combines Lemmas 4.2 and 4.3 of [Kovács et al., 2017] and Lemmas 5.2 and 5.3 of [Edelmann, 2022].

Lemma C.4.2. *In the above setting, suppose that*

$$\|\nabla e_h^0\|_{L^\infty(\Omega_h[\mathbf{x}^*])} \le \tfrac{1}{2} \,.$$

Then, for $0 \le \theta \le 1$*, the finite element functions* $u_h^\theta = \sum_{j=1}^N u_j \phi_j[\mathbf{x}^* + \theta\mathbf{e}]$ *on* Ω_h^θ *and* $w_h^\theta = \sum_{j=1}^{N_\Gamma} w_j \phi_j[\mathbf{x}^* + \theta\mathbf{e}]$ *on* Γ_h^θ *are bounded by*

$$\begin{aligned}
\|u_h^\theta\|_{L^p(\Omega_h^\theta)} &\le c_p \|u_h^0\|_{L^p(\Omega_h^\theta)}, \qquad & \|\nabla u_h^\theta\|_{L^p(\Omega_h^\theta)} &\le c_p \|\nabla u_h^0\|_{L^p(\Omega_h^0)}, \\
\|w_h^\theta\|_{L^p(\Gamma_h^\theta)} &\le c_p \|w_h^0\|_{L^p(\Gamma_h^0)}, \qquad & \|\nabla_{\Gamma_h^\theta} w_h^\theta\|_{L^p(\Gamma_h^\theta)} &\le c_p \|\nabla_{\Gamma_h^0} w_h^0\|_{L^p(\Gamma_h^0)},
\end{aligned} \tag{C.4.4}$$

for $1 \le p \le \infty$*, where* $c_p < \infty$ *is independent of* $\theta \in [0,1]$ *and of* h*.*

If $\|\nabla_{\Gamma_h[\mathbf{x}^*]} e_h^0\|_{L^\infty(\Gamma_h[\mathbf{x}^*])} \le \frac{1}{4}$, using the lemma for $w_h^\theta = e_h^\theta$ shows that

$$\|\nabla_{\Gamma_h^\theta} e_h^\theta\|_{L^\infty(\Gamma_h^\theta)} \le \tfrac{1}{2}, \qquad 0 \le \theta \le 1, \tag{C.4.5}$$

and then Lemma C.4.2 with $p = 2$ and interchanging the roles of $\mathbf{x}^*$ and $\mathbf{x}^* + \theta\mathbf{e}$ yield the following:

$$\begin{aligned}&\text{The norms } \|\cdot\|_{\mathbf{M}_{\bar\Omega}(\mathbf{x}^*+\theta\mathbf{e})} \text{ are } h\text{-uniformly equivalent for } 0 \le \theta \le 1,\\ &\text{and so are the norms } \|\cdot\|_{\mathbf{A}_{\bar\Omega}(\mathbf{x}^*+\theta\mathbf{e})},\ \|\cdot\|_{\mathbf{M}_\Gamma(\mathbf{x}^*+\theta\mathbf{e})},\ \|\cdot\|_{\mathbf{A}_\Gamma(\mathbf{x}^*+\theta\mathbf{e})}.\end{aligned} \tag{C.4.6}$$

Under the condition that $\varepsilon := \|\nabla_{\Gamma_h[\mathbf{x}^*]} e_h^0\|_{L^\infty(\Gamma_h[\mathbf{x}^*])} \le \frac{1}{4}$, using (C.4.5) in Lemma C.4.1 and applying the Cauchy–Schwarz inequality yields the bounds, with $c = c_\infty c_2^2$,

$$\begin{aligned}\mathbf{w}^T(\mathbf{M}_{\bar\Omega}(\mathbf{x}) - \mathbf{M}_{\bar\Omega}(\mathbf{x}^*))\mathbf{z} &\le c\varepsilon\, \|\mathbf{w}\|_{\mathbf{M}_{\bar\Omega}(\mathbf{x}^*)}\|\mathbf{z}\|_{\mathbf{M}_{\bar\Omega}(\mathbf{x}^*)},\\ \mathbf{w}^T(\mathbf{A}_{\bar\Omega}(\mathbf{x}) - \mathbf{A}_{\bar\Omega}(\mathbf{x}^*))\mathbf{z} &\le c\varepsilon\, \|\mathbf{w}\|_{\mathbf{A}_{\bar\Omega}(\mathbf{x}^*)}\|\mathbf{z}\|_{\mathbf{A}_{\bar\Omega}(\mathbf{x}^*)}\end{aligned} \tag{C.4.7}$$

and the analogous formulae for $\mathbf{M}_\Gamma$ and $\mathbf{A}_\Gamma$. We will also use similar bounds where we use the L^∞ norm of z_h or its gradient and the L^2 norm of the gradient of e_h.

Consider now a continuously differentiable function $\mathbf{x}\colon [0,T] \to \mathbb{R}^{3N}$ that defines a finite element domain $\Omega_h[\mathbf{x}(t)]$ for every $t \in [0,T]$, and assume that its time derivative $\mathbf{v}(t) = \dot{\mathbf{x}}(t)$ is the nodal vector of a finite element function $v_h(\cdot,t)$ that satisfies

$$\|\nabla v_h(\cdot,t)\|_{L^\infty(\Gamma_h[\mathbf{x}(t)])} \le K, \qquad 0 \le t \le T. \tag{C.4.8}$$

With $\mathbf{e} = \mathbf{x}(t) - \mathbf{x}(s) = \int_s^t \mathbf{v}(r)\,dr$, the bounds (C.4.7) then yield the following bounds, which were first shown in [Dziuk et al., 2012, Lemma 4.1] for surfaces: for $0 \le s,t \le T$ with $K|t-s| \le \frac{1}{4}$, we have with $C = cK$

$$\begin{aligned}\mathbf{w}^T\big(\mathbf{M}_{\bar\Omega}(\mathbf{x}(t)) - \mathbf{M}_{\bar\Omega}(\mathbf{x}(s))\big)\mathbf{z} &\le C\,|t-s|\,\|\mathbf{w}\|_{\mathbf{M}_{\bar\Omega}(\mathbf{x}(t))}\|\mathbf{z}\|_{\mathbf{M}_{\bar\Omega}(\mathbf{x}(t))},\\ \mathbf{w}^T\big(\mathbf{A}_{\bar\Omega}(\mathbf{x}(t)) - \mathbf{A}_{\bar\Omega}(\mathbf{x}(s))\big)\mathbf{z} &\le C\,|t-s|\,\|\mathbf{w}\|_{\mathbf{A}_{\bar\Omega}(\mathbf{x}(t))}\|\mathbf{z}\|_{\mathbf{A}_{\bar\Omega}(\mathbf{x}(t))}.\end{aligned} \tag{C.4.9}$$

Letting $s \to t$, this implies the bounds stated in [Kovács et al., 2017, Lemma 4.6] for surfaces and [Edelmann, 2022, Lemma 5.4] for domains:

$$\begin{aligned}\mathbf{w}^T\frac{\mathrm{d}}{\mathrm{d}t}\mathbf{M}_{\bar\Omega}(\mathbf{x}(t))\mathbf{z} &\le C\,\|\mathbf{w}\|_{\mathbf{M}_{\bar\Omega}(\mathbf{x}(t))}\|\mathbf{z}\|_{\mathbf{M}_{\bar\Omega}(\mathbf{x}(t))}\\ \mathbf{w}^T\frac{\mathrm{d}}{\mathrm{d}t}\mathbf{A}_{\bar\Omega}(\mathbf{x}(t))\mathbf{z} &\le C\,\|\mathbf{w}\|_{\mathbf{A}_{\bar\Omega}(\mathbf{x}(t))}\|\mathbf{z}\|_{\mathbf{A}_{\bar\Omega}(\mathbf{x}(t))}\end{aligned} \tag{C.4.10}$$

and analogously for surfaces. Patching together finitely many intervals over which $K|t-s| \le \frac{1}{4}$, we obtain the following:

$$\begin{aligned}&\text{The norms } \|\cdot\|_{\mathbf{M}_{\bar\Omega}(\mathbf{x}(t))} \text{ are } h\text{-uniformly equivalent for } 0 \le t \le T,\\ &\text{and so are the norms } \|\cdot\|_{\mathbf{A}_{\bar\Omega}(\mathbf{x}(t))},\end{aligned} \tag{C.4.11}$$

and analogously for surfaces.

C.4.2. Defects and errors for the coupled system

We consider finite element functions x_h^*, u_h^*, $v_h^* = (v_{\Gamma,h}^*, v_{\Omega,h}^*)$, and $w_h^* = (\mathrm{n}_h^*, H_h^*)$, with corresponding nodal vectors $\mathbf{u}^*$, $\mathbf{x}^*$, $\mathbf{v}^* = (\mathbf{v}_\Gamma^*; \mathbf{v}_\Omega^*)$, and $\mathbf{w}^* = (\mathbf{n}^*; \mathbf{H}^*)$, which are *suitable* finite element projections of the corresponding exact solution X, u, $v = (v_\Gamma, v_\Omega)$, and $w = (\mathrm{n}, H)$, respectively. The precise definition of these interpolations and Ritz-type projections will be given in Section C.5.2, where we will also prove that the obtained defects (i.e. consistency errors) are $O(h^k)$ in the appropriate norms.

For each variable the corresponding error vector will be denoted by a subscript, e.g. for X the error between the semi-discrete solution $\mathbf{x}$ and the finite element interpolation of the exact solution $\mathbf{x}^*$ is defined by

$$\mathbf{e}_\mathbf{x} = \mathbf{x} - \mathbf{x}^*,$$

which collects the nodal values of the finite element function e_x. The errors $\mathbf{e}_\mathbf{v}, \mathbf{e}_\mathbf{n}, \mathbf{e}_\mathbf{H}, \mathbf{e}_\mathbf{u}$ – and the corresponding finite element functions – are defined analogously.

C.4.2.1. Error equation for the generalized Robin boundary value problem

The nodal vectors $\mathbf{u}^*, \mathbf{x}^*, \mathbf{v}^*, \mathbf{n}^*, \mathbf{H}^*$ of the projected exact solution are inserted into the first equation of the numerical scheme (C.3.29a) and yield the defect $\mathbf{d}_\mathbf{u}$ defined by

$$\mathbf{L}(\mathbf{x}^*)\mathbf{u}^* = \mathbf{f}_u(\mathbf{x}^*, \mathbf{H}^*) + \mathbf{M}_{\bar\Omega}(\mathbf{x}^*)\mathbf{d}_\mathbf{u}\,. \tag{C.4.12}$$

Subtracting (C.4.12) from the first equation of (C.3.29), we obtain that the errors $\mathbf{e}_\mathbf{u}$ satisfy the error equation

$$\begin{aligned}\mathbf{L}(\mathbf{x})\mathbf{e}_\mathbf{u} = {}& \big(\mathbf{f}_u(\mathbf{x}, \mathbf{H}) - \mathbf{f}_u(\mathbf{x}^*, \mathbf{H}^*)\big) \\ & - \big(\mathbf{L}(\mathbf{x}) - \mathbf{L}(\mathbf{x}^*)\big)\mathbf{u}^* \\ & - \mathbf{M}_{\bar\Omega}(\mathbf{x}^*)\mathbf{d}_\mathbf{u}\,.\end{aligned} \tag{C.4.13}$$

C.4.2.2. Error equations for the forced mean curvature flow

When the nodal vectors of the projected exact solutions $\mathbf{u}^*, \mathbf{x}^*, \mathbf{v}^*, \mathbf{H}^*, \mathbf{n}^*$ are inserted into the numerical scheme (C.3.29b)–(C.3.29d), they yield defects $\mathbf{d}_\mathbf{n}, \mathbf{d}_\mathbf{H}$ and $\mathbf{d}_{\mathbf{v}_\Gamma}$ defined by

$$\begin{aligned}\mathbf{M}_\Gamma(\mathbf{x}^*)\dot{\mathbf{n}}^* + \mathbf{A}_\Gamma(\mathbf{x}^*)\mathbf{n}^* &= \mathbf{f}_\mathrm{n}(\mathbf{x}^*, \mathbf{n}^*) - \mathbf{D}_\Gamma(\mathbf{x}^*)\boldsymbol{\gamma}\mathbf{u}^* + \mathbf{M}_\Gamma(\mathbf{x}^*)\mathbf{d}_\mathbf{n}\,, \\ \mathbf{M}_\Gamma(\mathbf{x}^*)\dot{\mathbf{H}}^* + \mathbf{A}_\Gamma(\mathbf{x}^*)\mathbf{H}^* &= \mathbf{f}_H(\mathbf{x}^*, \mathbf{n}^*, -\mathbf{H}^* + \mathbf{u}^*) + \mathbf{A}_\Gamma(\mathbf{x}^*)\boldsymbol{\gamma}\mathbf{u}^* + \mathbf{M}_\Gamma(\mathbf{x}^*)\mathbf{d}_\mathbf{H}\,, \\ \mathbf{V}^* &= -\mathbf{H}^* + \mathbf{u}^* \\ \mathbf{v}_\Gamma^* &= \mathbf{V}^* \bullet \mathbf{n}^* + \mathbf{d}_{\mathbf{v}_\Gamma}.\end{aligned} \tag{C.4.14}$$

As before, we subtract (C.4.14) from (C.3.26a), (C.3.26b) and (C.3.25), and obtain that the

errors $\mathbf{e_n}$ and $\mathbf{e_H}$ satisfy the error equations

$$\begin{aligned}
\mathbf{M}_\Gamma(\mathbf{x})\dot{\mathbf{e}}_\mathbf{n} + \mathbf{A}_\Gamma(\mathbf{x})\mathbf{e_n} = & -\big(\mathbf{M}_\Gamma(\mathbf{x}) - \mathbf{M}_\Gamma(\mathbf{x}^*)\big)\dot{\mathbf{n}}^* \\
& -\big(\mathbf{A}_\Gamma(\mathbf{x}) - \mathbf{A}_\Gamma(\mathbf{x}^*)\big)\mathbf{n}^* \\
& +\big(\mathbf{f}_\mathrm{n}(\mathbf{x},\mathbf{n}) - \mathbf{f}_\mathrm{n}(\mathbf{x}^*,\mathbf{n}^*)\big) \\
& -\mathbf{D}_\Gamma(\mathbf{x}^*)\boldsymbol{\gamma}\mathbf{e_u} - \big(\mathbf{D}_\Gamma(\mathbf{x}) - \mathbf{D}_\Gamma(\mathbf{x}^*)\big)\boldsymbol{\gamma}\mathbf{u} \\
& -\mathbf{M}_\Gamma(\mathbf{x}^*)\mathbf{d_n}, \\
\mathbf{M}_\Gamma(\mathbf{x})\dot{\mathbf{e}}_\mathbf{H} + \mathbf{A}_\Gamma(\mathbf{x})\mathbf{e_H} = & -\big(\mathbf{M}_\Gamma(\mathbf{x}) - \mathbf{M}_\Gamma(\mathbf{x}^*)\big)\dot{\mathbf{H}}^* \\
& -\big(\mathbf{A}_\Gamma(\mathbf{x}) - \mathbf{A}_\Gamma(\mathbf{x}^*)\big)\mathbf{H}^* \\
& +\big(\mathbf{f}_H(\mathbf{x},\mathbf{n},-\mathbf{H}+\boldsymbol{\gamma}\mathbf{u}) - \mathbf{f}_H(\mathbf{x}^*,\mathbf{n}^*,-\mathbf{H}^*+\boldsymbol{\gamma}\mathbf{u}^*)\big) \\
& +\mathbf{A}_\Gamma(\mathbf{x}^*)\boldsymbol{\gamma}\mathbf{e_u} + \big(\mathbf{A}_\Gamma(\mathbf{x}) - \mathbf{A}_\Gamma(\mathbf{x}^*)\big)\boldsymbol{\gamma}\mathbf{u} \\
& -\mathbf{M}_\Gamma(\mathbf{x}^*)\mathbf{d_H}\,,
\end{aligned} \tag{C.4.15}$$

$$\tag{C.4.16}$$

and the error $\mathbf{e}_{\mathbf{v}_\Gamma}$ is obtained from

$$\mathbf{e}_{\mathbf{v}_\Gamma} = \mathbf{V}\bullet\mathbf{n} - \mathbf{V}^*\bullet\mathbf{n}^* - \mathbf{d}_{\mathbf{v}_\Gamma}. \tag{C.4.17}$$

Apart from the coupling terms with u included here, stable error propagation has been shown in [Kovács et al., 2019]. In the following we will therefore concentrate on the critical coupling terms involving $\mathbf{e_u}$ and $\mathbf{u}$.

C.4.2.3. Error equations for the harmonic velocity extension

The interpolated exact solution $\mathbf{v}^* = (\mathbf{v}^*_\Gamma; \mathbf{v}^*_\Omega)$ satisfies the numerical scheme (C.3.29f) up to a defect $\mathbf{d}_{\mathbf{v}_\Omega}$ defined by

$$\mathbf{A}_{\Omega\Omega}(\mathbf{x}^*)\mathbf{v}^*_\Omega = -\mathbf{A}_{\Omega\Gamma}(\mathbf{x}^*)\mathbf{v}^*_\Gamma + \mathbf{M}_{\Omega\Omega}(\mathbf{x}^*)\mathbf{d}_{\mathbf{v}_\Omega}\,. \tag{C.4.18}$$

Subtracting this equation from (C.3.27), we obtain the error equation

$$\begin{aligned}
\mathbf{A}_{\Omega\Omega}(\mathbf{x}^*)\mathbf{e}_{\mathbf{v}_\Omega} + \mathbf{A}_{\Omega\Gamma}(\mathbf{x}^*)\mathbf{e}_{\mathbf{v}_\Gamma} = & -\left(\mathbf{A}_{\Omega\Omega}(\mathbf{x}) - \mathbf{A}_{\Omega\Omega}(\mathbf{x}^*)\right)\mathbf{e}_{\mathbf{v}_\Omega} - \left(\mathbf{A}_{\Omega\Omega}(\mathbf{x}) - \mathbf{A}_{\Omega\Omega}(\mathbf{x}^*)\right)\mathbf{v}^*_\Omega \\
& -\left(\mathbf{A}_{\Omega\Gamma}(\mathbf{x}) - \mathbf{A}_{\Omega\Gamma}(\mathbf{x}^*)\right)\mathbf{e}_{\mathbf{v}_\Gamma} - \left(\mathbf{A}_{\Omega\Gamma}(\mathbf{x}) - \mathbf{A}_{\Omega\Gamma}(\mathbf{x}^*)\right)\mathbf{v}^*_\Gamma \\
& -\mathbf{M}_{\Omega\Omega}(\mathbf{x}^*)\mathbf{d}_{\mathbf{v}_\Omega}\,.
\end{aligned}$$

With $\mathbf{e_v} = (\mathbf{e}_{\mathbf{v}_\Gamma}; \mathbf{e}_{\mathbf{v}_\Omega})$ and $\mathbf{d_v} = (\mathbf{0}; \mathbf{d}_{\mathbf{v}_\Omega})$, this equation simplifies to

$$\begin{aligned}
\begin{pmatrix} 0 & 0 \\ 0 & \mathbf{I}_\Omega \end{pmatrix}\mathbf{A}_{\bar\Omega}(\mathbf{x}^*)\mathbf{e_v} = -\begin{pmatrix} 0 & 0 \\ 0 & \mathbf{I}_\Omega \end{pmatrix}\Big(& \left(\mathbf{A}_{\bar\Omega}(\mathbf{x}) - \mathbf{A}_{\bar\Omega}(\mathbf{x}^*)\right)\mathbf{e_v} \\
& + \left(\mathbf{A}_{\bar\Omega}(\mathbf{x}) - \mathbf{A}_{\bar\Omega}(\mathbf{x}^*)\right)\mathbf{v}^* \\
& + \mathbf{M}_{\bar\Omega}(\mathbf{x}^*)\mathbf{d_v}\Big).
\end{aligned} \tag{C.4.19}$$

C.4.3. Stability bound

We bound the errors at time t in terms of the defects up to time t and the errors in the initial values. The errors are bounded in the H^1 norms on the surface Γ and, where relevant, in the bulk Ω. For a nodal vector $\mathbf{e}$ associated with a surface finite element function $e \in \mathcal{S}_h[\mathbf{x}]$, we define with the symmetric positive definite matrix $\mathbf{K}_\Gamma(\mathbf{x}) = \mathbf{A}_\Gamma(\mathbf{x}) + \mathbf{M}_\Gamma(\mathbf{x})$

$$\|\mathbf{e}\|^2_{\mathbf{K}_\Gamma(\mathbf{x})} = \mathbf{e}^{\mathrm{T}}\mathbf{K}_\Gamma(\mathbf{x})\mathbf{e} = \|e\|^2_{H^1(\Gamma_h(\mathbf{x}))}\,,$$

and similarly for $\mathbf{e}$ associated with a bulk finite element function $e \in \mathcal{V}_h[\mathbf{x}]$, we define with the matrix $\mathbf{K}_{\bar\Omega}(\mathbf{x}) = \mathbf{A}_{\bar\Omega}(\mathbf{x}) + \mathbf{M}_{\bar\Omega}(\mathbf{x})$

$$\|\mathbf{e}\|^2_{\mathbf{K}_{\bar\Omega}(\mathbf{x})} = \mathbf{e}^{\mathrm{T}}\mathbf{K}_{\bar\Omega}(\mathbf{x})\mathbf{e} = \|e\|^2_{H^1(\Omega_h(\mathbf{x}))}.$$

With the matrix $\mathbf{L}(\mathbf{x}) = \mathbf{A}_{\bar\Omega}(\mathbf{x}) + \boldsymbol{\gamma}^{\mathrm{T}}\mathbf{A}_\Gamma(\mathbf{x})\boldsymbol{\gamma} + \boldsymbol{\gamma}^{\mathrm{T}}\mathbf{M}_\Gamma(\mathbf{x})\boldsymbol{\gamma}$ of (C.3.28) we set

$$\|\mathbf{e}\|^2_{\mathbf{L}(\mathbf{x})} = \mathbf{e}^{\mathrm{T}}\mathbf{L}(\mathbf{x})\mathbf{e} \sim \|e\|^2_{H^1(\Omega_h(\mathbf{x}))} + \|\gamma u_h\|^2_{H^1(\Gamma_h(\mathbf{x}))} = \|e\|^2_{H^1(\Omega_h(\mathbf{x}),\Gamma_h(\mathbf{x}))},$$

where the constant in the equivalence of norms (denoted above by the symbol $\sim$) is independent of h. To bound the defect $\mathbf{d}_\mathbf{v}$, we further need the following norm for a bulk nodal vector $\mathbf{d} \in \mathbb{R}^N$, which equals the dual norm for the corresponding finite element function $d \in \mathcal{V}_h[\mathbf{x}]$:

$$\|\mathbf{d}\|_{\star,\mathbf{x}} = \|d\|_{H_h^{-1}(\Omega_h[\mathbf{x}])} := \sup_{0\neq\varphi_h\in\mathcal{V}_h^0[\mathbf{x}]} \frac{\int_{\Omega_h[\mathbf{x}]} d\cdot\varphi_h}{\|\varphi_h\|_{H^1(\Omega_h[\mathbf{x}])}}\,.$$

The following result provides the key stability estimate, which bounds the errors in terms of the defects and the initial errors.

Proposition C.4.3. *Assume that the reference finite element functions*

$$x_h^*(\cdot,t),\ v_h^*(\cdot,t),\ u_h^*(\cdot,t),\ H_h^*(\cdot,t),\ \mathrm{n}_h^*(\cdot,t)$$

on the interpolated surface $\Gamma_h[\mathbf{x}^*(t)]$ and bulk $\Omega_h[\mathbf{x}^*(t)]$ have $W^{1,\infty}$ norms that are bounded independently of h, uniformly for all $t\in[0,T]$. Let

$$\begin{aligned}\delta = \max_{0\le t\le T}\Big(&\|\mathbf{d}_\mathbf{u}(t)\|_{\mathbf{M}_{\bar\Omega}(\mathbf{x}^*(t))} + \|\dot{\mathbf{d}}_\mathbf{u}(t)\|_{\mathbf{M}_{\bar\Omega}(\mathbf{x}^*(t))} + \|\mathbf{d}_\mathbf{H}(t)\|_{\mathbf{M}_\Gamma(\mathbf{x}^*(t))}\\ &+ \|\mathbf{d}_\mathbf{n}(t)\|_{\mathbf{M}_\Gamma(\mathbf{x}^*(t))} + \|\mathbf{d}_{\mathbf{v}_\Gamma}(t)\|_{\mathbf{K}_\Gamma(\mathbf{x}^*(t))} + \|\mathbf{d}_\mathbf{v}(t)\|_{\star,\mathbf{x}^*(t)}\Big)\end{aligned} \tag{C.4.20}$$

be a bound of the defects and

$$\varepsilon^0 = \|\mathbf{e}_\mathbf{H}(0)\|_{\mathbf{K}_\Gamma(\mathbf{x}^0)} + \|\mathbf{e}_\mathbf{n}(0)\|_{\mathbf{K}_\Gamma(\mathbf{x}^0)} \tag{C.4.21}$$

be a bound of the errors of the initial values. If the defects and initial errors are bounded by

$$\delta + \varepsilon^0 \le ch^\kappa \quad \text{for some } \kappa \text{ with } \frac{3}{2} < \kappa \le k, \tag{C.4.22}$$

then there exists $\bar h > 0$ such that the following stability bound holds for all $h \le \bar h$ and $0 \le t \le T$:

$$\begin{aligned}&\|\mathbf{e}_\mathbf{u}(t)\|_{\mathbf{L}(\mathbf{x}^*(t))} + \|\mathbf{e}_\mathbf{x}(t)\|_{\mathbf{L}(\mathbf{x}^*(t))} + \|\mathbf{e}_\mathbf{v}(t)\|_{\mathbf{L}(\mathbf{x}^*(t))}\\ &\quad + \|\mathbf{e}_\mathbf{H}(t)\|_{\mathbf{K}_\Gamma(\mathbf{x}^*(t))} + \|\mathbf{e}_\mathbf{n}(t)\|_{\mathbf{K}_\Gamma(\mathbf{x}^*(t))} \le C(\delta+\varepsilon^0),\end{aligned} \tag{C.4.23}$$

where C is independent of h and t, but depends on the final time T.

C.4.4. Proof of Proposition C.4.3

C.4.4.1. Preliminaries

Let $t^* \leq T$ be the maximal time such that the following inequalities hold true:

$$\begin{aligned}
\|e_x(\cdot,t)\|_{W^{1,\infty}(\Omega_h[\mathbf{x}^*(t)])} &\leq h^{(\kappa-3/2)/2} \\
\|e_v(\cdot,t)\|_{W^{1,\infty}(\Omega_h[\mathbf{x}^*(t)])} &\leq h^{(\kappa-3/2)/2} \\
\|e_u(\cdot,t)\|_{W^{1,\infty}(\Omega_h[\mathbf{x}^*(t)])} &\leq h^{(\kappa-3/2)/2} \qquad \text{for} \quad t \in [0,t^*]. \\
\|e_H(\cdot,t)\|_{W^{1,\infty}(\Gamma_h[\mathbf{x}^*(t)])} &\leq h^{(\kappa-1)/2} \\
\|e_{\mathrm{n}}(\cdot,t)\|_{W^{1,\infty}(\Gamma_h[\mathbf{x}^*(t)])} &\leq h^{(\kappa-1)/2}
\end{aligned} \tag{C.4.24}$$

We first prove the stated error bounds for $0 \leq t \leq t^*$. At the end of the proof we will show that t^* actually coincides with T.

Since the reference finite element functions $x_h^*(\cdot,t)$, $v_h^*(\cdot,t)$, $u_h^*(\cdot,t)$ and $H_h^*(\cdot,t)$, $\mathrm{n}_h^*(\cdot,t)$ on the interpolated bulk $\bar\Omega_h[\mathbf{x}^*(t)]$ and surface $\Gamma_h[\mathbf{x}^*(t)]$, respectively, have $W^{1,\infty}$ norms that are bounded independently of h for all $t \in [0,T]$, the bounds (C.4.24) together with Lemma C.4.2 imply that the $W^{1,\infty}$ norms of the bulk–surface finite element functions $x_h(\cdot,t), v_h(\cdot,t), u_h(\cdot,t)$ and $H_h(\cdot,t)$, $\mathrm{n}_h(\cdot,t)$ on $\bar\Omega_h[\mathbf{x}(t)]$ and $\Gamma_h[\mathbf{x}(t)]$, respectively, are also bounded independently of h and $t \in [0,t^*]$, and so are their lifts to $\bar\Omega_h[\mathbf{x}^*(t)]$ and $\Gamma_h[\mathbf{x}^*(t)]$.

The estimate on the position errors e_x in (C.4.24) and the $W^{1,\infty}$ bound on v_h immediately imply that the results of Section C.4.1 apply. In particular, due to the bounds in (C.4.24) (for a sufficiently small $h \leq h_0$), the main condition of Lemma C.4.2 and also (C.4.5) are satisfied (with $e_h^\theta = e_x^\theta$). Hence the h-uniform norm equivalences and estimates in (C.4.7) hold between the surfaces defined by $\mathbf{x}$ and $\mathbf{x}^*$. Similarly, again due to (C.4.24), the bound (C.4.8) also holds, and hence the estimates in (C.4.9), (C.4.10) and the h-uniform norm equivalences in time (C.4.11) also hold.

In the following, c and C denote generic constants that take different values on different occurrences. In contrast, constants with a subscript (such as c_0) will play a distinctive role in the proof and will not change their value between appearances.

C.4.4.2. Error bound for the generalized Robin boundary value problem

We test (C.4.13) with $\mathbf{e_u}$ and obtain

$$\begin{aligned}
\mathbf{e_u}^{\mathrm{T}}\mathbf{L}(\mathbf{x})\mathbf{e_u} = {}& \mathbf{e_u}^{\mathrm{T}}\big(\mathbf{f}_u(\mathbf{x},\mathbf{H}) - \mathbf{f}_u(\mathbf{x}^*,\mathbf{H}^*)\big) \\
& - \ \mathbf{e_u}^{\mathrm{T}}\big(\mathbf{L}(\mathbf{x}) - \mathbf{L}(\mathbf{x}^*)\big)\mathbf{u}^* \\
& - \ \mathbf{e_u}^{\mathrm{T}}\mathbf{M}_{\bar\Omega}(\mathbf{x}^*)\mathbf{d_u}\,.
\end{aligned} \tag{C.4.25}$$

We begin with estimating the first term on the right-hand side. We introduce finite element functions on the intermediate surface $\Gamma_h^\theta = \Gamma[\mathbf{x}^\theta]$ with $\mathbf{x}^\theta = \mathbf{x}^* + \theta\mathbf{e_x}$ $(0 \leq \theta \leq 1)$ that are

defined by

$$H_h^\theta = \sum_{i=1}^{N_\Gamma} (H_i^* + \theta(H_i - H_i^*))\varphi_i[\mathbf{x}^* + \theta \mathbf{e}_\mathbf{x}],$$
$$Q_h^\theta = \sum_{i=1}^{N_\Gamma} (Q_i^* + \theta(Q_i - Q_i^*))\varphi_i[\mathbf{x}^* + \theta \mathbf{e}_\mathbf{x}],$$

where Q_i^* and Q_i are the values of the source term Q at x_i^* and x_i, respectively. Their nodal vectors are denoted $\mathbf{H}^\theta = (H_i^\theta)$ and $\mathbf{Q}^\theta = (Q_i^\theta)$. We let e_u^θ be the finite element function on $\Omega_h^\theta = \Omega[\mathbf{x}^\theta]$ with nodal vector $\mathbf{e_u}$, and we set $e_u = e_u^0$ for later use. We then have

$$\begin{aligned} I := \mathbf{e_u}^{\mathrm{T}}\big(\mathbf{f}_u(\mathbf{x}, \mathbf{H}) - \mathbf{f}_u(\mathbf{x}^*, \mathbf{H}^*)\big) &= \int_0^1 \frac{\mathrm{d}}{\mathrm{d}\theta}\Big(\mathbf{e_u}^{\mathrm{T}}\mathbf{f}_u(\mathbf{x}^\theta, \mathbf{H}^\theta)\Big)\, d\theta \\ &= \int_0^1 \frac{\mathrm{d}}{\mathrm{d}\theta}\Big(-\int_{\Omega_h^\theta} e_u^\theta + \int_{\Gamma_h^\theta} e_u^\theta (H_h^\theta + Q_h^\theta)\Big)\mathrm{d}\theta. \end{aligned}$$

By the Leibniz formula and using that $\partial_\theta^\bullet e_u^\theta = 0$ by the transport property, this becomes

$$I = \int_0^1 \Big(-\int_{\Omega_h^\theta} e_u^\theta (\nabla \cdot e_x^\theta) + \int_{\Gamma_h^\theta} e_u^\theta (H_h^\theta + Q_h^\theta)(\nabla \cdot e_x^\theta) + \int_{\Gamma_h^\theta} e_u^\theta (\partial_\theta^\bullet H_h^\theta + \partial_\theta^\bullet Q_h^\theta)\Big)\mathrm{d}\theta,$$

which we bound with the Cauchy–Schwarz inequality, noting further that $\partial_\theta^\bullet H_h^\theta = e_H^\theta$ and $\partial_\theta^\bullet Q_h^\theta = e_Q^\theta$,

$$\begin{aligned} I \le \int_0^1 \Big(&\|e_u^\theta\|_{L^2(\Omega_h^\theta)} \|\nabla \cdot e_x^\theta\|_{L^2(\Omega_h^\theta)} + \|e_u^\theta\|_{L^2(\Gamma_h^\theta)} \|H_h^\theta + Q_h^\theta\|_{L^\infty(\Gamma_h^\theta)} \|\nabla \cdot e_x^\theta\|_{L^2(\Gamma_h^\theta)} \\ &+ \|e_u^\theta\|_{L^2(\Gamma_h^\theta)} \big(\|e_H^\theta + e_Q^\theta\|_{L^2(\Gamma_h^\theta)}\big)\Big)\mathrm{d}\theta. \end{aligned}$$

By Lemma C.4.2 and condition (C.4.24), which yields that H_h^θ is bounded in the maximum norm by a constant independent of h and θ, this integral can be further bounded by

$$I \le \|e_u\|_{L^2(\Omega_h[\mathbf{x}^*])} \|e_x\|_{H^1(\Omega_h[\mathbf{x}^*])} + c\|e_u\|_{L^2(\Gamma_h[\mathbf{x}^*])}\Big(\|e_x\|_{H^1(\Gamma_h[\mathbf{x}^*])} + \|e_H + e_Q\|_{L^2(\Gamma_h[\mathbf{x}^*])}\Big).$$

The second term (denoted II) on the right-hand side of (C.4.25) can be estimated with Lemma C.4.1. We obtain

$$II \le c\|e_u\|_{H^1(\Omega_h[\mathbf{x}^*],\Gamma_h[\mathbf{x}^*])} \|e_x\|_{H^1(\Omega_h[\mathbf{x}^*],\Gamma_h[\mathbf{x}^*])} \|u_h^*\|_{W^{1,\infty}(\Omega_h[\mathbf{x}^*],\Gamma_h[\mathbf{x}^*])}.$$

Finally, we have

$$III = -\mathbf{e_u}^{\mathrm{T}} \mathbf{M}_{\bar\Omega}(\mathbf{x}^*)\mathbf{d_u} = \int_{\Omega_h[\mathbf{x}^*]} e_u d_u \le c\|e_u\|_{L^2(\Omega_h[\mathbf{x}^*])} \cdot \|d_u\|_{L^2(\Omega_h[\mathbf{x}^*])},$$

so that altogether

$$\begin{aligned}\|\mathbf{e_u}\|_{\mathbf{L}(\mathbf{x}^*)} &= \|e_u\|_{H^1(\Omega_h[\mathbf{x}^*],\Gamma_h[\mathbf{x}^*])}\\ &\leq c\Big(\|e_x\|_{H^1(\Omega_h[\mathbf{x}^*],\Gamma_h[\mathbf{x}^*])} + \|e_H + e_Q\|_{L^2(\Gamma_h[\mathbf{x}^*])} + \|d_u\|_{L^2(\Omega_h[\mathbf{x}^*])}\Big)\\ &= c\Big(\|\mathbf{e_x}\|_{\mathbf{L}(\mathbf{x}^*)} + \|\mathbf{e_H} + \mathbf{e_Q}\|_{\mathbf{M}_\Gamma(\mathbf{x}^*))} + \|\mathbf{d_u}\|_{\mathbf{M}_{\bar\Omega}(\mathbf{x}^*)}\Big).\end{aligned}$$

Using that $\|\mathbf{e_Q}\|_{\mathbf{M}_\Gamma(\mathbf{x}^*))} \leq c\|\mathbf{e_x}\|_{\mathbf{M}_\Gamma(\mathbf{x}^*))} \leq c\|\mathbf{e_x}\|_{\mathbf{L}(\mathbf{x}^*)}$, this becomes

$$\|\mathbf{e_u}\|_{\mathbf{L}(\mathbf{x}^*)} \leq c\Big(\|\mathbf{e_x}\|_{\mathbf{L}(\mathbf{x}^*)} + \|\mathbf{e_H}\|_{\mathbf{M}_\Gamma(\mathbf{x}^*))} + \|\mathbf{d_u}\|_{\mathbf{M}_{\bar\Omega}(\mathbf{x}^*)}\Big). \tag{C.4.26}$$

In addition to this bound of e_u, we also need a bound for its material time derivative $\partial^\bullet e_u$. To this end we differentiate the error equation (C.4.13) with respect to time and test with $\dot{\mathbf{e}}_\mathbf{u}$. Using the same arguments as in bounding $\mathbf{e_u}$ before, together with the bound $\|\dot{\mathbf{e}}_\mathbf{Q}\|_{\mathbf{M}_\Gamma(\mathbf{x}^*)} \leq c\big(\|\mathbf{e_x}\|_{\mathbf{M}_\Gamma(\mathbf{x}^*)} + \|\mathbf{e_{v_\Gamma}}\|_{\mathbf{M}_\Gamma(\mathbf{x}^*)}\big)$, we find

$$\begin{aligned}\|\dot{\mathbf{e}}_\mathbf{u}\|_{\mathbf{L}(\mathbf{x}^*)} \leq c\Big(&\|\mathbf{e_u}\|_{\mathbf{L}(\mathbf{x}^*)} + \|\mathbf{e_x}\|_{\mathbf{L}(\mathbf{x}^*)} + \|\mathbf{e_v}\|_{\mathbf{L}(\mathbf{x}^*)}\\ &+\|\mathbf{e_H}\|_{\mathbf{M}_\Gamma(\mathbf{x}^*)} + \|\dot{\mathbf{e}}_\mathbf{H}\|_{\mathbf{M}_\Gamma(\mathbf{x}^*)} + \|\mathbf{d_u}\|_{\mathbf{M}_{\bar\Omega}(\mathbf{x}^*)} + \|\dot{\mathbf{d}}_\mathbf{u}\|_{\mathbf{M}_{\bar\Omega}(\mathbf{x}^*)}\Big).\end{aligned} \tag{C.4.27}$$

C.4.4.3. Error bound for the forced mean curvature flow

We test the error equation (C.4.16) for $\mathbf{e_H}$ with $\dot{\mathbf{e}}_\mathbf{H}$. On the left-hand side we obtain

$$\dot{\mathbf{e}}_\mathbf{H}^{\mathrm{T}}\mathbf{M}_\Gamma(\mathbf{x})\dot{\mathbf{e}}_\mathbf{H} + \dot{\mathbf{e}}_\mathbf{H}^{\mathrm{T}}\mathbf{A}_\Gamma(\mathbf{x})\mathbf{e_H} = \|\dot{\mathbf{e}}_\mathbf{H}\|^2_{\mathbf{M}_\Gamma(\mathbf{x})} + \frac{1}{2}\frac{\mathrm{d}}{\mathrm{d}t}\|\mathbf{e_H}\|^2_{\mathbf{A}_\Gamma(\mathbf{x})} - \frac{1}{2}\,\mathbf{e}_\mathbf{H}^{\mathrm{T}}\Big(\frac{\mathrm{d}}{dt}\mathbf{A}(\mathbf{x})\Big)\mathbf{e_H}.$$

On the right-hand side, the resulting terms that do not depend on u are estimated in exactly the same way as in [Kovács et al., 2019, Section 7], and for the extra terms we estimate as follows. The most critical term is $\dot{\mathbf{e}}_\mathbf{H}^T\mathbf{A}_\Gamma(\mathbf{x}^*)\boldsymbol{\gamma}\mathbf{e_u}$, whose direct estimation with the Cauchy–Schwarz inequality would contain the $\mathbf{A}_\Gamma(\mathbf{x}^*)$-norm of $\dot{\mathbf{e}}_\mathbf{H}$, which cannot be suitably bounded. Instead we rewrite

$$\dot{\mathbf{e}}_\mathbf{H}^T\mathbf{A}_\Gamma(\mathbf{x}^*)\boldsymbol{\gamma}\mathbf{e_u} = \frac{\mathrm{d}}{\mathrm{d}t}(\mathbf{e}_\mathbf{H}^T\mathbf{A}_\Gamma(x^*)\boldsymbol{\gamma}\mathbf{e}_u) - \mathbf{e}_\mathbf{H}^T\left(\frac{\mathrm{d}}{dt}\mathbf{A}_\Gamma(\mathbf{x}^*)\right)\boldsymbol{\gamma}\mathbf{e_u} - \mathbf{e}_H^T\mathbf{A}_\Gamma(\mathbf{x}^*)\boldsymbol{\gamma}\dot{\mathbf{e}}_\mathbf{u}.$$

For the last term with $\dot{\mathbf{e}}_\mathbf{u}$, after bounding via the Cauchy–Schwarz inequality and Young's inequality with a small $\rho > 0$,

$$\begin{aligned}\mathbf{e}_\mathbf{H}^T\mathbf{A}_\Gamma(\mathbf{x}^*)\boldsymbol{\gamma}\dot{\mathbf{e}}_\mathbf{u} &\leq \|\mathbf{e_H}\|_{\mathbf{A}_\Gamma(\mathbf{x}^*)}\|\boldsymbol{\gamma}\dot{\mathbf{e}}_\mathbf{u}\|_{\mathbf{A}_\Gamma(\mathbf{x}^*)}\\ &\leq \|\mathbf{e_H}\|_{\mathbf{K}_\Gamma(\mathbf{x}^*)}\|\dot{\mathbf{e}}_\mathbf{u}\|_{\mathbf{L}(\mathbf{x}^*)} \leq \tfrac{1}{2}\rho^{-1}\|\mathbf{e_H}\|^2_{\mathbf{K}_\Gamma(\mathbf{x}^*)} + \tfrac{1}{2}\rho\|\dot{\mathbf{e}}_\mathbf{u}\|^2_{\mathbf{L}(\mathbf{x}^*)},\end{aligned}$$

we use the bound (C.4.27) for $\|\dot{\mathbf{e}}_\mathbf{u}\|_{\mathbf{L}(\mathbf{x}^*)}$. We note that only the $\mathbf{M}_\Gamma$-norm of $\dot{\mathbf{e}}_\mathbf{H}$ appears in this bound, and $\|\dot{\mathbf{e}}_\mathbf{H}\|^2_{\mathbf{M}_\Gamma(\mathbf{x}^*)}$ times a small constant factor can be absorbed in the corresponding term on the left-hand side, since the $\mathbf{M}_\Gamma$-norms at $\mathbf{x}$ and $\mathbf{x}^*$ are equivalent uniformly in h.

The term $\mathbf{e}_\mathbf{H}^T\big(\mathbf{A}_\Gamma(\mathbf{x})-\mathbf{A}_\Gamma(\mathbf{x}^*)\big)\boldsymbol{\gamma}\mathbf{u}$ is of the same type as $\mathbf{e}_\mathbf{H}^T\big(\mathbf{A}_\Gamma(\mathbf{x})-\mathbf{A}_\Gamma(\mathbf{x}^*)\big)\mathbf{H}^*$, which was estimated in [Kovács et al., 2019, after (7.27)]. Here, the same proof and the use of condition (C.4.24) for $\mathbf{u}=\mathbf{u}^*+\mathbf{e}_\mathbf{u}$ yield the bound

$$\begin{aligned}
&\dot{\mathbf{e}}_\mathbf{H}^T\big(\mathbf{A}_\Gamma(\mathbf{x})-\mathbf{A}_\Gamma(\mathbf{x}^*)\big)\boldsymbol{\gamma}\mathbf{u}\\
&\le \frac{\mathrm{d}}{\mathrm{d}t}\Big(\mathbf{e}_\mathbf{H}^T\big(\mathbf{A}_\Gamma(\mathbf{x})-\mathbf{A}_\Gamma(\mathbf{x}^*)\big)\boldsymbol{\gamma}\mathbf{u}\Big)+c\,\|\mathbf{e}_\mathbf{H}\|_{\mathbf{A}_\Gamma(\mathbf{x}^*)}\big(\|\mathbf{e}_\mathbf{x}\|_{\mathbf{K}_\Gamma(\mathbf{x}^*)}+\|\mathbf{e}_\mathbf{v}\|_{\mathbf{K}_\Gamma(\mathbf{x}^*)}\big).
\end{aligned}$$

Proceeding as in [Kovács et al., 2019, after (7.30)], which includes an integration in time, we obtain a bound for $\mathbf{e}_\mathbf{H}$, cf. [Kovács et al., 2019, (7.33)],

$$\begin{aligned}
\|\mathbf{e}_\mathbf{H}(t)\|^2_{\mathbf{K}_\Gamma(\mathbf{x}^*(t))} \le c\int_0^t \Big(&\|\mathbf{e}_\mathbf{x}(s)\|^2_{\mathbf{L}(\mathbf{x}^*(s))}+\|\mathbf{e}_{\mathbf{v}_\Gamma}(s)\|^2_{\mathbf{K}_\Gamma(\mathbf{x}^*(s))}\\
&+\|\mathbf{e}_\mathbf{n}(s)\|^2_{\mathbf{K}_\Gamma(\mathbf{x}^*(s))}+\|\mathbf{e}_\mathbf{H}(s)\|^2_{\mathbf{K}_\Gamma(\mathbf{x}^*(s))}\Big)\mathrm{d}s\\
&+c\,\|\mathbf{e}_\mathbf{x}(t)\|^2_{\mathbf{K}_\Gamma(\mathbf{x}^*(t))}+c\,\|\mathbf{e}_\mathbf{H}(0)\|^2_{\mathbf{K}_\Gamma(\mathbf{x}^*(0))}\\
&+c\int_0^t \Big(\|\mathbf{d}_\mathbf{H}(s)\|^2_{\mathbf{M}_\Gamma(\mathbf{x}^*(s))}+\|\mathbf{d}_\mathbf{u}(s)\|^2_{\mathbf{M}_{\bar\Omega}(\mathbf{x}^*(s))}\\
&+\|\dot{\mathbf{d}}_\mathbf{u}(s)\|^2_{\mathbf{M}_{\bar\Omega}(\mathbf{x}^*(s))}\Big)\mathrm{d}s.
\end{aligned}\tag{C.4.28}$$

Testing the error equation (C.4.15) for $\mathbf{e}_\mathbf{n}$ with $\dot{\mathbf{e}}_\mathbf{n}$, we obtain in the same way, but now with terms that can be directly estimated, the bound for $\mathbf{e}_\mathbf{n}$,

$$\begin{aligned}
\|\mathbf{e}_\mathbf{n}(t)\|^2_{\mathbf{K}_\Gamma(\mathbf{x}^*(t))} \le c\int_0^t \Big(&\|\mathbf{e}_\mathbf{x}(s)\|^2_{\mathbf{L}(\mathbf{x}^*(s))}+\|\mathbf{e}_{\mathbf{v}_\Gamma}(s)\|^2_{\mathbf{K}_\Gamma(\mathbf{x}^*(s))}\\
&+\|\mathbf{e}_\mathbf{n}(s)\|^2_{\mathbf{K}_\Gamma(\mathbf{x}^*(s))}+\|\mathbf{e}_\mathbf{H}(s)\|^2_{\mathbf{K}_\Gamma(\mathbf{x}^*(s))}\Big)\mathrm{d}s\\
&+\|\mathbf{e}_\mathbf{x}(t)\|^2_{\mathbf{K}_\Gamma(\mathbf{x}^*(t))}+c\,\|\mathbf{e}_\mathbf{n}(0)\|^2_{\mathbf{K}_\Gamma(\mathbf{x}^*(0))}\\
&+c\int_0^t \Big(\|\mathbf{d}_\mathbf{n}(s)\|^2_{\mathbf{M}_\Gamma(\mathbf{x}^*(s))}+\|\mathbf{d}_\mathbf{u}(s)\|^2_{\mathbf{M}_{\bar\Omega}(\mathbf{x}^*(s))}\Big)\mathrm{d}s.
\end{aligned}\tag{C.4.29}$$

Noting $V=-H+u$ and using Lemma 5.3 of [Kovács et al., 2021] in (C.4.17) in the same way as in deriving the velocity error bound (5.44) of [Kovács et al., 2021], we obtain the following error bound for the boundary velocity:

$$\begin{aligned}
\|\mathbf{e}_{\mathbf{v}_\Gamma}(t)\|_{\mathbf{K}_\Gamma(\mathbf{x}^*(t))} \le c\Big(&\|\mathbf{e}_\mathbf{u}(t)\|_{\mathbf{K}_\Gamma(\mathbf{x}^*(t))}+\|\mathbf{e}_\mathbf{H}(t)\|_{\mathbf{K}_\Gamma(\mathbf{x}^*(t))}+\|\mathbf{e}_\mathbf{n}(t)\|_{\mathbf{K}_\Gamma(\mathbf{x}^*(t))}\Big)\\
&+\|\mathbf{d}_{\mathbf{v}_\Gamma}(t)\|_{\mathbf{K}_\Gamma(\mathbf{x}^*(t))}.
\end{aligned}\tag{C.4.30}$$

We have $\dot{\mathbf{e}}_\mathbf{x}=\mathbf{e}_\mathbf{v}$ and $\mathbf{e}_\mathbf{x}(0)=0$, and hence

$$\|\mathbf{e}_{\mathbf{x}_\Gamma}(t)\|_{\mathbf{K}_\Gamma(\mathbf{x}^*(t))} \le \int_0^t \|\mathbf{e}_{\mathbf{v}_\Gamma}(s)\|_{\mathbf{K}_\Gamma(\mathbf{x}^*(s))}\,\mathrm{d}s.\tag{C.4.31}$$

C.4.4.4. Error bound for the discrete harmonic velocity extension

The error equation (C.4.19) is the matrix–vector formulation of a discretized Dirichlet problem: Given $e_{v_\Gamma} \in \mathcal{S}_h[\mathbf{x}^*]$, find $e_v \in \mathcal{V}_h[\mathbf{x}^*]$ with $\gamma_h e_v = e_{v_\Gamma}$ such that

$$\int_{\Omega_h[\mathbf{x}^*]} \nabla e_v \cdot \nabla \varphi_h = \mathfrak{f}(\varphi_h) \qquad \text{for all } \varphi_h \in \mathcal{V}_h^0[\mathbf{x}^*], \tag{C.4.32}$$

where $\mathfrak{f}$ denotes the linear form on $\mathcal{V}_h^0[\mathbf{x}^*]$ that maps $\varphi_h \in \mathcal{V}_h^0[\mathbf{x}^*]$ with nodal vector $\boldsymbol{\varphi}$ to

$$\begin{aligned} \mathfrak{f}(\varphi_h) = &- \boldsymbol{\varphi}^{\mathrm{T}} \left(\mathbf{A}_{\bar\Omega}(\mathbf{x}) - \mathbf{A}_{\bar\Omega}(\mathbf{x}^*) \right) \mathbf{e_v} \\ &- \boldsymbol{\varphi}^{\mathrm{T}} \left(\mathbf{A}_{\bar\Omega}(\mathbf{x}) - \mathbf{A}_{\bar\Omega}(\mathbf{x}^*) \right) \mathbf{v}^* \\ &- \boldsymbol{\varphi}^{\mathrm{T}} \mathbf{M}_{\bar\Omega}(\mathbf{x}^*) \mathbf{d_v}. \end{aligned} \tag{C.4.33}$$

Proposition C.8.1 (concerning the Dirichlet data e_{v_Γ}) and standard finite element theory (concerning the functional $\mathfrak{f}$) give us the bound

$$\|e_v\|_{H^1(\Omega_h[\mathbf{x}^*])} \leq \|\mathfrak{f}\|_{H_h^{-1}(\Omega_h[\mathbf{x}^*])} + \|e_{v_\Gamma}\|_{H^{1/2}(\Gamma_h[\mathbf{x}^*])}\,, \tag{C.4.34}$$

where

$$\|\mathfrak{f}\|_{H_h^{-1}(\Omega_h[\mathbf{x}^*])} = \sup_{0 \neq \varphi_h \in \mathcal{V}_h^0[\mathbf{x}^*]} \frac{\mathfrak{f}(\varphi_h)}{\|\varphi_h\|_{H^1(\Omega_h[\mathbf{x}^*])}}.$$

We estimate the three terms of (C.4.33) separately. The steps are analogous to previous estimates based on Section C.4.1.

(i) For the first term we have, for sufficiently small h, using condition (C.4.24),

$$\begin{aligned} \boldsymbol{\varphi}^{\mathrm{T}} \left(\mathbf{A}_{\bar\Omega}(\mathbf{x}) - \mathbf{A}_{\bar\Omega}(\mathbf{x}^*) \right) \mathbf{e_v} &\leq c\, \|\varphi_h\|_{H^1(\Omega_h[\mathbf{x}^*])} \|\nabla e_x\|_{L^\infty(\Omega_h[\mathbf{x}^*])} \|e_v\|_{H^1(\Omega_h[\mathbf{x}^*])} \\ &\leq c\, h^{(\kappa-3/2)/2}\, \|\varphi_h\|_{H^1(\Omega_h[\mathbf{x}^*])} \|e_v\|_{H^1(\Omega_h[\mathbf{x}^*])} \\ &= c\, h^{(\kappa-3/2)/2}\, \|\varphi_h\|_{H^1(\Omega_h[\mathbf{x}^*])} \|\mathbf{e_v}\|_{\mathbf{K}_{\bar\Omega}(\mathbf{x}^*)}. \end{aligned}$$

(ii) For the second term we obtain

$$\boldsymbol{\varphi}^{\mathrm{T}} \left(\mathbf{A}_{\bar\Omega}(\mathbf{x}) - \mathbf{A}_{\bar\Omega}(\mathbf{x}^*) \right) \mathbf{v}^* \leq c \|\varphi_h\|_{H^1(\Omega_h[\mathbf{x}^*])} \|\nabla e_x\|_{L^2(\Omega_h[\mathbf{x}^*])} \|v_h^*\|_{W^{1,\infty}(\Omega_h[\mathbf{x}^*])}.$$

(iii) The third term is bounded by

$$\boldsymbol{\varphi}^{\mathrm{T}} \mathbf{M}_{\bar\Omega}(\mathbf{x}^*) \mathbf{d_v} \leq \|\varphi_h\|_{H^1(\Omega_h[\mathbf{x}^*])} \|\mathbf{d_v}\|_{\star,\mathbf{x}^*}.$$

Combining these estimates yields

$$\|\mathfrak{f}\|_{H_h^{-1}(\Omega_h[\mathbf{x}^*])} \leq c \left(h^{(\kappa-3/2)/2} \|\mathbf{e_v}\|_{\mathbf{K}_{\bar\Omega}(\mathbf{x}^*)} + \|\mathbf{e_x}\|_{\mathbf{A}_{\bar\Omega}(\mathbf{x}^*)} + \|\mathbf{d_v}\|_{\star,\mathbf{x}^*} \right).$$

For $h \leq h_0$ sufficiently small we can absorb the error $\mathbf{e_v}$ and insert the above estimate for $\mathfrak{f}$ in (C.4.34) to obtain

$$\|\mathbf{e_v}\|_{\mathbf{K}_{\bar\Omega}(\mathbf{x}^*)} \leq c \left(\|\mathbf{e_{v_\Gamma}}\|_{\mathbf{K}_\Gamma(\mathbf{x}^*)} + \|\mathbf{e_x}\|_{\mathbf{A}_{\bar\Omega}(\mathbf{x}^*)} + \|\mathbf{d_v}\|_{\star,\mathbf{x}^*} \right). \tag{C.4.35}$$

We have $\dot{\mathbf{e}}_\mathbf{x} = \mathbf{e_v}$ and $\mathbf{e_x}(0) = 0$, and hence

$$\|\mathbf{e_x}(t)\|_{\mathbf{K}_{\bar\Omega}(\mathbf{x}^*(t))} \leq \int_0^t \|\mathbf{e_v}(s)\|_{\mathbf{K}_{\bar\Omega}(\mathbf{x}^*(s))}\, \mathrm{d}s. \tag{C.4.36}$$

C.4.4.5. Combining the error bounds

By now we have the coupled inequalities (C.4.26), (C.4.28) and (C.4.29), (C.4.30) and (C.4.31), (C.4.35) and (C.4.36) for the error vectors $\mathbf{e_u}$, $\mathbf{e_H}$ and $\mathbf{e_n}$, $\mathbf{e_{v_\Gamma}}$ and $\mathbf{e_{x_\Gamma}}$, $\mathbf{e_v}$ and $\mathbf{e_x}$, respectively.

Combining the bounds (C.4.31) and (C.4.36) for $\mathbf{e_x}$, inserting the bounds (C.4.30) and (C.4.35) for $\mathbf{e_{v_\Gamma}}$ and $\mathbf{e_v}$ and noting that $\|\mathbf{e_x}\|^2_{\mathbf{L}(\mathbf{x}^*)} = \|\mathbf{e_x}\|^2_{\mathbf{K}_\Gamma(\mathbf{x}^*)} + \|\mathbf{e_x}\|^2_{\mathbf{K}_{\bar\Omega}(\mathbf{x}^*)}$, we obtain after using the Gronwall inequality to get rid of the term $\|\mathbf{e_x}\|_{\mathbf{L}(\mathbf{x}^*)}$ under the integral,

$$\begin{aligned}\|\mathbf{e_x}(t)\|_{\mathbf{L}(\mathbf{x}^*(t))} \le c\int_0^t \Big(\|\mathbf{e_u}(s)\|_{\mathbf{K}_\Gamma(\mathbf{x}^*(s))} + \|\mathbf{e_H}(s)\|_{\mathbf{K}_\Gamma(\mathbf{x}^*(s))} + \|\mathbf{e_n}(s)\|_{\mathbf{K}_\Gamma(\mathbf{x}^*(s))}\Big)\mathrm{d}s \\ + c\int_0^t \Big(\|\mathbf{d}_{\mathbf{v}_\Gamma}(s)\|_{\mathbf{K}_\Gamma(\mathbf{x}^*(s))} + \|\mathbf{d_v}(s)\|_{\star,\mathbf{x}^*(s)}\Big)\mathrm{d}s. \qquad \text{(C.4.37)}\end{aligned}$$

Inserting this bound into (C.4.26) and using the Gronwall inequality to get rid of the term $\|\mathbf{e_u}\|_{\mathbf{L}(\mathbf{x}^*)}$ under the integral yields

$$\begin{aligned}\|\mathbf{e_u}(t)\|_{\mathbf{L}(\mathbf{x}^*(t))} \le c\int_0^t \Big(\|\mathbf{e_H}(s)\|_{\mathbf{K}_\Gamma(\mathbf{x}^*(s))} + \|\mathbf{e_n}(s)\|_{\mathbf{K}_\Gamma(\mathbf{x}^*(s))}\Big)\mathrm{d}s \\ + c\,\|\mathbf{e_H}(t)\|_{\mathbf{M}_\Gamma(\mathbf{x}^*(t)))} + c\,\|\mathbf{d_u}(t)\|_{\mathbf{M}_{\bar\Omega}(\mathbf{x}^*(t))} \qquad \text{(C.4.38)} \\ + c\int_0^t \Big(\|\mathbf{d}_{\mathbf{v}_\Gamma}(s)\|_{\mathbf{K}_\Gamma(\mathbf{x}^*(s))} + \|\mathbf{d_v}(s)\|_{\star,\mathbf{x}^*(s)}\Big)\mathrm{d}s.\end{aligned}$$

Inserting (C.4.30), (C.4.37) and (C.4.38) into (C.4.28) yields

$$\begin{aligned}\|\mathbf{e_H}(t)\|^2_{\mathbf{K}_\Gamma(\mathbf{x}^*(t))} \le c\int_0^t \Big(\|\mathbf{e_H}(s)\|^2_{\mathbf{K}_\Gamma(\mathbf{x}^*(s))} + \|\mathbf{e_n}(s)\|^2_{\mathbf{K}_\Gamma(\mathbf{x}^*(s))}\Big)\mathrm{d}s + c\,\|\mathbf{e_H}(0)\|^2_{\mathbf{K}_\Gamma(\mathbf{x}^*(0))} \\ + c\int_0^t \Big(\|\mathbf{d_H}(s)\|^2_{\mathbf{M}_\Gamma(\mathbf{x}^*(s))} + \|\mathbf{d_u}(s)\|^2_{\mathbf{M}_{\bar\Omega}(\mathbf{x}^*(s))} + \|\dot{\mathbf{d}}_\mathbf{u}(s)\|^2_{\mathbf{M}_{\bar\Omega}(\mathbf{x}^*(s))} \qquad \text{(C.4.39)} \\ + \|\mathbf{d}_{\mathbf{v}_\Gamma}(s)\|^2_{\mathbf{K}_\Gamma(\mathbf{x}^*(s))} + \|\mathbf{d_v}(s)\|^2_{\star,\mathbf{x}^*(s)}\Big)\mathrm{d}s.\end{aligned}$$

Similarly, inserting (C.4.37) and (C.4.30) into (C.4.29) yields

$$\begin{aligned}\|\mathbf{e_n}(t)\|^2_{\mathbf{K}_\Gamma(\mathbf{x}^*(t))} \le c\int_0^t \Big(\|\mathbf{e_H}(s)\|^2_{\mathbf{K}_\Gamma(\mathbf{x}^*(s))} + \|\mathbf{e_n}(s)\|^2_{\mathbf{K}_\Gamma(\mathbf{x}^*(s))} + \|\mathbf{e_Q}(s)\|^2_{\mathbf{M}_\Gamma(\mathbf{x}^*(s))}\Big)\mathrm{d}s \\ + c\int_0^t \Big(\|\mathbf{d_n}(s)\|^2_{\mathbf{M}_\Gamma(\mathbf{x}^*(s))} + \|\mathbf{d_u}(s)\|^2_{\mathbf{M}_{\bar\Omega}(\mathbf{x}^*(s))} \qquad \text{(C.4.40)} \\ + \|\mathbf{d}_{\mathbf{v}_\Gamma}(s)\|^2_{\mathbf{K}_\Gamma(\mathbf{x}^*(s))} + \|\mathbf{d_v}(s)\|^2_{\star,\mathbf{x}^*(s)}\Big)\mathrm{d}s.\end{aligned}$$

Summing up (C.4.39) and (C.4.40) and using the Gronwall inequality thus yields

$$\begin{aligned}
&\|\mathbf{e_H}(t)\|^2_{\mathbf{K}_\Gamma(\mathbf{x}^*(t))} + \|\mathbf{e_n}(t)\|^2_{\mathbf{K}_\Gamma(\mathbf{x}^*(t))} \\
&\leq c\Big(\|\mathbf{e_H}(0)\|^2_{\mathbf{K}_\Gamma(\mathbf{x}^*(0))} + \|\mathbf{e_n}(0)\|^2_{\mathbf{K}_\Gamma(\mathbf{x}^*(0))}\Big) \\
&+ c\int_0^t \Big(\|\mathbf{d_H}(s)\|^2_{\mathbf{M}_\Gamma(\mathbf{x}^*(s))} + \|\mathbf{d_n}(s)\|^2_{\mathbf{M}_\Gamma(\mathbf{x}^*(s))} + \|\mathbf{d_u}(s)\|^2_{\mathbf{M}_{\bar\Omega}(\mathbf{x}^*(s))} \\
&\qquad + \|\dot{\mathbf{d}}_\mathbf{u}(s)\|^2_{\mathbf{M}_{\bar\Omega}(\mathbf{x}^*(s))} + \|\mathbf{d}_{\mathbf{v}_\Gamma}(s)\|^2_{\mathbf{K}_\Gamma(\mathbf{x}^*(s))} + \|\mathbf{d_v}(s)\|^2_{\star,\mathbf{x}^*(s)}\Big)\mathrm{d}s.
\end{aligned} \tag{C.4.41}$$

Inserting this bound first into (C.4.38), then both into (C.4.37) and finally that bound into (C.4.30) and (C.4.35) yields the stated stability bound (C.4.23) on the interval $[0, t^*]$.

It remains to show that $t^* = T$ if h is sufficiently small. We use the assumed defect bounds to obtain error bounds of order κ:

$$\|\mathbf{e_x}(t)\|_{\mathbf{L}(\mathbf{x}^*(t))} + \|\mathbf{e_v}(t)\|_{\mathbf{L}(\mathbf{x}^*(t))} + \|\mathbf{e_u}(t)\|_{\mathbf{L}(\mathbf{x}^*(t))} + \ \|\mathbf{e_H}(t)\|_{\mathbf{K}_\Gamma(\mathbf{x}^*(t))} + \|\mathbf{e_n}(t)\|_{\mathbf{K}_\Gamma(\mathbf{x}^*(t))} \leq Ch^\kappa.$$

By the inverse inequality [Brenner and Scott, 2008, Theorem 4.5.11], we then have for $t \in [0, t^*]$

$$\begin{aligned}
&\|e_x(\cdot,t)\|_{W^{1,\infty}(\Omega_h[\mathbf{x}^*(t)])} + \|e_v(\cdot,t)\|_{W^{1,\infty}(\Omega_h[\mathbf{x}^*(t)])} + \|e_u(\cdot,t)\|_{W^{1,\infty}(\Omega_h[\mathbf{x}^*(t)])} \\
&\leq ch^{-3/2}\big(\|\mathbf{e_x}(t)\|_{\mathbf{L}(\mathbf{x}^*(t))} + \|\mathbf{e_v}(t)\|_{\mathbf{L}(\mathbf{x}^*(t))} + \|\mathbf{e_u}(t)\|_{\mathbf{L}(\mathbf{x}^*(t))}\big) \leq cCh^{\kappa-3/2} \leq \tfrac{1}{2}h^{(\kappa-3/2)/2}
\end{aligned}$$

and

$$\begin{aligned}
&\|e_H(\cdot,t)\|_{W^{1,\infty}(\Gamma_h[\mathbf{x}^*(t)])} + \|e_\mathrm{n}(\cdot,t)\|_{W^{1,\infty}(\Gamma_h[\mathbf{x}^*(t)])} \\
&\leq ch^{-1}\big(\|\mathbf{e_H}(t)\|_{\mathbf{K}_\Gamma(\mathbf{x}^*(t))} + \|\mathbf{e_n}(t)\|_{\mathbf{K}_\Gamma(\mathbf{x}^*(t))}\big) \leq cCh^{\kappa-1} \leq \tfrac{1}{2}h^{(\kappa-1)/2}
\end{aligned}$$

for sufficiently small h. Hence we can extend the bounds (C.4.24) beyond t^*, which contradicts the maximality of t^* unless $t^* = T$. Therefore, we have the stability bound (C.4.23) on the whole interval $[0, T]$. □

C.4.5. Why not for the original Eyles–King–Styles model?

We cannot prove stability of the numerical method in the case $\mu = 0$, which corresponds to the model originally proposed in [Eyles et al., 2019]. The difficulty is caused by the term $\big(\mathbf{L}(\mathbf{x}) - \mathbf{L}(\mathbf{x}^*)\big)\mathbf{u}^*$ in the error equation (C.4.13) for $\mathbf{e_u}$, which in particular contains $\big(\mathbf{A}_{\bar\Omega}(\mathbf{x}) - \mathbf{A}_{\bar\Omega}(\mathbf{x}^*)\big)\mathbf{u}^*$. We see no way to bound the $L^2(\Omega_h[\mathbf{x}^*])$ norm (or the $H^{-1/2}$ norm) of the finite element function with this nodal vector in terms of the $H^1(\Omega_h[\mathbf{x}^*], \Gamma_h[\mathbf{x}^*])$ norm of the position error e_x. If such a bound had been available, then a result similar to Proposition C.8.3 (with an additional $H^{-1/2}(\Omega)$ forcing term in the bulk) would have allowed us to control the $H^1(\Gamma_h[\mathbf{x}^*])$ norm of the error function e_u, as is crucially required in the above proof. As Subsection C.4.4.2 shows, this obstacle does not appear with the generalized Robin boundary condition, for which the $H^1(\Gamma_h[\mathbf{x}^*])$ norm of the error function e_u can be controlled directly by energy estimates.

C.5. Consistency

In this section we prove that the initial values and the defects appearing in the stability bound of Proposition C.4.3 are indeed bounded as $O(h^k)$ in the appropriate norms that appear in the stability result. The defect estimates follow the ideas of [Dziuk and Elliott, 2013a, Kovács et al., 2017, Kovács et al., 2019, 2020].

C.5.1. Finite element projections of the exact solution

C.5.1.1. Interpolations and their errors

The Lagrange interpolation operator on the boundary is denoted by $I_h^\Gamma = (\widetilde{I}_h^\Gamma)^\ell$, and similarly the Lagrange interpolation operator in the bulk is denoted by $I_h^\Omega = (\widetilde{I}_h^\Omega)^\ell$. For vector valued functions both interpolations are defined componentwise.

The vectors $\mathbf{x}^*$ collect the nodal values of the interpolation of the exact solution X, i.e. of $X_h^*(\cdot,t) = \widetilde{I}_h^\Omega X(\cdot,t) \in \mathcal{V}_h[\mathbf{x}_*^0]^3$, with its lift $I_h X = (\widetilde{I}_h^\Omega X)^\ell$ being a function on the exact domain and its boundary.

We recall that the interpolation operators satisfy the error bounds, cf. [Elliott and Ranner, 2013, Demlow, 2009, Elliott and Ranner, 2021], for any $w \in H^{k+1}(\Omega)$ and any $z \in H^{k+1}(\Gamma)$, for $1 \le j \le k$ and $h \le h_0$,

$$\begin{aligned} \|w - I_h^\Omega w\|_{L^2(\Omega)} + h\|w - I_h^\Omega w\|_{H^1(\Omega)} &\le c h^{j+1} \|w\|_{H^{j+1}(\Omega)}, \\ \|z - I_h^\Gamma z\|_{L^2(\Gamma)} + h\|z - I_h^\Gamma z\|_{H^1(\Gamma)} &\le c h^{j+1} \|z\|_{H^{j+1}(\Gamma)}. \end{aligned} \tag{C.5.1}$$

C.5.1.2. Denoting bilinear forms

We briefly introduce a short yet general notation for bilinear forms on continuous and discrete domains. Let $\star$ denote any of the domains Ω, Γ or their interpolations Ω_h^*, Γ_h^*, then we define the following bilinear forms, for any w, φ in the appropriate space,

$$m_\star(w,\varphi) = \int_\star w\varphi \qquad \text{and} \qquad a_\star(w,\varphi) = \int_\star \nabla_\star w \cdot \nabla_\star \varphi,$$

i.e. the (semi-)inner products on $L^2(\star)$ and $H^1(\star)$, respectively.

For brevity we further introduce the notation $\bar{a}_\star = a_\star + m_\star$ for the $H^1(\star)$-scalar product on a continuous or discrete domain $\star \in \{\Omega, \Gamma, \Omega_h^*, \Gamma_h^*\}$.

C.5.1.3. A generalized surface Ritz map

Recall that Ω_h^* is the interpolation of the exact domain $\Omega[X]$, whose boundary $\partial\Omega_h^*$ is the nodal interpolation of the boundary $\Gamma[X]$, i.e. we have the relations $\Omega_h^* := \Omega_h[\mathbf{x}^*]$ where $\mathbf{x}^*$ collects the nodes of $\widetilde{I}_h^\Omega X$, and $\Gamma_h^* := \Gamma_h[\mathbf{x}_\Gamma^*] = \partial\Omega_h^*$ (depending only on the nodes $\mathbf{x}_\Gamma^*$ of $\widetilde{I}_h^\Gamma X$).

We will now define a few different (generalized) Ritz maps, which will play a crucial role in the consistency analysis. Note that since the bulk and the surface are time dependent, all these Ritz maps are depending on time as well, hence, for instance, they do not commute with time derivatives.

We start by defining a Ritz map on the boundary, cf. [Kovács, 2018, Section 6], which will be used for the geometric variables n and H determining the nodal values of the vectors $\mathbf{n}^*$ and $\mathbf{H}^*$. For any $w \in H^1(\Gamma[X])$ we first determine $\widetilde{R}_h^\Gamma w \in \mathcal{S}_h[\mathbf{x}^*]$ such that, for all $\varphi_h \in \mathcal{S}_h[\mathbf{x}^*]$,

$$\bar{a}_{\Gamma_h^*}(\widetilde{R}_h^\Gamma w, \varphi_h) = \bar{a}_\Gamma(w, (\varphi_h)^\ell), \tag{C.5.2}$$

and then defining the Ritz map via the lift $R_h^\Gamma w = (\widetilde{R}_h^\Gamma w)^\ell$. For vector valued functions the Ritz map is defined componentwise.

The above Ritz map R_h^Γ satisfies the error estimates, see [Kovács, 2018, Theorem 6.3–6.4], for any $w \in H^{k+1}(\Gamma)$ and for $1 \le j \le k$ and $h \le h_0$,

$$\begin{aligned} \|w - R_h^\Gamma w\|_{L^2(\Gamma)} + h\|w - R_h^\Gamma w\|_{H^1(\Gamma)} &\le c h^{j+1} \|w\|_{H^{j+1}(\Gamma)}, \\ \|\partial^\bullet (w - R_h^\Gamma w)\|_{L^2(\Gamma)} + h\|\partial^\bullet (w - R_h^\Gamma w)\|_{H^1(\Gamma)} &\le c h^{j+1} \Big(\|w\|_{H^{j+1}(\Gamma)} + \|\partial^\bullet w\|_{H^{j+1}(\Gamma)} \Big). \end{aligned} \tag{C.5.3}$$

C.5.1.4. A generalized bulk Ritz map

With the use of the interpolated bulk $\Omega_h^* = \widetilde{I}_h^\Omega X$, its boundary $\Gamma_h^* = \widetilde{I}_h^\Gamma X$, and the above defined boundary interpolation operators and the surface Ritz map (C.5.2) we will define a new bulk Ritz map.

The new bulk Ritz map will be defined via a Poisson problem with inhomogeneous Dirichlet boundary conditions using the Ritz map $\widetilde{R}_h^\Gamma$ as boundary data. Using such a Ritz map, with the appropriate boundary data (i.e. the boundary Ritz map of the trace), allows us to decouple certain bulk and surface terms during the consistency analysis.

For any $w \in H^1(\Omega;\Gamma)$ we define the bulk Ritz map $\widetilde{R}_h^{\mathrm{Ritz}} w$ such that it solves the following inhomogeneous Dirichlet problem using the *surface Ritz map* $\widetilde{R}_h^\Gamma(\gamma w)$ as Dirichlet boundary values, for any $\varphi_h \in \mathcal{V}_h^0[\mathbf{x}^*]$,

$$\begin{aligned} \bar{a}_{\Omega_h^*}(\widetilde{R}_h^{\mathrm{Ritz}} w, \varphi_h) &= \bar{a}_\Omega(w, \varphi_h^\ell), \\ \gamma_h^* \widetilde{R}_h^{\mathrm{Ritz}} w &= \widetilde{R}_h^\Gamma(\gamma w). \end{aligned} \tag{C.5.4}$$

As before, we set $R_h^{\mathrm{Ritz}} w = (\widetilde{R}_h^{\mathrm{Ritz}} w)^\ell$.

The following error estimates hold for the bulk Ritz map (C.5.4).

Lemma C.5.1. *For the bulk Ritz map defined by* (C.5.4) *we have the following bulk–surface error estimates. Using finite elements of polynomial degree at most k, for any $w \in H^{k+1}(\Omega;\Gamma)$, and for $j \le k$ and $h \le h_0$, we have*

$$\begin{aligned} \|w - R_h^{\mathrm{Ritz}} w\|_{L^2(\Omega;\Gamma)} + h\|w - R_h^{\mathrm{Ritz}} w\|_{H^1(\Omega;\Gamma)} &\le c h^{j+1} \|w\|_{H^{j+1}(\Omega;\Gamma)} \\ \|\partial_\Omega^\bullet (w - R_h^\Gamma w)\|_{L^2(\Omega;\Gamma)} + h\|\partial_\Omega^\bullet (w - R_h^\Gamma w)\|_{H^1(\Omega;\Gamma)} &\le c h^{j+1} \Big(\|w\|_{H^{j+1}(\Omega;\Gamma)} + \|\partial^\bullet w\|_{H^{j+1}(\Omega;\Gamma)} \Big). \end{aligned} \tag{C.5.5}$$

Proof. The proof is a technical adaptation of [Elliott and Ranner, 2021, Lemma 3.8 and 3.10] (handling the Dirichlet boundary data by the harmonic extension operator and its properties) in the setting [Elliott and Ranner, 2021, Section 8] (in particular note Lemma 8.24 therein). □

C.5.1.5. Stability of finite element projections

The above finite element projection errors directly imply the stability bounds, for $\mathcal{I}_h = I_h^\Omega, I_h^\Gamma$ and $\mathcal{P}_h = R_h^\Gamma, R_h^{\mathrm{Ritz}}$, with $h \le h_0$,

$$\|\mathcal{I}_h v\|_{H^1} \le (1+ch)\|v\|_{H^2} \quad \text{and} \quad \|\mathcal{P}_h v\|_{H^1} \le c\|v\|_{H^1}, \tag{C.5.6}$$

where the norm $\|\cdot\|_{H^j}$ denotes the suitable H^j-norm in the correct domain corresponding to the projection.

C.5.2. The chosen finite element projections of the exact solution

We now define the suitable finite element projections:

$$\begin{aligned} x_h^* &= \widetilde{I}_h^\Omega X, \\ u_h^* &= \widetilde{R}_h^{\mathrm{Ritz}} u, \qquad && \text{therefore} \qquad && \gamma_h^* u_h^* = \widetilde{R}_h^\Gamma(\gamma u), \\ v_h^* = (v_{\Gamma,h}^*, v_{\Omega,h}^*) &= \widetilde{I}_h^\Omega v, && \text{therefore} && \gamma_h^* v_h^* = v_{\Gamma,h}^* = \widetilde{I}_h^\Gamma(\gamma v), \\ w_h^* = (\mathrm{n}_h^*, H_h^*) &= (\widetilde{R}_h^\Gamma \mathrm{n}, \widetilde{R}_h^\Gamma H). \end{aligned} \tag{C.5.7}$$

With these choices the error estimate for the initial data (C.4.21) directly follows.

C.5.3. Consistency estimates for the coupled bulk–surface system

We will estimate the consistency errors (C.4.20) of the coupled system using the general strategy given below, which follows the ideas of [Dziuk and Elliott, 2013a, Kovács et al., 2017, Kovács et al., 2019, 2020, Edelmann, 2022].

The L_h^2 (either $L^2(\Omega_h^*)$ or $L^2(\Gamma_h^*)$) norm of a defect d_h is given by

$$\|d_h\|_{L_h^2} = \sup_{0 \neq \varphi_h \in L_h^2} \frac{m_h(d_h, \varphi_h)}{\|\varphi_h\|_{L_h^2}}.$$

We then estimate the scalar product using the following approach (see the above references as well):

(a) We first subtract the weak formulation of the continuous sub-problems from the corresponding defect equation from Section C.4.2 (given there in a matrix–vector form). Therefore the defect is rewritten as the sum of pairs comparing discrete and continuous objects.

(b) Crucial pairs will vanish using the definitions of the Ritz maps (C.5.2) and (C.5.4).

(c) We estimate the remaining pairs separately, using the following strategy: We add and subtract a suitable term, and then use the geometric approximation errors for the bilinear forms, see [Dziuk and Elliott, 2013a], [Kovács, 2018, Lemma 5.6], [Elliott and Ranner, 2021, Lemma 10.3] and apply the stability bounds (C.5.6) and the error bounds for the finite element projections (C.5.5), (C.5.3).

In the defect estimates below we will clearly indicate these steps.

As in the stability analysis, without loss of generality, we will again set the parameters

$$\alpha = \beta = \mu = 1.$$

C.5.3.1. Consistency estimates for the Robin boundary value problem

(a) Recalling that $u_h^* = \widetilde{R}_h^{\mathrm{Ritz}} u$, and by subtracting the weak formulation (C.2.11) with $\varphi^u = (\varphi_h^u)^\ell$ from (the abstract formulation of) the semi-discrete Robin problem (C.4.12), we obtain the following representations of the defect d_u:

$$\begin{aligned} m_{\Omega_h}(d_u, \varphi_h^u) = \; & a_{\Omega_h}(u_h^*, \varphi_h^u) - a_\Omega(u, (\varphi_h^u)^\ell) \\ & + \Big(a_{\Gamma_h}(\gamma_h^* u_h^*, \varphi_h^u) - a_\Gamma(\gamma u, (\varphi_h^u)^\ell) \Big) \\ & + \Big(m_{\Gamma_h}(\gamma_h u_h^*, \varphi_h^u) - m_\Gamma(\gamma u, (\varphi_h^u)^\ell) \Big) \\ & - \Big(\mathfrak{f}_h^*(\varphi_h^u) - \mathfrak{f}((\varphi_h^u)^\ell) \Big) \end{aligned} \tag{C.5.8}$$

for which we recall the definition of the (bi)linear forms a_Ω, a_Γ, m_Γ, and $\mathfrak{f}$ as well as their semi-discrete counterparts a_{Ω_h}, a_{Γ_h}, m_{Γ_h}, and $\mathfrak{f}_h^*$ (note that the definition of semi-discrete linear form $\mathfrak{f}_h^*$ contains the approximations $Q_h^* = \widetilde{I}_h Q$ and $H_h^* = \widetilde{R}_h^\Gamma H$).

(b) We start by analysing the first two pairs in d_u.

For the first two pairs, using the definition of the continuous and discrete bilinear forms a_Ω and a_{Ω_h}, a_Γ and a_{Γ_h}, and the definition of $u_h^* = \widetilde{R}_h^{\mathrm{Ritz}} u$ (C.5.4) together with the definition for its trace $\gamma_h^* u_h^* = \gamma_h^* \widetilde{R}_h^{\mathrm{Ritz}} u = \widetilde{R}_h^\Gamma(\gamma u)$ via (C.5.2), we directly compute

$$\begin{aligned} & \Big(a_{\Omega_h}(u_h^*, \varphi_h^u) - a_\Omega(u, (\varphi_h^u)^\ell) \Big) + \Big(a_{\Gamma_h}(\gamma_h^* u_h^*, \varphi_h^u) - a_\Gamma(\gamma u, (\varphi_h^u)^\ell) \Big) \\ & = \Big(a_{\Omega_h}(u_h^*, \varphi_h^u) - \bar{a}_\Omega(u, (\varphi_h^u)^\ell) \Big) + \Big(\bar{a}_{\Gamma_h}(\gamma_h^* u_h^*, \varphi_h^u) - \bar{a}_\Gamma(\gamma u, (\varphi_h^u)^\ell) \Big) \\ & - \Big(m_{\Omega_h}(u_h^*, \varphi_h^u) - m_\Omega(u, (\varphi_h^u)^\ell) \Big) - \Big(m_{\Gamma_h}(\gamma_h^* u_h^*, \varphi_h^u) - m_\Gamma(\gamma u, (\varphi_h^u)^\ell) \Big). \end{aligned}$$

Crucially, only the last two pairs remain here as the first two pairs vanish, by the definition of the bulk Ritz map $u_h^* = \widetilde{R}_h^{\mathrm{Ritz}} u$, see (C.5.4), in combination with the definition (C.5.2) and observing the proper choice of boundary condition $\gamma_h^* u_h^* = \gamma_h^* \widetilde{R}_h^{\mathrm{Ritz}} u = \widetilde{R}_h^\Gamma(\gamma u)$ in (C.5.4).

(c) The remaining pairs in d_u are therefore

$$\begin{aligned} m_{\Omega_h}(d_u, \varphi_h^u) = \; & - \Big(m_{\Omega_h}(u_h^*, \varphi_h^u) - m_\Omega(u, (\varphi_h^u)^\ell) \Big) \\ & - \Big(m_{\Gamma_h}(\gamma_h^* u_h^*, \varphi_h^u) - m_\Gamma(\gamma u, (\varphi_h^u)^\ell) \Big) \\ & + \Big(m_{\Gamma_h}(\gamma_h u_h^*, \varphi_h^u) - m_\Gamma(\gamma u, (\varphi_h^u)^\ell) \Big) \\ & - \Big(\mathfrak{f}_h^*(\varphi_h^u) - \mathfrak{f}((\varphi_h^u)^\ell) \Big). \end{aligned}$$

The first three pairs with the L^2-bilinear forms are estimated, using the error estimates (C.5.3) and the stability bound (C.5.6) for the Ritz map, and the bulk geometric approximation errors [Elliott and Ranner, 2021, Lemma 8.24], as

$$\begin{aligned} m_{\Omega_h}(u_h^*, \varphi_h^u) - m_\Omega(u, (\varphi_h^u)^\ell) &= m_{\Omega_h}(\widetilde{R}_h^{\mathrm{Ritz}} u, \varphi_h^u) - m_\Omega(R_h^{\mathrm{Ritz}} u, (\varphi_h^u)^\ell) + m_\Omega(R_h^{\mathrm{Ritz}} u - u, (\varphi_h^u)^\ell) \\ &\leq c h^{k+1} \|u\|_{H^{k+1}(\Omega;\Gamma)} \|(\varphi_h^u)^\ell\|_{L^2(\Omega)}. \end{aligned}$$

The two similar terms are estimated analogously (now using [Kovács, 2018, Lemma 5.6]), as $O(h^{k+1})$.

For the last pair, we will recall that the inhomogeneity Q_h^* is the interpolation $\widetilde{I}_h Q$ and H_h^* is the surface Ritz map $\widetilde{R}_h^\Gamma H$. We then estimate, using the error estimates (C.5.1), (C.5.3), the stability bounds (C.5.6), and the geometric approximation errors [Kovács, 2018, Lemma 5.6] and [Elliott and Ranner, 2021, Lemma 8.24], as

$$\begin{aligned} \mathfrak{f}_h^*(\varphi_h^u) - \mathfrak{f}((\varphi_h^u)^\ell) &= m_\Omega(1, (\varphi_h^u)^\ell) - m_{\Omega_h}(1, \varphi_h^u) \\ &\quad + m_{\Gamma_h}(Q_h^*, \gamma_h \varphi_h^u) - m_\Gamma(Q, \gamma(\varphi_h^u)^\ell) \\ &\quad + \Big(m_{\Gamma_h}(H_h^*, \gamma_h \varphi_h^u) - m_\Gamma(H, \gamma(\varphi_h^u)^\ell) \Big) \\ &\leq c h^{k+1} \Big(\|Q\|_{H^{k+1}(\Gamma)} + \|H\|_{H^{k+1}(\Gamma)} \Big) \|(\varphi_h^u)^\ell\|_{H^1(\Omega)}. \end{aligned}$$

Altogether we obtain the following defect bounds in the discrete dual norm:

$$\|d_u\|_{L^2(\Omega_h^*)} = O(h^{k+1}).$$

By differentiating (C.5.8) in time, and using similar arguments as above – analogously to [Kovács et al., 2021, Section 6] – yields the consistency bound

$$\|\dot{d}_u\|_{L^2(\Omega_h^*)} = O(h^{k+1}).$$

C.5.3.2. Consistency estimates for the forced mean curvature flow

The defects d_{n} and d_H in the forced mean curvature flow are estimated using the steps (a), (b), and (c), exactly as in [Kovács et al., 2019, 2020], heavily relying on the the *proper choice of boundary conditions* in the definition of R_h^{Ritz}, i.e.

$$\gamma_h^* u_h^* = \gamma_h^* \widetilde{R}_h^{\mathrm{Ritz}} u = \widetilde{R}_h^\Gamma(\gamma u).$$

The defect in the velocity d_v is directly estimated, using [Kovács et al., 2021, Lemma 5.3] and the interpolation error estimate on Γ (C.5.1) for $v_\Gamma^* = \widetilde{I}_h^\Gamma(\gamma v)$, as

$$\begin{aligned} \|d_{v_\Gamma}\|_{H^1(\Gamma_h^*)} &\leq c \big\| I_h^\Gamma \gamma v - \gamma v \big\|_{H^1(\Gamma)} + \big\| \widetilde{I}_h^\Gamma (V_h^* \, \mathrm{n}_h^*) - V^{-\ell} \, \mathrm{n}^{-\ell} \big\|_{H^1(\Gamma_h^*)} \\ &\leq c h^k \|\gamma v\|_{H^{k+1}(\Gamma)} + \|V_h^* \, \mathrm{n}_h^* - \widetilde{I}_h^\Gamma V \, \widetilde{I}_h^\Gamma \mathrm{n}\|_{H^1(\Gamma_h^*)} + 2 c h^k \big(\|V\|_{H^{k+1}(\Gamma)} + \|\mathrm{n}\|_{H^{k+1}(\Gamma)} \big). \end{aligned}$$

The middle term here is estimated further as $O(h^k)$, recalling that $V_h^* = -\widetilde{R}_h^\Gamma H + \gamma_h \widetilde{R}_h^{\mathrm{Ritz}} u$ and using multiple triangle inequalities, together with the approximation properties of the Ritz maps and the surface interpolation.

Altogether we proved the following defect bounds:

$$\|d_{\mathrm{n}}\|_{L^2(\Gamma_h^*)} = O(h^{k+1}), \quad \|d_H\|_{L^2(\Gamma_h^*)} = O(h^{k+1}), \quad \text{and} \quad \|d_{v_\Gamma}\|_{H^1(\Gamma_h^*)} = O(h^k).$$

C.5.3.3. Consistency estimates for the harmonic velocity extension

Recalling that we have set $v_h^* = \widetilde{I}_h^\Omega v$ hence $\gamma_h^* v_h^* = v_{\Gamma,h}^* = \widetilde{I}_h^\Gamma(\gamma v)$, which has nodal values $\mathbf{v}^* = (\mathbf{v}_\Gamma^*, \mathbf{v}_\Omega^*)^T \in \mathbb{R}^{3N}$ with $\mathbf{v}_\Gamma^*$ given as the nodal values of the surface interpolation.

In order to derive an expression for the defect in the velocity in Ω, we translate (C.4.18) to the semi-discrete functional analytic setting, and obtain that d_v satisfies the equation, for the given $v_h^* = \widetilde{I}_h^\Omega v$ and for any $\varphi_h^v \in \mathcal{V}_{h,0}[\mathbf{x}]^3$,

$$a_{\Omega_h^*}(\widetilde{I}_h^\Omega v, \varphi_h^v) = m_{\Omega_h^*}(d_v, \varphi_h^v).$$

Subtracting the equivalent weak formulation of the harmonic extension (C.2.13) from the above equation, setting $\varphi^v = (\varphi_h^v)^\ell \in H_0^1(\Omega)^3$, yields

$$m_{\Omega_h^*}(d_v, \varphi_h^v) = a_{\Omega_h^*}(\widetilde{I}_h^\Omega v, \varphi_h^v) - a_\Omega(v, (\varphi_h^v)^\ell).$$

By similar arguments as above we obtain

$$m_{\Omega_h^*}(d_v, \varphi_h^v) = a_{\Omega_h^*}(\widetilde{I}_h^\Omega v, \varphi_h^v) - a_\Omega(v, (\varphi_h^v)^\ell) \leq ch^k \|v\|_{H^{k+1}(\Omega)} \|\varphi_h^v\|_{H^1(\Omega)}.$$

using the bulk interpolation error estimate (C.5.1).

Altogether we proved the defect bound

$$\|d_v\|_{H_h^{-1}(\Omega_h^*)} = O(h^k).$$

C.6. Proof of Theorem C.3.1

The errors for all variables X, u, v, n, and H are decomposed using either interpolations or the appropriate Ritz maps, see (C.5.7), and using the definition of the composed lift ^{L} from Section C.3.1.1. As an example, for the flow map X we have

$$X_h^L - X = (\widehat{X}_h)^\ell - X = \big(\widehat{X}_h - X_h^*\big)^\ell + \big((X_h^*)^\ell - X\big),$$

the other functions are treated similarly.

The projections errors (cf. second term) are bounded in the (appropriate) H^1 norm by Ch^k, using interpolation or Ritz map error estimates.

For the errors between the numerical solution and the projections (cf. first term), we use the stability estimate of Proposition C.4.3 together with the defect bounds shown in Section C.5 to obtain

$$\|\mathbf{e_u}\|_{\mathbf{L}(\mathbf{x}^*)} + \|\mathbf{e_x}\|_{\mathbf{L}(\mathbf{x}^*)} + \|\mathbf{e_v}\|_{\mathbf{L}(\mathbf{x}^*)} + \|\mathbf{e_H}\|_{\mathbf{K}_\Gamma(\mathbf{x}^*)} + \|\mathbf{e_n}\|_{\mathbf{K}_\Gamma(\mathbf{x}^*)} \leq Ch^k.$$

By the equivalence of norms shown in [Dziuk, 1988, Lemma 3] and by the definition of discrete norms, we have

$$\|\big(\widehat{X}_h - X_h^*\big)^\ell\|_{H^1(\Omega[X^0],\Gamma[X^0])} \leq c\|\widehat{X}_h - X_h^*\|_{H^1(\Omega_h[\mathbf{x}_*^0],\Gamma_h[\mathbf{x}_*^0])} = c\|\mathbf{e_x}\|_{\mathbf{L}(\mathbf{x}^*)},$$

and similarly for the other errors. This proves the result. □

C.7. Numerical experiments

We performed numerical simulations and experiments for the coupled bulk–surface system (C.2.7)–(C.2.10) using its matrix–vector formulation (C.3.29) and linearly implicit BDF time discretizations, see the next Section C.7.1:

- We performed convergence experiments involving an example with radially symmetric exact solutions, and report on the convergence rates to illustrate the theoretical results of Theorem C.3.1. The same test example was used in [Eyles et al., 2019, Section 6.4.1]. Note that the parameter α here equals to $1/\alpha$ in [Eyles et al., 2019].

- We performed some numerical experiments from [Eyles et al., 2019, Section 6.4.3]: choosing the same parameters α and β, as well as using the three-dimensional analogues of the initial domain.

- We performed a numerical experiment which compares the numerical solution for various regularization parameters ($\mu = 0$, 0.01, 0.1, and 1).

The numerical experiments use quadratic evolving bulk–surface finite elements, for computing the finite element expressions quadratures of sufficiently high order were employed, such that their errors are negligible compared to discretisation errors. The parametrization of the quadratic elements was inspired by [Bartels et al., 2006]. The initial meshes were all generated using DistMesh [Persson and Strang, 2004], without taking advantage of any symmetry of the surface.

C.7.1. Linearly implicit full discretization

For the time discretization, we use a q-step linearly implicit backward difference formula with $q \leq 6$. For a step size $\tau > 0$, $t_n = n\tau \leq T$, we introduce for $n \geq q$ the discrete time derivative

$$\dot{\mathbf{u}}^n = \frac{1}{\tau} \sum_{j=0}^{q} \delta_j \mathbf{u}^{n-j}$$

and the extrapolated value

$$\widetilde{\mathbf{u}}^n = \sum_{j=0}^{q-1} \gamma_j \mathbf{u}^{n-1-j} \,.$$

The coefficients are given by the relations $\delta(\zeta) = \sum_{j=0}^{q} \delta_j \zeta^j = \sum_{\ell=1}^{q} \frac{1}{\ell}(1-\zeta)^\ell$ and $\gamma(\zeta) = \sum_{j=0}^{q-1} \gamma_j \zeta^j = (1-(1-\zeta)^q)/\zeta$, respectively.

We compute approximations $\mathbf{u}^n$ to $u(t_n)$, $\mathbf{p}^n$ to $p(t_n)$ etc. by the linearly implicit BDF

discretization

$$
\begin{aligned}
\big(\mathbf{A}_{\bar\Omega}(\widetilde{\mathbf{x}}^n) + \boldsymbol{\gamma}^{\mathrm{T}}\big(\mu\mathbf{A}_\Gamma(\widetilde{\mathbf{x}}^n) + \alpha\mathbf{M}_\Gamma(\widetilde{\mathbf{x}}^n)\big)\boldsymbol{\gamma}\big)\,\mathbf{u}^n &= \mathbf{f}_{\mathbf{u}}(\widetilde{\mathbf{x}}^n, \widetilde{\mathbf{H}}^n)\\
\mathbf{M}_\Gamma^{[3]}(\widetilde{\mathbf{x}}^n)\dot{\mathbf{n}}^n + \beta\mathbf{A}_\Gamma^{[3]}(\widetilde{\mathbf{x}}^n)\mathbf{n}^n &= \mathbf{f}_{\mathrm{n}}(\widetilde{\mathbf{x}}^n, \widetilde{\mathrm{n}}^n, \widetilde{\mathbf{H}}^n) - \alpha\mathbf{D}_\Gamma(\widetilde{\mathbf{x}}^n)\mathbf{u}^n,\\
\mathbf{M}_\Gamma(\widetilde{\mathbf{x}}^n)\dot{\mathbf{H}}^n + \beta\mathbf{A}_\Gamma(\widetilde{\mathbf{x}}^n)\mathbf{H}^n &= \mathbf{f}_V(\widetilde{\mathbf{x}}^n, \widetilde{\mathrm{n}}^n, \widetilde{\mathbf{H}}^n, \widetilde{\mathbf{u}}^n) + \alpha\mathbf{A}_\Gamma(\widetilde{\mathbf{x}}^n)\mathbf{u}^n.\\
\mathbf{V}^n &= -\beta\mathbf{H}^n + \alpha\mathbf{u}^n\\
\mathbf{v}_\Gamma^n &= \mathbf{V}^n \bullet \mathbf{n}^n\\
-\mathbf{A}_{\Omega\Omega}(\widetilde{\mathbf{x}}^n)\mathbf{v}_\Omega^n &= \mathbf{A}_{\Omega\Gamma}(\widetilde{\mathbf{x}}^n)\mathbf{v}_\Gamma^n\\
\dot{\mathbf{x}}^n &= \mathbf{v}^n\,.
\end{aligned}
\tag{C.7.1}
$$

C.7.2. Convergence experiments using radially-symmetric solutions

C.7.2.1. Constructing the radially-symmetric solutions in $\mathbb{R}^{m+1}$

We consider radially-symmetric solutions to the coupled bulk–surface problem (C.2.7)–(C.2.10) with $\mu = 0$ and a time-independent constant inhomogeneity Q. For curves in two dimensions the identical exact solutions were constructed and used in [Eyles et al., 2019, Section 6.4.1]. (Note that the parameter α here equals to $1/\alpha$ in [Eyles et al., 2019]). For later reference we performed these computations in m-dimensional surfaces in $\mathbb{R}^{m+1}$, and will report on experiments in $\mathbb{R}^3$.

We recall that the surface normal and mean curvature on a sphere $\Gamma(t)$ of radius $R(t)$ are given by

$$\mathrm{n} = \frac{x}{R(t)} \quad \text{and} \quad H = \frac{m}{R(t)}.$$

(a) Let us first construct the radially-symmetric solution of the Robin problem (C.2.7) with $\mu = 0$ (i.e. equation (C.2.3)).

Recall that in $\mathbb{R}^{m+1}$ the Laplace–Beltrami operator for a radially-symmetric function u is given by

$$\Delta u = \frac{1}{r^m}\partial_r\Big(r^m\partial_r u\Big).$$

Therefore,

$$u = u(r) = \frac{r^2}{2(m+1)} + c_0$$

satisfies the bulk equation (C.2.3a), i.e. $-\Delta u = -1$.

Now we need to determine the constant c_0 such that the Robin boundary condition (C.2.3b) holds. Recall that in $\mathbb{R}^{m+1}$ the gradient of a radially-symmetric function u is given by

$$\nabla u = \partial_r u\,\hat{\boldsymbol{r}},$$

where $\hat{\boldsymbol{r}}$ is the unit vector corresponding to the radial coordinate. We note here that on the sphere $\Gamma(t)$ we have $\hat{\boldsymbol{r}} = \mathrm{n}$.

We now plug in the solution into the boundary condition (C.2.3b) of the Robin problem, and compute on $\Gamma(t)$

$$\begin{aligned} Q + \beta H &= \Big(\partial_r\Big(\frac{r^2}{2(m+1)} + c_0\Big)\hat{\boldsymbol{r}}\Big)\Big|_{R(t)} \cdot \mathrm{n} + \alpha\Big(\frac{r^2}{2(m+1)} + c_0\Big)\Big|_{R(t)} \\ &= \frac{R(t)}{m+1} + \alpha\Big(\frac{R(t)^2}{2(m+1)} + c_0\Big). \end{aligned}$$

Upon plugging in $H = m/R(t)$ and rearranging, we obtain

$$c_0 = \frac{1}{\alpha}\left(Q + \beta\frac{m}{R(t)} - \frac{R(t)}{m+1}\right) - \frac{R(t)^2}{2(m+1)},$$

and hence the radially-symmetric solution of the Robin problem is given by

$$u(x,t) = u(r,t) = \frac{r^2}{2(m+1)} + \frac{1}{\alpha}\left(Q + \beta\frac{m}{R(t)} - \frac{R(t)}{m+1}\right) - \frac{R(t)^2}{2(m+1)}. \tag{C.7.2}$$

(b) We will now formulate the ODE governing the surface evolution and determine its solution. We start by recalling that $X(x^0,t) = R(t)x_0$ (with x^0 on the unit sphere) which satisfies $\dot{X} = v \circ X$, where

$$v = V\mathrm{n} = \big(-\beta H + \alpha u\big)\,\mathrm{n},$$

where the normal velocity, by the above computations, is given by

$$V = -\beta\frac{m}{R(t)} + \alpha u(R(t),t) = Q - \frac{R(t)}{m+1}.$$

The ODE for the radially-symmetric surface evolution therefore reduces to

$$\begin{aligned} \dot{R}(t) &= Q - \frac{R(t)}{m+1}, \\ R(0) &= R^0, \end{aligned}$$

which has the solution, for all t,

$$R(t) = (R^0 - (m+1)Q)e^{-t/(m+1)} + (m+1)Q. \tag{C.7.3}$$

C.7.2.2. Convergence experiments

For the convergence experiment we chose the following initial values and parameters: The initial surface Γ^0 is a two-dimensional sphere of radius $R^0 = 1.5$, the time-independent constant forcing is set to $Q = 1.5$, the initial concentration $u^0(x,0)$ is given by (C.7.2) for all $x \in \Gamma^0$. That is we are in a situation where a solution exists on $[0,\infty)$ and the exact solutions for $\Gamma[X]$ and $u(\cdot,t)$ are given in (C.7.3) and (C.7.2), respectively. The above choices are the exact same as the one chosen for [Eyles et al., 2019, Figure 3] (except the computations here are performed in the two-dimensional case), similarly to [Eyles et al., 2019] the parameters α and β are varied. The regularization parameter is set to $\mu = 0$.

We started algorithm (C.7.1) from the nodal interpolations of the exact initial values $\Gamma[X(\cdot,t_i)]$, $\mathrm{n}(\cdot,t_i)$, $H(\cdot,t_i)$, and $u(\cdot,t_i)$, for $i=0,\dots,q-1$. In order to illustrate the convergence results of Theorem C.3.1, we have computed the errors between the numerical solution (C.7.1) and (the nodal interpolation of the) exact solutions of the coupled bulk–surface problem (C.2.7)–(C.2.10) for the above radially-symmetric solution in dimension $m=2$.

In Figure C.1 we report on the errors between the numerical solution and the interpolation of the exact solution until the final time $T=1$, for a sequence of meshes (see plots) and for a sequence of time steps $\tau_{k+1}=\tau_k/2$. The logarithmic plots report on the $L^\infty(H^1)$ norm of the errors against the mesh width h in Figure C.1 top, and against the time step size τ in Figure C.1 bottom. The lines marked with different symbols and different colours correspond to different time step sizes and to different mesh refinements on the top and bottom, respectively.

In both plots in Figure C.1 we can observe two regions: On the top, a region where the spatial discretization error dominates, matching the $O(h^2)$ order of convergence of Theorem C.3.1 (see the reference lines), and a region, with small mesh size, where the temporal discretization error dominates (the error curves flatten out). For the graphs in the bottom, the same description applies, but with reversed roles. Convergence of fully discrete methods is not proved here, but $O(\tau^2)$ is expected for the 2-step BDF method, cf. [Kovács et al., 2019].

The convergence in time and in space as shown by Figure C.1 are in agreement with the theoretical convergence results (note the reference lines). We obtained similar convergence plots for varying α and β parameters.

C.7.3. Experiments on α and β dependence

As in [Eyles et al., 2019, Section 6.4.3] as an initial domain $\Omega\subset\mathbb{R}^3$ we choose the ellipsoid with radii 0.5, 0.5, and 1, i.e.

$$\Omega=\Big\{x\in\mathbb{R}^3 \mid \sqrt{\tfrac{x_1^2}{0.5^2}+\tfrac{x_2^2}{0.5^2}+x_3^2}\le 1\Big\},\qquad\text{and}\qquad \Gamma=\partial\Omega.$$

The initial domain and surface is approximated with quadratic bulk–surface finite elements with 7162 and 1430 degrees-of-freedom in the bulk and on the boundary, respectively. The time step size is set to $\tau=10^{-3}$. The model parameters are set to $Q=1.5$ and $\mu=0$, while α and β are varied for different experiments.

The initial data for the geometry (n_h^0 and H_h^0) were obtained by interpolation, while for the Robin problem u_h^0 solves the discretized Robin problem (C.3.13).

In Figure C.2 and C.3 we report on the numerical solution at different times with $\alpha=10$ and $\beta=1$ and $\alpha=1$ and $\beta=0.1$, respectively. For the sake of a direct comparison we are using the identical values as [Eyles et al., 2019, Figure 5] and [Eyles et al., 2019, Figure 6], respectively. The two experiments are performed in different dimensions. (Note that the parameter α here equals to $1/\alpha$ in [Eyles et al., 2019]).

C.7.4. Experiments on the effect of the regularization

We performed a numerical experiment reporting on the effect of the regularization (cf. Section C.2.2.4).

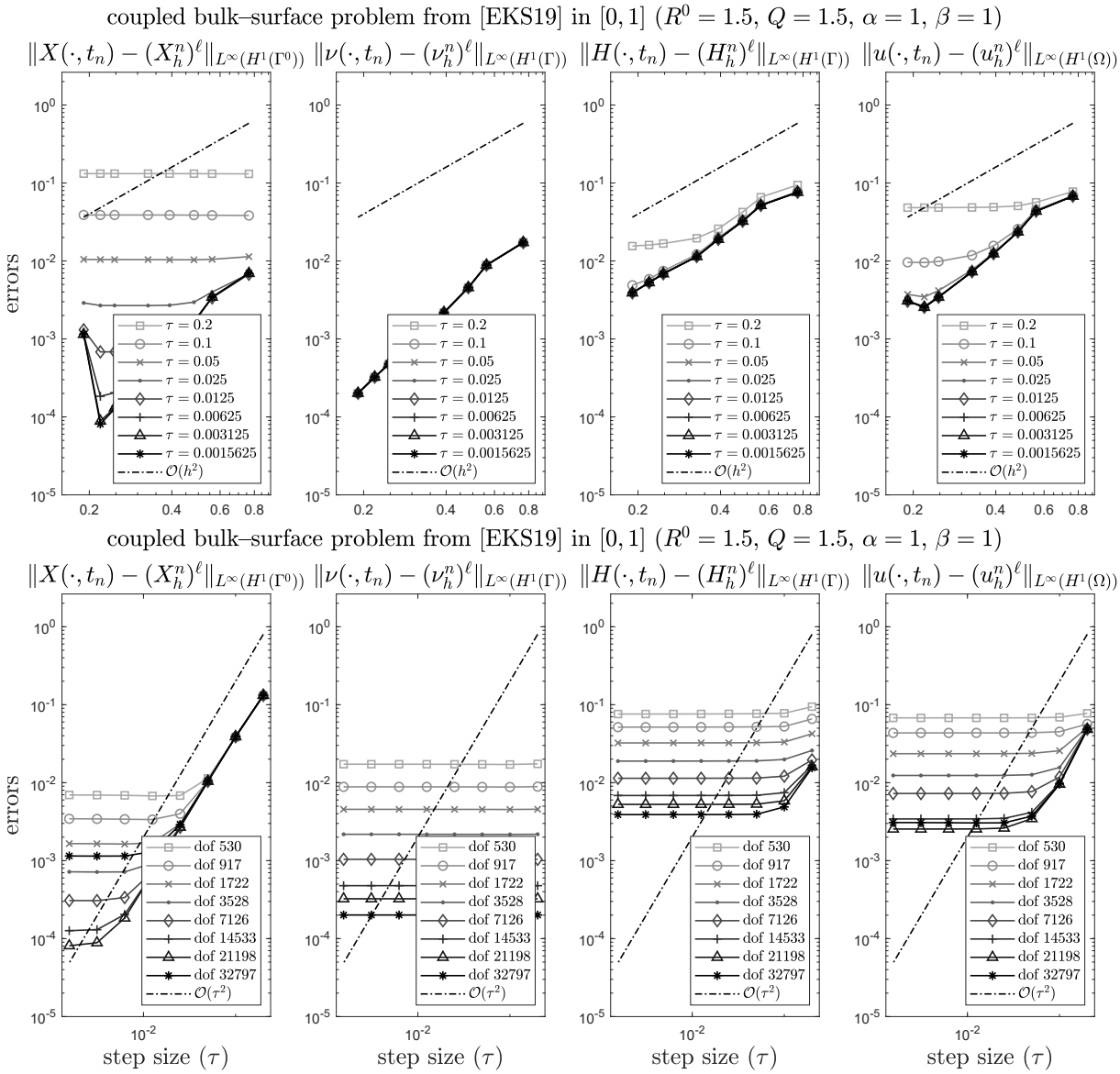

Figure C.1.: Spatial and temporal convergence of the BDF2 / quadratic ESFEM discretization of the coupled bulk–surface problem with $\alpha = 1$ and $\beta = 1$.

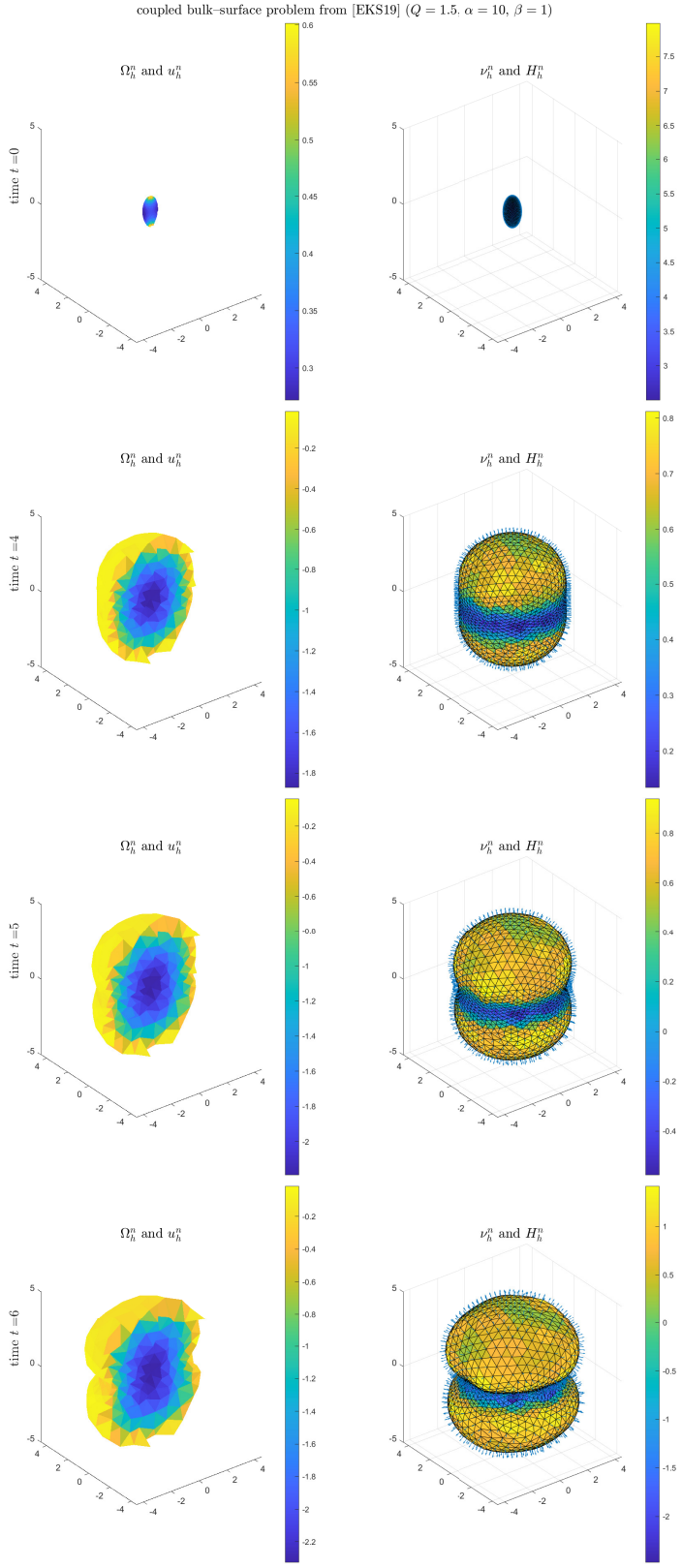

Figure C.2.: Numerical solution of the coupled bulk–surface problem with $\alpha = 10$ and $\beta = 1$.

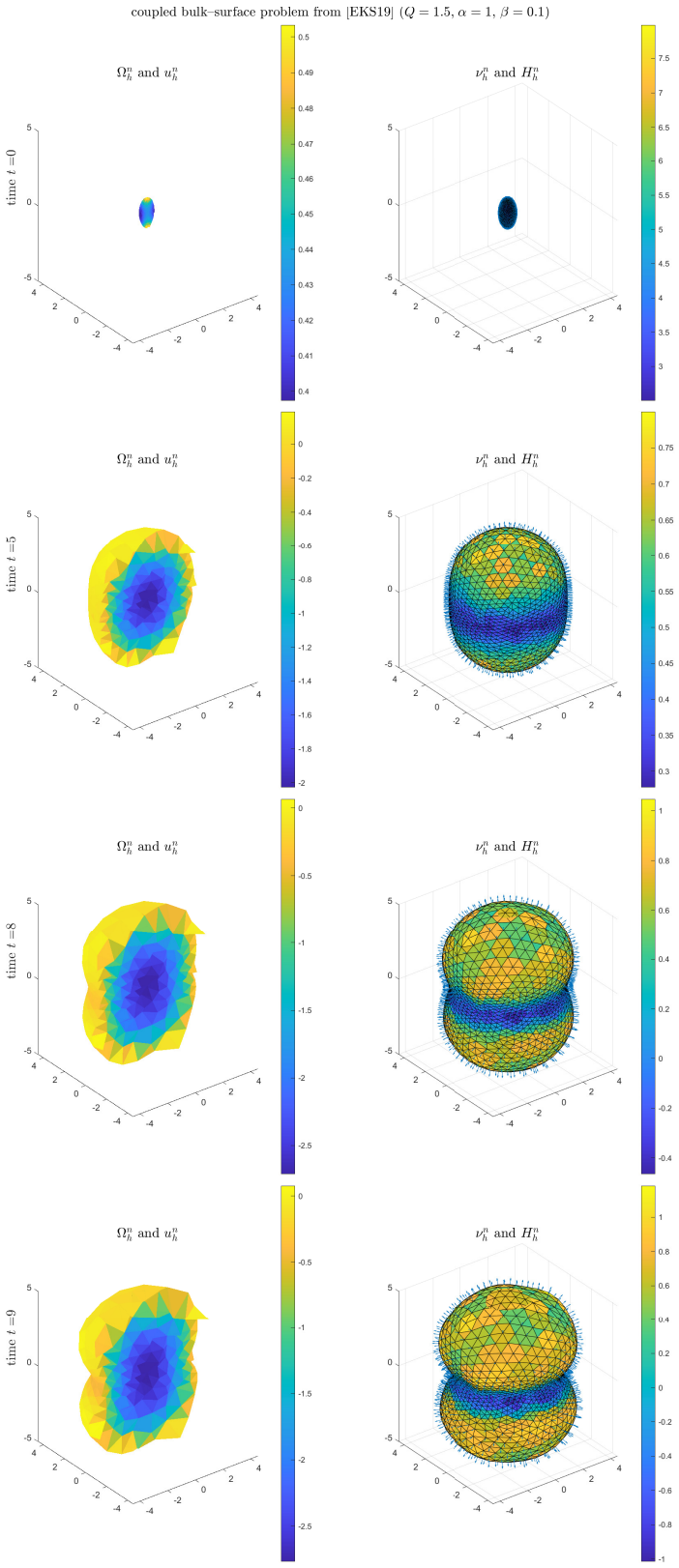

Figure C.3.: Numerical solution of the coupled bulk–surface problem with $\alpha = 1$ and $\beta = 0.1$.

The three columns of Figure C.4 show the numerical solution with varying regularization parameter $\mu = 0$, 0.01, 0.1, 1 (from left to right) with a fixed source $Q = 1.5$, and fixed model parameters $\alpha = 1$ and $\beta = 1$. The initial data were generated exactly as before. The bulk and surface mesh has 7162 and 1430 degrees-of-freedom, respectively, while the time step size is set to $\tau = 10^{-3}$. As observable in Figure C.4, the regularization (even with $\mu = 1$) has minimal effects both on the bulk–surface mesh evolution and the surface variable u_h^n.

C.8. Appendix: Stability bounds of finite element approximations to the Laplace equation with inhomogeneous boundary conditions

We give regularity estimates of finite element approximations to the Laplace equation with inhomogeneous Dirichlet and Robin boundary conditions. Such bounds play an important role in the stability analysis of the numerical method for the tumour growth model and are also of independent interest. As we are not aware of these finite element stability results in the literature, we present them here together with their proofs.

C.8.1. Dirichlet problem

Consider the Dirichlet problem

$$\begin{aligned} -\Delta u &= 0 \quad \text{in } \Omega, \\ u &= g \quad \text{on } \Gamma. \end{aligned}$$

It follows directly from the weak formulation and the trace theorem that

$$\|u\|_{H^1(\Omega)} \leq C \, \|g\|_{H^{1/2}(\Gamma)}. \tag{C.8.2}$$

Consider now a quasi-uniform finite element discretization of the Dirichlet problem, with boundary data given by the finite element function g_h on the boundary Γ_h of the computational domain Ω_h obtained by quasi-uniform finite element interpolation of the boundary Γ of Ω. There we have the bulk finite element space $\mathcal{V}_h$ and the boundary finite element space $\mathcal{S}_h$, which is the trace space of $\mathcal{V}_h$: For every $v_h \in \mathcal{V}_h$, its trace $\gamma_h v_h$ is in $\mathcal{S}_h$. We let $\mathcal{V}_h^0$ be the subspace of $\mathcal{V}_h$ with trace 0. For a given $g_h \in \mathcal{S}_h$, the finite element approximation $u_h \in \mathcal{V}_h$ is determined by

$$\int_{\Omega_h} \nabla u_h \cdot \nabla \varphi_h = 0 \quad \text{for all } \varphi_h \in \mathcal{V}_h^0, \qquad \gamma_h u_h = g_h.$$

There is a discrete bound analogous to (C.8.2).

Proposition C.8.1. *In the above situation, the finite element approximation u_h obtained from a quasi-uniform and shape-regular family of triangulations is bounded by*

$$\|u_h\|_{H^1(\Omega_h)} \leq C \, \|g_h\|_{H^{1/2}(\Gamma_h)}, \tag{C.8.3}$$

where C depends on bounds of finitely many derivatives of a parametrization of the boundary surface Γ and on the quasi-uniformity and shape regularity bounds, but is independent of h and $g_h \in \mathcal{S}_h \subset H^{1/2}(\Gamma_h)$.

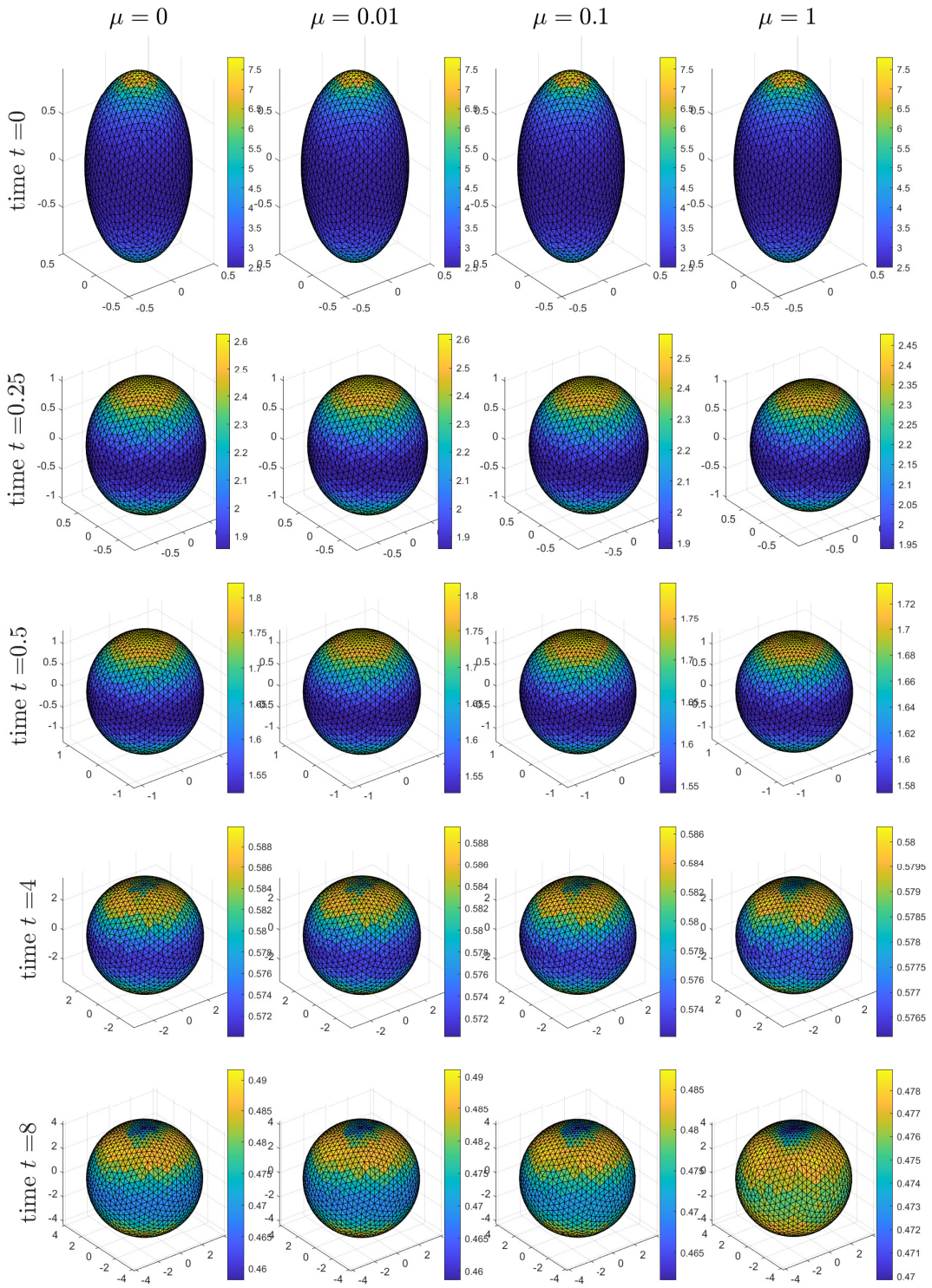

Figure C.4.: Numerical solution (Γ_h^n and u_h^n) of the coupled bulk–surface problem with varying regularization parameter $\mu = 0$, 0.01, 0.1, 1 (column-wise from left to right) $\alpha = 1$ and $\beta = 1$.

For linear finite elements on a two-dimensional polygonal domain Ω_h, such a bound was proved by Bramble, Pasciak & Schatz [Bramble et al., 1986], Lemma 3.2, and for linear finite elements on smooth domains, with a polygonal computational domain Ω_h, this was proved by Bramble & King [Bramble and King, 1994] (as an immediate corollary to their Theorem 1). We are not aware of a proof in the literature of the more general result for quadratic or higher-degree finite elements with non-polygonal computational domain, nor of the result in the three-dimensional case.

Proof. Let $\widetilde{I}_h^{\mathrm{SZ}}\colon H^1(\Omega_h) \to \mathcal{V}_h$ be the isoparametric Scott–Zhang finite element interpolation operator, see [Hansbo et al., 2020, Section 4.4], and see [Scott and Zhang, 1990] for the simpler case of polygonal domains, as well as [Camacho and Demlow, 2015] for the case of smooth closed surfaces. The operator $\widetilde{I}_h^{\mathrm{SZ}}$ is a stable projection that preserves nodal values, in particular boundary values in $\mathcal{S}_h$, i.e. $\gamma_h \widetilde{I}_h^{\mathrm{SZ}} v_h = \gamma_h v_h$ for all $v_h \in \mathcal{V}_h$.

Let $E\colon H^{1/2}(\Gamma) \to H^1(\Omega)$ be the solution operator of the Dirichlet problem: $u = Eg$, with $\|E\|_{H^1(\Omega)\leftarrow H^{1/2}(\Gamma)} \leq C$ by (C.8.2). We consider a discrete harmonic extension operator $E_h\colon S_h(\Gamma_h) \to S_h(\Omega_h)$ given by

$$E_h g_h = \widetilde{I}_h^{\mathrm{SZ}} (E g_h^\ell)^{-\ell}.$$

Note that $\gamma_h E_h g_h = g_h$. The finite element approximation u_h is defined equivalently by $u_h = E_h g_h + w_h$, where $w_h \in \mathcal{V}_h^0$ satisfies

$$\int_{\Omega_h} \nabla w_h \cdot \nabla \varphi_h = -\int_{\Omega_h} \nabla (E_h g_h) \cdot \nabla \varphi_h \qquad \text{for all } \varphi_h \in \mathcal{V}_h^0.$$

With $\varphi_h = w_h$, we obtain immediately

$$\|w_h\|_{H_0^1(\Omega_h)} \leq \|E_h g_h\|_{H^1(\Omega_h)} =: \alpha,$$

and so we have $\|u_h\|_{H^1(\Omega_h)} \leq 2\alpha$. We estimate (with different constants C)

$$\begin{aligned}
\alpha = \|\widetilde{I}_h^{\mathrm{SZ}} (E g_h^\ell)^{-\ell}\|_{H^1(\Omega_h)} &\leq C\, \|(E g_h^\ell)^{-\ell}\|_{H^1(\Omega_h)} \\
&\leq \|E g_h^\ell\|_{H^1(\Omega)} \\
&\leq C\, \|g_h^\ell\|_{H^{1/2}(\Gamma)} \\
&\leq C\, \|g_h\|_{H^{1/2}(\Gamma_h)},
\end{aligned}$$

where we obtained the estimates, in order, by the stability of the isoparametric Scott–Zhang interpolation, see [Hansbo et al., 2020, Eq. (4.45)] with $m = s = 1$; by the H^1 norm equivalence of lifted functions; by the bound (C.8.2); by the $H^{1/2}$ norm equivalence of the lift. This proves (C.8.3). □

C.8.2. Robin boundary value problem

Consider the Robin boundary value problem

$$\begin{aligned} -\Delta u &= 0 \quad \text{in } \Omega\,, \\ \partial_{\mathrm{n}} u + u &= g \quad \text{on } \Gamma, \end{aligned}$$

with the weak formulation to find $u \in H^1(\Omega)$ such that

$$\int_\Omega \nabla u \cdot \nabla \varphi + \int_\Gamma \gamma u \, \gamma\varphi = \int_\Gamma g \, \gamma\varphi \qquad \text{for all } \varphi \in H^1(\Omega). \tag{C.8.5}$$

We are particularly interested in the boundary value map $g \mapsto \gamma u$. We recall the following regularity result, which is readily obtained from e.g. [Taylor, 2011, Chapter 5].

Lemma C.8.2. *Let Ω be a sufficiently regular bounded domain with boundary Γ. For every $g \in L^2(\Gamma)$, the Robin boundary value problem* (C.8.4) *has a weak solution $u \in H^{3/2}(\Omega)$, and its trace is bounded by*

$$\|\gamma u\|_{H^1(\Gamma)} \leq C \|g\|_{L^2(\Gamma)}, \tag{C.8.6}$$

where C depends on bounds of finitely many derivatives of a parametrization of the boundary surface Γ.

Proof. The Lax–Milgram lemma provides a unique weak solution $u \in H^1(\Omega)$ for every $g \in H^{-1/2}(\Gamma)$, with

$$\|\gamma u\|_{H^{1/2}(\Gamma)} \leq c_\gamma \|u\|_{H^1(\Gamma)} \leq C \|g\|_{H^{-1/2}(\Gamma)}$$

by the trace theorem. Furthermore, by [Taylor, 2011], p. 410 and Section 5.7, we have $u \in H^2(\Omega)$ for every $g \in H^{1/2}(\Gamma)$, and

$$\|\gamma u\|_{H^{3/2}(\Gamma)} \leq c_\gamma \|u\|_{H^2(\Gamma)} \leq C \|g\|_{H^{1/2}(\Gamma)}.$$

The stated result then follows by interpolation of Sobolev spaces.

□

For the finite element approximation $u_h \in \mathcal{V}_h$, defined by

$$\int_{\Omega_h} \nabla u_h \cdot \nabla \varphi_h + \int_{\Gamma_h} \gamma_h u_h \, \gamma_h \varphi_h = \int_{\Gamma_h} g_h \, \gamma_h \varphi_h \qquad \text{for all } \varphi_h \in \mathcal{V}_h, \tag{C.8.7}$$

we have an analogous bound to Lemma C.8.2.

Proposition C.8.3. *In the situation of Lemma C.8.2, the finite element approximation u_h obtained from a quasi-uniform and shape-regular family of triangulations satisfies*

$$\|\gamma_h u_h\|_{H^1(\Gamma_h)} \leq C \|g_h\|_{L^2(\Gamma_h)},$$

where C depends on bounds of finitely many derivatives of a parametrization of the boundary surface Γ and on the quasi-uniformity and shape regularity bounds, but is independent of the mesh size h and of $g_h \in L^2(\Gamma_h)$.

Proof. We denote the left-hand sides of (C.8.5) and (C.8.7) by $a(u,\varphi)$ and $a_h(u_h,\varphi_h)$, respectively, and the right-hand sides by $m(g,\gamma\varphi)$ and $m_h(g_h,\gamma_h\varphi_h)$, respectively. Note that $a(\cdot,\cdot)$ is an $H^1(\Omega)$-elliptic bilinear form, and $m(\cdot,\cdot)$ is the $L^2(\Gamma)$ inner product.

We consider the Ritz map $\widetilde{R}_h\colon H^1(\Omega)\to\mathcal{V}_h\subset H^1(\Omega_h)$ that defines $\widetilde{R}_h w\in\mathcal{V}_h$ through

$$a_h(\widetilde{R}_h w,\varphi_h)=a(w,\varphi_h^\ell)\quad\text{ for all }\ \varphi_h\in\mathcal{V}_h.$$

We define $R_h\colon H^1(\Omega)\to\mathcal{V}_h^\ell\subset H^1(\Omega)$ by the lift $R_h w=(\widetilde{R}_h w)^\ell$. It is known from [Elliott and Ranner, 2021, Lemma 3.8] that

$$\begin{aligned}\|R_h w\|_{H^1(\Omega)}&\le C\,\|w\|_{H^1(\Omega)}&&\text{for all }\ w\in H^1(\Omega),\\ \|R_h w-w\|_{H^1(\Omega)}&\le Ch\,\|w\|_{H^2(\Omega)}&&\text{for all }\ w\in H^2(\Omega),\end{aligned}$$

which further implies, by interpolation of Sobolev spaces,

$$\|R_h w-w\|_{H^1(\Omega)}\le Ch^{1/2}\,\|w\|_{H^{3/2}(\Omega)}\quad\text{ for all }\ w\in H^{3/2}(\Omega).\tag{C.8.8}$$

In particular this holds true for the solution $u\in H^{3/2}(\Omega)$ of (C.8.4) with the lifted finite element function $g=g_h^\ell$.

We estimate

$$\|\gamma_h u_h\|_{H^1(\Gamma_h)}\le C\,\|\gamma_h(u_h-\widetilde{R}_h u)\|_{H^1(\Gamma_h)}+\|\gamma_h\widetilde{R}_h u\|_{H^1(\Gamma_h)}.\tag{C.8.9}$$

(i) Consider the first term on the right-hand side. By an inverse inequality and the trace inequality (via a pair of norm equivalences) we obtain

$$\|\gamma_h(u_h-\widetilde{R}_h u)\|_{H^1(\Gamma_h)}\le Ch^{-1/2}\|\gamma_h(u_h-\widetilde{R}_h u)\|_{H^{1/2}(\Gamma_h)}\le Ch^{-1/2}\|u_h-\widetilde{R}_h u\|_{H^1(\Omega_h)}\,.$$

To bound this term, we note that by the equations (C.8.5) and (C.8.7) for u and u_h and the definition of the Ritz map,

$$a_h(u_h-\widetilde{R}_h u,\varphi_h)=m_h(g_h,\gamma_h\varphi_h)-m(g_h^\ell,(\gamma_h\varphi)^\ell).$$

It is known from [Dziuk and Elliott, 2013a, Lemma 5.5], [Kovács, 2018, Lemma 5.6] that the right-hand side is bounded by

$$|m_h(g_h,\gamma_h\varphi_h)-m(g_h^\ell,(\gamma_h\varphi)^\ell)|\le Ch^2\|g_h\|_{L^2(\Gamma_h)}\,\|\gamma_h\varphi_h\|_{L^2(\Gamma_h)}\le Ch^2\|g_h\|_{L^2(\Gamma_h)}\,\|\varphi_h\|_{H^1(\Omega_h)}.$$

(For isoparametric finite elements of polynomial degree k the above estimate holds with h^{k+1} instead of h^2.)

By the h-uniform equivalence of the norm induced by a_h and the $H^1(\Omega_h)$-norm on $\mathcal{V}_h$, this yields

$$\|u_h-\widetilde{R}_h u\|_{H^1(\Omega_h)}\le Ch^2\|g_h\|_{L^2(\Gamma_h)}$$

and hence

$$\|\gamma_h(u_h-\widetilde{R}_h u)\|_{H^1(\Gamma_h)}\le Ch^{3/2}\|g_h\|_{L^2(\Gamma_h)}.$$

(ii) Now we turn to the second term on the right-hand side of (C.8.9). By the H^1 norm equivalence under the lift [Demlow, 2009, equation (2.16)] we have, with $R_h u = (\widetilde{R}_h u)^\ell$,

$$\|\gamma_h \widetilde{R}_h u\|_{H^1(\Gamma_h)} \le C \|(\gamma_h \widetilde{R}_h u)^\ell\|_{H^1(\Gamma)} = C \|\gamma R_h u\|_{H^1(\Gamma)} .$$

Let $R_h^\Gamma \colon H^1(\Gamma) \to \mathcal{S}_h^\ell \subset H^1(\Gamma)$ be the Ritz map for $-\Delta_\Gamma u + u = 0$ on Γ (see, e.g., [Kovács, 2018, Definition 6.1]), i.e., $R_h^\Gamma w = (\widetilde{R}_h^\Gamma w)^\ell$, where $w_h = \widetilde{R}_h^\Gamma w \in \mathcal{S}_h$ is determined by

$$\int_{\Gamma_h} \Big(\nabla_\Gamma w_h \cdot \nabla_\Gamma \varphi_h + w_h \, \varphi_h \Big) = \int_\Gamma \Big(\nabla_\Gamma w \cdot \nabla_\Gamma \varphi_h^\ell + w \, \varphi_h^\ell \Big) \quad \text{for all } \varphi_h \in \mathcal{S}_h.$$

By the proof of Theorem 6.3 [Kovács, 2018] (working with $k = 0$ and the H^1 stability of the Ritz map in the estimates of part (b) of the proof therein) that

$$\begin{aligned} \|R_h^\Gamma w\|_{H^1(\Gamma)} &\le C \, \|w\|_{H^1(\Gamma)} && \text{for all } \ w \in H^1(\Gamma), \\ \|R_h^\Gamma w - w\|_{L^2(\Gamma)} &\le Ch \, \|w\|_{H^1(\Gamma)} && \text{for all } \ w \in H^2(\Gamma). \end{aligned}$$

Note that we have formulated the error estimate such that we have the $H^1(\Gamma)$ norm on the right-hand side. By interpolation of Sobolev spaces this further yields

$$\|R_h^\Gamma w - w\|_{H^{1/2}(\Gamma)} \le Ch^{1/2} \, \|w\|_{H^1(\Gamma)}. \tag{C.8.10}$$

We estimate

$$\|\gamma R_h u\|_{H^1(\Gamma)} \le \|\gamma R_h u - R_h^\Gamma \gamma u\|_{H^1(\Gamma)} + \|R_h^\Gamma \gamma u\|_{H^1(\Gamma)}.$$

Using first an inverse inequality (via a pair of norm equivalences) and then the trace inequality with (C.8.8) and (C.8.10), (C.8.6) (where $g = g_h^\ell$), the first term on the right-hand side is bounded by

$$\begin{aligned} \|\gamma R_h u - R_h^\Gamma \gamma u\|_{H^1(\Gamma)} &\le Ch^{-1/2} \|\gamma R_h u - R_h^\Gamma \gamma u\|_{H^{1/2}(\Gamma)} \\ &\le Ch^{-1/2} \big(\|\gamma R_h u - \gamma u\|_{H^{1/2}(\Gamma)} + \|\gamma u - R_h^\Gamma \gamma u\|_{H^{1/2}(\Gamma)} \big) \\ &\le Ch^{-1/2} \big(\|R_h u - u\|_{H^1(\Omega)} + \|\gamma u - R_h^\Gamma \gamma u\|_{H^{1/2}(\Gamma)} \big) \\ &\le Ch^{-1/2} \big(Ch^{1/2} \|u\|_{H^{3/2}(\Omega)} + Ch^{1/2} \|\gamma u\|_{H^1(\Gamma)} \big) \\ &\le C \|g\|_{L^2(\Gamma)}. \end{aligned}$$

The second term is bounded by

$$\|R_h^\Gamma \gamma u\|_{H^1(\Gamma)} \le C \, \|\gamma u\|_{H^1(\Gamma)} \le C \|g\|_{L^2(\Gamma)}.$$

Combining the bounds of (i) and (ii) and noting that the L^2 norm equivalence under the lift yields $\|g\|_{L^2(\Gamma)} = \|g_h^\ell\|_{L^2(\Gamma)} \le C \|g_h\|_{L^2(\Gamma_h)}$, we finally obtain the stated bound for $\|\gamma_h u_h\|_{H^1(\Gamma_h)}$. □

D. Appendix: Isoparametric finite element implementation

In this section, we give a brief summary on how to implement the finite element method in the three-dimensional case. We start with linear finite elements both for the bulk and the surface and then extend it to second-degree polynomials, where the transformation from the reference element is no longer affine. The topic of mesh generation is not covered here.

D.1. Linear bulk finite elements

We denote by N the number of nodes of the triangulation and by T the number of elements. The mesh is given by an array `nodes` $\in \mathbb{R}^{N\times 3}$, where `nodes(k,:)` is the k-th node, and an array `elements` $\in \mathbb{R}^{T\times 4}$, where `elements(k,j)` is the index of the j-th node of the k-th element, i.e. `nodes(elements(k,j),:)` is the j-th node of element k.

We denote by N_Γ the number of points that lie on the boundary $\Gamma = \partial\Omega$ and assume for simplicity that the array `nodes` is ordered such that exactly the first N_Γ nodes are the boundary nodes.

In the following, we explain how to compute the local mass and stiffness matrices corresponding to each element.

We use the notational convention that capital X denotes points in $\mathbb{R}^3$ whereas lower-case x, y, z denote the three variables ($X = (x, y, z)$). Basis functions are denoted by φ, element transformations by Φ. Matrices are denoted by bold–face capital letters. Every quantity with a hat corresponds to the reference element.

The reference element is the unit simplex

$$\widehat{E} = \{(x, y, z) \in \mathbb{R}^3 : 0 \le x + y + z \le 1,\ x \ge 0,\ y \ge 0,\ z \ge 0\}\,.$$

We denote the corners by $\widehat{X}_1, \dots \widehat{X}_4$. The Lagrangian basis functions $\widehat{\varphi}_j$ are defined by the property $\widehat{\varphi}_j(\widehat{X}_k) = \delta_{jk}$.

Integrals of functions $f = f(x, y, z)$ defined on $\widehat{E}$ are parametrized by

$$\int_{\widehat{E}} f(x, y, z)\mathrm{d}(x, y, z) = \int_0^1 \int_0^{1-x} \int_0^{1-x-y} f(x, y, z)\mathrm{d}z\mathrm{d}y\mathrm{d}x\,.$$

For an arbitrary element E with nodes $X_i = (x_i, y_i, z_i)^{\mathrm{T}}$, $i = 1, 2, 3, 4$, the transformation

$\Phi_E : \widehat{E} \to E$ and its inverse are given by

$$\begin{aligned}\Phi_E(X) &= \mathbf{B}X + X_1\,,\\ \Phi_E^{-1}(Y) &= \mathbf{B}^{-1}(Y - X_1)\,, \quad \text{where}\\ \mathbf{B} &= \begin{pmatrix} X_2 - X_1 & X_3 - X_1 & X_4 - X_1 \end{pmatrix} \in R^{3\times 3}\,.\end{aligned}$$

The reference mass matrix $\widehat{\mathbf{M}}^\Omega$ is defined by $\widehat{\mathbf{M}}^\Omega_{jk} = \int_{\widehat{E}} \widehat{\varphi}_j \widehat{\varphi}_k$ and can be precomputed and stored. For an arbitrary element E with corresponding affine transformation $\Phi_E(X) = \mathbf{B}X + b$, the transformation formula yields $\mathbf{M}^\Omega = |\det(\mathbf{B})|\widehat{\mathbf{M}}^\Omega$ for the local mass matrix corresponding to E.

The reference stiffness matrix $\widehat{\mathbf{A}}^\Omega$ is defined by $\widehat{\mathbf{A}}^\Omega_{jk} = \int_{\widehat{E}} \nabla\widehat{\varphi}_j \cdot \nabla\widehat{\varphi}_k$. In order to apply the transformation formula, it is convenient to define matrices $\widehat{\mathbf{A}}^\Omega_{xx}$, $\widehat{\mathbf{A}}^\Omega_{xy}$, $\widehat{\mathbf{A}}^\Omega_{xz}$, $\widehat{\mathbf{A}}^\Omega_{yy}$, $\widehat{\mathbf{A}}^\Omega_{yz}$ and $\widehat{\mathbf{A}}^\Omega_{zz}$ by

$$(\widehat{\mathbf{A}}^\Omega_{xy})_{jk} = \int_{\widehat{E}} \partial_x\widehat{\varphi}_j \partial_y\widehat{\varphi}_k \tag{D.1.1}$$

and the remaining ones defined analogously. As for the stiffness matrix, these are precomputed and stored. For an arbitrary element E with corresponding transformation $\Phi_E(X) = \mathbf{B}X + b$, the chainrule and tranformation formula yield

$$\int_E \nabla\varphi_j \cdot \nabla\varphi_k = \int_{\widehat{E}} \nabla\widehat{\varphi}_j^{\mathrm{T}} \mathbf{B}^{-1}\mathbf{B}^{-\mathrm{T}} \nabla\widehat{\varphi}_k |\det(B)|\,.$$

Writing $\mathbf{C} = \mathbf{B}^{-1} \in \mathbb{R}^{3\times 3}$, an elementary calculation shows

$$\begin{aligned}\frac{1}{|\det(\mathbf{B})|}\mathbf{A}^\Omega = {} & (C_{11}^2 + C_{12}^2 + C_{13}^2)\widehat{\mathbf{A}}^\Omega_{xx}\\ & + (C_{11}C_{21} + C_{12}C_{22} + C_{13}C_{23})(\widehat{\mathbf{A}}^\Omega_{xy} + (\widehat{\mathbf{A}}^\Omega_{xy})^{\mathrm{T}})\\ & + (C_{11}C_{31} + C_{12}C_{32} + C_{13}C_{33})(\widehat{\mathbf{A}}^\Omega_{xz} + (\widehat{\mathbf{A}}^\Omega_{xz})^{\mathrm{T}})\\ & + (C_{21}^2 + C_{22}^2 + C_{23}^2)\widehat{\mathbf{A}}^\Omega_{yy}\\ & + (C_{21}C_{31} + C_{22}C_{32} + C_{23}C_{33})(\widehat{\mathbf{A}}^\Omega_{yz} + (\widehat{\mathbf{A}}^\Omega_{yz})^{\mathrm{T}})\\ & + (C_{31}^2 + C_{32}^2 + C_{33}^2)\widehat{\mathbf{A}}^\Omega_{zz}\end{aligned} \tag{D.1.2}$$

from which we obtain the local stiffness matrix.

D.2. Linear surface finite elements

The reference element $\widehat{E} \subset \mathbb{R}^3$ is given by the nodes

$$\widehat{X}_1 = \begin{pmatrix}0\\0\\0\end{pmatrix}\,, \quad \widehat{X}_2 = \begin{pmatrix}1\\0\\0\end{pmatrix}\,, \quad \widehat{X}_3 = \begin{pmatrix}0\\1\\0\end{pmatrix}$$

and the normal vector $\widehat{\mathbf{n}} = (0,0,1)^{\mathrm{T}}$. The Lagrangian basis functions $\widehat{\varphi}_j$ are defined by the property $\widehat{\varphi}_j(\widehat{X}_k) = \delta_{jk}$. In particular: $\partial_z \widehat{\varphi}_j = 0$.

For an arbitrary element E with nodes $X_i = (x_i, y_i, z_i)^{\mathrm{T}}$, $i = 1,2,3$, the transformation $\Phi_E : \widehat{E} \to E$ is given by

$$\begin{aligned}\Phi_E(X) &= \mathbf{B}X + X_1\,, \quad \text{where}\\ \mathbf{B} &= \begin{pmatrix} X_2 - X_1 & X_3 - X_1 & \frac{(X_2-X_1)\times(X_3-X_1)}{\|(X_2-X_1)\times(X_3-X_1)\|}\end{pmatrix}.\end{aligned}$$

The $\times$ denotes the cross product. Note that we have the relation $\mathbf{n} = \mathbf{B}\widehat{\mathbf{n}}$, where $\mathbf{n}$ denotes the normal vector of E. This can be rewritten as $D\Phi_K(\cdot)\widehat{\mathbf{n}} = \mathbf{n}$, which will be crucial for isoparametric elements.

The reference surface mass matrix $\widehat{\mathbf{M}}^\Gamma$ is defined by $\widehat{\mathbf{M}}^\Gamma_{jk} = \int_{\widehat{E}} \widehat{\varphi}_j \widehat{\varphi}_k$ which is precomputed and is simply the reference mass matrix for linear bulk finite elements in $\mathbb{R}^2$. For an arbitrary element E with corresponding transformation $\Phi_E(X) = \mathbf{B}X + b$, the transformation formula yields $\mathbf{M}^\Gamma = |\det(\mathbf{B})|\widehat{\mathbf{M}}^\Gamma$ for the corresponding local surface mass matrix.

The reference surface stiffness matrices $\widehat{\mathbf{A}}^\Gamma_{xx}$, $\widehat{\mathbf{A}}^\Gamma_{xy}$, $\widehat{\mathbf{A}}^\Gamma_{yy}$ are defined as analogously to (D.1.1) For an arbitrary element E with corresponding transformation $\Phi_E(X) = \mathbf{B}X + b$, the relation $\varphi_j(Y) = \widehat{\varphi}_j(\Phi_E^{-1}(Y))$ and the chain rule yield

$$\nabla_Y \varphi_j(Y) = \mathbf{C}^{\mathrm{T}} \nabla_X \widehat{\varphi}_j(X) = \begin{pmatrix} C_{11}\partial_x\widehat{\varphi}_j + C_{21}\partial_y\widehat{\varphi}_j \\ C_{12}\partial_x\widehat{\varphi}_j + C_{22}\partial_y\widehat{\varphi}_j \\ C_{13}\partial_x\widehat{\varphi}_j + C_{23}\partial_y\widehat{\varphi}_j \end{pmatrix},$$

where $\mathbf{C} = \mathbf{B}^{-1}$ and $Y = \Phi_E(X)$. Here we have used $\partial_z\widehat{\varphi}_j = 0$. For the tangential gradient on E, it is easily seen that

$$\nabla_E \varphi_j = \mathbf{C}^{\mathrm{T}} \nabla \widehat{\varphi}_j\,.$$

Applying the transformation formula together with the above relations yields that the local surface stiffness matrix is given by

$$\begin{aligned}\widehat{\mathbf{A}}^\Gamma &= (C_{11}^2 + C_{12}^2 + C_{13}^2)\widehat{\mathbf{A}}^\Gamma_{xx}\\ &\quad + (C_{11}C_{21} + C_{12}C_{22} + C_{13}C_{23})(\widehat{\mathbf{A}}^\Gamma_{xy} + (\widehat{\mathbf{A}}^\Gamma_{xy})^{\mathrm{T}})\\ &\quad + (C_{21}^2 + C_{22}^2 + C_{23}^2)\widehat{\mathbf{A}}^\Gamma_{yy}\,.\end{aligned}$$

D.3. Second order finite elements (polygonal)

Before deriving how to implement second order isoparametric elements, we start with the case of polygonal local elements. Note that for curved domains, where the boundary is approximated by piecewise polynomials, only the *boundary elements*, i.e. those simplices with more than one node on the boundary are curved. The interior simplices with at most one node on the boundary are tetrahedrons and the parametrization from the reference element is affine. Exploiting that, quadrature formulas to approximate the integrals are only needed for the boundary bulk elements.

The reference element $\widehat{E}$ is again the unit simplex but now considered with the 10 standard second order nodes $\widehat{X}_1, \dots, \widehat{X}_{10}$. The Lagrangian basis functions are defined by $\widehat{\varphi}_i(X_j) = \delta_{ij}$.

For an arbitrary plain element E with nodes $X_i = (x_i, y_i, z_i)^{\mathrm{T}}$, $i = 1, \dots, 10$, the affine transformation $\Phi_E = \widehat{E} \to E$ and its inverse are determined by $X_1, \dots, X_4$ and given as in the linear case.

The reference bulk mass matrix $\widehat{\mathbf{M}}^\Omega$ is given by $\widehat{\mathbf{M}}^\Omega_{jk} = \int_{\widehat{E}} \widehat{\varphi}_j \widehat{\varphi}_k$ and is yet again computed and stored once. For an arbitrary element E with corresponding affine transformation $\Phi_E(X) = \mathbf{B}X + b$, the transformation formula yields $\mathbf{M}^\Omega = |\det(\mathbf{B})| \widehat{\mathbf{M}}^\Omega$ for the local mass matrix.

The reference bulk stiffness matrices $\widehat{\mathbf{A}}^\Omega_{xx}$ etc. are defined as in the linear case, for instance $\widehat{\mathbf{A}}^\Omega_{xz} = (\int_{\widehat{E}} \partial_x \widehat{\varphi}_j \partial_z \widehat{\varphi}_k)_{jk}$.

For an arbitrary element E with corresponding transformation $\Phi_E(X) = \mathbf{B}X + b$, we denote $\mathbf{C} = \mathbf{B}^{-1}$. The chain rule, the transformation formula and the same calculation yield the same result as (D.1.2).

D.4. Isoparametric bulk elements

In this section, we explain how to deal with the isoparametric bulk elements, i.e. the boundary elements of the bulk triangulation with more than one node on the boundary. We refer to Bartels et al. [2006], where isoparametric implementations are explained for two-dimensional bulk domains.

D.4.1. Mesh data

Starting from the order-1-mesh, the boundary elements are those with more than one node on the boundary. When creating an order-2-mesh, the new nodes that are created on the edge between boundary nodes have to be projected orthogonally onto the boundary. In the simple case of a mesh on the unit ball, this is achieved by normalizing the new nodes. The new elements have

- Zero or one boundary node, if the initial element has zero or one boundary node,
- three boundary nodes, if the initial element has two boundary nodes,
- six boundary nodes, if the initial element has three boundary nodes.

The curved elements are those with three or six boundary nodes. We add another column in the `elements` array, where the the last column counts the number of boundary nodes.

Note that the following isoparametric procedure, when applied to polygonial (interior) elements is equivalent to the affine procedure presented previously. If one aims to keep a short code, it is not necessary to distinguish between boundary and interior elements. However, the isoparametric procedure is computationally more expensive, which is why we use it only on the boundary elements, where it is necessary.

D.4.2. Isoparametric parametrization

The reference simplex $\widehat{E}$ is the same as for the plain bulk elements and given by the nodes $\widehat{X}_j$, $j = 1, \dots, 10$. Consider we are given a curved simplex E with nodes P_j, $j = 1, \dots, 10$. We assume that $P_1, \dots, P_4$ are the corners and $P_5, \dots, P_{10}$ lie on the respective (curved) line segments (edges) of the (curved) simplex.

The isoparametric transformation $\Phi_E : \widehat{E} \to E$ is given by

$$\Phi_E(x) = \sum_{j=1}^{10} P_j \widehat{\varphi}_j(x)\,, \quad x \in \widehat{E}\,,$$

where $\widehat{\varphi}_j$ are the Lagrangian basis functions on the reference element.

D.4.3. Mass matrix

On a curved simplex $E = \Phi_E(\widehat{E})$, we apply the transformation formula and a quadrature rule $(x_m, \kappa_m)_{m=1}^{14}$ (see Section D.4.5) on $\widehat{E}$:

$$\begin{aligned}\int_E \varphi_j \varphi_k &= \int_{\widehat{E}} \widehat{\varphi}_j(x)\widehat{\varphi}_k(x) |\det D\Phi_E(x)| \mathrm{d}x \\ &\approx \sum_{m=1}^{14} \kappa_m \widehat{\varphi}_j(x_m)\widehat{\varphi}_k(x_m) |\det D\Phi_E(x_m)| = \mathbf{M}^{\Omega}_{jk}\,.\end{aligned}$$

The factors $\widehat{\varphi}_l(x_m)$ do not depend on the element E and thus not on the transformation. They are precomputed once and stored in a matrix $\boldsymbol{\varphi} \in \mathbb{R}^{14\times 10}$, such that $\boldsymbol{\varphi}_{ml} = \widehat{\varphi}_l(x_m)$. We then obtain in matrix–vector form:

$$\mathbf{M}^{\Omega} = \sum_{m=1}^{14} \kappa_m |\det D\Phi_E(x_m)| \boldsymbol{\varphi}_m^{\mathrm{T}} \boldsymbol{\varphi}_m\,, \tag{D.4.1}$$

where $\boldsymbol{\varphi}_m$ denotes the m-th row of $\boldsymbol{\varphi}$.

For the derivative, we see that

$$\partial_k \Phi_E = \sum_{j=1}^{10} P_j \partial_k \widehat{\varphi}_j = \mathbf{P} \cdot \partial_k \widehat{\boldsymbol{\varphi}}\,,$$

where

$$\mathbf{P} = \begin{pmatrix} P_1 & \cdots & 10 \end{pmatrix} \in \mathbb{R}^{3\times 10}\,, \quad \widehat{\boldsymbol{\varphi}} = \begin{pmatrix} \widehat{\varphi}_1 \\ \vdots \\ \widehat{\varphi}_{10} \end{pmatrix} \in \mathbb{R}^{10\times 1}\,.$$

We thus have

$$D\Phi_E(x_m) = \begin{pmatrix} \mathbf{P}\cdot\partial_1\widehat{\varphi}(x_m) & \mathbf{P}\cdot\partial_2\widehat{\varphi}(x_m) & \mathbf{P}\cdot\partial_3\widehat{\varphi}(x_m) \end{pmatrix} \in \mathbb{R}^{3\times 3}\,.$$

The values of the derivatives of the reference basis functions in the nodes are independent of the transformation. They are precomputed once and stored in matrices $\boldsymbol{\varphi}_x$, $\boldsymbol{\varphi}_y$, $\boldsymbol{\varphi}_z \in \mathbb{R}^{14\times 10}$.

D.4.4. Stiffness matrix

The chain rule yields $\nabla\varphi(y) = D\Phi_E^{-\mathrm{T}}\widehat{\varphi}(x)$ (where $y = \Phi_E(x)$) so the transformation formula and a quadrature rule yield

$$\begin{aligned}\int_E \nabla\varphi_j \cdot \nabla\varphi_k &= \int_{\widehat{E}} \nabla\widehat{\varphi}_j^{\mathrm{T}}(D\Phi_E)^{-1}(D\Phi_E)^{-\mathrm{T}}\nabla\widehat{\varphi}_k |\det D\Phi_E| \\ &\approx \sum_{m=1}^{14} \kappa_m \nabla\widehat{\varphi}_j(x_m)^{\mathrm{T}} D\Phi_E(x_m)^{-1} D\Phi_E(x_m)^{-\mathrm{T}} \nabla\widehat{\varphi}_k(x_m) |\det D\Phi_E(x_m)| \\ &= \mathbf{A}_{jk}^{\Omega}\,.\end{aligned}$$

for the local stiffness matrix.

Collecting the values $\nabla\widehat{\varphi}_j(x_m)$ in an array $\nabla\widehat{\varphi}(x_m) \in \mathbb{R}^{3\times 10}$ and denoting

$$\mathbf{B}_m := D\Phi_E(x_m)^{-\mathrm{T}}\nabla\widehat{\varphi}(x_m) \in \mathbb{R}^{3\times 10}\,,$$

we can write

$$\mathbf{A}^{\Omega} = \sum_{m=1}^{14} \kappa_m |\det D\Phi_E(x_m)| \mathbf{B}_m^{\mathrm{T}}\mathbf{B}_m\,. \tag{D.4.2}$$

Note that (D.4.2) looks similar to (D.4.1), but the matrix $\mathbf{B}_m$ depends on both the transformation and the quadrature node, so it has to be computed for each element and each quadrature node.

D.4.5. Quadrature rule on $\widehat{E}$

The quadrature rule we apply on $\widehat{E}$ has 14 nodes and is of order 5. It has the form

$$\int_{\widehat{E}} f(x)\mathrm{d}x \approx \sum_{m=1}^{14} \kappa_m f(x_m)\,.$$

The nodes and weights are taken from [Gellert and Harbord, 1991, Table VI] and are not listed here.

D.5. Isoparametric surface elements

D.5.1. Isoparametric parametrization

Consider we are given a curved triangle $E \subset \mathbb{R}^3$ with nodes $P_1, \ldots, P_6$. We assume that P_1, P_2 and P_3 are the corners and that P_4, P_5 and P_6 are on the line segment (P_1, P_2), (P_2, P_3) and (P_3, P_1), respectively. We denote by $\widehat{E} \subset \mathbb{R}^2$ the reference element. The isoparametric transformation of E is given by

$$\Phi_E : \widehat{E} \to E\,, \quad (\xi,\eta) \mapsto \sum_{j=1}^{6} P_j \widehat{\varphi}_j(\xi,\eta)\,,$$

where φ_j, $j = 1, \ldots, 6$ are the basis functions on the reference element.

D.5.2. Mass matrix

On a curved triangle $E = \Phi_E(\widehat{E})$, we apply the definition of a surface integral and a quadrature rule on $\widehat{E}$:

$$\begin{aligned}\int \varphi_j \varphi_k &= \int_{\widehat{E}} \widehat{\varphi}_j \widehat{\varphi}_k \|\partial_\xi \Phi_E \times \partial_\eta \Phi_E\|_2 \\ &\approx \sum_{m=1}^{7} \kappa_m \widehat{\varphi}_j(\xi_m, \eta_m) \widehat{\varphi}_k(\xi_m, \eta_m) \|(\partial_\xi \Phi_E \times \partial_\eta \Phi_E)(\xi_m, \eta_m)\|_2 =: \mathbf{M}^\Gamma_{jk} \,.\end{aligned}$$

The factors $\widehat{\varphi}_j(\xi_m, \eta_m)$ do not depend on the transformation. They are precomputed once and then stored in a matrix $\boldsymbol{\varphi} \in \mathbb{R}^{7\times 6}$, where $\boldsymbol{\varphi}_{jk} = \widehat{\varphi}_k(\xi_j, \eta_j)$. In matrix–vector form, we obtain

$$\mathbf{M}^\Gamma = \sum_{m=1}^{7} \kappa_m \boldsymbol{\varphi}_m^{\mathrm{T}} \boldsymbol{\varphi} \|(\partial_\xi \Phi_E \times \partial_\eta \Phi_E)(\xi_m, \eta_m)\|_2 \,,$$

where $\boldsymbol{\varphi}_m$ denotes the m-th row of $\boldsymbol{\varphi}$.

For the derivative, we see that

$$\partial_\xi \Phi_E = \mathbf{P} \cdot \partial_\xi \widehat{\varphi} \,, \quad \partial_\eta \Phi_E = \mathbf{P} \cdot \partial_\eta \widehat{\varphi} \,,$$

where

$$\mathbf{P} = \begin{pmatrix} P_1 & \cdots & P_6 \end{pmatrix} \in \mathbb{R}^{3\times 6} \,, \quad \widehat{\varphi} = \begin{pmatrix} \widehat{\varphi}_1 \\ \vdots \\ \widehat{\varphi}_6 \end{pmatrix} \in \mathbb{R}^{6\times 1} \,.$$

The values of the derivatives of the basis functions in the nodes are independent of the transformation. They are precomputed once and stored in matrices $\boldsymbol{\varphi}_\xi$, $\boldsymbol{\varphi}_\eta$.

D.5.3. Stiffness matrix

We follow a construction similar to the curved line segments in $\mathbb{R}^2$. The map Φ_E, considered as a map $\mathbb{R}^3 \to \mathbb{R}^3$ is not invertible. We construct a map

$$\overline{\Phi} : \mathbb{R}^3 \to \mathbb{R}^3 \,, \quad (\xi, \eta, z) \mapsto \overline{\Phi}(\xi, \eta, z)$$

such that $\overline{\Phi}(\xi, \eta, 0) = \Phi_E(\xi, \eta)$. We require that the Jacobian matrix satisfies

$$(D\overline{\Phi})(\xi, \eta, 0)\widehat{\mathbf{n}} = \mathbf{n}\left(\Phi_E(\xi, \eta)\right) \,.$$

Note that for $x = \Phi_E(\xi, \eta) \in E$, the unit normal vector is given by

$$\mathbf{n}(x) = \pm \frac{\partial_\xi \Phi_E(\xi, \eta) \times \partial_\eta \Phi_E(\xi, \eta)}{\|\partial_\xi \Phi_E(\xi, \eta) \times \partial_\eta \Phi_E(\xi, \eta)\|_2} \,.$$

This implies that the Jacobian satisfies (at $(\xi,\eta,0)\in\mathbb{R}^3$)

$$D\overline{\Phi}(\xi,\eta,0)=\begin{pmatrix}\partial_\xi\Phi_E(\xi,\eta) & \partial_\eta\Phi_E(\xi,\eta) & \frac{\partial_\xi\Phi_E(\xi,\eta)\times\partial_\eta\Phi_E(\xi,\eta)}{\|\partial_\xi\Phi_E(\xi,\eta)\times\partial_\eta\Phi_E(\xi,\eta)\|_2}\end{pmatrix}=:\mathbf{B}(\xi,\eta)\,.$$

For a basis function $\widehat{\varphi}=\widehat{\varphi}_j$, $\mathbb{R}^2\to\mathbb{R}$, we set

$$\widetilde{\widehat{\varphi}}:\mathbb{R}^3\to\mathbb{R}\,,\quad \widetilde{\widehat{\varphi}}(\xi,\eta,z)=\widehat{\varphi}(\xi,\eta)\,.$$

We have

$$\widetilde{\widehat{\varphi}}(\xi,\eta,0)=\widehat{\varphi}(\xi,\eta)=\varphi(\Phi_E(\xi,\eta))=\varphi(\overline{\Phi}(\xi,\eta,0))$$

and thus with the chainrule, writing $x=\Phi_E(\xi,\eta)$,

$$\begin{pmatrix}\partial_\xi\widehat{\varphi}(\eta,\xi)\\ \partial_\eta\widehat{\varphi}(\eta,\xi)\\ 0\end{pmatrix}=\mathbf{B}(\xi,\eta)^{\mathrm{T}}\nabla\varphi(x)\,.$$

We set $\mathbf{C}(\xi,\eta):=\mathbf{B}(\xi,\eta)^{-1}$ and thus have

$$\begin{aligned}\nabla\varphi_j(x)&=\mathbf{C}(\xi,\eta)^{\mathrm{T}}\nabla\widetilde{\widehat{\varphi}}(\xi,\eta,0)\\&=\begin{pmatrix}C_{11}(\xi,\eta)\partial_\xi\widehat{\varphi}(\xi,\eta)+C_{21}(\xi,\eta)\partial_\eta\widehat{\varphi}(\xi,\eta)\\ C_{12}(\xi,\eta)\partial_\xi\widehat{\varphi}(\xi,\eta)+C_{22}(\xi,\eta)\partial_\eta\widehat{\varphi}(\xi,\eta)\\ C_{13}(\xi,\eta)\partial_\xi\widehat{\varphi}(\xi,\eta)+C_{23}(\xi,\eta)\partial_\eta\widehat{\varphi}(\xi,\eta)\end{pmatrix}\end{aligned}$$

Now we use that $\mathbf{B}(\xi,\eta)\widehat{\mathbf{n}}=\mathbf{n}(\Phi_E(\xi,\eta))=\mathbf{n}(x)$ and thus $\mathbf{n}(x)^{\mathrm{T}}=\widehat{\mathbf{n}}^{\mathrm{T}}\mathbf{B}(\xi,\eta)^{\mathrm{T}}$ and compute

$$\begin{aligned}\nabla_E\varphi_j(x)&=(I-\mathbf{n}(x)\mathbf{n}(x)^{\mathrm{T}})\nabla\varphi_j(x)\\&=\mathbf{C}(\xi,\eta)^{\mathrm{T}}\nabla\widetilde{\widehat{\varphi}}_j(\xi,\eta,0)-\mathbf{n}(x)\mathbf{n}(x)^{\mathrm{T}}\mathbf{C}(\xi,\eta)^{\mathrm{T}}\widetilde{\widehat{\varphi}}(\xi,\eta,0)\\&=\mathbf{C}(\xi,\eta)^{\mathrm{T}}\nabla\widetilde{\widehat{\varphi}}_j(\xi,\eta,0)\,.\end{aligned}$$

For the stiffness matrix, we obtain

$$\begin{aligned}\int_E\nabla_E\varphi_j\cdot\nabla_E\varphi_k&=\int_{\widehat{E}}\mathbf{C}^{\mathrm{T}}\nabla\widetilde{\widehat{\varphi}}_j\cdot\mathbf{C}^{\mathrm{T}}\nabla\widetilde{\widehat{\varphi}}_k\|\partial_\xi\Phi_E\times\partial_\eta\Phi_E\|_2\\&\approx\sum_{m=1}^{7}\kappa_m\left(\nabla\widetilde{\widehat{\varphi}}_j\mathbf{C}\mathbf{C}^{\mathrm{T}}\nabla\widetilde{\widehat{\varphi}}_k\right)(\xi_m,\eta_m)\|(\partial_\xi\Phi\cdot\partial_\eta\Phi)(\xi_m,\eta_m)\|_2=:\mathbf{A}^\Gamma_{jk}\,.\end{aligned}$$

We write

$$\nabla\widehat{\varphi}(\xi_m,\eta_m)=\begin{pmatrix}\partial_\xi\widehat{\varphi}_1(\xi_m,\eta_m) & \cdots & \partial_\xi\widehat{\varphi}_6(\xi_m,\eta_m)\\ \partial_\eta\widehat{\varphi}_1(\xi_m,\eta_m) & \cdots & \partial_\eta\widehat{\varphi}_6(\xi_m,\eta_m)\\ 0 & \cdots & 0\end{pmatrix}\in\mathbb{R}^{3\times6}$$

and set $\mathbf{B}_m:=\mathbf{C}(\xi_m,\eta_m)^{\mathrm{T}}\nabla\widehat{\varphi}(\xi_m,\eta_m)\in\mathbb{R}^{3\times6}$. We then obtain in matrix–vector form

$$\mathbf{A}^\Gamma=\sum_{m=1}^{7}\kappa_m\mathbf{B}_m^{\mathrm{T}}\mathbf{B}_m\|(\partial_\xi\Phi_E\times\partial_\eta\Phi_E)(\xi_m,\eta_m)\|_2\,.$$

Bibliography

S. Badia and R. Codina. Analysis of a stabilized finite element approximation of the transient convection–diffusion equation using an ale framework. *SIAM Journal on Numerical Analysis*, 44(5):2159–2197, 2006.

S. Bartels, C. Carstensen, and A. Hecht. P2Q2Iso2D = 2D Isoparametric FEM in Matlab. *Journal of Computational and Applied Mathematics*, 192(2):219–250, 2006.

C. Bernardi. Optimal finite-element interpolation on curved domains. *SIAM Journal on Numerical Analysis*, 26(5):1212–1240, 1989.

D. Boffi and L. Gastaldi. Stability and geometric conservation laws for ale formulations. *Computer Methods in Applied Mechanics and Engineering*, 193(42-44):4717–4739, 2004.

J. H. Bramble and J. T. King. A robust finite element method for nonhomogeneous Dirichlet problems in domains with curved boundaries. *Math. Comp.*, 63(207):1–17, 1994.

J. H. Bramble, J. E. Pasciak, and A. H. Schatz. The construction of preconditioners for elliptic problems by substructuring. I. *Math. Comp.*, 47(175):103–134, 1986.

S. C. Brenner and R. Scott. *The mathematical theory of finite element methods*, volume Texts in Applied Mathematics, 15. Springer, New York, 2008.

F. Camacho and A. Demlow. L_2 and pointwise a posteriori error estimates for FEM for elliptic PDEs on surfaces. *IMA J. Numer. Anal.*, 35(3):1199–1227, 2015.

P. G. Ciarlet and P. A. Raviart. Interpolation theory over curved elements, with applications to finite element methods. *Computer Methods in Applied Mechanics and Engineering*, 1(2): 217–249, 1972.

K. Deckelnick, G. Dziuk, and C. M. Elliott. Computation of geometric partial differential equations and mean curvature flow. *Acta Numerica*, 14:139–232, 2005.

A. Demlow. Higher-order finite element methods and pointwise error estimates for elliptic problems on surfaces. *SIAM Journal on Numerical Analysis*, 47(2):805–827, 2009.

F. Dubois. Discrete vector potential representation of a divergence-free vector field in three-dimensional domains: numerical analysis of a model problem. *SIAM Journal on Numerical Analysis*, 27(5):1103–1141, 1990.

G. Dziuk. Finite elements for the Beltrami operator on arbitrary surfaces. In *Partial Differential Equations and Calculus of Variations*, pages 142–155. Springer, 1988.

G. Dziuk. An algorithm for evolutionary surfaces. *Numerische Mathematik*, 58(1):603–611, 1990.

G. Dziuk and C. M. Elliott. Finite elements on evolving surfaces. *IMA Journal of Numerical Analysis*, 27(2):262–292, 2007a.

G. Dziuk and C. M. Elliott. Surface finite elements for parabolic equations. *J. Comput. Math.*, 25(4):385–407, 2007b.

G. Dziuk and C. M. Elliott. L^2–estimates for the evolving surface finite element method. *Mathematics of Computation*, 82(281):1–24, 2013a.

G. Dziuk and C. M. Elliott. Finite element methods for surface PDEs. *Acta Numerica*, 22:289, 2013b.

G. Dziuk, C. Lubich, and D. Mansour. Runge–Kutta time discretization of parabolic differential equations on evolving surfaces. *IMA Journal of Numerical Analysis*, 32(2):394–416, 2012.

G. Dziuk, D. Kröner, and T. Müller. Scalar conservation laws on moving hypersurfaces. *Interfaces Free Bound.*, 15(2):203–236, 2013.

K. Ecker. *Regularity theory for mean curvature flow*. Springer, 2012.

D. Edelmann. Isoparametric finite element analysis of a generalized robin boundary value problem on curved domains. *SMAI J. Comput. Math.*, 7:57–73, 2021.

D. Edelmann. Finite element analysis for a diffusion equation on a harmonically evolving domain. *IMA J. Numer. Anal.*, 42:1866–1901, 2022.

D. Edelmann, B. Kovács, and C. Lubich. Numerical analysis of an evolving bulk–surface model of tumour growth, 2024.

C. M. Elliott and T. Ranner. Finite element analysis for a coupled bulk–surface partial differential equation. *IMA Journal of Numerical Analysis*, 33(2):377–402, 2013.

C. M. Elliott and T. Ranner. A unified theory for continuous-in-time evolving finite element space approximations to partial differential equations in evolving domains. *IMA J. Numer. Anal.*, 41(3):1696–1845, 2021.

J. Eyles, J. R. King, and V. Styles. A tractable mathematical model for tissue growth. *Interfaces Free Bound.*, 21(4):463–493, 2019.

L. Formaggia and F. Nobile. A stability analysis for the arbitrary Lagrangian Eulerian formulation with finite elements. *East-West Journal of Numerical Mathematics*, 7(2):105–132, 1999.

L. Formaggia and F. Nobile. Stability analysis of second-order time accurate schemes for ale–fem. *Computer Methods in Applied Mechanics and Engineering*, 193(39-41):4097–4116, 2004.

M. J. Gander and L. Halpern. Optimized Schwarz waveform relaxation methods for advection reaction diffusion problems. *SIAM Journal on Numerical Analysis*, 45(2):666–697, 2007.

L. Gastaldi. A priori error estimates for the arbitrary lagrangian eulerian formulation with finite elements. *Journal of Numerical Mathematics*, 9(2):123–156, 2001.

M. Gellert and R. Harbord. Moderate degree cubature formulas for 3-d tetrahedral finite-element approximations. *Communications in applied numerical methods*, 7(6):487–495, 1991.

L. Gerardo-Giorda, F. Nobile, and C. Vergara. Analysis and optimization of Robin–Robin partitioned procedures in fluid-structure interaction problems. *SIAM Journal on Numerical Analysis*, 48(6):2091–2116, 2010.

F. Gesztesy and M. Mitrea. Generalized Robin boundary conditions, Robin-to-Dirichlet maps, and Krein-type resolvent formulas for Schrödinger operators on bounded Lipschitz domains. *arXiv preprint arXiv:0803.3179*, 2008.

G. R. Goldstein. Derivation and physical interpretation of general boundary conditions. *Advances in Differential Equations*, 11(4):457–480, 2006.

L. Halpern. Optimized Schwarz waveform relaxation: roots, blossoms and fruits. In *Domain Decomposition Methods in Science and Engineering XVIII*, pages 225–232. Springer, 2009.

P. Hansbo, M. G. Larson, and K. Larsson. Analysis of finite element methods for vector Laplacians on surfaces. *IMA J. Numer. Anal.*, 40(3):1652–1701, 2020.

T. Kashiwabara, C. M. Colciago, L. Dedè, and A. Quarteroni. Well-posedness, regularity, and convergence analysis of the finite element approximation of a generalized Robin boundary value problem. *SIAM J. Numer. Anal.*, 53(1):105–126, 2015.

J. King and C. Venkataraman. Free boundary problems for Stokes flow, with applications to the growth of biological tissues. *Interfaces Free Bound.*, 23(4):433–458, 2021.

B. Kovács. High-order evolving surface finite element method for parabolic problems on evolving surfaces. *IMA J. Numer. Anal.*, 38(1):430–459, 2018.

B. Kovács and C. Lubich. Linearly implicit full discretization of surface evolution. *Numer. Math.*, 140(1):121–152, 2018.

B. Kovács, B. Li, C. Lubich, and C. A. Power Guerra. Convergence of finite elements on a solution-driven evolving surface. *Numerische Mathematik*, 137(3):643–689, 2017.

B. Kovács, B. Li, and C. Lubich. A convergent evolving finite element algorithm for mean curvature flow of closed surfaces. *Numer. Math.*, 143:797–853, 2019.

B. Kovács, B. Li, and C. Lubich. A convergent algorithm for forced mean curvature flow driven by diffusion on the surfaces. *Interfaces and Free Boundaries*, 22(4):443–464, 2020.

B. Kovács, B. Li, and C. Lubich. A convergent evolving finite element algorithm for Willmore flow of closed surfaces. *Numer. Math.*, 149:595–644, 2021.

M. Lenoir. Optimal isoparametric finite elements and error estimates for domains involving curved boundaries. *SIAM Journal on Numerical Analysis*, 23(3):562–580, 1986.

P. Persson and G. Strang. A simple mesh generator in MATLAB. *SIAM Review*, 46(2):329–345, 2004.

A. Quarteroni and A. Valli. *Domain decomposition methods for partial differential equations*. Oxford University Press, 1999.

L. R. Scott and S. Zhang. Finite element interpolation of nonsmooth functions satisfying boundary conditions. *Math. Comp.*, 54(190):483–493, 1990.

M. E. Taylor. *Partial differential equations I. Basic theory*, volume 115 of *Applied Mathematical Sciences*. Springer, New York, second edition, 2011.

S. W. Walker. *The shape of things: a practical guide to differential geometry and the shape derivative*. SIAM, Philadelphia, 2015.